Method Development for Comprehensive Lipidome Profiling of Cells using LC-MS

by

Barinder Bajwa

A thesis submitted in partial fulfillment of the requirements for the degree of

Master of Science

Department of Chemistry
University of Alberta

Abstract

Lipidomics aims to research lipid metabolism inside various samples or biological organisms. Through the research of lipidomics, information regarding the diversity, abundance, and function of lipids can determined. Although lipids can be categorized into 8 lipid classes, the variability between head groups and acyl chains results in over 100,000's of unique structures. These unique lipids encompass a wide range of biological functions in living organisms such as cell signaling, energy storage, and cell compartmentalization. Mass spectrometry (MS) makes for an ideal analysis technique for lipid research, as it allows for the comprehensive profiling of lipid species from complex matrices as a result of its high sensitivity and ability to be coupled with separation techniques. Additionally, through the employment of tandem MS, the structural identifications of lipid molecules can be determined, helping validate MS results.

A fundamental step in the analysis of lipids involves lipid extraction, in which solvents are used to efficiently extract as many lipid classes and species as possible from the biological organism. Due to the structural diversity of lipids, lipids tend to have a wide range of physiochemical properties, making the extraction of all lipid classes impossible. The use of an appropriate extraction protocol is critical, as lipid extraction tends to be one of the preliminary steps in lipidomics research, thus will have a considerable effect on the quality of results obtained from the analysis. Biphasic extraction is often utilized as it incorporates the use of a non-polar organic solvent for lipid extraction, along with a polar solvent for the solubilization of polar contaminants. In chapter 2, a slightly modified version of the Folch and MTBE, along with the original MTBE method were evaluated to determine an optimal extraction protocol for the lipidomics analysis of cell lines. Metrics such as the time for lipid extraction, reproducibility of extraction, ease of extraction, and extraction efficiency were assessed using *Saccharomyces cerevisiae* cells. Although the MTBE protocol was more efficient at extracting polar lipids,

the modified Folch protocol was chosen as the optimal extraction method due to its high reproducibility and short extraction time. Furthermore, it was found that an increased incubation time in the MTBE protocol was detrimental to its reproducibility, based on RSD values and intragroup separation in PCA. Finally, the modified Folch protocol was used for tandem MS of yeast cell extracts in which 401 and 398 features were identified using Metaboscape 4.0 and LipidMatch, respectively. Our tandem MS protocol had applied unique collision energies to specific lipid classes, which resulted in more lipid identifications compared to previous literature that focused on profiling the yeast lipidome.

Research into the lipidomes of various cancer cell lines through liquid chromatography mass spectrometry (LC-MS) has increased over the past decade. In particular, MCF-7 breast cancer cells are a useful model for cancer research due to their ability to simulate human breast cancers, and have been successfully used to demonstrate abnormal lipid changes relative to healthy cells. In chapter 3, we first found the optimal cell lysis protocol by evaluating the lysis efficiency between MCF-7 cells disrupted via thermal lysis and bead lysis. Cells subjected to bead lysis were found to have a better cell lysis efficiency, homogenized better in the lysis solvent, and had lower intra-group variability. Additionally, comprehensive lipid profiling of MCF-7 cells was performed through our untargeted tandem MS protocol. After evaluating our identifications against literature, our profiling method was able to identify more lipid species in every lipid class compared, with the exception of phosphatidylserines. Through the employment of our protocol, we can get a better understanding of the MCF-7 lipidome, which could potentially lead to biomarker discovery for breast cancer in the future.

Preface

Samples in Chapter 2 were obtained from Dr Shuang Zhao. The cell lysis protocol was adapted from Dr Xian Luo. The modified Folch protocol was adapted from Adriana Zardini Buzatto. I prepared the samples, helped with design of the experiment, collected and processed data, and generated tables and figures. The conceptualization of the experiment was derived by Dr Liang Li, along with being involved in the experimental design.

Sample stock in Chapter 3 was obtained from Gareth Lambkin, but were grown to confluency by myself. I prepared the samples, helped with design of the experiment, collected and processed data, and generated tables and figures. The conceptualization of the experiment was derived by Dr Liang Li, along with being involved in the experimental design.

Acknowledgments

I would like to express my heartfelt thanks and gratitude towards my supervisor, Dr Liang Li, for his guidance, inspiration, and mostly his patience. Throughout my time here, I have learnt a great deal regarding problem solving, troubleshooting, lipidomics, and data analysis in the field of Mass Spectrometry. The biweekly meetings were a tremendous help with my projects, and I was able to receive invaluable feedback from the discussions.

I wish to extend my great appreciation and gratitude towards my supervisory committee for their advice and participating in my oral examination.

I would like to thank my group members for their helpful feedback and support over the years. My sincere thanks to Adriana Zardini Buzatto and Carlos Canez Quijada for teaching me the ropes in lipidomics, Dr Xian Luo and Gareth Lambkin for showing me how to culture cells, and Xiaohang Wang, Dr Yunong Li, Dr Wei Han, and Dr Shuang Zhao for their mentorship. To my fellow and past friends in the chemistry department, Yunong, Erik, Kamran, Carlos, Zeenat, Trevor, Luis, and Rene, I want to thank you for your support and all the memories we shared together over the past years.

Finally, I would like to thank my parents and family for everything they have done in my life.

Table of Contents

List of Tables viii

List of Figures ix

List of Abbreviations xi

List of Symbols xiii

Chapter 1: Introduction 1

1.1: Introduction to Lipidomics 1

1.2: Benefits of Lipidomics Research 2

1.3: Strategies into Extracting Lipids 4

1.4: Lipidomics Instrumentation 6

1.5: Scope of the Thesis 10

1.6: Literature Cited 11

Chapter 2: Development of a Lipid Extraction Protocol and Lipidome Profiling of *Saccharomyces cerevisiae* using Liquid Chromatography Mass Spectrometry (LC-MS) 15

2.1: Introduction 15

2.2: Experimental 17

2.2.1: Chemicals and Reagents 17

2.2.2: Media and Culture Conditions for the Growth of *Saccharomyces cerevisiae* 17

2.2.3: Cell lysis 18

2.2.4: Sample Preparation 18

2.2.5: LCMS Conditions 21

2.2.6: Data Processing and Analysis 23

2.3: Results and Discussion 24

2.3.1: Time Assessment 25

2.3.2: Safety and Cost Assessment 26

2.3.3: Extraction Efficiency Assessment 27

2.3.4: Ease of Extractability 34

2.3.5: Assessment of Method Reproducibility 35

2.3.6: Assessment of Method Repeatability 37

2.3.7: MSMS Analysis of *Saccharomyces cerevisiae* using a Modified Folch Lipid Extraction Protocol 40

2.4: Conclusion 47
2.5: Literature Cited 48
Chapter 3: Comparison of Cell Lysis Techniques and Lipid Profiling of MCF-7 Breast Cancer Cells using Liquid Chromatography Mass Spectrometry (LC-MS) 51
3.1: Introduction 51
3.2: Experimental 53
3.2.1: Chemicals and Reagents 53
3.2.2: Media and Culture Conditions for the Growth of MCF-7 Breast Cancer Cells 54
3.2.3: Cell Lysis 54
3.2.4: Sample Preparation 55
3.2.5: LCMS Conditions 57
3.2.6: Data Processing and Analysis 58
3.3: Results and Discussion 59
3.3.1: Assessment of Lysis Efficiency 60
3.3.2: Assessment of Method Reproducibility 66
3.3.3: Assessment of Homogenization 68
3.3.4: MSMS Analysis of MCF-7 Breast Cancer Cells using a Modified Folch Lipid Extraction Protocol 69
3.4: Conclusion 75
3.5: Literature Cited 75
Chapter 4: Conclusions and Future Work 79
4.1: Thesis Summary 79
4.2: Future Work 80
4.3: Literature Cited 81
Bibliography 82
Appendix 91

List of Tables

Table 2.3.1: Summary of RSD values calculated from intensities of internal standards and putatively identified features for samples extracted on different days……..38

Appendix Table 1: Summary of MSMS methods used on the yeast samples for lipid identification. CE refers to collision energy……91

Appendix Table 2: List of annotated lipid species from Metaboscape 4.0 libraries (LC-MS-MS Positive mode; LC-MS-MS Negative mode; MSDIAL; RIKEN Oxidized Phospholipids) and LipidMatch. Feature names in bold were detected through both annotation software……..94

Appendix Table 3: Summary of MSMS methods used on the MCF-7 samples for lipid identification. CE refers to collision energy……110

Appendix Table 4: List of annotated lipid species detected in MCF-7 breast cancer cells through Metaboscape 4.0 libraries (Bruker LipidBlast; Mass Bank; RIKEN Oxidized Phospholipids; LC-MSMS Positive; and LC-MSMS Negative) and LipidMatch. Feature names in bold were detected through both annotation software……..111

List of Figures

Figure 1.1: A representation of structures of the 8 main classes of lipids as defined by the International Lipid Classification and Nomenclature Committee (Adapted from LipidMap Tools. https://www.lipidmaps.org/resources/tools/index.php?tab=structure. accessed August 3rd, 2020)……2

Figure 2.3.1: Summed signal intensities for internal standards detected for each sample in ESI positive and negative mode……29

Figure 2.3.2: Comparison of average signal intensities for internal standards detected from each extraction method. Error bars represent the standard deviation of the average……29

Figure 2.3.3: Summed signal intensities for putatively identified lipids detected for each sample in ESI positive mode in the comparison between different extraction methods……30

Figure 2.3.4: Summed signal intensities for putatively identified lipids detected for each sample in ESI negative mode in the comparison between different extraction methods……31

Figure 2.3.5: Number of missing features for each extraction method in ESI positive mode from a total of 1826 putatively identified features from all extraction methods……32

Figure 2.3.6: Number of missing features for each extraction method in ESI positive mode from a total of 441 putatively identified features from all extraction methods……33

Figure 2.3.7: PCA plots of putatively identified features detected from different lipid extraction protocols and QCs. Features from ESI positive and negative modes were merged before generating the PCA plot……36

Figure 2.3.8: PCA plots of putatively identified features detected from samples and QCs extracted using the Folch method on different days. Features from ESI positive and negative modes were merged before generating the PCA plot……39

Figure 2.3.9: List of putatively identified features identified through LipidMaps that were incorporated into SPLs for MSMS of yeast cells……41

Figure 2.3.10: Bar graph comparing the number of lipids annotated in different lipid classes between Metaboscape 4.0 libraries, LipidMatch library, and literature……45

Figure 2.3.11: Spectra obtained by Münger et al. obtained at 30 eV in ESI positive mode for ergosterol with a precursor m/z of 379.337[32]……46

Figure 2.3.12: Experimental ESI-MSMS spectra obtained at 30.8 eV in ESI positive mode for ergosterol with precursor m/z of 379.336……47

Figure 3.3.1: Comparison of average signal intensities for internal standards detected from each cell lysis method. Error bars represent the standard deviation of the average……61

Figure 3.3.2: Summed signal intensities for putatively identified lipids detected for each sample in ESI positive mode in the comparison between different cell lysis methods……62

Figure 3.3.3: Summed signal intensities for putatively identified lipids detected for each sample in ESI negative mode in the comparison between different cell lysis methods……..63

Figure 3.3.4: Number of missing features for each cell lysis method in ESI positive mode from a total of 1853 putatively identified features from all tested protocols……..65

Figure 3.3.5: Number of missing features for each cell lysis method in ESI negative mode from a total of 1066 putatively identified features from all tested protocols……65

Figure 3.3.6: PCA plots of putatively identified features detected from different cell disruption protocols, alongside QC samples. Features from ESI positive and negative modes were merged before generating the PCA plot……..67

Figure 3.3.7: Microscope image obtained under 20x magnification of cells lysed using: (**a**) thermal lysis through freeze that cycles; and (**b**) bead lysis with assistance through vortexing……69

Figure 3.3.8: List of putatively identified features identified through LipidMaps that were incorporated into SPLs for MSMS of MCF-7 cells……70

Figure 3.3.9: Bar graph comparing the number of lipids annotated in different lipid classes between Metaboscape 4.0 libraries, LipidMatch library, and literature in breast cancer cells……74

Appendix Figure 1: Summed signal intensities for all internal standards extracted from yeast cells using a modified Folch protocol. Samples were extracted on different days and run in both ESI modes……93

Appendix Figure 2: Summed signal intensities for putatively identified lipids extracted from yeast cells using a modified Folch protocol. Samples were extracted on different days and run in ESI positive mode……..93

Appendix Figure 3: Summed signal intensities for putatively identified lipids extracted from yeast cells using a modified Folch protocol. Samples were extracted on different days and run in ESI negative mode……..94

List of Abbreviations

ACN	Acetonitrile
APCI	Atmospheric pressure chemical ionization
B&D	Bligh and Dyer
BMP	Bis(monoacylglycero)phosphate
CE	Collision energy
CL	Cardiolipin
Chol	Cholesterol
CholE	Cholesterol esters
Cer	Ceramide
CID	Collision induced dissociation
CIL	Chemical isotope labeling
CO_2	Carbon Dioxide
DCM	Dichloromethane
DG	Diacylglycerols
EDTA	Ethylenediaminetetraacetic acid
ESI	Electrospray Ionization
FBS	Fetal Bovine Serum
FA	Fatty acid
FT	Freeze thaw
GC	Gas chromatography
H_2O	Water
HPLC	High performance liquid chromatography
ID	Identification
IPA	Isopropyl alcohol
IPC	Inositol Phosphoryl ceramide
LC	Liquid chromatography
LPA	Lysophosphatidic Acid
LPC	Lysophosphatidylcholine
LPE	Lysophosphatidylethanolamine
LPG	Lysophosphatidylglycerols

LPI	Lysophosphatidylinositol
LPL	Lysophospholipids
MIPC	Mannosylinositol phosphorylceramide
MCF-7	Michigan Cancer Foundation-7
MeOH	Methanol
MG	Monoacylglycerols
MPA	Mobile phase A
MPB	Mobile phase B
MS	Mass spectrometry
MSMS	Tandem MS
MTBE	Methyl tert-butyl ether
NMR	Nuclear magnetic resonance
PBS	Phosphate Buffer Saline
PA	Phosphatidic Acid
PC	Phosphatidylcholines
PCA	Principal component analysis
PE	Phosphatidylethanolamine
PG	Phosphatidylglycerols
PI	Phosphatidylinositol
PS	Phosphatidylserine
QC	Quality Control
QToF	Quadrupole time of flight
RSD	Relative standard deviation
RP	Reversed phase
SPL	Scheduled precursor list
SM	Sphingomyelin
Sph	Sphingoid bases
TG	Triacylglycerols
TLC	Thin-layer chromatography
UHPLC	Ultra-high performance liquid chromatography
WE	Wax ester

List of Symbols

°C	Degrees Celsius
Cc	Cubic centimeter
Cm	Centimeter
Da	Daltons
eV	Electron volts
g	G Force
g/mL	Grams per milliliter
Hz	Hertz
kV	Kilovolts
M	Molar
mDa	Milli Dalton
mL	Milliliter
mm	Millimeter
mM	Millimolar
m/z	Mass to charge ratio
min	Minutes
ppm	Parts per million
rpm	Revolutions per minute
S/N	Signal to noise
µL	Microliter
V	Volts
v/v	Volume per volume
w/v	Weight per volume

Chapter 1: Introduction

1.1: Introduction to Lipidomics

Lipidomics aims to study the metabolism of lipids inside cells and biological pathways through techniques utilized in analytical chemistry[1]. Lipidome is a term used to describe the total lipid content inside a biological source and the lipidome can be quite complex in terms of abundance and diversity, mainly attributed to the different types of biochemical transformations that lipids undergo during lipid synthesis[2][3]. The International Lipid Classification and Nomenclature Committee describes lipids as small molecules that are hydrophobic or amphipathic in nature which are comprised of carbanion-based condensation of thioesters and/or carbocation-based condensation of isoprene units[4]. Using this definition, lipids can be classified into 8 major classes of lipids as shown in Figure 1.1 (fatty acyls (FA), glycerolipids, glycerophospholipids, sphingolipids, saccharolipids, polyketides, prenol lipids, and sterol lipids), and further divided into subclasses depending on their head group, aliphatic chains, and the type of linkage between their head group and aliphatic chains[1][2]. The diversity of lipids regarding their head groups and acyl chains leads to over 100,000's of potential structures[1]. For example, phosphatidylethanolamines (PE) can differ in terms of the length of carbons in their acyl chain, stereochemistry the of acyl chains, number of double bonds, position of double bonds, and presence of oxygen groups[5]**.** Since 2003, lipidomics has become a rapidly evolving field, leading to important discoveries through the use of analytical instruments[6]. Mass spectrometry (MS), a common analytical approach, has the benefit of detecting small perturbations of lipids due to its high sensitivity, making it suitable for the analysis of the cell lipidome and other complex biological matrices[7].

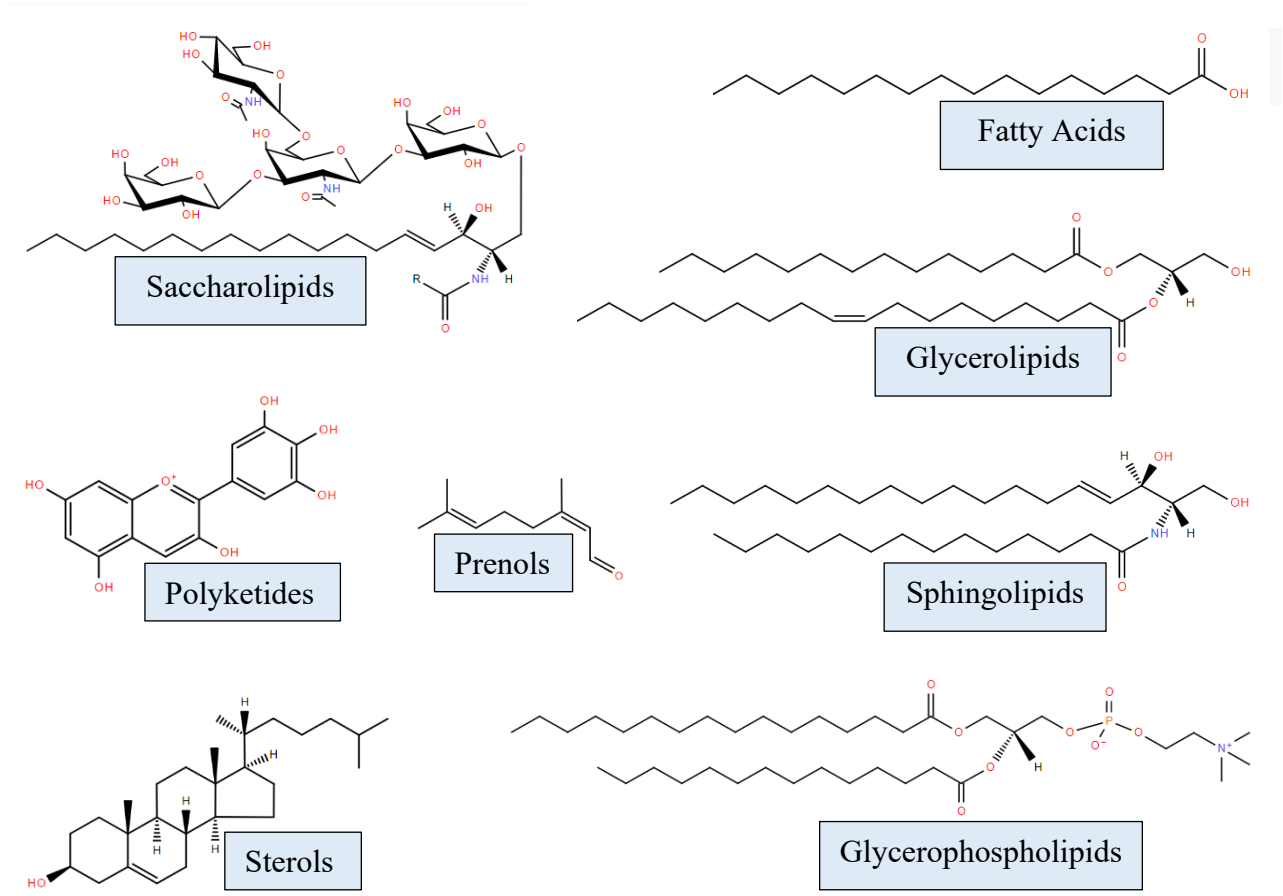

Figure 1.1: A representation of structures of the 8 main classes of lipids as defined by the International Lipid Classification and Nomenclature Committee (Adapted from LipidMap Tools. https://www.lipidmaps.org/resources/tools/index.php?tab=structure. accessed August 3rd, 2020).

1.2: Benefits of Lipidomics Research

Lipids are comprised of many lipid subclasses resulting in a broad range of structures and biological functions. Previous knowledge states that lipids are involved in cell signaling, energy storage, and cell compartmentalization, but recent studies have found that lipids play an additional role in cell apoptosis, inflammation, immunity, and disease pathology[8]-[12]. An emphasis has been placed on neurodegenerative diseases, as lipids comprise of fifty percent of the dry weight of the brain[13].

Neurodegenerative disorders are of high interest due to the lack of cure for diseases such as Alzheimer's, Parkinson's, and Huntington's, and research into lipids may provide insights into disease progression and pathogenesis. By focusing research into cells involved in neurodegenerative disorders or diseases such as cancer, biomarkers can potentially be discovered through monitoring changes in cell lipidomes. Biomarkers can help monitor new treatment options, help assess the severity of the disease, and lead to the discovery of novel drugs. Cancer cells are particularly well researched, and it has been shown in past research that due to the increased proliferation exhibited by cancer cells, they require an increase in nutrient uptake compared to healthy cells[14]. Altered changes in the lipidome such as increased FA uptake[15], as well as the upregulation of de novo lipogenesis has been linked in cancer cells[16]. Studies in the field of lipidomics into antibiotic resistance has found major differences in the lipidomes between antibiotic sensitive and resistance bacterial strains, suggesting that the lipid composition of cells might contribute to drug resistance[17]-[19]. These studies can have profound impact into the discovery of new antimicrobial therapies to combat existing antimicrobial strains, and help provide information into the mechanisms behind antibiotic resistance. Lipids serve as good indicators of the status of a biological system as they respond to both intrinsic (genome, proteome) and extrinsic (diet, environment) stimuli[6]. Many industries incorporate microorganisms and plants to produce lipids for commercial products such as biodiesel, cosmetics, and food, thus the accurate quantification and quantitation of lipids in cells is emphasized in research[20]-[22]. Lipids are also involved in modifications with proteins to form lipoproteins[6]. Taking into account all the lipid modifications; cell lipidomes are quite complex due to the number of lipids, concentration ranges of lipids, and the constant regulation in response to physiological perturbations, making lipids difficult to monitor[6]. Techniques need to be employed to effectively and efficiently extract as much information from the lipidome as possible.

1.3: Strategies into Extracting Lipids

One of the preliminary steps in extracting lipids from cells is the lysis of the cell membrane or cell wall to release the intercellular contents of the cell. There are many cell lysis techniques that can be employed to achieve the disruption of the membrane, and can be chosen based on the ease of purification, type of target molecule for analysis, and quality of the final products[23]. The type of cell can also influence the type of lysis method used. Cells such as gram negative bacteria, which contain a cell wall, plasma membrane, and an outer membrane, typically are more difficult to lyse compared to mammalian cells, and require harsher lysis methods[24]. Cell lysis methods can be defined as either mechanical or non-mechanical lysis. Mechanical lysis uses shear forces to disrupt the cell membrane, and includes methods such as bead lysis and high-pressure homogenization. These methods are widely used due to their applicability to a wide range of cells, high lysis efficiency, and high throughput. A caveat to consider is that they tend to produce heat, which can potentially degrade analytes of interest[23]. Non-mechanical lysis can be subdivided into three categories: Physical lysis; chemical lysis; and biological lysis. Physical lysis utilizes external forces to lyse the cell, achieved without any contact with the cell. There are many physical lysis methods, but only thermal lysis will be discussed. Thermal lysis uses temperature to disrupt the cell membrane, and a prime example is freeze-thaw lysis, in which cells are repeatedly frozen and thawed. The continuous freeze-thaw cycles cause ice crystals to form, which will help lyse the membrane of the cell[23]. Although the method isn't suitable for industrial applications and is time consuming, it does not require any external tools such as beads, which can impede lipid extraction. Chemical lysis employs buffers and detergents[25], but is avoided in MS as the chemicals can cause ion suppression, matrix effects, or might interfere with downstream analyses. Biological lysis utilizes enzymes, but can be quite expensive and results in partial lysis of the cell membrane[23]. Similar to chemical lysis, it is often difficult to purify the lysate, resulting in interference during analysis via MS.

To obtain a comprehensive idea of a lipidome in a biological source, one needs to efficiently extract as many lipids as possible. This can be a challenging task caused by the structural diversity and modifications of lipids, which can range from polar (lysophosphatidylcholines) to apolar (cholesterol esters) lipids[26]. As a result, lipids will have different physiochemical properties, making it impossible to extract all lipid classes and subclasses using a singular extraction technique. Consequently, extraction techniques tend to either focus on specific lipid classes or try to extract as many lipids as possible. Another complication that arises is that complex biological matrices such as tissue, cells, and bio-fluids, often contain unwanted proteins, salts, carbohydrates, and metabolites, which will impede with downstream specificity and interfere with high performance liquid chromatography (HPLC) separation[27]. Biphasic lipid extraction utilizes a polar aqueous phase and a relatively non-polar organic phase[1]. Biphasic lipid extraction is frequently used when extracting lipids from bio-fluids, cells, or tissues, as the aqueous phase is able to remove cell debris, polar contaminants, and proteins, all the while isolating lipids in the organic phase. Popular extraction protocols include the Folch and the Bligh and Dyer (B&D), which were developed in 1957 and 1959 respectively[28][29]. Both protocols employ chloroform/methanol/water in different ratios (2:2:1.8 v/v/v for B&D and 8:4:3 v/v/v for Folch). Due to chloroform being cariogenic, dichloromethane can serve as optimal substituent for the organic phase as it is less toxic. Although the Folch and B&D are the more commonly used methods, there have been recent protocols published, such as the Methyl-tert-butyl ether (MTBE) protocol by Matyash et al[30]. MTBE is an organic solvent which has a lower density than water, which is unique in that the organic layer remains on top during the extraction, allowing for more accessible solvent extraction[30].

Internal standards are introduced into the biological sample before extraction and serve to normalize sample loss during extraction and is necessary for analyte quantification[31]. Ideally, internal standards should be isotopes of common analytes in the sample as they will have similar

physicochemical properties to the analyte, and the effects of sample preparation, elution patterns, and ionization will be nearly identical. An internal standard for each lipid species would be ideal, but due to the complex nature of lipids, it would be near impossible to obtain an isotope labelled internal standard for every lipid. Additionally, there would be huge cost complications. Ionization efficiency of lipids during MS analysis is dependent on the head group of the lipid subclass, thus each lipid subclass requires its own internal standard for reliable MS analysis[1].

To improve the detectability of lipids in downstream analysis, one can derivatize specific functional groups of certain lipid subclasses. Lipid subclasses such as triacylglycerides (TG) and FAs have a difficult time ionizing under electrospray ionization (ESI) negative and positive mode respectively. Derivatization is an optional procedure which can enhance analyte sensitivity and help determine the absolute quantification of specific lipid subclasses[27]. Some examples of derivatization include methylation of FAs for gas chromatography mass spectrometry (GC-MS)[32], determining double bond positions in phospholipids through the Paternò–Büchi reaction[33], and the use of diazomethane to increase sensitivity of PEs and phosphatidylcholines (PC)[34]. Some drawbacks of lipid derivatization is that the technique can be laborious, reduce sample throughput, introduce background interference, and increase the cost per analysis[6].

1.4: Lipidomics Instrumentation

Techniques for lipidomics have advanced over the years and one of the leading applications has been the field of MS. Due to its customizable coverage (targeted vs. untargeted) and its ability to be combined with separation techniques, it consistently outperforms other analysis platforms such as nuclear magnetic resonance (NMR), thin-layer chromatography (TLC), and fluorescence spectroscopy[7].

MS is also highly sensitive, can detect multiple compounds at once, has high throughput, and a high mass accuracy[35][36]. The general principle of MS is to detect ions based on their mass to charge ratio (m/z) and relating the abundance of ions into a signal. Due to complexity of lipidome, it is common to find isomeric lipids, underlying importance of confidently identifying lipids based on not just the m/z alone. We can employ tandem MS (MSMS) to isolate and fragment a specific mass compound to obtain a molecular fingerprint, as each analyte fragments in a unique way due to structural differences. MSMS can provide information on the double bond positions of lipids, lipid subclass head groups, structural information, or FA tail constituents[1].

Analytes are required to be ionized into the gas phase for MS to operate. Several ionization techniques have been developed, yet Atmospheric Pressure Chemical Ionization (APCI) and ESI are used almost exclusively in the lipidomics field[27]. APCI pumps sample dissolved in solvent through a capillary. Once the sample reaches the end of the capillary, the sample and solvent are aerosolized and vaporized into the gas phase using high temperatures and nitrogen gas. The solvent and sample are ionized through the use of a corona discharge needle at atmospheric pressure[37]. APCI is often incorporated when analyzing polar and thermally stable lipids such as sphingolipids. Samples ionized through APCI tend to be efficiently ionized and undergo little fragmentation. Due to high temperatures involved in the process, thermally unstable, non-volatile, and high molecule weight analytes have difficulty ionizing[37]. ESI remains prevalent in literature and common amongst the lipidomics community, attributable to its ability to ionize non-volatile lipids effectively, as well as the low energy used during ionization[27]. The low energy requirement of ESI prevents the fragmentation of intact lipid molecules, thus obtaining accurate information on the mass of the molecule. The basic principle of ESI is that charged droplets are produced through the use of an electrical field, after which the droplets slowly evaporate and transfer the charge over to individual analytes[39]. Lipids that contain a charge in their

natural state have increased sensitivity, but neutral lipids can also form ions through adduct formation through the addition of specific salts into the sample. A drawback of ESI is that it suffers from ion suppression when analyzing complex biological matrices, but the effect can be mitigated through the use of chromatographic methods[7].

Ion suppression is a result of non-volatile analytes which impact the efficiency in which droplets in ESI form or evaporate, thus affecting the number of charged ions present. This results in analytes of interest having low sensitivity, and in return, can result in inaccurate portrayal of the true concentration of the analyte[40]. Minimizing ion suppression can be achieved through purifying the sample in order to reduce the complexity of the mixture. Some techniques used in conjunction with MS that function to minimize ion suppression are liquid and gas chromatography[39]. These techniques employ the use of a column which separates the sample mixture based on the physicochemical properties (polarity, hydrophobicity, size, charge, affinity) of analytes. The column separates chemicals by incorporating two phases; a mobile phase and stationary phase. As the mixture is carried through the column via the mobile phase, analytes interact with the stationary phase and are retained based on their affinity for the stationary phase, thus providing another dimension of identification[7]. GC uses inert gases as mobile phase to carry analytes while LC uses liquid solvents. Although both separation techniques are common, LC is more widely used as lipids tend to be dissolved in liquid solvent after lipid extraction. GC requires samples to be volatile and derivatization is often required to bring the analyte into the gas phase, making it unsuitable for untargeted analysis[38]. Generally reversed phase columns are used in lipidomics which contain a stationary phase consisting of C8-C18 hydrocarbons. For the mobile phase, a ramp is used starting from an aqueous to an organic solvent to elute analytes that are partitioned inside the stationary phase[27].

Mass analyzers are a fundamental part of MS as they allow for the separation of analytes based on the m/z[41]. Many forms of mass analyzers exist, but only the Quadrupole Time of Flight (QToF) will be discussed. Ions enter the first quadrupole, which functions as a mass filter to select ions with a specific m/z, depending on the RF and DC voltage applied. The first quadrupole can also be set to RF only mode, in which all ions will be filtered through into the second quadrupole[42]. The second quadrupole functions as a collision cell, if tandem MS is performed. A collision gas consisting of a neutral gas such as nitrogen is released into the quadrupole for collision induced dissociation. An electric voltage is then applied to increase the kinetic energy of the ions, causing the ions to collide with the gas. The kinetic energy of the ions gets converted into internal energy, resulting in fragmentation of the precursor ions. After leaving the quadrupole, ions get released into the ToF tube, where a short electric pulse will be applied to send ions into the reflectron. The reflectron consists of a series of metal plates, in which an electric potential is applied and will push ions back towards a detector. Ions with a smaller m/z will experience a stronger electric pulse in the ToF tube, and will reach the detector faster compared to ions with a larger m/z[42]. The reflectron functions to increase the flight time of the ions to improve resolution, and also help correct spatial variability of the ions. Ions with a higher kinetic energy relative to ions with the same m/z ratio will penetrate deeper into the reflectron, and will take a slightly longer path to the detector. The ions will ultimately reach the detector in a similar time frame compared to ions with a lower kinetic energy[42]. QToFs combines the fragmentation efficiency of the quadrupole ion focusing device and the mass accuracy, sensitivity, and resolution of the time of flight analyzer. QToFs are often used in research involving untargeted analysis of metabolites due to their ability to detect multiple analytes[7]. In lipidomics, achieving a high resolution and mass accuracy is necessary to help distinguish between the various isomers, adducts, subclasses, and fatty acyl saturations that exist[41]. High data acquisition speeds also allow for the QToF mass analyzer to be coupled to ultra-high performance liquid chromatography (UHPLC), resulting in increased sample throughput[41].

1.5: Scope of the Thesis

The objective of this research is to develop new untargeted lipidomics techniques for cells through the use of ESI-UHPLC-MS. In Chapter 2, a lipid extraction protocol for cells is developed and tested with *Saccharomyces cerevisiae*. Lipid extraction protocols are critical in lipid analysis of cells, as it will determine the types and quantity of lipids extracted, along with impacting the quality of data. Modified versions of the Folch and MTBE lipid extraction protocols are assessed through parameters such as time, reproducibility, and extraction efficiency, to find the optimal lipid extraction protocol. Once an optimal lipid extraction protocol is determined, the repeatability needs to be tested to ensure that there is little variance between samples extracted in different batches. Finally, the optimized lipid extraction protocol is applied to profile the lipidome of *Saccharomyces cerevisiae* through untargeted analysis using tandem MS. Compared to past literature, we focus on a more untargeted approach for lipid identification, and utilize unique collision energies for specific lipid classes. This allows us to obtain efficient fragmentation of lipid classes and improving analyte annotations through the use of lipid libraries.

In Chapter 3, the lipid extraction protocol is employed for MCF-7 breast cancer cells. The optimal cell lysis method for breast cancer cells is developed by comparing cells lysed using thermal lysis and bead lysis. Parameters such as reproducibility, homogenization, and lysis efficiency are assessed. Since cell lysis tends to be a preliminary step in lipid analysis, it has a considerable impact on the downstream results and data. Having a cell lysis protocol which can efficiently lyse the cells will improve the amount of lipids extracted, and help provide an accurate representation of the cellular lipidome. The lipidome of MCF-7 is also analyzed through untargeted analysis, and lipid profiling is performed through tandem MS. Identifications obtained from our tandem MS analysis method are compared to literature to assess the effectiveness of our protocol.

1.6: Literature Cited

[1] B. Brügger, Lipidomics: Analysis of the Lipid Composition of Cells and Subcellular Organelles by Electrospray Ionization Mass Spectrometry, Annu. Rev. Biochem. (2014). https://doi.org/10.1146/annurev-biochem-060713-035324.

[2] X. Han, Lipidomics for studying metabolism, Nat. Rev. Endocrinol. (2016). https://doi.org/10.1038/nrendo.2016.98.

[3] E. Fahy, D. Cotter, M. Sud, S. Subramaniam, Lipid classification, structures and tools, Biochim. Biophys. Acta - Mol. Cell Biol. Lipids. (2011). https://doi.org/10.1016/j.bbalip.2011.06.009.

[4] E. Fahy, S. Subramaniam, R.C. Murphy, M. Nishijima, C.R.H. Raetz, T. Shimizu, F. Spener, G. Van Meer, M.J.O. Wakelam, E.A. Dennis, Update of the LIPID MAPS comprehensive classification system for lipids, J. Lipid Res. (2009). https://doi.org/10.1194/jlr.R800095-JLR200.

[5] S.A. Murphy, A. Nicolaou, Lipidomics applications in health, disease and nutrition research, Mol. Nutr. Food Res. (2013). https://doi.org/10.1002/mnfr.201200863.

[6] K. Yang, X. Han, Lipidomics: Techniques, Applications, and Outcomes Related to Biomedical Sciences, Trends Biochem. Sci. (2016). https://doi.org/10.1016/j.tibs.2016.08.010.

[7] L. Li, J. Han, Z. Wang, J. Liu, J. Wei, S. Xiong, Z. Zhao, Mass spectrometry methodology in lipid analysis, Int. J. Mol. Sci. (2014). https://doi.org/10.3390/ijms150610492.

[8] F.M. Vaz, M. Pras-Raves, A.H. Bootsma, A.H.C. van Kampen, Principles and practice of lipidomics, J. Inherit. Metab. Dis. (2014). https://doi.org/10.1007/s10545-014-9792-6.

[9] A. Swiader, H. Nahapetyan, J. Faccini, R. D'Angelo, E. Mucher, M. Elbaz, P. Boya, C. Vindis, Mitophagy acts as a safeguard mechanism against human vascular smooth muscle cell apoptosis induced by atherogenic lipids, Oncotarget. (2016). https://doi.org/10.18632/oncotarget.8936.

[10] K.R. Feingold, C. Grunfeld, The Effect of Inflammation and Infection on Lipids and Lipoproteins, 2000.

[11] M.H. den Brok, T.K. Raaijmakers, E. Collado-Camps, G.J. Adema, Lipid Droplets as Immune Modulators in Myeloid Cells, Trends Immunol. (2018). https://doi.org/10.1016/j.it.2018.01.012.

[12] S. Borgquist, T. Butt, P. Almgren, D. Shiffman, T. Stocks, M. Orho-Melander, J. Manjer, O. Melander, Apolipoproteins, lipids and risk of cancer, Int. J. Cancer. (2016). https://doi.org/10.1002/ijc.30013.

[13] K.D. Bruce, A. Zsombok, R.H. Eckel, Lipid processing in the brain: A key regulator of systemic metabolism, Front. Endocrinol. (Lausanne). (2017). https://doi.org/10.3389/fendo.2017.00060.

[14] S.R. Islam, S.K. Manna, Lipidomic analysis of cancer cell and tumor tissues, in: Methods Mol. Biol., 2019. https://doi.org/10.1007/978-1-4939-9027-6_11.

[15] A. Carracedo, L.C. Cantley, P.P. Pandolfi, Cancer metabolism: Fatty acid oxidation in the limelight, Nat. Rev. Cancer. (2013). https://doi.org/10.1038/nrc3483.

[16] P. Sun, S. Xia, B. Lal, X. Shi, K.S. Yang, P.A. Watkins, J. Laterra, Lipid metabolism enzyme ACSVL3 supports glioblastoma stem cell maintenance and tumorigenicity, BMC Cancer. (2014). https://doi.org/10.1186/1471-2407-14-401.

[17] W. Hewelt-Belka, J. Nakonieczna, M. Belka, T. Bączek, J. Namieśnik, A. Kot-Wasik, Untargeted Lipidomics Reveals Differences in the Lipid Pattern among Clinical Isolates of Staphylococcus aureus Resistant and Sensitive to Antibiotics, J. Proteome Res. (2016). https://doi.org/10.1021/acs.jproteome.5b00915.

[18] K.M. Hines, A. Waalkes, K. Penewit, E.A. Holmes, S.J. Salipante, B.J. Werth, L. Xu, Characterization of the Mechanisms of Daptomycin Resistance among Gram-Positive Bacterial Pathogens by Multidimensional Lipidomics, MSphere. (2017). https://doi.org/10.1128/msphere.00492-17.

[19] H.M. Adams, L.R. Joyce, Z. Guan, R.L. Akins, K.L. Palmer, Streptococcus mitis and S. oralis lack a requirement for CdsA, the enzyme required for synthesis of major membrane phospholipids in bacteria, Antimicrob. Agents Chemother. (2017). https://doi.org/10.1128/AAC.02552-16.

[20] C. Breil, M. Abert Vian, T. Zemb, W. Kunz, F. Chemat, "Bligh and Dyer" and Folch methods for solid–liquid–liquid extraction of lipids from microorganisms. Comprehension of solvatation mechanisms and towards substitution with alternative solvents, Int. J. Mol. Sci. (2017). https://doi.org/10.3390/ijms18040708.

[21] K. Appala, K. Bimpeh, C. Freeman, K.M. Hines, Recent applications of mass spectrometry in bacterial lipidomics, Anal. Bioanal. Chem. (2020). https://doi.org/10.1007/s00216-020-02541-8.

[22] E.K. Matich, M. Ghafari, E. Camgoz, E. Caliskan, B.A. Pfeifer, B.Z. Haznedaroglu, G.E. Atilla-Gokcumen, Time-series lipidomic analysis of the oleaginous green microalga species Ettlia oleoabundans under nutrient stress, Biotechnol. Biofuels. (2018). https://doi.org/10.1186/s13068-018-1026-y.

[23] M.S. Islam, A. Aryasomayajula, P.R. Selvaganapathy, A review on macroscale and microscale cell lysis methods, Micromachines. (2017). https://doi.org/10.3390/mi8030083.

[24] E.R. Rojas, G. Billings, P.D. Odermatt, G.K. Auer, L. Zhu, A. Miguel, F. Chang, D.B. Weibel, J.A. Theriot, K.C. Huang, The outer membrane is an essential load-bearing element in Gram-negative bacteria, Nature. (2018). https://doi.org/10.1038/s41586-018-0344-3.

[25] R.B. Brown, J. Audet, Current techniques for single-cell lysis, J. R. Soc. Interface. (2008). https://doi.org/10.1098/rsif.2008.0009.focus.

[26] Z. Liu, A. Logan, B.G. Cocks, S. Rochfort, Seasonal variation of polar lipid content in bovine milk, Food Chem. (2017). https://doi.org/10.1016/j.foodchem.2017.06.038.

[27] S.W.J. Shields, C.R. Canez, K. V. Wasslen, H. Lee, D. Stalinski, L. Trouborst, S. Joudan, S. Whitton, H.P. Weinert, J.M. Manthorpe, J.C. Smith, Enhancing the analysis of complex lipid samples through developments in chromatography and chemical derivatization, in: NATO Sci. Peace

Secur. Ser. A Chem. Biol., 2017. https://doi.org/10.1007/978-94-024-1113-3_11.

[28] J. FOLCH, M. LEES, G.H. SLOANE STANLEY, A simple method for the isolation and purification of total lipides from animal tissues., J. Biol. Chem. (1957). https://doi.org/10.3989/scimar.2005.69n187.

[29] E.G. BLIGH, W.J. DYER, A rapid method of total lipid extraction and purification., Can. J. Biochem. Physiol. (1959). https://doi.org/10.1139/o59-099.

[30] V. Matyash, G. Liebisch, T. V. Kurzchalia, A. Shevchenko, D. Schwudke, Lipid extraction by methyl-terf-butyl ether for high-throughput lipidomics, in: J. Lipid Res., 2008. https://doi.org/10.1194/jlr.D700041-JLR200.

[31] S. Vinter, Variations in internal standard: An inspector's perspective, Bioanalysis. (2019). https://doi.org/10.4155/bio-2019-0232.

[32] M. Gómez-Brandón, M. Lores, J. Domínguez, Comparison of extraction and derivatization methods for fatty acid analysis in solid environmental matrixes, Anal. Bioanal. Chem. (2008). https://doi.org/10.1007/s00216-008-2274-7.

[33] W. Zhang, D. Zhang, Q. Chen, J. Wu, Z. Ouyang, Y. Xia, Online photochemical derivatization enables comprehensive mass spectrometric analysis of unsaturated phospholipid isomers, Nat. Commun. (2019). https://doi.org/10.1038/s41467-018-07963-8.

[34] C.R. Canez, S.W.J. Shields, M. Bugno, K. V. Wasslen, H.P. Weinert, W.G. Willmore, J.M. Manthorpe, J.C. Smith, Trimethylation Enhancement Using 13C-Diazomethane (13C-TrEnDi): Increased Sensitivity and Selectivity of Phosphatidylethanolamine, Phosphatidylcholine, and Phosphatidylserine Lipids Derived from Complex Biological Samples, Anal. Chem. (2016). https://doi.org/10.1021/acs.analchem.5b04524.

[35] F.F. Hsu, Mass spectrometry-based shotgun lipidomics – a critical review from the technical point of view, Anal. Bioanal. Chem. (2018). https://doi.org/10.1007/s00216-018-1252-y.

[36] I. Aretz, D. Meierhofer, Advantages and pitfalls of mass spectrometry based metabolome profiling in systems biology, Int. J. Mol. Sci. (2016). https://doi.org/10.3390/ijms17050632.

[37] C. Pitman, W. LaCourse, Desorption Atmospheric Pressure Chemical Ionization: A Brief Review, Anal. Chim. Acta. (2020). https://doi.org/https://doi.org/10.1016/j.aca.2020.05.073.

[38] B. Silva Barbosa Correia, R. Susana Torrinhas, W. Yutaka Ohashi, L. Tasic, Analytical Tools for Lipid Assessment in Biological Assays, in: Adv. Lipid Metab., 2020. https://doi.org/10.5772/intechopen.81523.

[39] C.S. Ho, C.W.K. Lam, M.H.M. Chan, R.C.K. Cheung, L.K. Law, L.C.W. Lit, K.F. Ng, M.W.M. Suen, H.L. Tai, Electrospray ionisation mass spectrometry: principles and clinical applications., Clin. Biochem. Rev. (2003).

[40] A.J. Taylor, A. Dexter, J. Bunch, Exploring Ion Suppression in Mass Spectrometry Imaging of a Heterogeneous Tissue, Anal. Chem. (2018). https://doi.org/10.1021/acs.analchem.7b05005.

[41] S.B. Breitkopf, S.J.H. Ricoult, M. Yuan, Y. Xu, D.A. Peake, B.D. Manning, J.M. Asara, A relative quantitative positive/negative ion switching method for untargeted lipidomics via high resolution LC-MS/MS from any biological source, Metabolomics. (2017). https://doi.org/10.1007/s11306-016-1157-8.

[42] D.R. Allen, B.C. McWhinney, Quadrupole Time-of-Flight Mass Spectrometry: A Paradigm Shift in Toxicology Screening Applications, Clin. Biochem. Rev. (2019). https://doi.org/10.33176/aacb-19-00023.

Chapter 2: Development of a Lipid Extraction Protocol and Lipidome Profiling of *Saccharomyces cerevisiae* using Liquid Chromatography Mass Spectrometry (LC-MS)

2.1: Introduction

All living organisms are composed of one or more cells; thus, cells tend to be described as the building block of life. Cells can be specialized to have a wide variety of functions, and these differences can be explained through the study of genomics, proteomics, transcriptomics, metabolomics, and lipidomics. Cellular lipidomics are involved in numerous industries such as production of biofuels, nutritional lipidomics, cosmetics, and biomarker discovery[1]. Although more emphasis has been placed in recent years, studying the cellular lipidome can be quite a daunting task due to the sheer number of lipids found in cells, all with varying degrees of abundance, structure, and function. Yeast are unicellular, eukaryotic organisms which have advanced the field of lipid research and studying them has led to novel information regarding cancer and neurodegenerative diseases[2][3]. Albeit being simple organisms, there is a significant overlap between biological pathways and genes of human cells, which include signal transduction, protein folding, metabolism, and cell apoptosis[4]. With a cell doubling time of 90 minutes, ease of growth, robustness, and affordable nutrients for growth, the yeast strain *Saccharomyces cerevisiae* makes for an ideal candidate for method testing[5]. Furthermore, the entire genome of *Saccharomyces cerevisiae* has been sequenced, making it suitable for genetic engineering, as well as understanding the function of genes and how they affect metabolic pathways.

MS is an ideal approach for the study of lipidomics as it offers high sensitivity, allows for the detection of miniscule perturbations of lipids between cells, and offers the ability to identify multiple analytes simultaneously, which can compensate for the diversity and abundance of cellular lipids. HPLC is often used in conjunction with high resolution MS as it reduces sample complexity and ion

suppression, and improves specificity to aid in lipid identification[6]. With the support of MSMS, lipid identifications can be verified based on either their distinct fragmentation patterns, or similarity to MSMS spectra libraries[7][8]. Untargeted lipidomics analysis is prevalent in method testing, biomarker analysis, and studying molecular mechanisms as it allows for the simultaneous detection of multiple lipid classes. Merging these analytical techniques will provide a comprehensive view on the relative concentrations and identifications of lipids found in cells. Additionally, this approach will help distinguish between isobaric and isomeric lipid species, leading to a more thorough understanding of the roles and mechanisms of lipids involved in biological processes[9].

It is critical to have an efficient extraction protocol as it tends to be the preliminary step in lipid analysis, and thus has a considerable impact on downstream results and the amount of information obtained from the analysis. Additionally, any contaminants that result from an inadequate extraction protocol can result in columns being clogged, ion suppression of analytes, reduced sensitivity, and lower reproducibility of experiments[10]. Due to the chemical diversity of lipids, no signal extraction protocol is able to successfully extract every lipid class, which would be ideal for untargeted analytical approaches. Organic solvents play a fundamental part in the performance of a lipid extraction technique due to the ability to partition lipid classes into the organic solvent. Lipid extraction techniques such as the Folch, and more recently the MTBE method, are particularly popular due to the incorporation of a biphasic solvent system[11][12]. The combination of methanol with a non-polar organic solvent allows for the extraction of a diverse set of lipid classes, after which water is added to solubilize polar contaminants and to induce phase separation.

In this study, multiple extraction techniques for cellular lipid extraction were compared and an optimized protocol was developed. Multiple aspects of lipid extraction were evaluated, such as the time, reproducibility, ease of extraction, and extraction efficiency. The proposed protocol was then tested for its batch to batch repeatability by performing extractions on different days and statistically analyzing the

data. Finally, MSMS was performed on the *Saccharomyces cerevisiae* lipid extracts, which yielded novel lipids after comparing to literature. This work indicates that the proposed protocol can be applied to cell lines for comprehensive profiling of cellular lipidomes, relative to current literature.

2.2: Experimental

2.2.1: Chemicals and Reagents

All chemicals and reagents were obtained from Sigma-Aldrich Canada (Markham, ON, Canada), except those otherwise noted. LC-MS grade water (H_2O), acetonitrile (ACN), methanol (MeOH), and isopropyl alcohol (IPA) were from Honeywell (Calgary, AB, Canada). LC-MS grade dichloromethane (DCM) and MTBE were obtained from Thermo Fisher Scientific (Edmonton, AB, Canada). 0.5 mm diameter glass beads were acquired from Biospec Products.

2.2.2: Media and Culture Conditions for the Growth of *Saccharomyces cerevisiae*

Saccharomyces cerevisiae BY4741 was chosen for the experiment as the entire genome and mutations are known[13]. The growth media selected for the experiment was synthetic complete minimal with 2% w/v glucose supplemented with 0.5% w/v ammonium sulfate[14]. Cells were grown at 30 °C in a 225rpm shaking incubator for 24 hours, after which the growth media was removed and resuspended with fresh growth media. The cells were further incubated for 6 hours before harvesting via centrifugation for 10 minutes at 4640 g and 4 °C. 1 mL of cold LC-MS grade H_2O was added to resuspend the cell pellet, which was removed after micro-centrifuging for 1 minute at 16000 g and 4 °C. The cells were washed with LC-MS grade H_2O two more times to remove any residual growth media

which could interfere with downstream analysis. After the last wash, cells were aliquoted into 2 mL Eppendorf tubes, with each tube containing 4E07 yeast cells. The cells were then quickly frozen in liquid nitrogen and stored in a -80 °C freezer.

2.2.3: Cell lysis

0.150 cc (mL) of glass beads were added to a 2mL Eppendorf tube containing thawed BY4741 yeast cells, 25 µL of LC-MS grade H_2O, 19 µL MeOH, and 6 µL deuterated lipid internal standards[14]. To add a consistent volume of glass beads, a 200 µL pipette tip was labelled with a marker to indicate the appropriate volume of beads to add. The glass beads were poured into the pipette tip to the specified mark (0.150 mL), and were then transferred into the Eppendorf tube containing the sample. Cells were lysed by vortexing using a Vortex-Genie 2 mixer at 3200 rpm (Fisher Scientific) for 1 minute, alternated with 1 minute of incubation in an ice-water bath. The cell lysis step was repeated for a total of 5 intervals.

2.2.4: Sample Preparation

Methyl tert-butyl ether lipid extraction:

The MTBE protocol was adapted for reduced sample volumes from the paper published by Matyash et al[12]. Although the volumes of reagents were modified, our protocol utilized the appropriate ratio of solvents. 400 µL of MTBE and 95 µL of MeOH was added to each sample before vortexing at 3200 rpm for 1 minute. The sample was then incubated at room temperature for either 10 minutes or 60 minutes using a Vortex-Genie 2 mixer (Setting 7). After incubation, 75 µL of H_2O was added to obtain a solvent ratio of 10/3/2.5 ratio of MTBE/MeOH/H_2O, and samples were vortexed for 10

seconds. Samples were then centrifuged for 10 minutes at 12000 rpm and 4 °C to separate the aqueous and organic layers. 300 µL of the top organic layer, comprising of MeOH and MTBE, was extracted into a new 2 mL Eppendorf tube and placed inside a 4 °C fridge. A second lipid extraction was performed for improved extraction efficiency by adding 200 µL of MTBE, 60 µL of MeOH, and 50 µL H_2O to the original sample to maintain the original solvent ratio. The samples were vortexed for 10 seconds, incubated for 10 minutes, and then centrifuged for 10 minutes at 12000 rpm and 4 °C. 230 µL of the top organic layer was extracted and merged with the previous extract. The extracted supernatant was dried down at room temperature using a Savant SC110A Speed Vac for 90 minutes. Once removed from the Speed Vac, samples were purged with nitrogen gas, flash-frozen using liquid nitrogen, and stored in a -80 °C freezer for long term storage.

Folch lipid extraction:

The Folch protocol was adapted for reduced sample volumes, and had substituted DCM in lieu of chloroform[11]. Although the volumes of reagents were modified, our protocol utilized the appropriate ratio of solvents. 275 µL of MeOH was added to each sample before vortexing for 20 seconds using a Vortex-Genie 2 at 3200 rpm. A total of 600 µL of DCM was added before vortexing each sample for 20 seconds, after which 200 µL of H_2O was added to reach a solvent ratio of 8/4/3 of DCM/MeOH/H_2O. After vortexing for 10 seconds, samples were incubated for 10 minutes at room temperature to equilibrate the lipids. Samples were then centrifuged for 10 minutes at 12000 rpm and 4 °C, after which 350 µL of the lower organic phase (DCM) was extracted into a fresh 2 mL Eppendorf tube. The Eppendorf tube containing the extracted DCM was placed inside a 4 °C fridge. 350 µL of fresh DCM was added to the original Eppendorf tube containing the sample and the tube was vortexed for 20 seconds. Samples were further incubated for 10 minutes at room temperature and subjected to

centrifugation for an additional 10 minutes at 12000 rpm and 4 °C. 350 µL of DCM was extracted and was combined with the previous lipid extract. The extracted supernatant was dried down at room temperature using a Savant SC110A Speed Vac for 50 minutes. Once removed from the Speed Vac, samples were purged with nitrogen gas, flash-frozen using liquid nitrogen, and stored in a -80 °C freezer for long term storage.

Sample Resuspension:

Before running the samples on the LCMS, they were taken out of the - 80 °C freezer, thawed, and resuspended. Samples were first re-dissolved in 1.5 µL of mobile phase A (MPA) and 1.5 µL mobile phase B (MPB), then vortexed for 30 seconds using the Vortex-Genie 2. Afterwards, 27 µL of MPA was further added, and the samples were vortexed for an additional 30 seconds. The total reconstitution of the sample comprised of 95% MPA and 5% MPB for a 0x dilution. Samples could be further diluted through the addition of the same ratio of mobile phases. After resuspension, samples were transferred into glass inserts. MPA was comprised of 50% MeOH, 40% ACN, 10% H_2O (v/v/v), with 10mM ammonium formate. MPB was comprised of 95% IPA, 5% H_2O (v/v), with 10mM ammonium formate.

Blank and Quality Control preparation:

Extraction blanks underwent the same cell lysis and lipid extraction protocol as samples, but contained no yeast cells, and the internal standard was substituted with the same volume of methanol. Quality control samples were made by pooling multiple samples extracted from the same lipid extraction protocol together.

2.2.5: LCMS Conditions

Maxis II QToF:

3 replicates and 1 blank, along with 3 Quality Controls (QCs), were extracted for each of the following lipid extraction protocols: Folch; MTBE with 10-minute incubation; and MTBE with a 60-minute incubation. Samples were separated through the use of a Dionex UltiMate 3000 (Dionex, Sunnyvale, CA, USA) ultra-high performance liquid chromatography employing an Agilent reversed-phase Eclipse Plus C18 column (10 cm × 2.1 mm, 1.8 µm particle size) in ESI positive and negative mode. A flow rate of 250 µL/min was used during sample analysis with a column temperature of 40°C for all runs. A sample dilution of 0x and 10x was used for ESI negative and positive mode respectively. Injection volumes of 9 µL and 6 µL were used for ESI negative and positive mode respectively. The chromatographic gradient for analyte separation was as followed: t = 0 min, 5% MPB; t = 1.8 min, 5% MPB; t = 8.5 min, 30% MPB; t = 18 min, 95% MPB; t = 25 min, 95% MPB; with a 10-minute re-equilibration gradient afterwards. The UHPLC was coupled to a Maxis II QToF mass spectrometer with an ESI source. Spectra of analytes with a mass between 150 to 1500 m/z range was acquired at a rate of 1 Hz. The capillary voltage of the ionization source was set to 4500 V, along with an end plate offset of 500 V. The nebulizer gas pressure was set to 1.4 bar, and the flowrate of the dry gas was set to 4.0 L/min, at a temperature of 230°C. Each sample had a 1-minute segment at the end of each run in which 10mM of sodium formate mass calibrant solution was injected into the ion source.

Impact QToF:

3 replicate and 1 blank sample were extracted using the Folch method on 3 different days, along with 3 QCs, to test the day to day extraction reproducibility of the Folch method. Samples were

separated through the use of a Dionex UltiMate 3000 UHPLC employing an Agilent reversed-phase Eclipse Plus C18 column (10 cm × 2.1 mm, 1.8 µm particle size) in ESI positive and negative mode. A flow rate of 250 µL/min was used during the analysis with a column temperature of 40°C. A sample dilution of 0x was used for both ESI negative and positive mode. Injection volumes of 12 µL and 8 µL were used for ESI negative and positive mode respectively. The chromatographic gradient for analyte separation was as followed: t = 0 min, 5% MPB; t = 1.8 min, 5% MPB; t = 8.5 min, 30% MPB; t = 18 min, 95% MPB; t = 25 min, 95% MPB; with a 10-minute re-equilibration gradient afterwards. The UHPLC was coupled to an Impact QToF mass spectrometer with an ESI source. Spectra of analytes with a mass between 150 to 1500 m/z range was acquired at a rate of 1 Hz. The capillary voltage of the ionization source was set to 4500 V, along with an end plate offset of 500 V. The nebulizer gas pressure was set to 1.4 bar, and the flowrate of the dry gas was set to 4.0 L/min, at a temperature of 230°C. Each sample had a 1-minute segment at the beginning of each run in which 10mM of sodium formate mass calibrant solution was injected into the ion source.

Impact II QToF:

3 samples were extracted using the Folch protocol and pooled to produce QCs. The QCs were run on the Impact II QToF to generate a list of lipids present in yeast cells. Scheduled precursor lists were composed of lipids found in 100% of the QCs, and MSMS analysis was performed using collision energies compiled from literature (Appendix Table 1). MSMS was performed using QC samples under ESI positive and negative mode. Samples were separated through the use of a Dionex UltiMate 3000 UHPLC employing a Waters Acquity BEH C18 column (10 cm × 2.1 mm, 1.74 µm particle size) in ESI positive and negative mode. A flow rate of 250 µL/min was used during the analysis with a column temperature of 40°C. A sample dilution of 2x and 5x was used for ESI negative and positive mode respectively, while

injection volumes of 9 µL and 6 µL were used for ESI negative and positive mode respectively. The chromatographic gradient for analyte separation was as followed: t = 0 min, 2% MPB; t = 3 min, 5% MPB; t = 8 min, 40% MPB; t = 22 min, 95% MPB; t = 25 min, 95% MPB; with a 10-minute re-equilibration gradient afterwards. The UHPLC was coupled to an Impact II QToF mass spectrometer with an ESI source. MS spectra of analytes with a mass between 150 to 1500 m/z range was acquired at a rate of 1.44 Hz. MSMS spectra was acquired using a quadrupole isolation width of 2 Daltons, MS acquisition time of 0.4 seconds, and an MSMS acquisition time of 1 second. Precursor ions were chosen for fragmentation if they fell within a m/z tolerance of 0.05 Daltons and a 30 second RT tolerance from the proposed mass in the SPL. The capillary voltage of the ionization source was set to 4500 V, along with an end plate offset of 500 V. The nebulizer gas pressure was set to 1 bar, and the flowrate of the dry gas was set to 4.0 L/min, at a temperature of 230°C. Each sample had a 1-minute segment at the beginning of each run, in which sodium formate mass calibrant solution was injected into the ion source.

2.2.6: Data Processing and Analysis

After samples were run on the UHPLC-ESI-QToF-MS, the data was processed through Bruker Metaboscape 4.0. The software served to extract peaks from the chromatograms and process them through alignment, re-calibration, filtering, and adduct identification. The software outputted information compiled from multiple samples regarding m/z, retention time, adduct formation, and relative peak intensity for each unique analyte. The parameters for analyte detection were set to 5.0 mDa for the precursor m/z tolerance and 15 seconds for the retention time tolerance. Analytes were then identified putatively through the use of the LipidMaps database with a m/z tolerance of 5.0 mDa. Analytes were filtered and ranked based on the expected retention time, number of carbons in the fatty acyl chains, adduct formation, number of double bonds, and the number of functional groups found in

the lipid. Analytes were then normalized using in-house designed excel formulas. Normalization was performed by first matching the lipid class of the analyte to one of the 14 lipid classes belonging to the deuterated internal standards. Finally, the ratios of the intensities for the analyte and its class matched internal standard were taken. Multivariate statistical analysis plots such as principal component analysis (PCA) were generated through the use of MetaboAnalyst using features that contained relative standard deviation (RSD) values <30% for QCs. MSMS data was processed using Metaboscape 4.0 and the MSMS spectra of fragment ions were matched to spectra libraries (MSDIAL; RIKEN Oxidized Phospholipids; LC-MSMS Positive; and LC-MSMS Negative) through Metabscape 4.0 with a precursor mass tolerance of 10.0 mDa, mSigma tolerance of 100, and MSMS score threshold of 100. Spectra matching was based off adduct formation, intensity of fragment ions, and m/z tolerance. Spectra of fragment ions were also run through LipidMatch software, which is an in-silico fragmentation library, for lipid identification. The mass accuracy window for matching the experimental and in-silico precursor m/z was set to 20 mDa.

2.3: Results and Discussion

The Folch, MTBE, and modified MTBE lipid extraction protocols were investigated for their effectiveness in extracting lipids from cells through the use of UHPLC-ESI-MS. Parameters that were tested were: the total time for lipid extraction, the cost per analysis, extraction efficiency of the method, ease of extraction, and reproducibility of the method. Before any lipid extraction took place, it was critical to place emphasis on proper sample handling in order to reduce any sample variation, which could influence downstream results, rather than the factors being examined. Yeast cells were an appropriate organism for testing the efficiency of lipid extraction protocols on cells as the yeast lipidome has been thoroughly researched and defined[15]-[17]. The small size of yeast cells also allows the cells to be more dispersed in aqueous solution, which prevents cell aggregation, and reduces the variance

between samples after aliquoting. Additionally, through performing the lipid extractions in triplicates, variation in sample handling was further reduced and helped to validate experimental results[18]. Instrumental drift was also reduced through randomizing the order of sample injections which would assist in appraising protocol reproducibility.

2.3.1: Time Assessment

Time was a necessary parameter in determining the optimal lipid extraction method as biological samples can degrade overtime, which will lead to changes in the metabolome and lipidome. Thus, to accurately portray the true chemical nature of cells, it is essential to have a quick lipid extraction protocol. One major issue in lipidomics is the peroxidation of lipids, which involves oxidative degeneration of lipids. Polyunsaturated lipids contain double bonds which possess highly reactive hydrogen molecules which will form radicals after reacting with reactive oxygen species[19][20]. The unstable acyl radical will then react with oxygen molecules to form a lipid peroxide along with a radical species, which will continue to react with free fatty acids. This will continue until the free radical reacts with another radical species, which results in a wide variety of oxidized lipids[19][20]. Lipids can also oxidize in the presence of light, which is termed photo-oxidation[20]. Overall, it is important to minimize exposure of lipid samples to air and light, to reduce lipid peroxidation and preserve sample integrity. The MTBE protocol described by Matyash et al had a 60-minute incubation step which potentially could introduce lipid peroxidation; thus, the incubation step of the MTBE protocol was modified to 10 minutes and was tested against the original protocol[12]. In terms of time it took to complete extraction, the 10-minute MTBE and Folch were similar, whereas the original MTBE protocol was 50 minutes longer due to the prolonged incubation step. Since the Folch and MTBE methods utilized different extraction solvents, the time for the solvent to evaporate using the SpeedVac was evaluated. Since the Folch method

employed the use of the highly volatile DCM, the time to evaporate 700 µL solvent was 50 minutes. Extraction protocols employing the use of MTBE had an inconsistent evaporation time for 530 µL of solvent, from anywhere between 75 to 90 minutes. Since MeOH and MTBE have a much lower volatility compared to DCM (Boiling point of MeOH: 64.6°C; Boiling point of MTBE: 55.2°C; Boiling point of DCM: 39.6°C)[21], it would take longer to evaporate the MTBE/MeOH solvent mixture which would increase the overall time for solvent evaporation. Since cell lysis was consistent for all lipid extraction protocols, the extraction protocols were evaluated based on the amount of time it took to extract the lipids from the cells, and the time it took for the solvent to dry. The Folch protocol was the most suitable method for rapid extraction of lipids from cells, due to the short and consistent solvent drying time. The second fastest protocol was the MTBE method with the 10-minute incubation period, while the original MTBE protocol took the longest due to having a 60-minute incubation period[12].

2.3.2: Safety and Cost Assessment

Chloroform was used in the original Folch method, but was substituted for dichloromethane in the current experiment. DCM offers the benefit of being a safer alternative, as chloroform is considered of being a probable human carcinogen[22]. Although DCM is still considered toxic to humans, it has a higher occupational exposure limit than its counterpart (50 ppm for DCM; and 10 ppm for chloroform in Alberta)[23][24]. In addition, DCM is also less hazardous to the environment and is cheaper than chloroform[22].

A brief cost analysis was performed for the MTBE and Folch method in which the cost per sample extraction was evaluated. The only difference between the two extraction methods was the types and volumes of solvent used. The Folch method utilized 950 µL of DCM, 300 µL of MeOH, and 225 µL of H_2O for a total cost of CAD $0.086/extraction, whereas the MTBE method utilized 600 µL of DCM,

180 µL of MeOH, and 150 µL H_2O for a total cost of CAD $0.092/ extraction. Both methods were similar in cost and neither method had an advantage over the other. In an experiment containing 1000 samples, the Folch method would only be $6 cheaper.

2.3.3: Extraction Efficiency Assessment

Features and internal standards were extracted from LCMS spectra through Metaboscape 4.0 software and included information on the intensity of the ions and their corresponding retention times. All features were putatively matched to the LipidMaps library according to their m/z. The extraction efficiency of each lipid extraction method was determined through summing the relative intensities of internal standards found in each sample, as well as the intensities of all putatively identified features in both ionization modes. Intensities of each individual internal standard was also compared between extraction methods. Since the same cell lysis protocol, sample volume, dilution factor, and LCMS conditions were used for all samples, ion intensities of internal standards and putative features could be used to compare between extraction protocols, as the peak intensities would be dependent on the quantity of lipids extracted through each protocol. However, the relative intensities for the features could not be applied for estimating the absolute quantification of lipids due to the variances in ionization efficiencies between lipid groups. Certain lipid classes are able to ionize more efficiently based on their head group, which results in a greater peak intensity and causes signal suppression in lipid classes that are difficult to ionize[25].

When looking at the total intensities of the internal standards extracted in ESI positive and negative mode (Figure 2.3.1), the Folch extraction had the lowest average intensity of 2.54E07 (RSD of 3.95%), the MTBE extraction with the 60 minute incubation had an average intensity of 2.55E07 (RSD of 17.00%), while the MTBE extraction with the 10 minute incubation had the highest average intensity of

3.06E07 (RSD 3.30%). All of the deuterated lipid internal standards with the exception of MG and PS, were detected in ESI positive and negative mode in all samples. When comparing the two MTBE extraction methods, utilizing a 10-minute incubation was optimal in extracting internal standards, also signifying that the extra incubation period was detrimental to the extraction of internal standards. When comparing the 10-minute MTBE method to the Folch method, it was clear that using MTBE as a solvent was more efficient in extracting the internal standards, due to the incorporation of both methanol and MTBE in the organic phase. The polar methanol was able to solubilize polar lipids more readily, whereas the organic phase in the Folch method comprised only of non-polar DCM. Comparing the average intensities of individual internal standards (Figure 2.3.2), it was clear that the 10 min MTBE method was able to extract every class of internal standard more efficiently than the Folch and the 60 min MTBE. In the comparison between the Folch and the 60 min MTBE, there was a small variance in the extractability of the PE, lyso-phosphatidylethanolamine (LPE), and cholesterol internal standards. The Folch method was more suitable in extracting the lyso-phosphatidylcholine (LPC), TG, and cholesterol ester (CholE) internal standards over the 60 min MTBE method. However, the Folch method showed lower extractability for the phosphatidylglycerol (PG), phosphatidylinositol (PI), sphingomyelin (SM), Diacylglycerol (DG), and phosphatidic acid (PA) internal standards compared to the 60 min MTBE. Between the 60 min MTBE and Folch, the Folch was more suitable for the extraction of hydrophobic internal standards (TG and CholE) potentially as a result of its more hydrophobic organic phase, whereas the 60 min MTBE was able to efficiently extract more polar lipid classes (SM, PI, PG, PA) potentially due to its more polar organic phase.

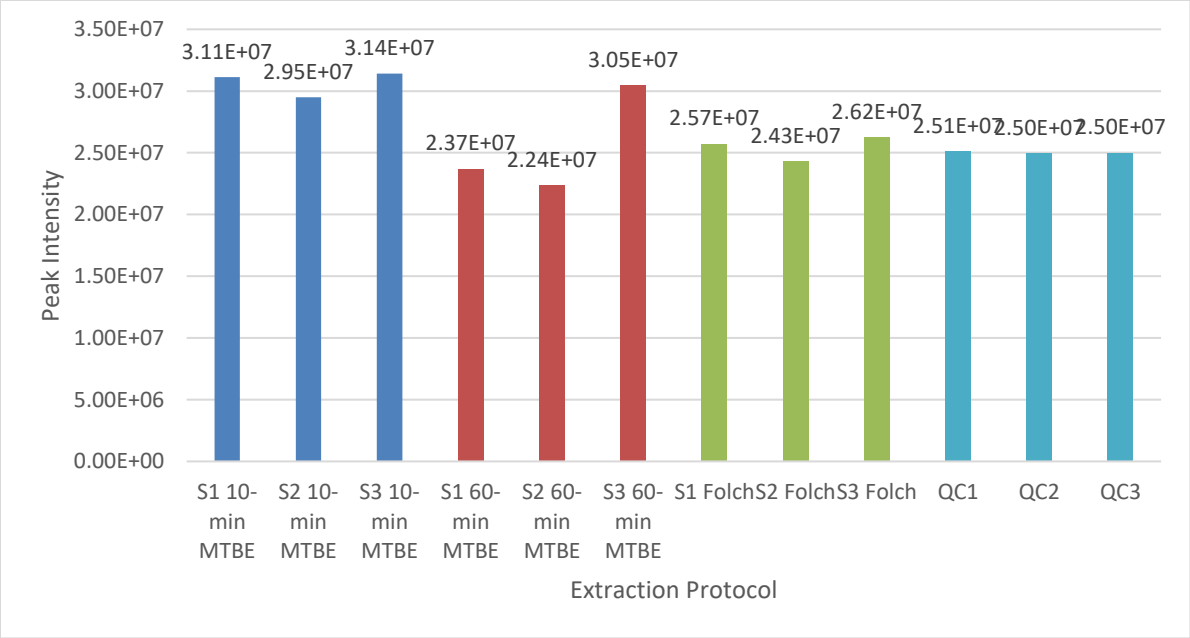

Figure 2.3.1: Summed signal intensities for internal standards detected for each sample in ESI positive and negative mode.

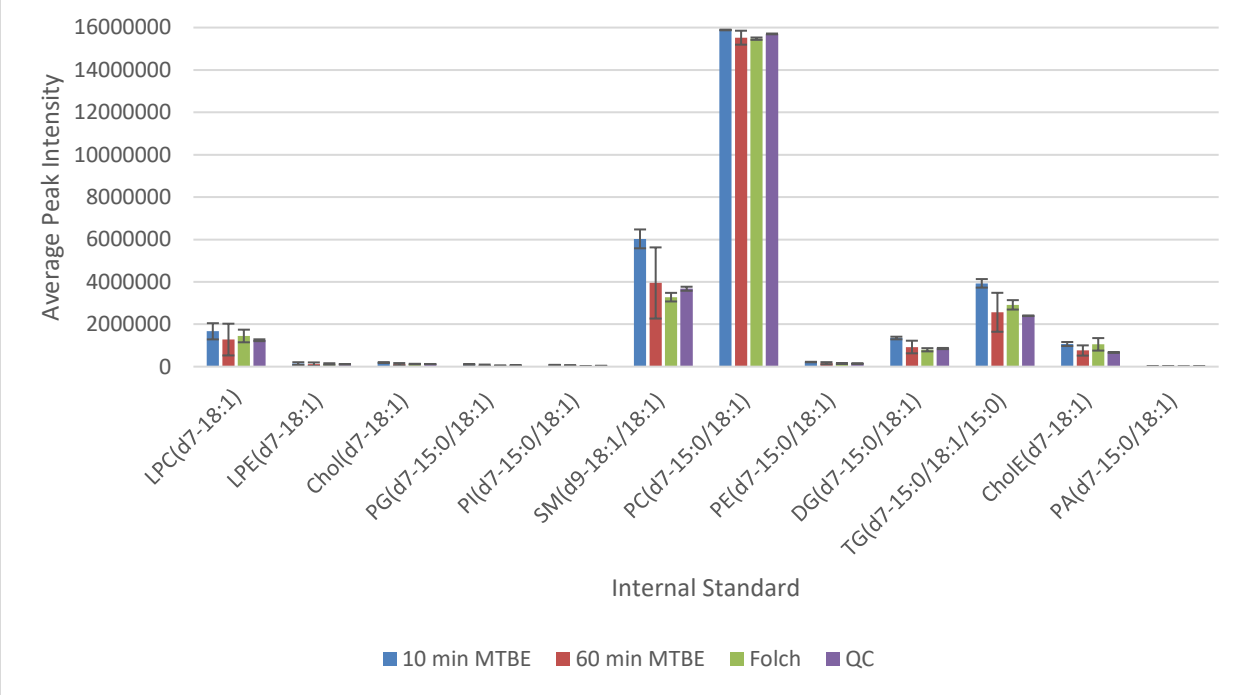

Figure 2.3.2: Comparison of average signal intensities for internal standards detected from each extraction method. Error bars represent the standard deviation of the average.

Next, the number and total intensities of putatively identified lipids were compared to further evaluate the extraction efficiency between extraction protocols. The average intensities for the extraction protocols in ESI positive mode (Figure 2.3.3) followed a similar trend to the average intensities for the internal standards. The 10-minute MTBE protocol had the highest average intensity of 3.48E08 (RSD of 4.21%), followed by the 60-minute MTBE protocol with an average intensity of 3.32E08 (RSD of 5.94%), and lastly the Folch protocol with the lowest average intensity of 3.14E08 (RSD of 5.27%). For ESI negative mode (Figure 2.3.4), the 60 minute MTBE extraction protocol had the highest average intensity of 2.12E07 (RSD of 9.09%), while the 10 minute MTBE extraction protocol had an average intensity of 2.02E07 (RSD of 6.50%), whereas the Folch extraction method had the lowest average intensity at 1.36E07 (RSD of 7.81%).

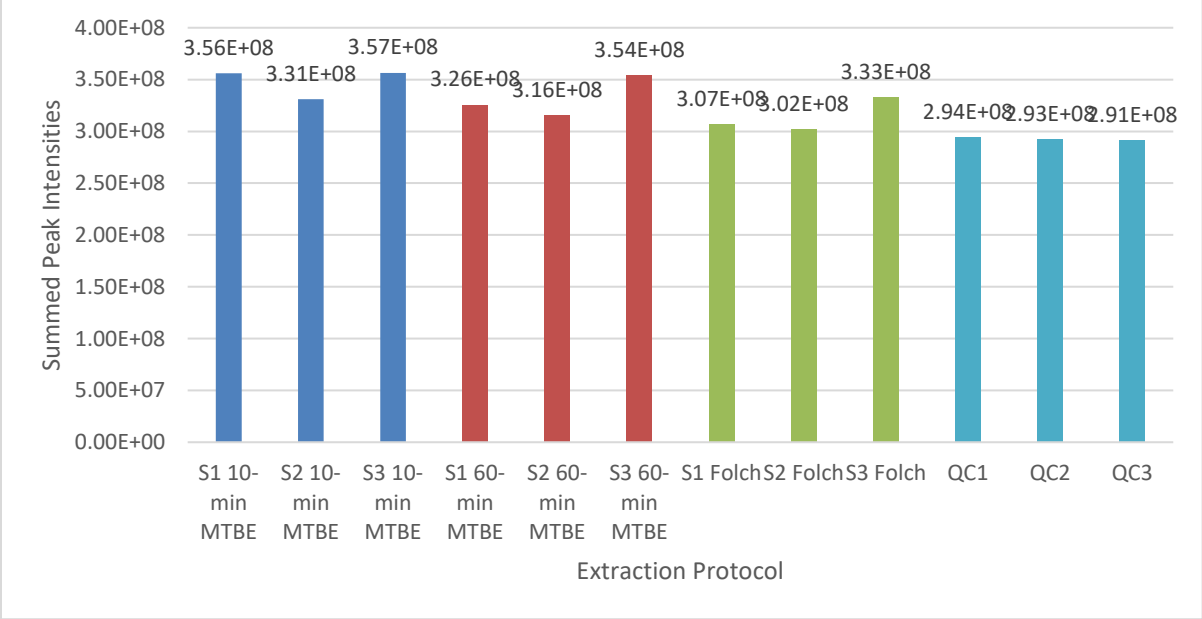

Figure 2.3.3: Summed signal intensities for putatively identified lipids detected for each sample in ESI positive mode in the comparison between different extraction methods.

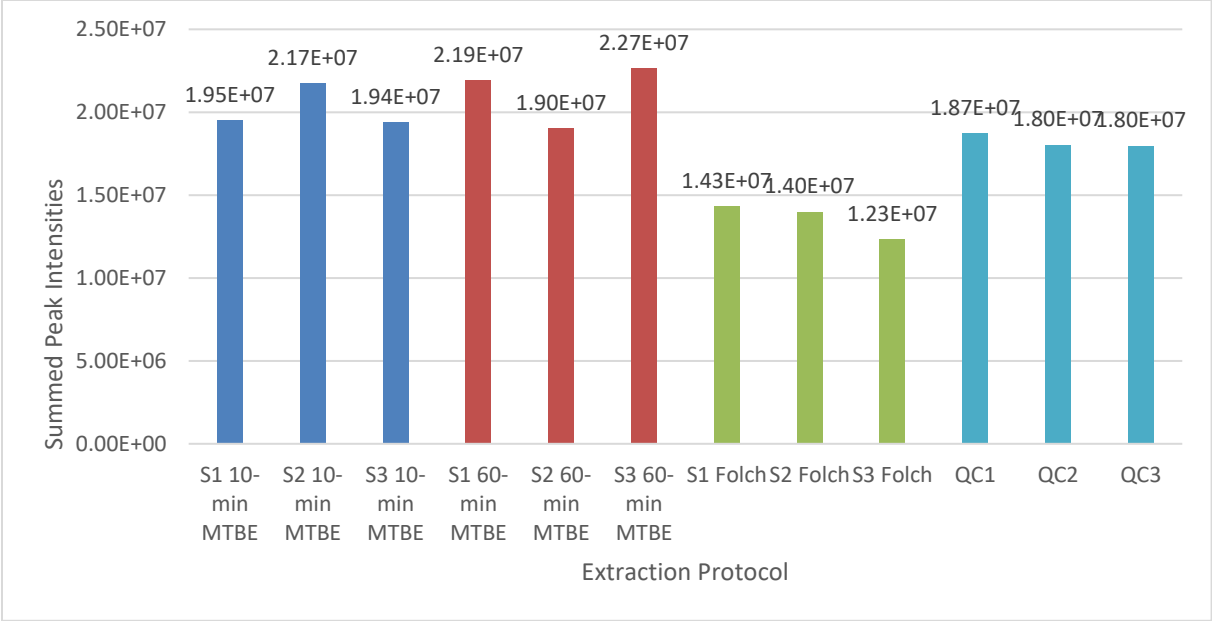

Figure 2.3.4: Summed signal intensities for putatively identified lipids detected for each sample in ESI negative mode in the comparison between different extraction methods.

The number of putatively identified features detected in each extraction protocol was another form of evaluating the extraction efficiency, which would give an indication on how the organic solvents affect the lipid classes extracted. Figures 2.3.5 and 2.3.6 displayed the number of missing features belonging to each lipid subclass in ESI positive and negative mode respectively. A total of 1826 features were putatively identified in all samples through the use of LipidMaps in ESI positive mode, while 441 Lipids were identified in ESI negative mode. The Folch protocol had the greatest number of missing features, with 58 missing features in ESI positive mode and 20 features in ESI negative mode. The 60-minute MTBE protocol had 9 missing features in ESI positive and 2 missing features in ESI negative mode. Finally, the 10-minute MTBE protocol had 8 and 0 missing features in ESI positive and negative mode respectively. Both MTBE extraction protocols had similar amounts of missing features, indicating that the major contributor to the lipid subclasses extracted in a protocol was reliant more so on the solvent used, regardless of the incubation time of the method. The Folch protocol had the least range of lipid coverage as it was unable to extract as many lipid subclasses than either of the MTBE methods. All

the missing features that were unable to be detected in the Folch method for ESI negative mode (Figure 2.1.5), with the exception of DG, eluted earlier than 3 minutes in the chromatographic run. This indicated that most of the missing features were polar in nature, and that the Folch method had a difficult time extracting polar lipids compared to the MTBE protocols.

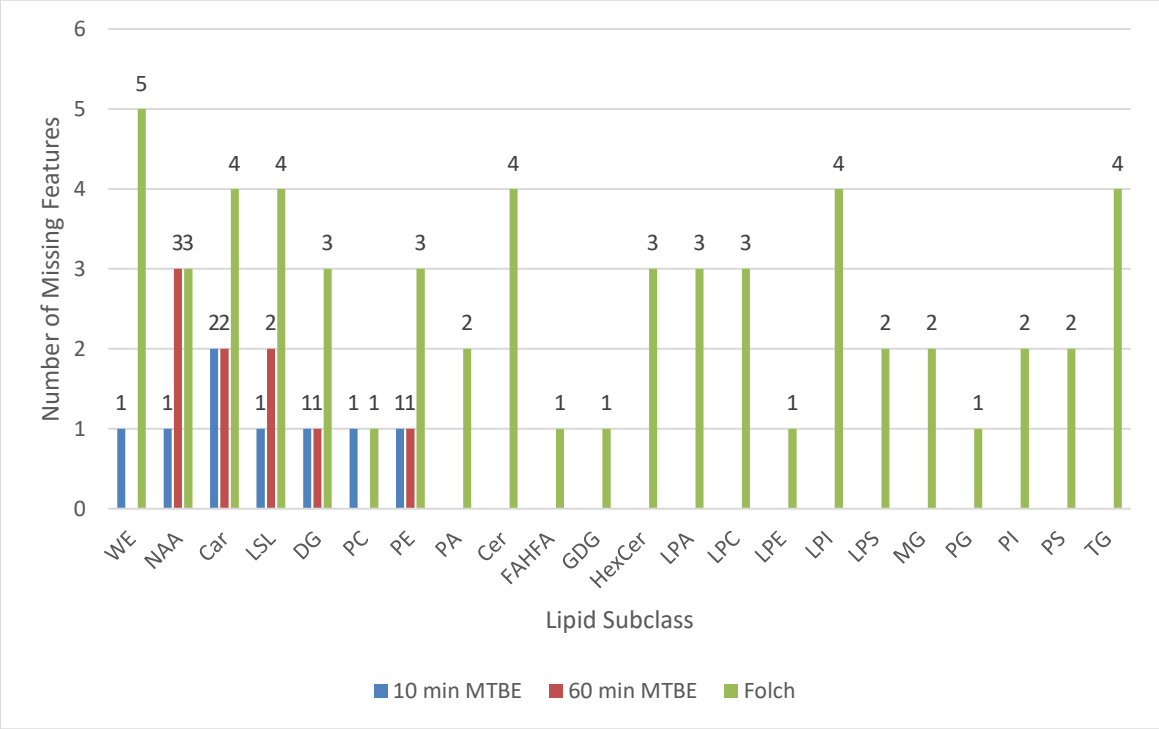

Figure 2.3.5: Number of missing features for each extraction method in ESI positive mode from a total of 1826 putatively identified features from all extraction methods.

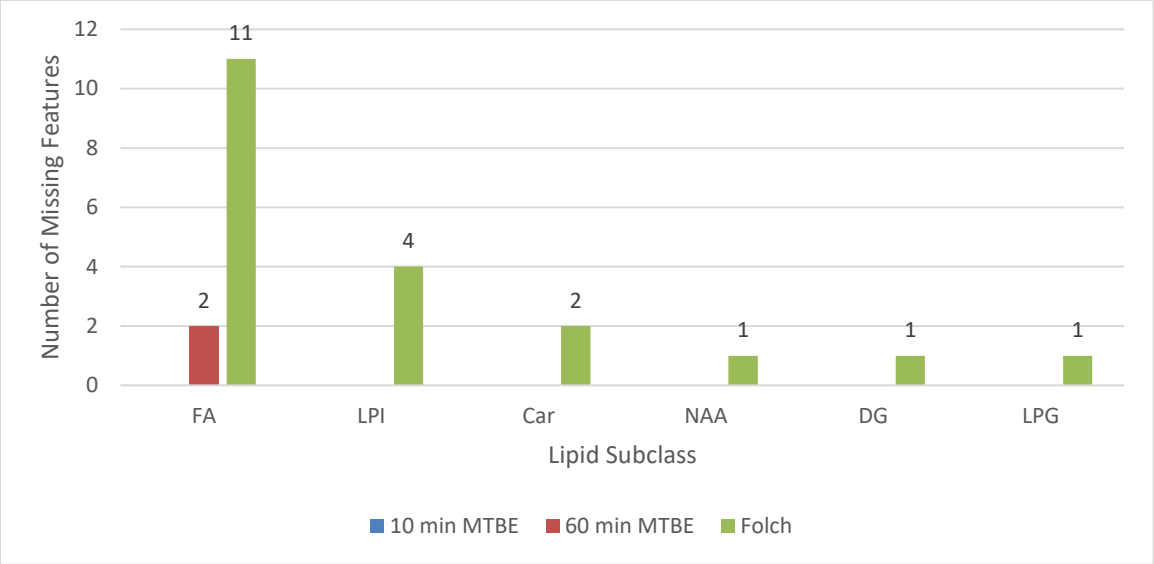

Figure 2.3.6: Number of missing features for each extraction method in ESI positive mode from a total of 441 putatively identified features from all extraction methods.

The missing features for each extraction method corroborated with the intensities for putatively identified lipids. The Folch method had the highest number of missing features out of all the extraction methods, which resulted in having the lowest average intensity in ESI positive and negative mode. The increased polarity of the methanol employed in the MTBE protocol allowed for the attraction of polar lipids such as fatty acids and wax esters, into the organic phase. Meanwhile, the MTBE was able to solubilize several hydrophobic lipids, such as TGs, DGs, and cholesterol esters. In the Folch method, the nonpolar DCM limited the extraction of polar lipids into the organic phase, resulting in fewer lipids being extracted. Overall, due to the polar nature of methanol in the organic phase, the MTBE protocol was more efficient in extracting a wide variety of lipids, as well as the amount of lipids which was signified by the higher intensities in Figures 2.3.1, 2.3.3, and 2.3.4. The prolonged incubation time in the 60 min MTBE method did not affect the types of lipid classes extracted, demonstrated by the number of missing features in Figures 2.3.5 and 2.3.6. However, the overall intensity of extracted features was lower in Figures 2.3.1, 2.3.3, and 2.3.4, signifying the loss of lipids due to prolonged incubation.

2.3.4: Ease of Extractability

The ease in which the organic layer was able to be extracted was considered when choosing the most optimal extraction protocol. A simple extraction protocol allows for a novice to follow the protocol with reproducible results. The MTBE protocol provided the benefit of having the organic layer remain at the top of the biphasic solution, making it easily accessible for solvent extraction. MTBE and methanol have a density of 0.74 g/mL and 0.79 g/mL respectively, while H_2O has a density of 1.00 g/mL[21]. DCM however has a density greater than H_2O (1.33g/mL)[21], which results in the organic layer remaining at the bottom. When extracting the organic phase in the Folch method, the pipette tip must travel through the upper aqueous phase and the protein pellet, which can potentially lead to disruption of the protein pellet or withdrawal of some of the aqueous phase. Salts, contaminants, and proteins residing in the aqueous phase can then cause ion suppression, clogging of the column, matrix effects, or a loss in sample reproducibility[26]. Since the protocol utilizes beads for cell lysis, the beads congregate to the bottom of the tube with the organic phase, such that the user will need to pipette between the beads and the aqueous phase in order to extract the organic phase. DCM also has a lower viscosity and is prone to drip out of the pipette tip during sample transfer, potentially leading to sample loss for inexperienced users, and affecting sample reproducibility. This effect can be mitigated by pre-rinsing the pipette tip with fresh DCM prior to sample transfer, making the DCM less prone to drippage, thus leading to accurate volume transfer. The modified Folch extraction protocol was also designed to leave adequate room for the withdrawal of the organic phase, as 350 µL out of the 600 µL of DCM was transferred each time during lipid extraction. The organic phase was extracted twice to increase the total amount of lipids recovered and increasing the extraction efficiency. By having the organic layer on top, the MTBE method does not require the user to bypass the aqueous and protein layers. Additionally, since the aqueous phase and non-extractable residue is located at the bottom of the tube, the beads do not impede sample extraction.

2.3.5: Assessment of Method Reproducibility

Figure 2.3.7 shows a PCA score plot for total putatively identified lipids extracted from various extraction protocols. Features that had an RSD value below 30% in QC samples were kept for the generation of the PCA plot, which included 1805 out of the total 1826 features for ESI positive mode data, and 440 out of the 441 total lipids for ESI negative mode data. Data filtering was performed to remove features that were likely to be classified as non-informative variables. Non informative variables could result from baseline noise and are unlikely of use for data models. It is highly recommended to remove these features from untargeted metabolomics datasets as they can result from instrument noise or contaminants, and impede future downstream data models such as pathway analysis and biomarker discovery[27][28]. The sample data was inputted into Metaboanalyst and was normalized via Autoscaling through the program. The tight clustering of the triplicate QC data points displayed in Figure 2.3.7 signified that the mass spectrometer had good reproducibility. Samples extracted using the Folch method displayed the lowest intragroup variability, indicating that there was little difference in the types of features and feature intensities between the samples. The 60-minute MTBE method displayed the highest variability amongst samples, denoted by the large confidence interval region and distance between samples in Figure 2.3.7, suggesting that the extraction was not as reproducible compared to the other protocols tested. The low reproducibility of the 60-minute MTBE method might be contributed by the increased incubation time, which could have affected the solubility lipids in the organic phase caused by the prolonged shaking. MeOH plays a critical role in lipid extraction as it breaks hydrogen bonds or electrostatic interactions between lipids and lipid-protein complexes, allowing for lipids to be solubilized by the non-polar solvent[26]. The prolonged shaking may have prevented the MeOH from properly disrupting the various interactions involved in the cell lipidome. Samples extracted using the 10-minute MTBE protocol displayed the second lowest intragroup variability, with S210min displaying the highest degree of variance from all samples extracted in the group. Although the MTBE protocols

had a more accessible organic layer, making lipid extraction easier, it exhibited higher sample variance in the PCA plot compared to their Folch counterpart. The low reproducibility may have been attributed by the inconsistent drying time of the organic phase in the SpeedVac during solvent evaporation. The different drying times of MTBE samples were due to inconsistent volumes of methanol or H_2O in the organic phase, potentially caused by poor partitioning of the biphasic solvent layers. MTBE is able to solubilize H_2O at 1.4%, which would be increased in the presence of MeOH[29]. Having different volumes of H_2O in the organic phase would affect the drying rate of solvent evaporation, as well as the solubility of lipids during sample extraction, thus affecting the reproducibility of the results. It is important to note that since the organic phase of the Folch method was composed of only DCM, the drying time was much more consistent.

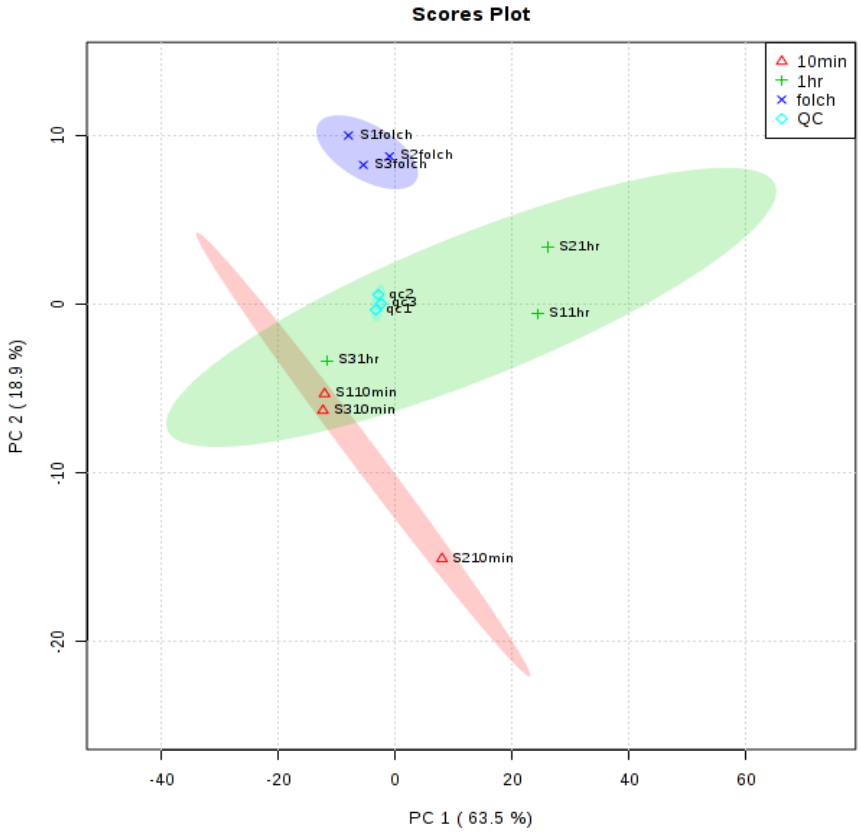

Figure 2.3.7: PCA plots of putatively identified features detected from different lipid extraction protocols and QCs. Features from ESI positive and negative modes were merged before generating the PCA plot.

The Folch method was chosen for future cell lipid extractions. The MTBE method had a better extraction efficiency, demonstrated by the higher intensities and number of detected features, and had a more accessible organic phase for extraction. However, the limitations of the MTBE method outweighed the benefits. The PCA plot (Figure 2.3.7) showed that cells extracted with the MTBE methods had a lower reproducibility than their Folch counterpart. Reproducibility was a key factor when deciding on the optimal protocol as it is critical for lipidomics studies to have high precision. Studies in which samples are compared, such as biomarker analysis or clinical studies, require workflows to be reproducible as a small variance in sample handling can lead to inaccurate downstream analysis and false results[21]. These variances in sample handling will in turn mask actual biological variances between sample groups. The Folch method was also more time efficient as the time for solvent evaporation took 50 minutes compared to a maximum time of 90 minutes for the MTBE protocol. The prolonged solvent evaporation step in the MTBE protocol could allow for the oxidation of lipid species, potentially leading to inaccurate lipidome analysis. Although the Folch method was more challenging to extract, the issue could be resolved through practicing the method. Although neither of the MTBE methods were chosen for future cell studies, it was important to note that the modified 10-minute was preferred over the 60-minute protocol. The 10-minute protocol provided the advantage of being 50 minutes faster and being more reproducible.

2.3.6: Assessment of Method Repeatability

To test the repeatability of the Folch method, three sample extractions and a blank were performed on yeast cells on three separate days. After lipid extraction, samples were purged with nitrogen gas for 30 seconds before storing in a -80 °C freezer in order to reduce lipid oxidation. QCs were prepared by pooling all samples together with the exception of blanks. Once all samples were

extracted, an Impact UHPLC-ESI-QToF instrument was used to analyze the samples in ESI positive and negative mode.

Repeatability was monitored through the RSD values of sample and internal standard intensities. Good repeatability would result in similar intensities between batches indicating low variability in the amount of lipids extracted. RSD is an excellent measure of how close samples are to one another and how precise the average is. RSD differs from standard deviation as it relates the standard deviation to the average, allowing for comparisons between variables of different magnitudes and units[30]. Generally, an acceptable RSD value for precision is 15-20% from the average, when evaluating repeatability[31]. The RSD of the summed intensity for all internal standards, as well as putatively identified features for ESI negative and positive mode (Table 2.3.1), were found to be 7.95%, 5.22%, and 9.88% respectively. All the calculated value fell below the 15% threshold, either between samples from the same batch, or between the entire set of samples, providing a good indication that the method displayed a degree of repeatability. The summed intensity for all internal standards (Appendix Figure 1), and putatively identified features for ESI negative (Appendix Figure 2) and positive mode (Appendix Figure 2) allowed for a better visualization of the RSDs. Neither of the figures displayed a high degree of variance; either intergroup or intragroup.

Table 2.3.1: Summary of RSD values calculated from intensities of internal standards and putatively identified features for samples extracted on different days.

	Nov 19, 2019 (N=3)	**Dec 9, 2019 (N=3)**	**Dec 16, 2019 (N=3)**	**All Days (N=9)**
RSDs of summed intensity for features detected in ESI Pos (%)	**5.75**	**9.70**	**7.05**	**7.95**
RSDs of summed intensity for features detected in ESI Neg (%)	**4.82**	**4.15**	**1.66**	**5.22**
RSDs of summed intensity for I.S. detected in ESI Pos and Neg (%)	**5.88**	**12.80**	**7.79**	**9.88**

A PCA plot (Figure 2.3.8) was also generated to validate the reproducibility between all sample sets after filtering features with an RSD value above 30% in QC samples (36 out of 1080 total features were filtered out). Autoscaling was performed on the data set before generating the PCA plot. No clear separation between sample groups was observed, which was expected as all samples were from the same batch of yeast, and were processed using identical extraction protocols and instruments. However, if separation was observed, it would have indicated that the protocol was not reproducible due to either sample handling or processing, making the protocol unsuitable an experiment conducted on different days. Furthermore, no batch effects were seen due to storage conditions, allowing for samples to be purged with nitrogen gas and flash frozen directly after extraction for future experiments. These steps would grant the ability to store samples prior to analysis via MS, thus minimizing variation caused by instrumental drift.

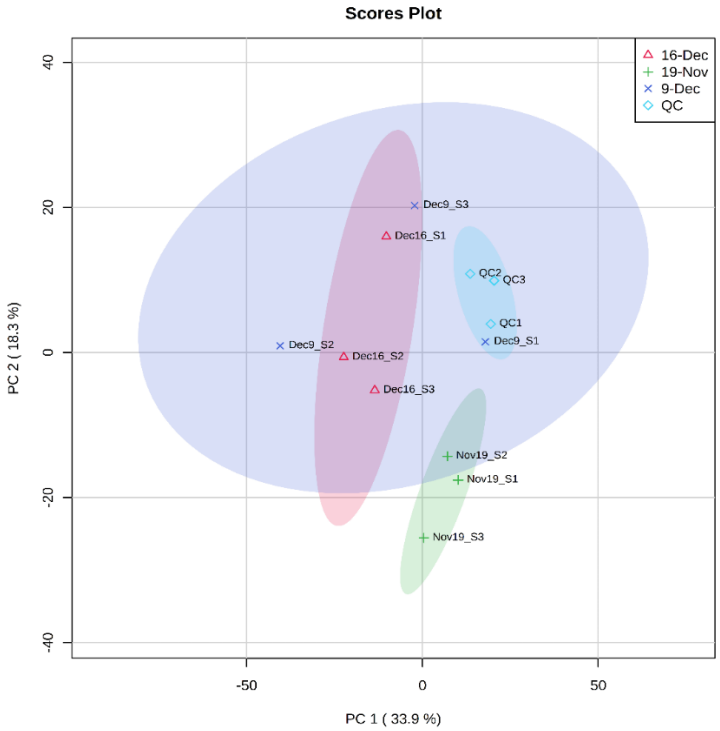

Figure 2.3.8: PCA plots of putatively identified features detected from samples and QCs extracted using the Folch method on different days. Features from ESI positive and negative modes were merged before generating the PCA plot.

2.3.7: MSMS Analysis of *Saccharomyces cerevisiae* using a Modified Folch Lipid Extraction Protocol

The objective of this experiment was to use the modified Folch protocol for qualitative analysis of *Saccharomyces cerevisiae* BY4741 cells through performing MSMS. All analyses were performed using an Impact II UHPLC-ESI-QToF. Multiple yeast cell lysates were extracted using the Folch protocol before pooling them to make a QC. The QCs were either diluted two or fivefold for positive and negative mode respectively. MS analysis was performed on a triplicate QCs to obtain a list of features for the generation of a scheduled precursor list (SPL). Only features present in all QC samples were kept in order to filter out instrument noise or contaminants. Through LCMS lipidomics, 2346 and 1075 lipids were putatively identified through LipidMaps under ESI positive and negative mode respectively (Figure 2.3.9). In total, 32 lipid subclasses were identified in ESI positive, while 29 lipid subclasses were identified in ESI negative mode. The putatively identified lipids were used for the development of SPLs. The SPL would be uploaded into a MSMS method in which the mass spectrometer would schedule the fragmentation of precursors specified by the SPL within a defined m/z and retention time range. In time periods in which no precursors were scheduled for fragmentation, the mass spectrometer would choose features with a strong peak intensity for MSMS.

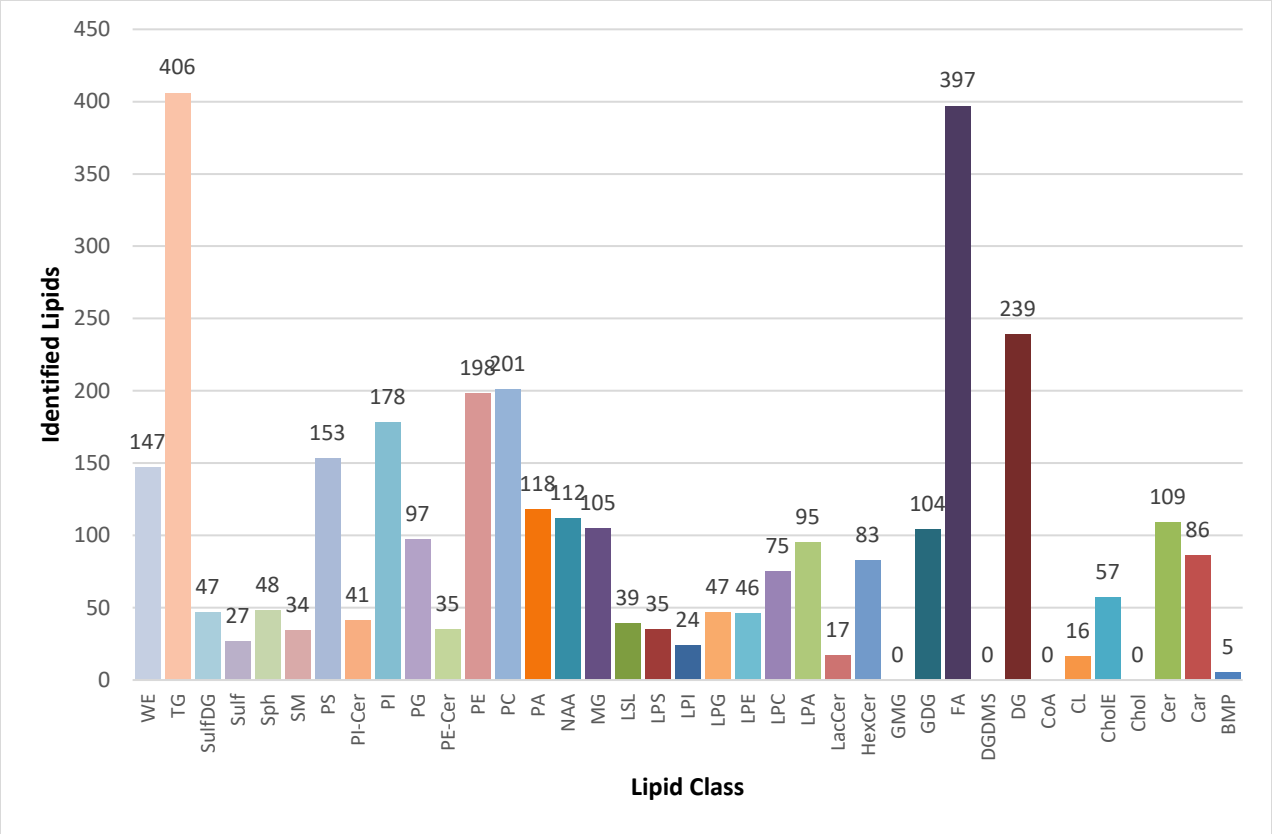

Figure 2.3.9: List of putatively identified features identified through LipidMaps that were incorporated into SPLs for MSMS of yeast cells.

For SPL development, lipid subclasses were merged together to reduce the amount of MSMS runs in the experiment, which would increase throughput, reduce sample consumption, and reduce analysis time. Lipid subclasses which could share isomers and similar retention times with other subclasses were merged together, as lipid identification was performed putatively. For example, PC $[32:0+H]^+$ will share a monoisotopic mass with PE $[35:0+H]^+$ of 733.56216, thus PC and PE groups were merged. A retention time tolerance of 15 seconds and a mass tolerance of 50 mDa were used for SPL construction, which would indicate the precursor mass range and retention time range during MSMS fragmentation. We aimed for 10 features per 30 second window in each SPL to help reduce ion suppression. If there were a large number of features within a 30 second interval, the SPL was split into multiple lists. A total of 21 scheduled precursor lists were constructed for ESI positive MSMS, while 11

SPLs were made for ESI negative MSMS. The collision energies for the MSMS methods were modified according to the lipid classes present in the SPL uploaded. Collison energies for MSMS methods were obtained through previously published research for both ionization modes (Appendix Table 1).

After performing MSMS analysis on the QC samples, the data was processed through Metaboscape 4.0, and spectral IDs were annotated through the software. Metaboscape 4.0 assigned a score to how close the spectra of a precursor matched with experimental spectra from a library. The m/z tolerance for library matching was set such that a mass delta of 5 mDa or lower would be considered a high score, and a mass delta between 5-10 mDa would constitute a low score. Furthermore, if an annotation had an MSMS score between 100-500, the annotation was considered a weak match, whereas a MSMS score between 500-1000 was considered a strong match. After deleting duplicate annotations, there were a total of 212 matches for ESI positive mode and 189 matches for ESI negative mode (Appendix Table 2). The libraries used for spectral matching were the following: MSDIAL; RIKEN Oxidized Phospholipids; LC-MSMS Positive; and LC-MSMS Negative. A total of 23 features had a m/z tolerance between 5-10 mDa, while the rest were successfully annotated with a m/z tolerance below 5 mDa, denoting accurate mass calibration by the software. A total of 135 and 119 features had an MSMS score above 500 in ESI positive and negative mode respectively (Appendix Table 2).

MSMS data was correspondingly uploaded to the LipidMatch software for lipid identification in order to validate annotations from Metaboscape 4.0 and for further lipid elucidation. LipidMatch matched lipids to an in-silico fragmentation library containing fragmentation patterns of over 250,000 unique lipids spanning over 56 lipid species. Annotation matching was accomplished through rule-based identification in which class specific fragmentation patterns of known lipids in the LipidMatch library were searched through sample MSMS spectra and correspondingly matched. Default fragmentation rules for feature annotation were applied. The mass accuracy for matching experimental and in-silico precursor m/z was set to ±10 mDa. Duplicate identifications were removed from the total list of

annotations, and identifications were further filtered through the removal of all annotation classifications with the exception of "1_". Annotations numbered as "1_" were matched based on lipid class (head group) and fatty acyl constituents, making it the most stringent classification[7]. Classifications labelled as "3_" denoted that only a class specific fragment was able to be matched, with no information regarding the fatty acyl group, thus were removed from the identifications to help increase the confidence in the matches[7]. Some matches contained multiple lipid matches, but lipids with the highest probability were kept. A total of 223 lipids were matched for ESI positive mode and an additional 175 lipids for ESI negative mode (Appendix Table 2). The libraries were merged with a retention time and mass windows of 30 seconds and 20 mDa respectively. A total of 118 lipids for ESI positive and 89 lipids for ESI negative were corroborated between the two libraries (Appendix Table 2 bolded), helping increase the confidence in the results and providing novel lipid identifications.

MSMS identifications matched from both libraries were compared to a study titled "LILY-lipidome isotope labeling of yeast: *in vivo* synthesis of ^{13}C labeled reference lipids for quantification by mass spectrometry" by Rampler et al. on the *Pichia pastoris* yeast strain[17]. The comparison was performed to gauge how well our workflow was able to characterize lipid species against other methods. Although the study used a different yeast strain for lipidome analysis, it was published in 2017. MS is a rapidly evolving field with constant advancements, making it critical to compare studies within a similar timeframe. For the sake of comparative analysis, only lipids classes detected in the reference paper were evaluated. Identifications with matches in both ESI positive and negative mode were manually merged. The reference study annotated lipids via LipidXplorer, as well as manual assignment from fragments generated through LC-MSMS[17]. LipidXplorer utilizes rule based annotation for lipid identification, but the user must manually input fragmentation rules, making it inefficient in terms of time compared to LipidMatch[32]. The reference study was able to identify 215 unique lipids, whereas our method was successfully able to identify 273 lipids using Metaboscape 4.0 for lipid

annotation and 314 lipids using LipidMatch for lipid annotation between 14 lipid classes (Figure 2.3.10). Our untargeted approach had detected 46 and 84 TGs for Metaboscape 4.0 and LipidMatch respectively, while Rampler et al. only detected 26 TGs shown in Figure 2.3.10. PCs were also able to be detected by a significant margin in our method, in which 60 and 58 PCs were detected by Metaboscape 4.0 and LipidMatch, while Rampler et al. detected 28. Our approach was able to detect a considerable amount more TGs and PCs, indicating the diversity of TGs and PCs in yeast was greater than what had been suggested by past literature. By using two programs for lipid annotation, they were able to work in conjunction with one another allowing for more lipids to be detected along with validating results. Our method was able to detect more lipids belonging to ceramide (Cer), cardiolipin (CL), lyso-phospholipid (LPL), PE, PI, and phosphatidylserine (PS) lipid classes contrasted to Rampler et al., not to mention lipid classes that weren't detected in Rampler's paper such as FAs, bis(monoacylglycero)phosphates (BMP), monoacylglycerides (MG), and oxidized lipids. Rampler et al. acquired MSMS spectra by applying a relative collision energy of 24 and 21 eV for ESI positive and negative modes respectively[17]. Our method had incorporated unique collision energies for specific lipid classes, allowing for efficient fragmentation of lipid species, thus yielding more MSMS spectra and information regarding the structural identity of lipids. This in turn would assist in increasing the number of annotations after matching against lipid libraries versus relying on a single collision energy to efficiently fragment all lipid classes. The reference study was able to detect more lipids belonging to the inositol phosphoryl ceramide (IPC), mannosylinositol phosphoryl ceramide (MIPC), DG, and PG subclass. No lipids belonging to the MIPC or IPC subclasses were detected in our method due to lack of coverage for these subclasses in the libraries referenced for annotation.

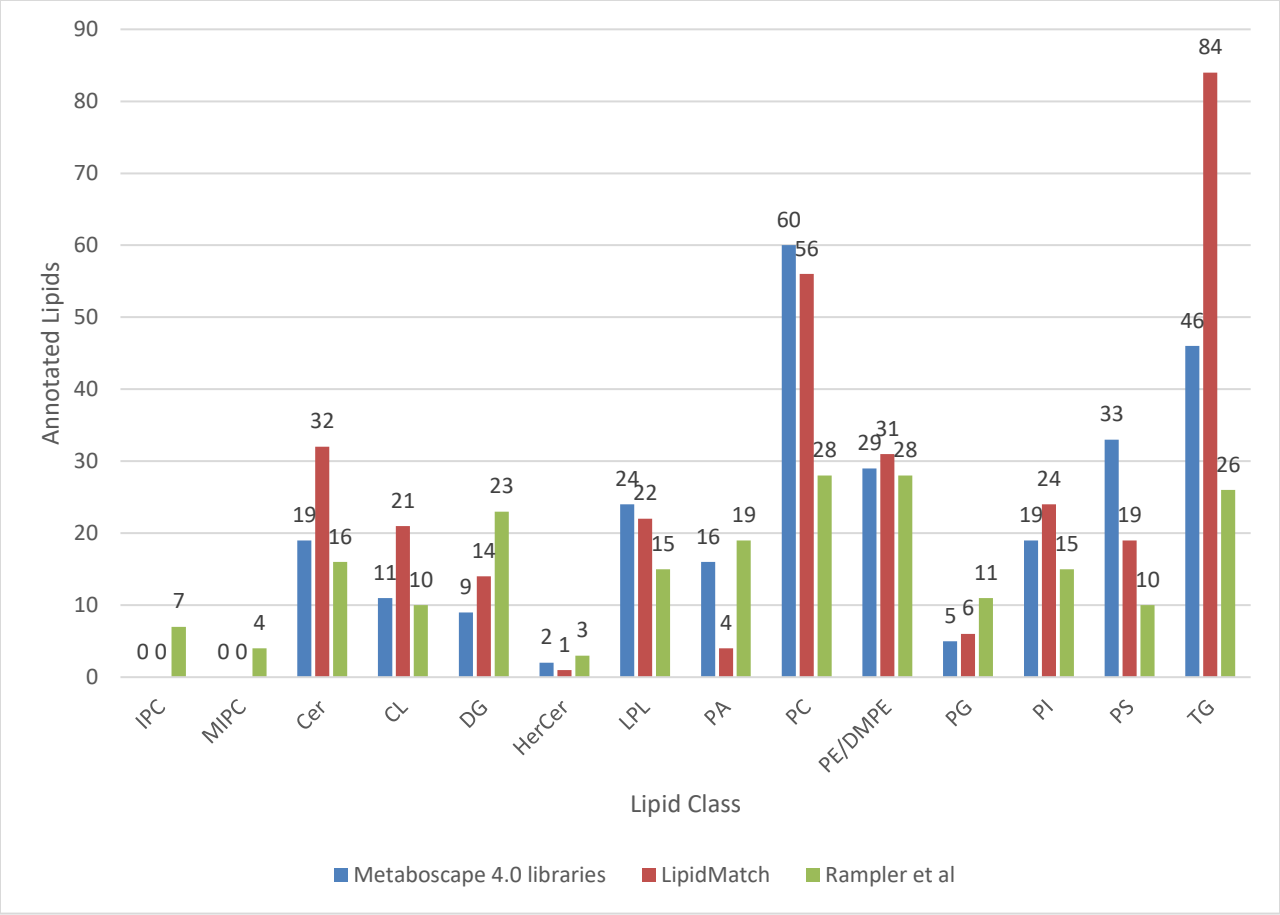

Figure 2.3.10: Bar graph comparing the number of lipids annotated in different lipid classes between Metaboscape 4.0 libraries, LipidMatch library, and literature.

Ergosterol is the most abundant sterol present in yeast cell membranes, and plays a critical role in maintaining membrane permeability and fluidity[33]. Although ergosterol is present in high concentrations in *Saccharomyces cerevisiae* and has been successfully quantified in literature, no annotation was found in our study[34]. Through manual interpretation of MSMS spectra in ESI positive mode by using the precursor m/z of 379.336, we were able to find the fragmentation pattern of ergosterol. To help validate the identity of ergosterol due to lack of reference library matches, we compared the MSMS spectra to literature. In particular, the fragmentation pattern (Figure 2.3.11) of ergosterol obtained through ESI positive MSMS by Münger et al. was successfully matched with the

MSMS spectra (Figure 2.3.12) we acquired[35]. All major fragmentation peaks between a m/z of 145-380 were positively matched between the two spectra. It is important to note that our method utilized a collision energy of 30.8 eV for the fragmentation of ergosterols precursor ion, similar to the 30 eV used by Münger et al., revealing the importance of using unique collision energies for specific lipid classes[35]. An issue we experienced during annotating lipids was the lack of spectra matching to libraries. In total there were 2048 MSMS spectra obtained for ESI positive mode and 959 MSMS spectra obtained for ESI negative mode, yet a small portion of those spectra were successfully annotated using Metaboscape 4.0 and LipidMatch. Through the manual identification of ergosterol, it is safe to assume that many lipid species went unidentified through the limitations provided by lipid libraries. LipidMatch allows the user to create fragmentation patterns for specific lipid classes in order to aid identification. In the current study, only the default fragmentation rules for default lipid classes were used, but in the future this feature can be employed for the identification of uncommon lipid classes such as ergosterol, IPCs, and MIPCs.

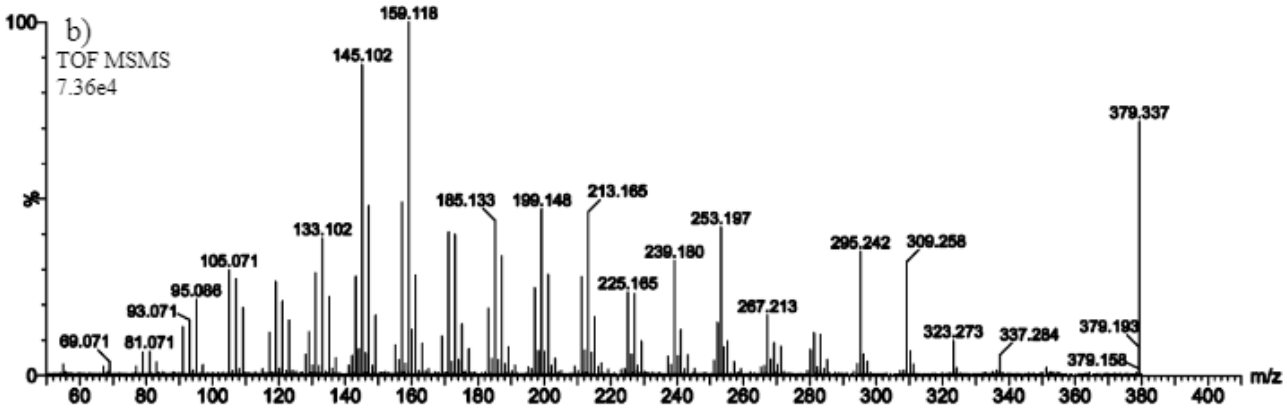

Figure 2.3.11: Spectra obtained by Münger et al. obtained at 30 eV in ESI positive mode for ergosterol with a precursor m/z of 379.337[35].

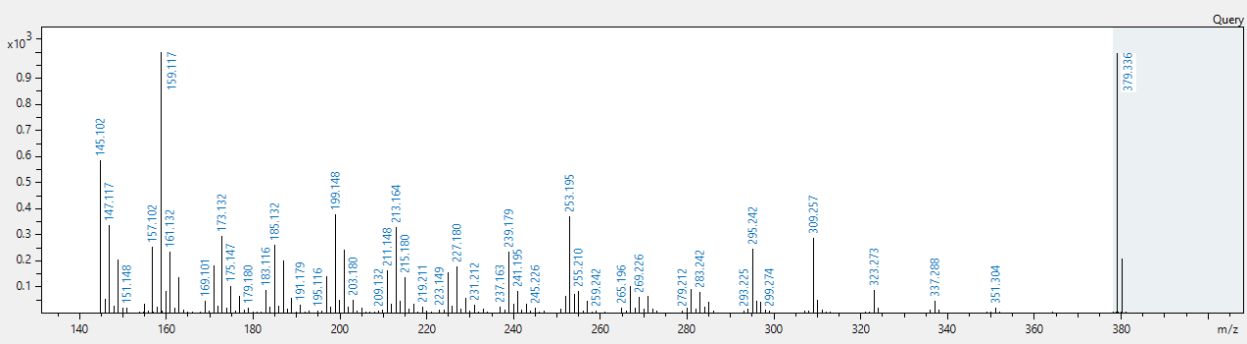

Figure 2.3.12: Experimental ESI-MSMS spectra obtained at 30.8 eV in ESI positive mode for ergosterol with precursor m/z of 379.336.

2.4: Conclusion

In a comparative lipidomics study, we assessed the cost, time, ease of extraction, extraction efficiency, and reproducibility of a few lipid extraction protocols. A modified version of the Folch protocol was chosen for future studies for untargeted lipidome analysis in cells as a result of its high reproducibility and short extraction time. Additionally, the day to day sample repeatability was evaluated through PCA analysis and RSD values. Furthermore, we successfully annotated 401 features using Metaboscape 4.0 and 398 features using LipidMatch, with a total of 207 corroborated lipids between them. Our method was comprehensive in defining the lipidome for *Saccharomyces cerevisiae* as a considerable amount of lipid species were able to be identified compared to literature[17]. We also noted a high number of unannotated spectra that went unmatched due to the lack of coverage provided by lipid libraries, and helped validate the finding through manual interpretation of ergosterol. We note that the number of annotations could potentially be improved through the manual input of fragmentation rules for new lipid classes using LipidMatch. In the future, we will consider employing this protocol for the absolute quantification of lipid species in cell lines. It should also be worth extracting the upper aqueous layer during lipid extraction for the analysis of polar metabolites.

2.5: Literature Cited

[1] Y.J. Zhou, N.A. Buijs, V. Siewers, J. Nielsen, Fatty acid-derived biofuels and chemicals production in Saccharomyces cerevisiae, Front. Bioeng. Biotechnol. (2014). https://doi.org/10.3389/fbioe.2014.00032.

[2] A. Geller, R. Shrestha, J. Yan, Yeast-derived β-glucan in cancer: Novel uses of a traditional therapeutic, Int. J. Mol. Sci. (2019). https://doi.org/10.3390/ijms20153618.

[3] A. V. Oliveira, R. Vilaça, C.N. Santos, V. Costa, R. Menezes, Exploring the power of yeast to model aging and age-related neurodegenerative disorders, Biogerontology. (2017). https://doi.org/10.1007/s10522-016-9666-4.

[4] S. Mohammadi, B. Saberidokht, S. Subramaniam, A. Grama, Scope and limitations of yeast as a model organism for studying human tissue-specific pathways, BMC Syst. Biol. (2015). https://doi.org/10.1186/s12918-015-0253-0.

[5] R. Salari, R. Salari, Investigation of the Best Saccharomyces cerevisiae Growth Condition, Electron. Physician. (2017). https://doi.org/10.19082/3592.

[6] C.Z. Ulmer, R.E. Patterson, J.P. Koelmel, T.J. Garrett, R.A. Yost, A robust lipidomics workflow for mammalian cells, plasma, and tissue using liquid-chromatography high-resolution tandem mass spectrometry, Methods Mol. Biol. (2017). https://doi.org/10.1007/978-1-4939-6996-8_10.

[7] J.P. Koelmel, N.M. Kroeger, C.Z. Ulmer, J.A. Bowden, R.E. Patterson, J.A. Cochran, C.W.W. Beecher, T.J. Garrett, R.A. Yost, LipidMatch: An automated workflow for rule-based lipid identification using untargeted high-resolution tandem mass spectrometry data, BMC Bioinformatics. (2017). https://doi.org/10.1186/s12859-017-1744-3.

[8] T. Kind, K.H. Liu, D.Y. Lee, B. Defelice, J.K. Meissen, O. Fiehn, LipidBlast in silico tandem mass spectrometry database for lipid identification, Nat. Methods. (2013). https://doi.org/10.1038/nmeth.2551.

[9] M.R. Wenk, Lipidomics: New tools and applications, Cell. (2010). https://doi.org/10.1016/j.cell.2010.11.033.

[10] M. Cruz, M. Wang, J. Frisch-Daiello, X. Han, Improved Butanol–Methanol (BUME) Method by Replacing Acetic Acid for Lipid Extraction of Biological Samples, Lipids. (2016). https://doi.org/10.1007/s11745-016-4164-7.

[11] J. FOLCH, M. LEES, G.H. SLOANE STANLEY, A simple method for the isolation and purification of total lipides from animal tissues., J. Biol. Chem. (1957). https://doi.org/10.3989/scimar.2005.69n187.

[12] V. Matyash, G. Liebisch, T. V. Kurzchalia, A. Shevchenko, D. Schwudke, Lipid extraction by methyl-terf-butyl ether for high-throughput lipidomics, in: J. Lipid Res., 2008. https://doi.org/10.1194/jlr.D700041-JLR200.

[13] W. Runguphan, J.D. Keasling, Metabolic engineering of Saccharomyces cerevisiae for production of fatty acid-derived biofuels and chemicals, Metab. Eng. (2014). https://doi.org/10.1016/j.ymben.2013.07.003.

[14] X. Luo, S. Zhao, T. Huan, D. Sun, R.M.N. Friis, M.C. Schultz, L. Li, High-performance chemical isotope labeling liquid chromatography-mass spectrometry for profiling the metabolomic reprogramming elicited by ammonium limitation in yeast, J. Proteome Res. (2016). https://doi.org/10.1021/acs.jproteome.6b00070.

[15] C.S. Ejsing, J.L. Sampaio, V. Surendranath, E. Duchoslav, K. Ekroos, R.W. Klemm, K. Simons, A. Shevchenko, Global analysis of the yeast lipidome by quantitative shotgun mass spectrometry, Proc. Natl. Acad. Sci. U. S. A. (2009). https://doi.org/10.1073/pnas.0811700106.

[16] C. Klose, M.A. Surma, M.J. Gerl, F. Meyenhofer, A. Shevchenko, K. Simons, Flexibility of a eukaryotic lipidome - insights from yeast lipidomics, PLoS One. (2012). https://doi.org/10.1371/journal.pone.0035063.

[17] E. Rampler, C. Coman, G. Hermann, A. Sickmann, R. Ahrends, G. Koellensperger, LILY-lipidome isotope labeling of yeast:: In vivo synthesis of 13C labeled reference lipids for quantification by mass spectrometry, Analyst. (2017). https://doi.org/10.1039/c7an00107j.

[18] D.L. Vaux, F. Fidler, G. Cumming, Replicates and repeats—what is the difference and is it significant?, EMBO Rep. (2012). https://doi.org/10.1038/embor.2012.36.

[19] A. Ayala, M.F. Muñoz, S. Argüelles, Lipid peroxidation: Production, metabolism, and signaling mechanisms of malondialdehyde and 4-hydroxy-2-nonenal, Oxid. Med. Cell. Longev. (2014). https://doi.org/10.1155/2014/360438.

[20] R. Domínguez, M. Pateiro, M. Gagaoua, F.J. Barba, W. Zhang, J.M. Lorenzo, A comprehensive review on lipid oxidation in meat and meat products, Antioxidants. (2019). https://doi.org/10.3390/antiox8100429.

[21] E.. Morgan, Vogel's textbook of practical organic chemistry. 5th edn., Endeavour. (1990). https://doi.org/10.1016/0160-9327(90)90017-l.

[22] U.S. Department of Health and Human Services, Report on Carcinogens, 14th Edition, 2016.

[23] Dichloromethane Profile, (n.d.). https://www.carexcanada.ca/profile/dichloromethane/ (accessed June 19, 2020).

[24] Chloroform Profile, (n.d.). https://www.carexcanada.ca/profile/chloroform/ (accessed June 19, 2020).

[25] A.J. Taylor, A. Dexter, J. Bunch, Exploring Ion Suppression in Mass Spectrometry Imaging of a Heterogeneous Tissue, Anal. Chem. (2018). https://doi.org/10.1021/acs.analchem.7b05005.

[26] C.Z. Ulmer, C.M. Jones, R.A. Yost, T.J. Garrett, J.A. Bowden, Optimization of Folch, Bligh-Dyer, and Matyash sample-to-extraction solvent ratios for human plasma-based lipidomics studies, Anal. Chim. Acta. (2018). https://doi.org/10.1016/j.aca.2018.08.004.

[27] A.J. Hackstadt, A.M. Hess, Filtering for increased power for microarray data analysis, BMC Bioinformatics. (2009). https://doi.org/10.1186/1471-2105-10-11.

[28] C. Schiffman, L. Petrick, K. Perttula, Y. Yano, H. Carlsson, T. Whitehead, C. Metayer, J. Hayes, S. Rappaport, S. Dudoit, Filtering procedures for untargeted lc-ms metabolomics data, BMC Bioinformatics. (2019). https://doi.org/10.1186/s12859-019-2871-9.

[29] K. Watanabe, N. Yamagiwa, Y. Torisawa, Cyclopentyl methyl ether as a new and alternative

process solvent, Org. Process Res. Dev. (2007). https://doi.org/10.1021/op0680136.

[30] Y. Gao, M.G. Ierapetritou, F.J. Muzzio, Determination of the confidence interval of the relative standard deviation using convolution, J. Pharm. Innov. (2013). https://doi.org/10.1007/s12247-012-9144-8.

[31] G. Tiwari, R. Tiwari, Bioanalytical method validation: An updated review, Pharm. Methods. (2010). https://doi.org/10.4103/2229-4708.72226.

[32] R. Herzog, K. Schuhmann, D. Schwudke, J.L. Sampaio, S.R. Bornstein, M. Schroeder, A. Shevchenko, Lipidxplorer: A software for consensual cross-platform lipidomics, PLoS One. (2012). https://doi.org/10.1371/journal.pone.0029851.

[33] M.L. Rodrigues, The multifunctional fungal ergosterol, MBio. (2018). https://doi.org/10.1128/mBio.01755-18.

[34] T.H. Toh, B.A. Prior, M.J. Van Der Merwe, Quantification of plasma membrane ergosterol of Saccharomyces cerevisiae by direct-injection atmospheric pressure chemical ionization/tandem mass spectrometry, Anal. Biochem. (2001). https://doi.org/10.1006/abio.2000.4877.

[35] L.H. Münger, S. Boulos, L. Nyström, UPLC-MS/MS based identification of dietary steryl glucosides by investigation of corresponding free sterols, Front. Chem. (2018). https://doi.org/10.3389/fchem.2018.00342.

Chapter 3: Comparison of Cell Lysis Techniques and Lipid Profiling of MCF-7 Breast Cancer Cells using Liquid Chromatography Mass Spectrometry (LC-MS)

3.1: Introduction

Cells are considered the building block of all living organisms and are involved in every biological processes. Although cells share characteristic features, there is a large diversity in how cells function. Multicellular organisms contain specialized cells which play specific roles such as transmission of information[1], energy storage[2], and immune response[3]. Differences in function can be explained through the regulation and expression of DNA, lipids, proteins, and metabolites. In humans and animals, the nervous system is composed of a high abundance of lipids which allow for signal transmission and a source of energy[4], compared to muscle cells which will express lower levels of lipids but will have a higher protein content. Structural integrity, size, and other mechanical properties of cells will also influence cell growth, apoptosis, and differentiation[5]. Slight perturbations in any of the processes involved in regulation and maintenance of cell homeostasis may disrupt the cell's natural physiology, and lead to diseases such as cancer.

Breast cancer is the most common malignancy diagnosed amongst Canadian women, and it is expected that 1 in 8 women will develop breast cancer in their lifetime[6]. All healthy cells undergo cell apoptosis which involves genetically programmed cell death. Disruptions in genetics involved in the regulation of cell apoptosis may lead to an imbalance between cell proliferation and death, resulting in the formation of tumors[7]. Current methods used for diagnosis such as mammography, magnetic resonance imaging, and clinical breast examination are often subjective which leads to poor or inaccurate diagnosis[8]. Early detection or improved treatment of breast cancer would improve the

survival rate for patients, reduce financial burdens, or help reduce phycological stress which may be induced through currents treatments such as chemotherapy[9]. Cell lines play an integral role as in-vitro model systems in cancer research as they can be used for molecular diagnosis, test therapeutic efficiency of drugs, and serve as a reliable source of biological material[9][10]. In particular, MCF-7 lines are a popular cell line in breast cancer research due to being one of few cell lines to express estrogen receptor alpha[11]. Due to its ability to express the estrogen receptor, it is able to simulate human breast cancers which exhibit the same receptors[11]. Furthermore, many discoveries have been made in cancer research through MCF-7 cells, making it a suitable cell line for experiments[9].

The human lipidome is quite complex, and involves a constant regulation of lipid catabolism, anabolism, transport, and intake. Previous studies have demonstrated that these processes are disrupted in cancer cells, causing abnormal levels of lipids. Fatty acid synthase has found to be upregulated in cancer cells, which results in increased concentration of long chain fatty acids[12]. Additionally, a clinical study examined the relationship between serum lipids such as TG, total cholesterol, HDL-C, and LDL-C, and the risk of breast cancer[13]. Incorporating over 1000 patients with breast cancer, the study found that TGs and total cholesterol levels were significantly higher in breast cancer patients compared to healthy controls[13]. Despite all the research linking lipid levels to breast cancer, very few studies focus on utilizing an untargeted approach for the profiling of the lipidome of the MCF-7 cell line. LC-MS would allow for excellent separation of analytes and provide high sensitivity, enabling the detection and identification of lipids from a complex cell matrix through untargeted analysis.

The first step in lipid analysis of cells involves the lysis of cells in order to release the cellular contents of cells through the disruption of their outer membrane. The effectiveness of the lysis method will influence the amount of lipids released, yielding an accurate representation of the physiological make-up of the cell. MCF-7 cells are classified as eukaryotic cells and lack a cell wall[14], allowing their

inter-cellular contents to be easily accessible through various forms of cell lysis. Mechanical lysis methods such as bead lysis are commonly used amongst cell research[15]-[17] due to its high lysis efficiency and ability to effectively disrupt cell walls[14]. Alternative methods such as thermal lysis and sonication utilize an external force for cell rupture[14], and benefit from the lack of beads which can potentially interfere with lipid extraction. Our study focused on bead and thermal lysis to assist in the extraction of lipids from MCF-7 cells.

In this chapter, we compared the effect on extraction efficiency of lipids between bead and thermal lysis of MCF-7 breast cancer cells. After cell lysis, samples were extracted using a modified Folch lipid extraction protocol before separating lipid analytes using UHPLC and analyzing the lipids through untargeted QToF MS. Once an optimal lysis method was selected, the protocol was employed for MSMS analysis for a comprehensive profiling of the MCF-7 cell lipidome. Identifications obtained through lipid annotation software were evaluated against literature. By identifying the MCF-7 lipidome via untargeted analysis, we can get a better understanding of lipids present in cancer cells, and potentially lead to biomarkers for prognosis or the development of suitable treatments.

3.2: Experimental

3.2.1: Chemicals and Reagents

All chemicals and reagents were obtained from Sigma-Aldrich Canada (Markham, ON, Canada), except those otherwise noted. LC-MS grade water (H_2O), acetonitrile (ACN), methanol (MeOH), and isopropyl alcohol (IPA) were from Honeywell (Calgary, AB, Canada). LC-MS grade dichloromethane (DCM) and MTBE were obtained from Thermo Fisher Scientific (Edmonton, AB, Canada). 0.5 mm diameter glass beads were acquired from Biospec Products.

3.2.2: Media and Culture Conditions for the Growth of MCF-7 Breast Cancer Cells

MCF-7 cells (ATCC HTB-22) were cultured in Hyclone DMEM growth medium using either t-25 or t-75 culture flasks. The growth medium was supplemented with 10% fetal bovine serum (FBS) and 0.01 mg/mL human recombinant insulin. Cells were grown at 37 °C in a humidified atmosphere with 5% CO_2. Every two days, prior growth media was removed and cells were resuspended in fresh media until an optimal cell count was reached. Harvesting of cells was achieved by adding 0.25% (w/v) trypsin and 0.53 mM EDTA for 10 minutes at 37 °C in order to detach cells from the culture flask. Trypsin was inhibited through the addition of fresh growth media. The trypsin and growth media were separated from the cells via centrifugation for 7 minutes at 900 g. Supernatant was removed using a sterile vacuum, after which cells were suspended in fresh cold PBS solution. PBS was removed by centrifuging for 7 minutes at 900 g and vacuuming out. The washing step was repeated an additional two times. Cells were suspended in PBS and counted through a hemocytometer and a Zeiss Axiovert 25 inverted microscope (Oberkochen, Germany). Approximately 3.5E05 cells were aliquoted into Eppendorf tubes and the tubes were purged with nitrogen gas, flash frozen in liquid nitrogen, and stored at −80 °C freezer until further use. Cells were sub cultured every 4 days by adding 0.25% (w/v) trypsin and 0.53 mM EDTA for 10 minutes at 37 °C. After the addition of fresh growth media, cells were viewed under a microscope to determine confluency. After centrifuging for 7 minutes at 900 g, the supernatant was vacuumed out and fresh growth media was added. Cells were homogenized and split into two culture flasks. The culture flasks were then incubated at 37 °C in a humidified atmosphere with 5% CO_2.

3.2.3: Cell Lysis

Bead Lysis:

0.150 cc (mL) of glass beads were added to a 2mL Eppendorf tube containing thawed MCF-7 breast cancer cells, 25 µL of LC-MS grade H_2O, 20 µL MeOH, and 5 µL deuterated lipid internal standards. To add a consistent volume of glass beads, a 200 µL pipette tip was labelled with a marker to indicate the appropriate volume of beads to add. The glass beads were poured into the pipette tip to the specified mark (0.150 mL), and were then transferred into the Eppendorf tube containing the sample. Cells were lysed by vortexing using a Vortex-Genie 2 mixer at 3200 rpm (Fisher Scientific) for 1 minute, alternated with 1 minute of incubation in an ice-water bath. The cell lysis step was repeated for a total of 5 intervals.

Thermal Lysis:

Cell pellets were suspended in 25 µL of LC-MS grade H_2O, 20 µL MeOH, and 5 µL deuterated lipid internal standards. Cell lysis was achieved by submerging the sample vial in liquid nitrogen for 5 seconds before thawing at room temperature for 4 minutes. The freeze thaw cycle was repeated for a total of 5 intervals.

3.2.4: Sample Preparation

Folch Lipid Extraction:

The Folch protocol was adapted for reduced sample volumes and substituted DCM in lieu of chloroform[18]. Although the volumes of reagents were modified, our protocol utilized the appropriate ratios of solvents. 275 µL of MeOH was added to each sample before vortexing for 20 seconds using a Vortex-Genie 2 at 3200 rpm. A total of 600 µL of DCM was added before vortexing each sample for 20 seconds, after which 200 µL of H_2O was added to reach a solvent ratio of 8/4/3 of DCM/MeOH/H_2O.

After vortexing for 10 seconds, samples were incubated for 10 minutes at room temperature to equilibrate the lipids. Samples were then centrifuged for 10 minutes at 12000 rpm and 4 °C, and 350 µL of the lower organic phase (DCM) was extracted into a fresh 2 mL Eppendorf tube. The Eppendorf tube containing the extracted DCM was placed inside a 4 °C fridge. 350 µL of fresh DCM was added to the original Eppendorf tube containing the sample and the tube was vortexed for 20 seconds. Samples were further incubated for 10 minutes at room temperature and subjected to centrifugation for an additional 10 minutes at 12000 rpm and 4 °C. 350 µL of DCM was extracted and was combined with the previous lipid extract. The extracted supernatant was dried down at room temperature using a Savant SC110A Speed Vac for 50 minutes. Once removed from the Speed Vac, samples were purged with nitrogen gas, flash-frozen using liquid nitrogen, and stored in a -80 °C freezer for long term storage.

Sample Resuspension:

Before running the samples on the LCMS, they were taken out of the - 80 °C freezer, thawed, and resuspended. Samples were first re-dissolved in 1.5 µL of mobile phase A (MPA) and 1.5 µL mobile phase B (MPB), then vortexed for 30 seconds using the Vortex-Genie 2. Afterwards, 27 µL of MPA was further added, and the samples were vortexed for an additional 30 seconds. The total reconstitution of the sample comprised of 95% MPA and 5% MPB for a 0x dilution. Samples could be further diluted through the addition of the same ratio of mobile phases. After resuspension, samples were transferred into glass inserts. MPA was comprised of 50% MeOH, 40% ACN, 10% H_2O (v/v/v), and 10mM ammonium formate. MPB was comprised of 95% IPA, 5% H_2O (v/v), and 10mM ammonium formate.

Blank and Quality Control preparation:

Extraction blanks underwent the same cell lysis and lipid extraction protocol as samples, but contained no MCF-7 cells and the internal standard was substituted with the same volume of methanol. Quality control samples were made by pooling multiple samples extracted from the same lipid extraction protocol together.

3.2.5: LCMS Conditions

Impact II QToF:

MCF-7 samples were lysed in triplicates, along with 1 blank, using either the bead lysis or thermal lysis protocols. Samples were then extracted using the Folch protocol and a portion of the samples were pooled to produce QCs. Samples were run on a UHPLC-MS system to evaluate the types of lipids extracted from each cell lysis method through putative identification. Samples were separated through the use of a Dionex UltiMate 3000 UHPLC employing a Waters Acquity BEH C18 column (10 cm × 2.1 mm, 1.74 µm particle size) in ESI positive and negative mode. A flow rate of 250 µL/min was used during the analysis with a column temperature of 40°C. A sample dilution of 2x and 5x was used for ESI negative and positive mode respectively. Injection volumes of 9 µL and 6 µL were used for ESI negative and positive mode respectively. The chromatographic gradient for analyte separation was as followed: t = 0 min, 2% MPB; t = 3 min, 5% MPB; t = 8 min, 40% MPB; t = 22 min, 95% MPB; t = 25 min, 95% MPB; with a 10-minute re-equilibration gradient afterwards. The UHPLC was coupled to an Impact II QToF mass spectrometer with an ESI source. MS spectra of analytes with a mass between 150 to 1500 m/z range was acquired at a rate of 1.44 Hz. MSMS spectra was acquired using a quadrupole isolation width of 2 Daltons, MS acquisition time of 0.4 seconds, and an MSMS acquisition time of 1 second. The

capillary voltage of the ionization source was set to 4500 V, along with an end plate offset of 500 V. The nebulizer gas pressure was set to 1 bar, and the flowrate of the dry gas was set to 4.0 L/min, at a temperature of 230°C. Each sample had a 1-minute segment at the beginning of each run, in which sodium formate mass calibrant solution was injected into the ion source. QCs were run in order to generate a scheduled precursor list of lipids present in MCF-7 cells. Scheduled precursor lists were composed of lipids detected in 100% of the QCs through UHPLC-MS. MSMS analysis was performed using collision energies compiled from literature (Appendix Table 3) in which each MSMS method had a unique SPL. MSMS was performed using QC samples under ESI positive and negative mode. Precursor ions were chosen for fragmentation if they fell within a m/z tolerance of 0.05 Daltons and a 30 second retention time tolerance from the proposed mass in the SPL.

3.2.6: Data Processing and Analysis

After samples were run on the UHPLC-ESI-QToF-MS, the data was processed through Bruker Metaboscape 4.0. The software served to extract peaks from the chromatograms and process them through alignment, re-calibration, filtering, and adduct identification. The software outputted information compiled from multiple samples regarding m/z, retention time, adduct formation, and relative peak intensity for each unique analyte. The parameters for analyte detection were set to 5.0 mDa for the precursor m/z tolerance and 15 seconds for the retention time tolerance. Analytes were then identified putatively through the use of the LipidMaps database with an m/z tolerance of 5.0 mDa. Analytes were filtered and ranked based on the expected retention time, number of carbons in the fatty acyl chains, adduct formation, and the number of double bonds and functional groups found in the lipid. Analytes were then normalized using in-house designed excel formulas. Normalization was performed by first matching the lipid class of the analyte to one of the 14 lipid classes belonging to the deuterated

internal standards. Finally, the ratios of the intensities for the analyte and its class matched internal standard were taken. Multivariate statistical analysis plots such as principal component analysis (PCA) were generated through the use of MetaboAnalyst 4.0 using features that contained RSD values <30% for QCs. MSMS chromatograms were processed using Metaboscape 4.0 and the MSMS spectra of fragment ions were matched to spectra libraries (Bruker LipidBlast; Mass Bank; RIKEN Oxidized Phospholipids; LC-MSMS Positive; and LC-MSMS Negative) through Metaboscape 4.0 with a precursor mass tolerance of 20.0 mDa, mSigma tolerance of 100, and MSMS threshold of 100. Spectra matching was based off adduct formation, intensity of fragment ions, and m/z tolerance. Spectra of fragment ions was also run through LipidMatch software, which is an in-silico fragmentation library. The mass accuracy tolerance for matching the experimental and in-silico precursor m/z was set to 20 mDa. Annotations from the two software's were consolidated using a m/z window of 20 mDa and retention time window of 15 seconds.

3.3: Results and Discussion

Bead lysis is a type of mechanical lysis in which glass beads are vortexed at high velocity to physically rupture cell membranes via shearing or friction[14]. This allows for high efficiency cell lysis and is for the most part independent on the cell type. A caveat of bead lysis is that intracellular components of cells could potentially be damaged due to heat generated from prolonged vortexing, however this effect was mitigated through chilling cell samples on ice directly after each vortex cycle[14]. Another disadvantage to bead lysis is that the beads reduce the available organic phase to be extracted during lipid extraction. A modified Folch protocol had been applied for lipid extraction in which the bottom organic phase was comprised of DCM. Due to the density of the beads, the beads also resided in the bottom of the sample vial, making solvent extraction difficult. Lysis of cells through freeze

thaw lysis circumvented this issue as no beads were employed for cell disruption. Cells were snap frozen in liquid nitrogen and were allowed to thaw back to room temperature, causing cell lysis through the formation of ice crystals in the cell membrane[14]. The lack of a cell wall in MCF-7 cells allowed for the cell membrane to more susceptible to cell lysis, thus increasing the effectiveness of thermal lysis[19]. Although the organic phase in thermal lysis was more accessible, the throughput of the method was lower than bead lysis. Bead lysis could incorporate the use of bead mills which could lyse multiple samples at once, whereas thermal lysis is limited to the speed of the user.

3.3.1: Assessment of Lysis Efficiency

Bead and thermal lysis methods were evaluated for their efficiency to lyse MCF-7 breast cancer cells. Cell lysis effectiveness was assessed through the intensities of putatively identified lipids extracted via a modified Folch protocol. Triplicates of cells were lysed using either thermal lysis or through beads, and were analyzed through ESI-LC-MS after lipid extraction. Cell disruption plays an integral part in lipidomics analysis of cells as it allows for intracellular components to be extracted, achieved through the lysis of the outer membrane(s)[20]. An efficient protocol would allow for lipids stored in the cellular components to become more obtainable, thus improving the variety and yields of lipids extracted. Figure 3.3.1 shows the summed intensities for various lipid internal standards detected in both ESI positive and negative modes in relation to the cell lysis protocol utilized. The results had indicated that the quantity of internal standards extracted were similar, which was expected as the internal standard was only a representative of the effectiveness of the lipid extraction protocol employed, rather than the cell lysis protocol. Since both cell lysis protocols utilized the exact same lipid extraction protocol, and were analyzed using the same conditions, the intensities of internal standards between the two protocols should have been approximately equivalent.

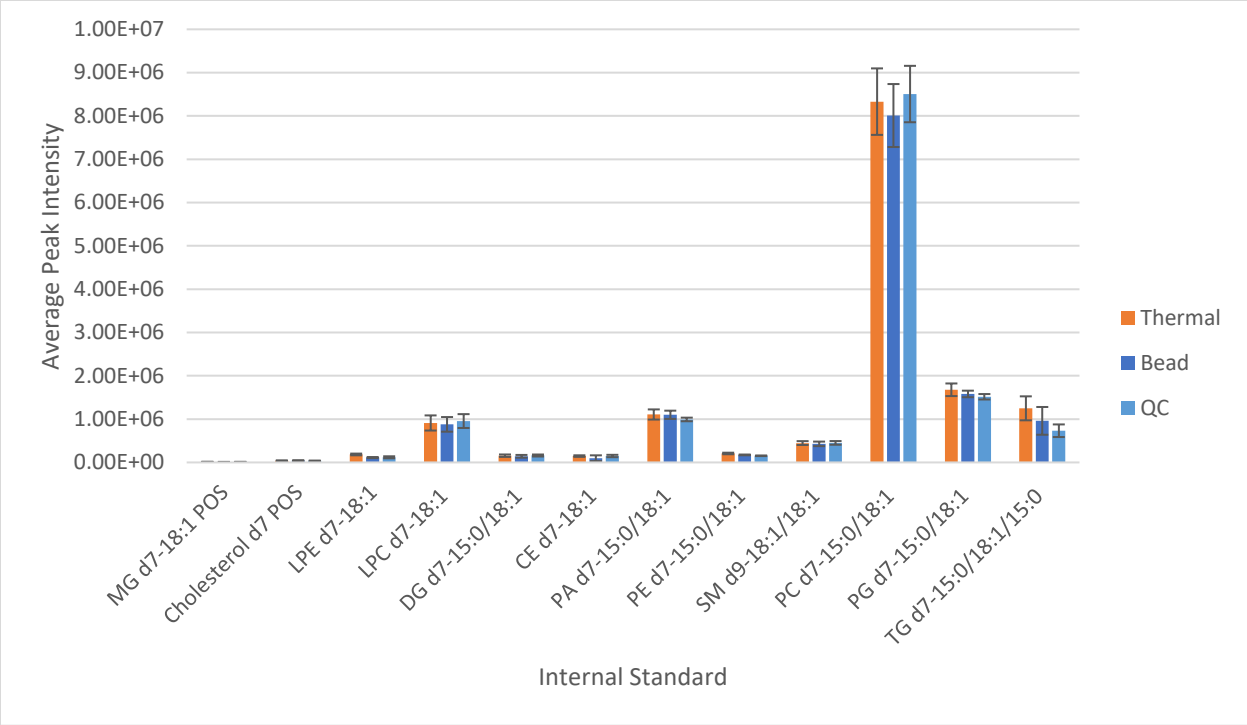

Figure 3.3.1: Comparison of average signal intensities for internal standards detected from each cell lysis method. Error bars represent the standard deviation of the average.

The mean summed intensities for putatively identified lipids in ESI positive and negative mode presented in Figures 3.3.2 and 3.3.3 had indicated that the total yield of lipids extracted from both cell disruption methods were similar. The highest lipid yield in ESI positive mode was achieved following bead lysis (1.66E8, with a standard deviation of 2.53E07), whereas thermal lysis had an average summed intensity of 1.63E08 with a standard deviation of 1.19E07. However, it was observed that the lipid yield detected in ESI negative mode for thermal lysis was slightly higher than cells lysed using beads (Figure 3.3.3). Average of summed signal intensities for thermal lysis were 9.39E07 (Standard deviation of 7.02E06) compared to 8.58E07 (Standard deviation of 3.89E06) for cells using bead lysis. Although summed signal intensities were similar in both ionization modes, the standard deviation for thermal lysis were considerably higher, signifying the lack of reproducibility in lipid extraction of the protocol compared to cell disruption via beads. Figure 3.3.1 showed that internal standards extracted from both

cell lysis methods had similar reproducibility, whereas Figures 3.3.2 and 3.3.3 demonstrated distinct differences in reproducibility between both methods. Since the extraction of internal standards were not affected by the lysis protocol, but rather the lipid extraction protocol, the variance in reproducibility in the lipid intensities in Figures 3.3.2 and 3.3.3 were mainly a result of the cell lysis protocol utilized.

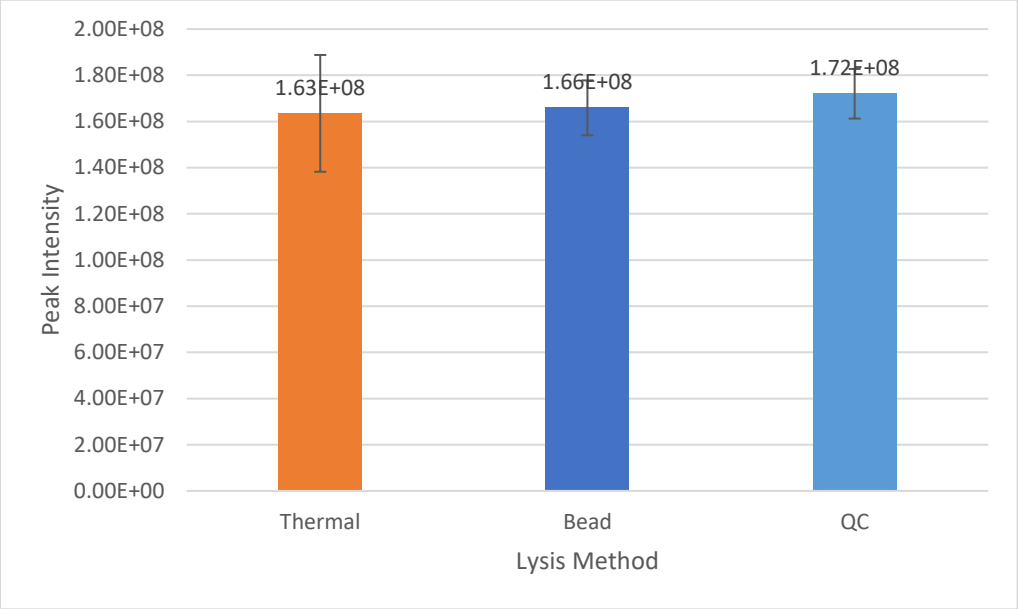

Figure 3.3.2: Summed signal intensities for putatively identified lipids detected for each sample in ESI positive mode in the comparison between different cell lysis methods.

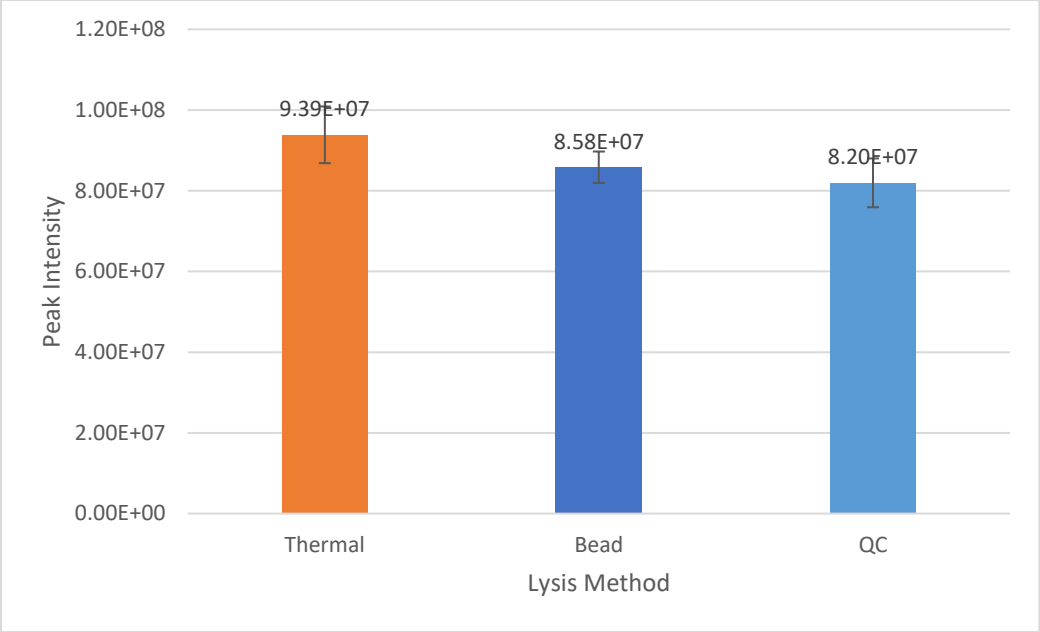

Figure 3.3.3: Summed signal intensities for putatively identified lipids detected for each sample in ESI negative mode in the comparison between different cell lysis methods.

The lysis efficiency was also monitored through identifying the number of missing lipids from each lipid class, which could help explain the variance seen between the two lysis methods via principle component analysis. 53 lipids belonging to 20 lipid subclasses were identified to be missing for cells lysed via thermal lysis in ESI positive mode, compared to 1 missing lipid identified for cells lysed via bead lysis (Figure 3.3.4). Additionally, 65 lipids belonging to 14 lipid subclasses were unable to be detected for cells disrupted through thermal lysis in ESI negative mode, with no missing features detected for cells disrupted through bead lysis (Figure 3.3.5). Lipids belonging to the sterol lipid subclass mostly comprised the total number of missing lipids for thermal lysis in ESI positive mode, with a total of 20 lipids. The top three lipid classes containing of the majority of the missing lipids for ESI negative mode for thermal lysis were sterols (20 missing), LPAs (15 missing), and PAs (8 missing). Sterol lipids are commonly found in membranes of cells and function to help regulate the fluidity of the membrane, along with maintaining membrane structure, and controlling biological processes[21]. Additionally, sterols form lipid rafts which

are present in membranes, and play important roles in asymmetric growth, infectious diseases, cellular sorting, and signal transduction[21]. Due to their involvement in cell growth and signal transduction, sterol levels have found to be unregulated in cancer cells and contribute to malignant transformation of cells, making it crucial for sterols to be detected and identified[22]. PA and LPA are other types of membrane lipid which are found to be upregulated in cancer cells[23]. PA affects many cellular processes such as signal transduction, cell proliferation, and cell reproduction[24], whereas LPA has found to promote breast cancer cell proliferation, migration, and invasion[25]. High abundance of missing sterol, LPA, and PA species detected in Figures 3.3.4 and 3.3.5 for thermal lysis might be due to inefficient lysis of the cell membrane. This claim can be supported by the fact that sterols, LPAs, and PAs are all play critical roles in membranes of cancer cells, and poor cell membrane lysis will result in inadequate recovery of these lipid species during lipid extraction. Moreover, 45 out of the 65 missing lipids for thermal lysis under ESI negative mode had eluted before 5 minutes, revealing that most of the missing features were polar. Due to their amphiphilic nature, membrane lipids tend to form micelles. Through a lack of homogenization of cells in the solvent, the micelles could potentially reduce the surface area in which the extraction solvent was able to solubilize the polar lipids, thus reducing extraction efficiency. The extraction solvent comprising of DCM, employed by the modified Folch method, is non-polar in nature, further limiting the affinity for the extraction of polar membrane lipids if they had formed micelles.

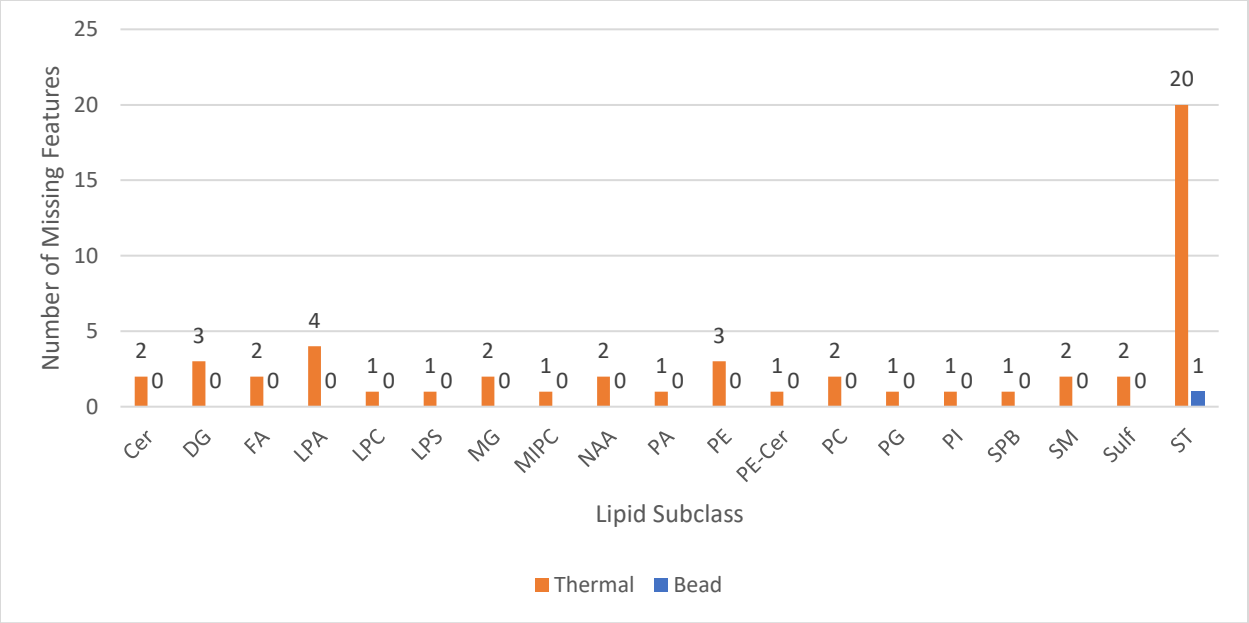

Figure 3.3.4: Number of missing features for each cell lysis method in ESI positive mode from a total of 1853 putatively identified features from all tested protocols.

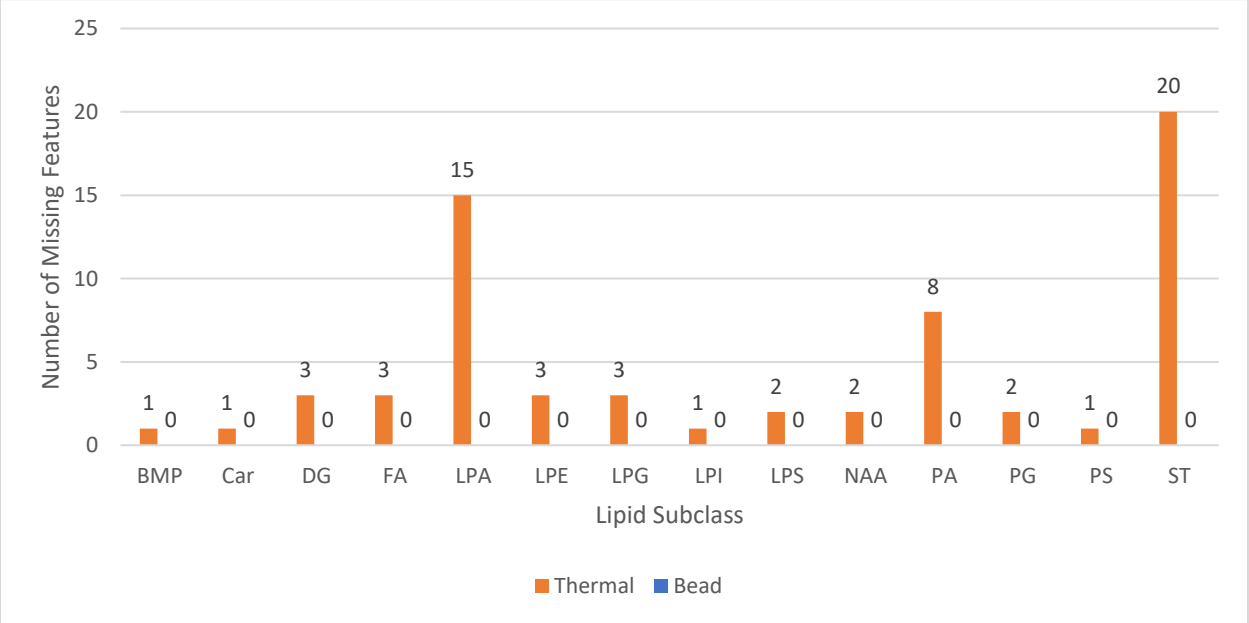

Figure 3.3.5: Number of missing features for each cell lysis method in ESI negative mode from a total of 1066 putatively identified features from all tested protocols.

3.3.2: Assessment of Method Reproducibility

Reproducibility of the cell disruption methods were also evaluated via a PCA plot generated through Metaboanalyst (Figure 3.3.6). Unlike PLSDA, PCA is an unsupervised multivariate analysis method in which information regarding the sample group is not supplied, thus separation of components is considered unbiased[26]. Data filtering was performed to remove features that were likely to be classified as non-informative variables. Features that had an RSD value below 30% in QC samples were kept for the generation of the PCA plot, which included 1796 out of the total 1853 features for ESI positive mode data, and 1033 out of the 1066 total lipids for ESI negative mode data identified through putative identification via LipidMaps. The sample data was inputted into Metaboanalyst and was normalized via Autoscaling through the program. Autoscaling was performed through centering the data around the mean and dividing each feature by the standard deviation of each variable in their respective sample groups, thus normalizing the data around the mean. The benefit of Autoscaling is that it changes the emphasis from features with a high concentration, and allows for all features to be equally weighted[27]. The caveat of this scaling method is that noise variables get inflated, but by performing peak filtering before scaling the data, it helps mitigate variables generated via noise[27]. The two cell lysis groups were demonstrated to be well separated in Figure 3.3.6. In the PCA plot, 38.1% and 16.7% of the total variances between the groups were captured through the first and second principal component respectively. Majority of the intergroup variation was explained through the first principal component, whereas the intragroup separation was explained through the second principal component, shown by the vertical stacking of samples in the PCA plot along the first principal component. In terms of reproducibility, samples that were subjected to thermal lysis through freeze thaw cycles had a larger confidence region and a higher degree of sample separation, particularly along the second principal component. Cell lysis performed via beads were more clustered together and had a smaller confidence region, indicating that samples had lower intragroup variability, thus making

the method more reproducible. A similar trend was seen in the standard deviations of the summed intensities of putatively identified lipids in Figures 3.3.2 and 3.3.3, where samples subjected to thermal lysis displayed the highest degree of standard deviation in contrast to bead lysed samples. The high standard deviation exhibited by the thermal lysis samples denoted a lower reproducibility, which was evident in the PCA plot in Figure 3.3.6.

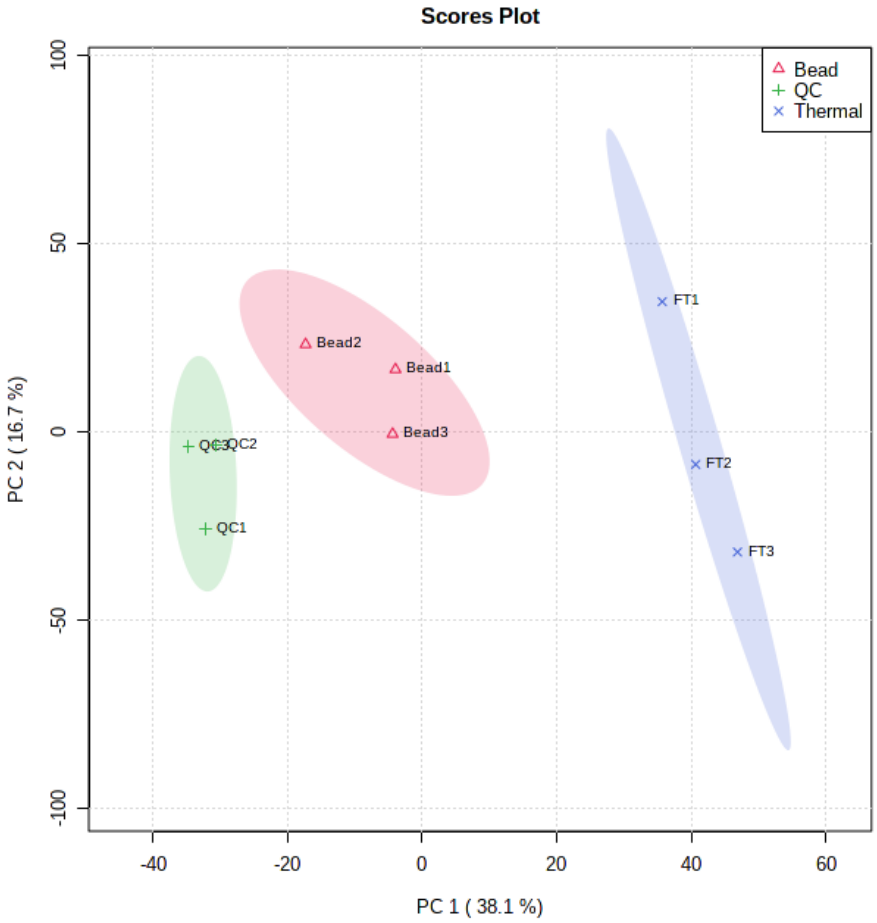

Figure 3.3.6: PCA plots of putatively identified features detected from different cell disruption protocols, alongside QC samples. Features from ESI positive and negative modes were merged before generating the PCA plot.

3.3.3: Assessment of Homogenization

Homogenization of the cell lysate was investigated through the employment of a Zeiss Axiovert 25 inverted microscope under 20x magnification. Pictures of the homogenate were taken for both lysis methods and were shown in Figures 3.3.7a and 3.3.7b. Cells disrupted through freeze thaw cycles via thermal lysis (Figure 3.3.7a) had shown poor homogenization of cells in the lysis solvent comprising of 50:50 water/methanol, due to the clustering of cells. 50:50 water/methanol was chosen as the lysis solvent due to a study which found that the ratio was methanol and water was the most optimal in providing the best cell lysis efficiency[28]. The lysis solvent was also useful in that both solvents were already incorporated into the Folch method, thus no additional solvents had to be introduced, which could potentially hinder lipid extraction. Cells disrupted through bead vortexing had shown excellent homogenization (Figure 3.3.7b), with no clumping of cells. Cell debris was uniformly dispersed in the lysis solvent, demonstrating that bead lysis was effective in rupturing the cell membranes and breaking apart the cell pellet as a result of consistent vortexing. Furthermore, clumps of cells were clearly visible without the use of a microscope in the thermal lysis samples, which may have led to the formation of micelles and limited the extraction of polar lipids (Figure 3.3.5). Literature focused on comparing and finding optimal cell lysis protocols for breast cancer cells could not be found. Similar studies have been carried out in which several lysis techniques were compared using various cell lines such as *Chlorella vulgaris*[29], *Candida albicans*[30], and colon cancer cells[31]. It should be emphasized that different cell lines contain highly variable cell membrane or cell wall structures, thus the cell lines will respond differently to the same cell lysis protocols[32]. Due to optimal cell lysis being dependent on the species of cells, and the cell membrane composition, it is not ideal to generalize or compare the results of one species to another[32].

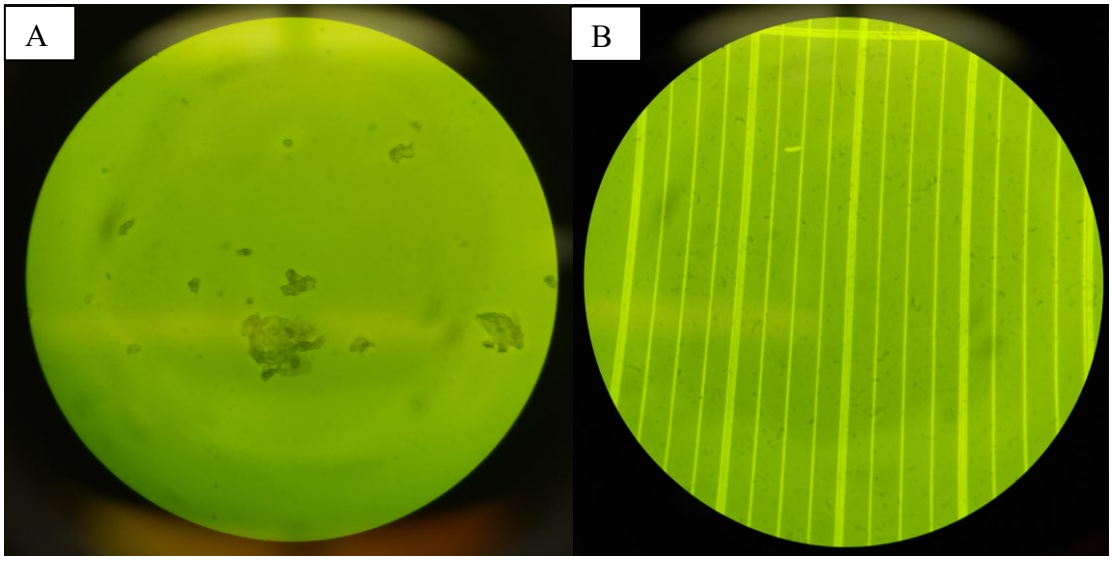

Figure 3.3.7: Microscope image obtained under 20x magnification of cells lysed using: (**a**) thermal lysis through freeze that cycles; and (**b**) bead lysis with assistance through vortexing.

Bead lysis was chosen as the optimal cell disruption method for the lysis of MCF-7 breast cancer cells. The beads coupled with vortexing, were able to collide with the cells to disrupt the cell membranes, allowing the cells to homogenize in the solvent. The lipid extraction solvent would have an increased surface area to extract lipids from the homogenized cell lysates via bead disruption, therefore increasing lipid extraction efficiency. Cells lysed using beads were also shown to be more reproducible through PCA plots and standard deviation of intensities of putatively identified lipids. Moreover, thermal lysis was unable to detect as many lipids as bead lysis in both ESI modes.

3.3.4: MSMS Analysis of MCF-7 Breast Cancer Cells using a Modified Folch Lipid Extraction Protocol

Lipidomics profiling of MCF-7 breast cancer cells disrupted through bead lysis was performed using UHPLC-MS to investigate the profiles of major lipid compounds present in breast cancer cells. MCF-7 breast cancer cells were extracted using a modified Folch protocol for lipid extraction after cell

lysis. Cell extracts were pooled to for QC samples, after which were diluted either two or fivefold for ESI positive of negative mode respectively. Scheduled precursor lists (SPLs) were produced comprising of a list of putatively identified features detected in all QC samples. Through LCMS lipidomics, 3466 and 743 lipids were putatively identified through LipidMaps under ESI positive and negative mode respectively (Figure 3.3.8). In total, 31 lipid subclasses were identified in ESI positive, while 30 lipid subclasses were identified in ESI negative mode.

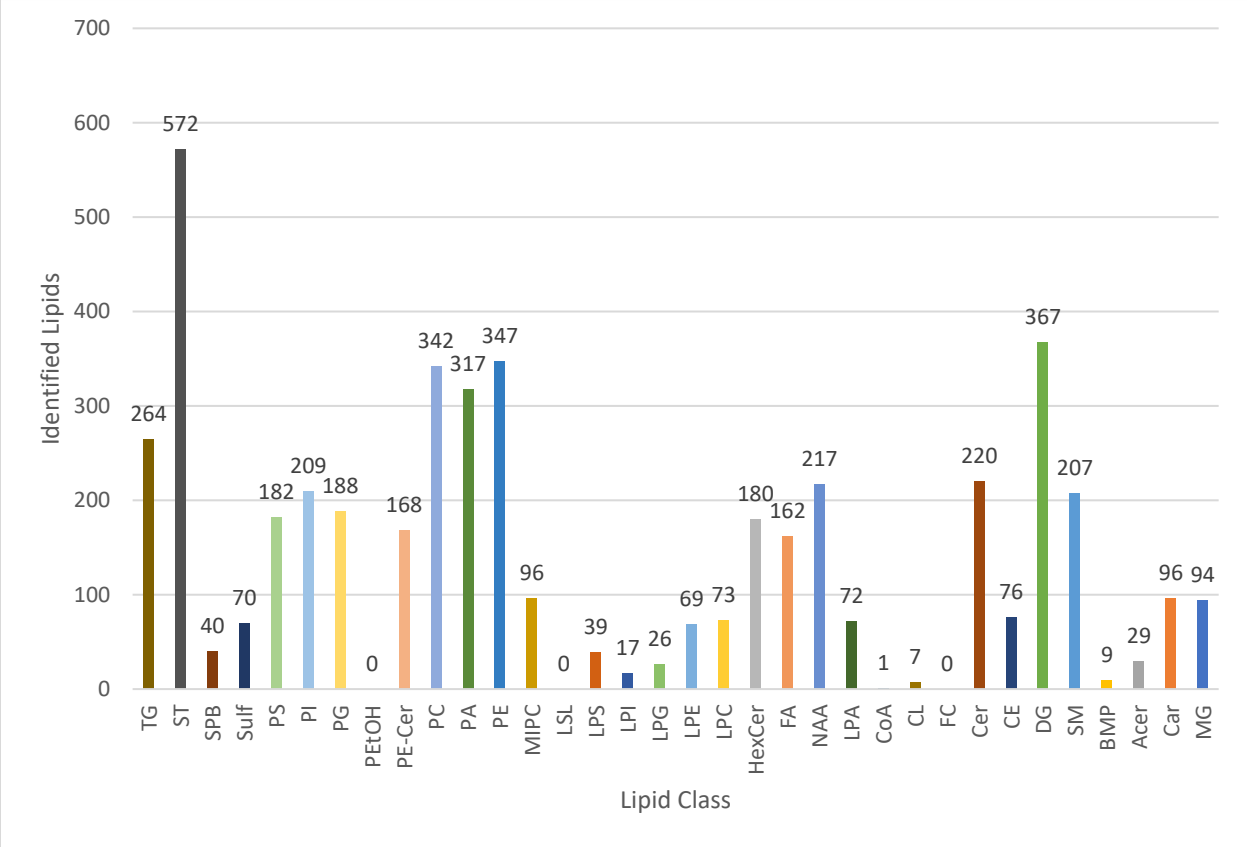

Figure 3.3.8: List of putatively identified features identified through LipidMaps that were incorporated into SPLs for MSMS of MCF-7 cells.

SPLs were uploaded into unique MSMS methods which were set to specific collision energies (Appendix Table 3) corresponding to the lipid classes present in the SPL. A retention time tolerance of 15 seconds and a mass tolerance of 50 mDa were applied for SPL construction, which would indicate the

precursor mass range and retention time range for MSMS fragmentation. 36 SPLs were generated for ESI positive MSMS, and an additional 10 SPLs were constructed for ESI negative MSMS. Collision energies for MSMS methods were obtained through previously published research for both ionization modes. QC samples were analyzed through LC-MSMS, after which the data was processed using Metaboscape 4.0 for peak identification, peak alignment, mass calibration, and adduct identification. The MSMS data was then annotated using either the LipidMatch library, or Metaboscape 4.0 which contained multiple metabolite and lipid libraries integrated into the software. The libraries used for spectral matching through the Metaboscape 4.0 software were the following: Bruker LipidBlast; Mass Bank; RIKEN Oxidized Phospholipids; LC-MSMS Positive; and LC-MSMS Negative. A mass tolerance filter of 10 mDa or lower was applied for library matching, additionally only annotation with a MSMS score above 100 were kept, with those above a score of 500 being considered as strong matches. Duplicate annotations were deleted, resulting in a total of 398 lipids identified in MCF-7 breast cancer cells, with 336 of them having an MSMS score above 500 (Appendix Table 4). MSMS data was further uploaded and annotated through the LipidMatch software to improve confidence in the lipid identifications obtained from Metaboscape 4.0. Default fragmentation rules for lipid identification using LipidMatch were applied such that for positive annotation, a lipid required a match based on both the lipid head group and fatty acyl tail constituents. Duplicate annotations for lipids were removed, and for matches containing multiple possible identifications, the most probable match was kept. The mass tolerance for matching experimental and in-silico precursor m/z was set to 20 mDa. Appendix Table 4 showed that 472 lipids were successfully annotated to the LipidMatch library under both ESI modes. Annotations from Metaboscape 4.0 and LipidMatch were consolidated with a retention time and mass windows of 30 seconds and 20 mDa respectively, for a total of 205 lipids present in both libraries (Appendix Table 4**,** Bolded IDs). Combining both libraries allowed for validation of results and helped discover novel lipid identifications, which otherwise would have been missed if only one annotation software was

employed. It is important to note that not all identifications in Appendix Table 4 were naturally occurring lipids in MCF-7 cells. Certain identifications such as erucamide and dibutyl phthalate, which were annotated through Metaboscape 4.0 libraries, were hydrophobic plasticizers that were extracted using the equipment employed. These identifications were left to show that our method had the ability to detect contaminants that resulted from sample handling, extraction, or analysis.

MSMS identifications from Metaboscape 4.0 and LipidMatch were compared to similar studies conducted in the past 4 years, focusing on the lipid profiling of MCF-7 cells. “Comparative metabolic and lipidomic profiling of human breast cancer cells with different metastatic potentials” by Kim et al. was chosen for comparison of phospholipids such as PC, PE, PG, PI, and PS[33]. The study by Kang et al. titled “Spheroid-induced epithelial-mesenchymal transition provokes global alterations of breast cancer lipidome: A multi-layered omics analysis” was chosen for its detection of Cer, LPC, PC, PE, and SM lipid classes[34]. There were limited studies focusing on untargeted lipidomics profiling of MCF-7 breast cancer cells, thus multiple studies were used to obtain a broad range of lipid classes in order to gauge how well our workflow characterized lipid species against other methods. Only lipid classes that were exclusively detected in the reference papers were compared to evaluate how effective our method was in identifying lipids through MSMS analysis. Annotations obtained through our protocol that contained matches in both ESI positive and negative mode were manually merged before comparing. The reference studies by Kim et al. and Kang et al. had annotated lipids via an in-house lipid library and through Agilent SimLipid software respectively[33][34]. The study by Kim et al. had identified 44 phospholipids from breast cancer cells, whereas Kang et al. had identified 144 lipids from MCF-7 cells (Figure 3.3.9). Our method was able to successfully identify 262 lipids using Metaboscape 4.0, and 242 lipids using LipidMatch between the 9 lipid classes compared (Figure 3.3.9). Our untargeted approach was able to identify more lipids in every lipid class, with the exception of PS, and had identified additional lipid classes such as FAs, CholEs, CLs, and DGs, which were not detected in any of the studies

referenced. The largest discrepancy was seen between the PC lipid class in which 67 and 125 PCs were detected by LipidMatch and Metaboscape 4.0, while 41 and 11 PCs were identified by Kang et al., and Kim et al. respectively. Ceramides were also identified by a significant margin, as 21 ceramides were annotated by LipidMatch, in contrast to the 5 ceramides detected by Kang et al. TGs displayed the highest similarity in which 49 and 43 TGs were identified through LipidMatch and Metaboscape 4.0, whereas Kang et al. had identified 44 TGs. Using LipidMatch and Metaboscape 4.0 in tandem had resulted in an increase in number of unique lipids identified. Our approach employed multiple MSMS methods tailored to specific lipid classes, allowing for efficient fragmentation of lipids, thus increasing the total number of lipids and lipid classes identified, compared to Kang et al. which had performed MSMS using a single collision energy of 30eV[34]. Higher mass compounds typically require a higher collision energy for efficient fragmentation relative to lower mass compounds, emphasizing the importance of adjusting collision energy in relation to m/z[35]. Although individual lipids couldn't be quantified due to different ionization efficiencies between lipid classes, the diversity in lipid classes could be explored. Our method had found that PCs in MCF-7 cells had the most diversity, as seen by the number of unique PCs detected, followed by TGs, PEs, and SMs. PCs, PEs, and SMs are all naturally abundant lipids present in mammalian cell membranes. In particular, PCs and PEs comprise a large percentage of the endoplasmic reticulum, Golgi apparatus, mitochondria, endosomes/lysosomes, and the plasma membrane[23]. PCs and PEs are also zwitterionic and are able to be easily detected in both ESI modes. Furthermore, due to their zwitterionic headgroups, the ionization efficiency of these lipid subclasses is increased, allowing them to be detected at low concentrations. TGs function as the main source for energy storage for the cell and to serve as a source of fatty acids for membrane biosynthesis[36]. Sphingomyelins are the most abundant complex sphingolipid species in mammalian cells[37] and serve as structural components in the plasma membrane, along with acting as signaling molecules[38]. All these lipid classes play critical roles in mammalian cells, and as a result are required at

high abundance, making it no surprise to see a wide range of lipid species from these subclasses as shown in Figure 3.3.9. Our approach for MSMS identification of MCF-7 breast cancer cells was able to identify a substantial amount of lipids compared to similar literature, alongside revealing a greater diversity of the MCF-7 lipidome. This was in part due to utilizing a combination of analytical techniques such as the appropriate cell lysis protocol coupled with an efficient and reproducible lipid extraction protocol. The sensitivity and resolution of the QToF allowed for the detection of low abundance species and ability to distinguish between isobaric species. The incorporation of two annotation libraries for lipid identification also enabled the ability to detect novel lipid species, and allowed for over 200 lipid species to be corroborated between the two libraries.

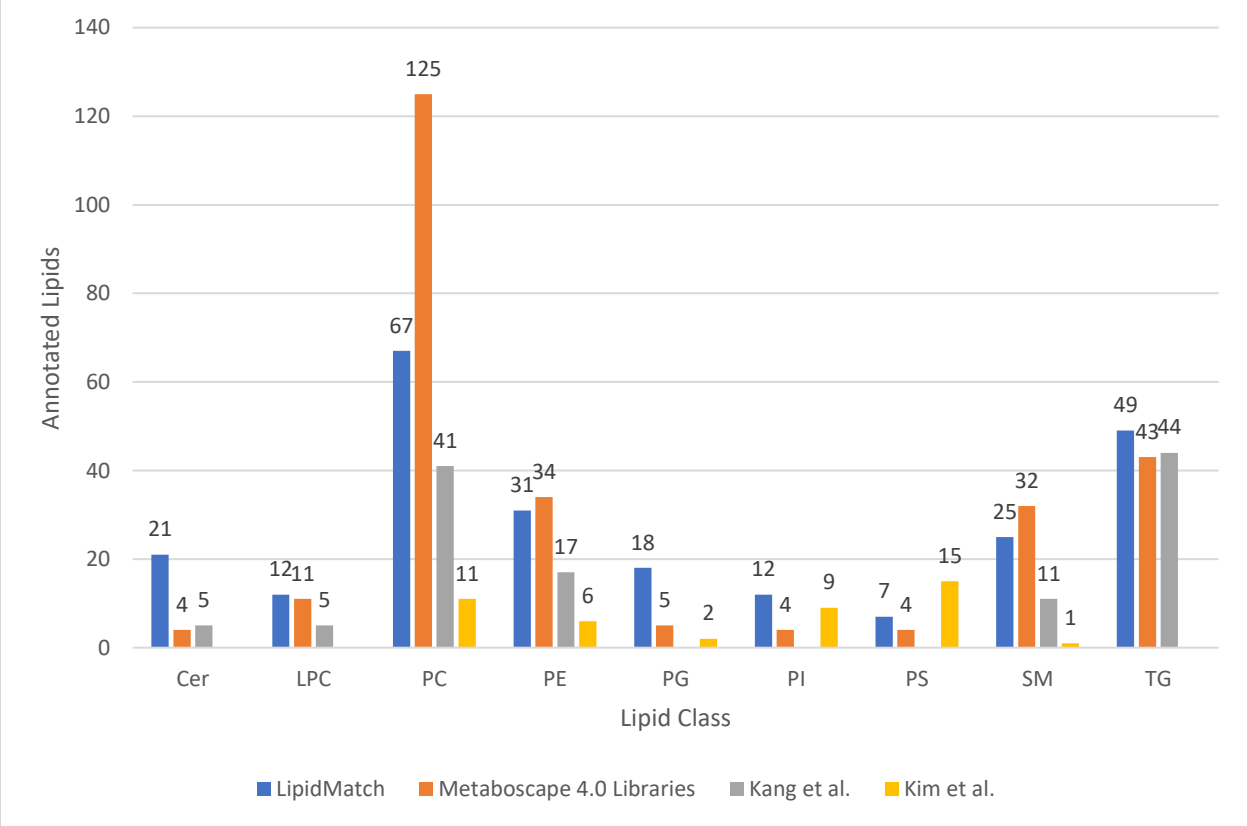

Figure 3.3.9: Bar graph comparing the number of lipids annotated in different lipid classes between Metaboscape 4.0 libraries, LipidMatch library, and literature in breast cancer cells.

3.4: Conclusion

We have developed and applied a comprehensive lipidomics protocol for lipid profiling of MCF-7 breast cancer cells. Bead lysis was compared against thermal lysis in order to determine the optimal cell disruption method. We demonstrated that bead lysis was more reproducible, had a higher lysis efficiency, and was able to homogenize the cell lysate more effectively in the lysis solvent. The lipidomics protocol using beads was then applied for the untargeted MSMS analysis of MCF-7 cells in order to identify as many unique lipid species as possible. Furthermore, we successfully annotated 398 features using Metaboscape 4.0 and 472 features using LipidMatch, with a total of 205 corroborated lipids between them, helping validate our findings. Annotated lipids were compared with past literature, and among the lipid groups examined, our results suggested that the MCF-7 lipidome diversity was far greater than previously reported. In the future, biomarker analysis can be probed in which the lipidome of healthy breast tissue or epithelial cells can be compared to breast cancer tissue at various stages of metastasis. Relative quantification of lipids can be performed to observe any regulation of lipids, which can potentially serve as biomarkers for disease prognosis.

3.5: Literature Cited

[1] K. Sidiropoulou, E.K. Pissadaki, P. Poirazi, Inside the brain of a neuron, EMBO Rep. (2006). https://doi.org/10.1038/sj.embor.7400789.

[2] K. Ikeda, P. Maretich, S. Kajimura, The Common and Distinct Features of Brown and Beige Adipocytes, Trends Endocrinol. Metab. (2018). https://doi.org/10.1016/j.tem.2018.01.001.

[3] S. Sakaguchi, T. Yamaguchi, T. Nomura, M. Ono, Regulatory T Cells and Immune Tolerance, Cell. (2008). https://doi.org/10.1016/j.cell.2008.05.009.

[4] L. Rodríguez-Berdini, B.L. Caputto, Lipid metabolism in neurons: A brief story of a novel c-Fos-dependent mechanism for the regulation of their synthesis, Front. Cell. Neurosci. (2019). https://doi.org/10.3389/fncel.2019.00198.

[5] C.T. Lim, E.H. Zhou, S.T. Quek, Mechanical models for living cells - A review, J. Biomech. (2006).

https://doi.org/10.1016/j.jbiomech.2004.12.008.

[6] Canadian Cancer Statistics Advisory Committee, Canadian Cancer Statistics 2019, 2019.

[7] R. Simstein, M. Burow, A. Parker, C. Weldon, B. Beckman, Apoptosis, chemoresistance, and breast cancer: Insights from the MCF-7 cell model system, Exp. Biol. Med. (2003). https://doi.org/10.1177/153537020322800903.

[8] C. Johnson, S. Manna, K. Krausz, J. Bonzo, R. Divelbiss, M. Hollingshead, F. Gonzalez, Global Metabolomics Reveals Urinary Biomarkers of Breast Cancer in a MCF-7 Xenograft Mouse Model, Metabolites. (2013). https://doi.org/10.3390/metabo3030658.

[9] Ş. Comşa, A.M. Cîmpean, M. Raica, The story of MCF-7 breast cancer cell line: 40 Years of experience in research, Anticancer Res. (2015).

[10] J.P. Gillet, S. Varma, M.M. Gottesman, The clinical relevance of cancer cell lines, J. Natl. Cancer Inst. (2013). https://doi.org/10.1093/jnci/djt007.

[11] A. V. Lee, S. Oesterreich, N.E. Davidson, MCF-7 Cells - Changing the Course of Breast Cancer Research and Care for 45 Years, J. Natl. Cancer Inst. (2015). https://doi.org/10.1093/jnci/djv073.

[12] J. Long, C.-J. Zhang, N. Zhu, K. Du, Y.-F. Yin, X. Tan, D.-F. Liao, L. Qin, Lipid metabolism and carcinogenesis, cancer development., Am. J. Cancer Res. (2018).

[13] L.J. Wei, C. Zhang, H. Zhang, X. Wei, S.X. Li, J.T. Liu, X.B. Ren, [A case-control study on the association between serum lipid level and the risk of breast cancer]., Zhonghua Yu Fang Yi Xue Za Zhi. 50 (2016) 1091–1095. https://doi.org/10.3760/cma.j.issn.0253-9624.2016.12.013.

[14] M.S. Islam, A. Aryasomayajula, P.R. Selvaganapathy, A review on macroscale and microscale cell lysis methods, Micromachines. (2017). https://doi.org/10.3390/mi8030083.

[15] C.S. Ejsing, J.L. Sampaio, V. Surendranath, E. Duchoslav, K. Ekroos, R.W. Klemm, K. Simons, A. Shevchenko, Global analysis of the yeast lipidome by quantitative shotgun mass spectrometry, Proc. Natl. Acad. Sci. U. S. A. (2009). https://doi.org/10.1073/pnas.0811700106.

[16] J.S. Kruger, N.S. Cleveland, R.Y. Yeap, T. Dong, K.J. Ramirez, N.J. Nagle, A.C. Lowell, G.T. Beckham, J.D. McMillan, M.J. Biddy, Recovery of Fuel-Precursor Lipids from Oleaginous Yeast, ACS Sustain. Chem. Eng. (2018). https://doi.org/10.1021/acssuschemeng.7b01874.

[17] R.M. Taskova, H. Zorn, U. Krings, H. Bouws, R.G. Berger, A comparison of cell wall disruption techniques for the isolation of intracellular metabolites from Pleurotus and Lepista sp., Zeitschrift Fur Naturforsch. - Sect. C J. Biosci. (2006). https://doi.org/10.1515/znc-2006-5-608.

[18] J. FOLCH, M. LEES, G.H. SLOANE STANLEY, A simple method for the isolation and purification of total lipides from animal tissues., J. Biol. Chem. (1957). https://doi.org/10.3989/scimar.2005.69n187.

[19] A. Vermassen, S. Leroy, R. Talon, C. Provot, M. Popowska, M. Desvaux, Cell wall hydrolases in bacteria: Insight on the diversity of cell wall amidases, glycosidases and peptidases toward peptidoglycan, Front. Microbiol. (2019). https://doi.org/10.3389/fmicb.2019.00331.

[20] D. Wang, Y. Li, X. Hu, W. Su, M. Zhong, Combined enzymatic and mechanical cell disruption and lipid extraction of green alga Neochloris oleoabundans, Int. J. Mol. Sci. (2015). https://doi.org/10.3390/ijms16047707.

[21] E.J. Dufourc, Sterols and membrane dynamics, J. Chem. Biol. (2008). https://doi.org/10.1007/s12154-008-0010-6.

[22] L. Gabitova, A. Gorin, I. Astsaturov, Molecular pathways: Sterols and receptor signaling in cancer, Clin. Cancer Res. (2014). https://doi.org/10.1158/1078-0432.CCR-13-0122.

[23] D. Casares, P. V. Escribá, C.A. Rosselló, Membrane lipid composition: Effect on membrane and organelle structure, function and compartmentalization and therapeutic avenues, Int. J. Mol. Sci. (2019). https://doi.org/10.3390/ijms20092167.

[24] X. Wang, S.P. Devaiah, W. Zhang, R. Welti, Signaling functions of phosphatidic acid, Prog. Lipid Res. (2006). https://doi.org/10.1016/j.plipres.2006.01.005.

[25] A. Boucharaba, B. Guillet, F. Menaa, M. Hneino, A.J. Van Wijnen, P. Clézardin, O. Peyruchaud, Bioactive lipids lysophosphatidic acid and sphingosine 1-phosphate mediate breast cancer cell biological functions through distinct mechanisms, Oncol. Res. (2009). https://doi.org/10.3727/096504009790217399.

[26] B. Worley, R. Powers, Multivariate Analysis in Metabolomics, Curr. Metabolomics. (2013). https://doi.org/10.2174/2213235x11301010092.

[27] R.A. van den Berg, H.C.J. Hoefsloot, J.A. Westerhuis, A.K. Smilde, M.J. van der Werf, Centering, scaling, and transformations: Improving the biological information content of metabolomics data, BMC Genomics. (2006). https://doi.org/10.1186/1471-2164-7-142.

[28] X. Luo, S. Zhao, T. Huan, D. Sun, R.M.N. Friis, M.C. Schultz, L. Li, High-performance chemical isotope labeling liquid chromatography-mass spectrometry for profiling the metabolomic reprogramming elicited by ammonium limitation in yeast, J. Proteome Res. (2016). https://doi.org/10.1021/acs.jproteome.6b00070.

[29] J.Y. Lee, C. Yoo, S.Y. Jun, C.Y. Ahn, H.M. Oh, Comparison of several methods for effective lipid extraction from microalgae, in: Bioresour. Technol., 2010. https://doi.org/10.1016/j.biortech.2009.03.058.

[30] A. Rodríguez, M. Vaneechoutte, Comparison of the efficiency of different cell lysis methods and different commercial methods for RNA extraction from Candida albicans stored in RNAlater, BMC Microbiol. (2019). https://doi.org/10.1186/s12866-019-1473-z.

[31] J.N. Myers, P. V. Rekhadevi, A. Ramesh, Comparative evaluation of different cell lysis and extraction methods for studying benzo(a)pyrene metabolism in HT-29 colon cancer cell cultures, Cell. Physiol. Biochem. (2011). https://doi.org/10.1159/000331732.

[32] A.R. Byreddy, A. Gupta, C.J. Barrow, M. Puri, Comparison of cell disruption methods for improving lipid extraction from thraustochytrid strains, Mar. Drugs. (2015). https://doi.org/10.3390/md13085111.

[33] H.Y. Kim, K.M. Lee, S.H. Kim, Y.J. Kwon, Y.J. Chun, H.K. Choi, Comparative metabolic and lipidomic profiling of human breast cancer cells with different metastatic potentials, Oncotarget. (2016). https://doi.org/10.18632/oncotarget.11560.

[34] Y.P. Kang, J.H. Yoon, N.P. Long, G.B. Koo, H.J. Noh, S.J. Oh, S.B. Lee, H.M. Kim, J.Y. Hong, W.J. Lee, S.J. Lee, S.S. Hong, S.W. Kwon, Y.S. Kim, Spheroid-induced epithelial-mesenchymal transition provokes global alterations of breast cancer lipidome: A multi-layered omics analysis, Front.

Oncol. (2019). https://doi.org/10.3389/fonc.2019.00145.

[35] B. MacLean, D.M. Tomazela, S.E. Abbatiello, S. Zhang, J.R. Whiteaker, A.G. Paulovich, S.A. Carr, M.J. MacCoss, Effect of collision energy optimization on the measurement of peptides by selected reaction monitoring (SRM) mass spectrometry, Anal. Chem. (2010). https://doi.org/10.1021/ac102179j.

[36] G. Van Meer, D.R. Voelker, G.W. Feigenson, Membrane lipids: Where they are and how they behave, Nat. Rev. Mol. Cell Biol. (2008). https://doi.org/10.1038/nrm2330.

[37] C.R. Gault, L.M. Obeid, Y.A. Hannun, An overview of sphingolipid metabolism: From synthesis to breakdown, Adv. Exp. Med. Biol. (2010). https://doi.org/10.1007/978-1-4419-6741-1_1.

[38] M.L. Kraft, Sphingolipid organization in the plasma membrane and the mechanisms that influence it, Front. Cell Dev. Biol. (2017). https://doi.org/10.3389/fcell.2016.00154.

Chapter 4: Conclusions and Future Work

4.1: Thesis Summary

The application of liquid chromatography mass spectrometry in the research of cellular lipidomics had become popular due to its ability to reduce the complexity of biological matrices, and the high sensitivity which enables the detection of low abundant lipids. In Chapter 2, several lipid extraction methods were compared using yeast cells to determine the optimal protocol for lipid extraction. Several factors such as cost, time, reproducibility, and extraction efficiency were evaluated. Although the Folch protocol was not as efficient in extracting lipids, the method was more reproducible and more time efficient in contrast to the other protocols compared. The modified Folch extraction protocol was monitored for repeatability through the extraction of yeast samples on different days. It was found through the generation of PCA plots, that samples extracted on different days had very little variability. We applied the modified Folch protocol for the MSMS analysis of *Saccharomyces cerevisiae* and were able to identify 401 and 398 respective features through Metaboscape 4.0 and LipidMatch annotation software. 207 of the lipids were corroborated between the two software, helping validate our findings. Our lipid identifications were compared to similar untargeted MSMS lipidomics studies of yeast cells, and demonstrated that our method was comprehensive in defining the lipidome of *Saccharomyces cerevisiae*. We also noted a high number of unannotated spectra that went unmatched due to the lack of coverage provided by lipid libraries, which was validated through the manual interpretation of ergosterol from our unannotated spectra.

Chapter 3 investigated the optimal cell lysis technique for the disruption of MCF-7 breast cancer cells. Thermal lysis through freeze-thaw cycles using liquid nitrogen were compared against bead lysis with the aid of a vortex. Through monitoring the cell lysis efficiency, reproducibility, and viewing how

well cells homogenized after lysis, we were able to conclude that bead disruption was more effective in lysing breast cancer cells. Our lipidomics protocol, which utilized unique MSMS collision energies for specific lipid classes, was applied for MSMS analysis of MCF-7 breast cancer cells for lipidomics profiling. 398 features were successfully annotated through Metaboscape 4.0 and an additional 472 features via LipidMatch. 205 of the lipids were able to be corroborated between the two software. Past literature on untargeted lipid profiling of MCF-7 cells was compared to evaluate the effectiveness of our protocol. Our method had identified more lipids in every lipid class compared with the exception of PS, and detected lipid classes such as FAs, BMPs, CEs, CLs, DGs which were not found in the reference studies. The high level of coverage with our technique suggested that the MCF-7 lipidome diversity was far greater than previously reported.

4.2: Future Work

We hope to expand the coverage of this protocol by integrating chemical isotope labelling (CIL) for metabolomics profiling. This can be achieved by extracting the top aqueous layer during solvent extraction in the Folch protocol, such that the top aqueous layer would extract polar metabolites, while the bottom DCM layer would extract lipids. By merging these techniques together, not only would the method provide a more comprehensive view on the metabolome and lipidome of cells, it would also reduce sample consumption. Cell samples in which only a limited number of cells are available, such as in clinical studies, would particularly benefit from the amount of sample required for complete metabolite profiling. Our research group already has CIL LC-MS based protocols for the profiling of amine/phenol, carboxylic, hydroxyl, and carbonyl submetabolomes, and some have even been applied for determining the metabolome of several cell lines[1][2].

With the excellent lipidomics coverage of our protocol, hopefully biomarker analysis of cell lines can be explored in the near future. Previous literature has found substantial changes in the lipidome of cancer cells compared to healthy cells, along with changes relating to the various stages of metastasis[3]-[5]. Typically cancer cells express increased expression of lipids and metabolites required for oncogenic processes[3], but the lack of coverage through the techniques employed tends limits the information obtained. By comparing the lipidome profiles and their relative intensities between normal and diseased cells using our method, potential biomarkers or insights into disease progression might be discovered.

4.3: Literature Cited

[1] X. Luo, S. Zhao, T. Huan, D. Sun, R.M.N. Friis, M.C. Schultz, L. Li, High-performance chemical isotope labeling liquid chromatography-mass spectrometry for profiling the metabolomic reprogramming elicited by ammonium limitation in yeast, J. Proteome Res. (2016). https://doi.org/10.1021/acs.jproteome.6b00070.

[2] X. Luo, L. Li, Metabolomics of Small Numbers of Cells: Metabolomic Profiling of 100, 1000, and 10000 Human Breast Cancer Cells, Anal. Chem. (2017). https://doi.org/10.1021/acs.analchem.7b03100.

[3] J. Roy, P. Dibaeinia, T.M. Fan, S. Sinha, A. Das, Global analysis of osteosarcoma lipidomes reveal altered lipid profiles in metastatic versus nonmetastatic cells, J. Lipid Res. (2019). https://doi.org/10.1194/jlr.M088559.

[4] F.F. Eiriksson, M.K. Nøhr, M. Costa, S.K. Bödvarsdottir, H.M. Ögmundsdottir, M. Thorsteinsdottir, Lipidomic study of cell lines reveals differences between breast cancer subtypes, PLoS One. (2020). https://doi.org/10.1371/journal.pone.0231289.

[5] H.Y. Kim, K.M. Lee, S.H. Kim, Y.J. Kwon, Y.J. Chun, H.K. Choi, Comparative metabolic and lipidomic profiling of human breast cancer cells with different metastatic potentials, Oncotarget. (2016). https://doi.org/10.18632/oncotarget.11560.

Bibliography

[1] Dichloromethane Profile, (n.d.). https://www.carexcanada.ca/profile/dichloromethane/ (accessed June 19, 2020).

[2] Chloroform Profile, (n.d.). https://www.carexcanada.ca/profile/chloroform/ (accessed June 19, 2020).

[3] H.M. Adams, L.R. Joyce, Z. Guan, R.L. Akins, K.L. Palmer, Streptococcus mitis and S. oralis lack a requirement for CdsA, the enzyme required for synthesis of major membrane phospholipids in bacteria, Antimicrob. Agents Chemother. (2017). https://doi.org/10.1128/AAC.02552-16.

[4] D.R. Allen, B.C. McWhinney, Quadrupole Time-of-Flight Mass Spectrometry: A Paradigm Shift in Toxicology Screening Applications, Clin. Biochem. Rev. (2019). https://doi.org/10.33176/aacb-19-00023.

[5] K. Appala, K. Bimpeh, C. Freeman, K.M. Hines, Recent applications of mass spectrometry in bacterial lipidomics, Anal. Bioanal. Chem. (2020). https://doi.org/10.1007/s00216-020-02541-8.

[6] I. Aretz, D. Meierhofer, Advantages and pitfalls of mass spectrometry based metabolome profiling in systems biology, Int. J. Mol. Sci. (2016). https://doi.org/10.3390/ijms17050632.

[7] A. Ayala, M.F. Muñoz, S. Argüelles, Lipid peroxidation: Production, metabolism, and signaling mechanisms of malondialdehyde and 4-hydroxy-2-nonenal, Oxid. Med. Cell. Longev. (2014). https://doi.org/10.1155/2014/360438.

[8] E.G. BLIGH, W.J. DYER, A rapid method of total lipid extraction and purification., Can. J. Biochem. Physiol. (1959). https://doi.org/10.1139/o59-099.

[9] S. Borgquist, T. Butt, P. Almgren, D. Shiffman, T. Stocks, M. Orho-Melander, J. Manjer, O. Melander, Apolipoproteins, lipids and risk of cancer, Int. J. Cancer. (2016). https://doi.org/10.1002/ijc.30013.

[10] A. Boucharaba, B. Guillet, F. Menaa, M. Hneino, A.J. Van Wijnen, P. Clézardin, O. Peyruchaud, Bioactive lipids lysophosphatidic acid and sphingosine 1-phosphate mediate breast cancer cell biological functions through distinct mechanisms, Oncol. Res. (2009). https://doi.org/10.3727/096504009790217399.

[11] C. Breil, M. Abert Vian, T. Zemb, W. Kunz, F. Chemat, “Bligh and Dyer” and Folch methods for solid–liquid–liquid extraction of lipids from microorganisms. Comprehension of solvatation mechanisms and towards substitution with alternative solvents, Int. J. Mol. Sci. (2017). https://doi.org/10.3390/ijms18040708.

[12] S.B. Breitkopf, S.J.H. Ricoult, M. Yuan, Y. Xu, D.A. Peake, B.D. Manning, J.M. Asara, A relative quantitative positive/negative ion switching method for untargeted lipidomics via high resolution LC-MS/MS from any biological source, Metabolomics. (2017). https://doi.org/10.1007/s11306-016-1157-8.

[13] R.B. Brown, J. Audet, Current techniques for single-cell lysis, J. R. Soc. Interface. (2008). https://doi.org/10.1098/rsif.2008.0009.focus.

[14] K.D. Bruce, A. Zsombok, R.H. Eckel, Lipid processing in the brain: A key regulator of systemic metabolism, Front. Endocrinol. (Lausanne). (2017). https://doi.org/10.3389/fendo.2017.00060.

[15] B. Brügger, Lipidomics: Analysis of the Lipid Composition of Cells and Subcellular Organelles by Electrospray Ionization Mass Spectrometry, Annu. Rev. Biochem. (2014). https://doi.org/10.1146/annurev-biochem-060713-035324.

[16] A.R. Byreddy, A. Gupta, C.J. Barrow, M. Puri, Comparison of cell disruption methods for improving lipid extraction from thraustochytrid strains, Mar. Drugs. (2015). https://doi.org/10.3390/md13085111.

[17] Canadian Cancer Statistics Advisory Committee, Canadian Cancer Statistics 2019, 2019.

[18] C.R. Canez, S.W.J. Shields, M. Bugno, K. V. Wasslen, H.P. Weinert, W.G. Willmore, J.M. Manthorpe, J.C. Smith, Trimethylation Enhancement Using 13C-Diazomethane (13C-TrEnDi): Increased Sensitivity and Selectivity of Phosphatidylethanolamine, Phosphatidylcholine, and Phosphatidylserine Lipids Derived from Complex Biological Samples, Anal. Chem. (2016). https://doi.org/10.1021/acs.analchem.5b04524.

[19] A. Carracedo, L.C. Cantley, P.P. Pandolfi, Cancer metabolism: Fatty acid oxidation in the limelight, Nat. Rev. Cancer. (2013). https://doi.org/10.1038/nrc3483.

[20] D. Casares, P. V. Escribá, C.A. Rosselló, Membrane lipid composition: Effect on membrane and organelle structure, function and compartmentalization and therapeutic avenues, Int. J. Mol. Sci. (2019). https://doi.org/10.3390/ijms20092167.

[21] Ş. Comşa, A.M. Cîmpean, M. Raica, The story of MCF-7 breast cancer cell line: 40 Years of experience in research, Anticancer Res. (2015).

[22] M. Cruz, M. Wang, J. Frisch-Daiello, X. Han, Improved Butanol–Methanol (BUME) Method by Replacing Acetic Acid for Lipid Extraction of Biological Samples, Lipids. (2016). https://doi.org/10.1007/s11745-016-4164-7.

[23] M.H. den Brok, T.K. Raaijmakers, E. Collado-Camps, G.J. Adema, Lipid Droplets as Immune Modulators in Myeloid Cells, Trends Immunol. (2018). https://doi.org/10.1016/j.it.2018.01.012.

[24] R. Domínguez, M. Pateiro, M. Gagaoua, F.J. Barba, W. Zhang, J.M. Lorenzo, A comprehensive review on lipid oxidation in meat and meat products, Antioxidants. (2019). https://doi.org/10.3390/antiox8100429.

[25] E.J. Dufourc, Sterols and membrane dynamics, J. Chem. Biol. (2008). https://doi.org/10.1007/s12154-008-0010-6.

[26] F.F. Eiriksson, M.K. Nøhr, M. Costa, S.K. Bödvarsdottir, H.M. Ögmundsdottir, M. Thorsteinsdottir, Lipidomic study of cell lines reveals differences between breast cancer subtypes, PLoS One. (2020). https://doi.org/10.1371/journal.pone.0231289.

[27] C.S. Ejsing, J.L. Sampaio, V. Surendranath, E. Duchoslav, K. Ekroos, R.W. Klemm, K. Simons, A. Shevchenko, Global analysis of the yeast lipidome by quantitative shotgun mass spectrometry, Proc. Natl. Acad. Sci. U. S. A. (2009). https://doi.org/10.1073/pnas.0811700106.

[28] E. Fahy, D. Cotter, M. Sud, S. Subramaniam, Lipid classification, structures and tools, Biochim. Biophys. Acta - Mol. Cell Biol. Lipids. (2011). https://doi.org/10.1016/j.bbalip.2011.06.009.

[29] E. Fahy, S. Subramaniam, R.C. Murphy, M. Nishijima, C.R.H. Raetz, T. Shimizu, F. Spener, G. Van Meer, M.J.O. Wakelam, E.A. Dennis, Update of the LIPID MAPS comprehensive classification system for lipids, J. Lipid Res. (2009). https://doi.org/10.1194/jlr.R800095-JLR200.

[30] K.R. Feingold, C. Grunfeld, The Effect of Inflammation and Infection on Lipids and Lipoproteins, 2000.

[31] J. FOLCH, M. LEES, G.H. SLOANE STANLEY, A simple method for the isolation and purification of total lipides from animal tissues., J. Biol. Chem. (1957). https://doi.org/10.3989/scimar.2005.69n187.

[32] L. Gabitova, A. Gorin, I. Astsaturov, Molecular pathways: Sterols and receptor signaling in cancer, Clin. Cancer Res. (2014). https://doi.org/10.1158/1078-0432.CCR-13-0122.

[33] Y. Gao, M.G. Ierapetritou, F.J. Muzzio, Determination of the confidence interval of the relative standard deviation using convolution, J. Pharm. Innov. (2013). https://doi.org/10.1007/s12247-012-9144-8.

[34] C.R. Gault, L.M. Obeid, Y.A. Hannun, An overview of sphingolipid metabolism: From synthesis to breakdown, Adv. Exp. Med. Biol. (2010). https://doi.org/10.1007/978-1-4419-6741-1_1.

[35] A. Geller, R. Shrestha, J. Yan, Yeast-derived β-glucan in cancer: Novel uses of a traditional therapeutic, Int. J. Mol. Sci. (2019). https://doi.org/10.3390/ijms20153618.

[36] J.P. Gillet, S. Varma, M.M. Gottesman, The clinical relevance of cancer cell lines, J. Natl. Cancer Inst. (2013). https://doi.org/10.1093/jnci/djt007.

[37] M. Gómez-Brandón, M. Lores, J. Domínguez, Comparison of extraction and derivatization methods for fatty acid analysis in solid environmental matrixes, Anal. Bioanal. Chem. (2008). https://doi.org/10.1007/s00216-008-2274-7.

[38] A.J. Hackstadt, A.M. Hess, Filtering for increased power for microarray data analysis, BMC Bioinformatics. (2009). https://doi.org/10.1186/1471-2105-10-11.

[39] X. Han, Lipidomics for studying metabolism, Nat. Rev. Endocrinol. (2016). https://doi.org/10.1038/nrendo.2016.98.

[40] R. Herzog, K. Schuhmann, D. Schwudke, J.L. Sampaio, S.R. Bornstein, M. Schroeder, A. Shevchenko, Lipidxplorer: A software for consensual cross-platform lipidomics, PLoS One. (2012). https://doi.org/10.1371/journal.pone.0029851.

[41] W. Hewelt-Belka, J. Nakonieczna, M. Belka, T. Bączek, J. Namieśnik, A. Kot-Wasik, Untargeted Lipidomics Reveals Differences in the Lipid Pattern among Clinical Isolates of Staphylococcus aureus Resistant and Sensitive to Antibiotics, J. Proteome Res. (2016). https://doi.org/10.1021/acs.jproteome.5b00915.

[42] K.M. Hines, A. Waalkes, K. Penewit, E.A. Holmes, S.J. Salipante, B.J. Werth, L. Xu, Characterization of the Mechanisms of Daptomycin Resistance among Gram-Positive Bacterial Pathogens by Multidimensional Lipidomics, MSphere. (2017). https://doi.org/10.1128/msphere.00492-17.

[43] C.S. Ho, C.W.K. Lam, M.H.M. Chan, R.C.K. Cheung, L.K. Law, L.C.W. Lit, K.F. Ng, M.W.M. Suen, H.L. Tai, Electrospray ionisation mass spectrometry: principles and clinical applications., Clin. Biochem. Rev. (2003).

[44] F.F. Hsu, Mass spectrometry-based shotgun lipidomics – a critical review from the technical point of view, Anal. Bioanal. Chem. (2018). https://doi.org/10.1007/s00216-018-1252-y.

[45] K. Ikeda, P. Maretich, S. Kajimura, The Common and Distinct Features of Brown and Beige Adipocytes, Trends Endocrinol. Metab. (2018). https://doi.org/10.1016/j.tem.2018.01.001.

[46] M.S. Islam, A. Aryasomayajula, P.R. Selvaganapathy, A review on macroscale and microscale cell lysis methods, Micromachines. (2017). https://doi.org/10.3390/mi8030083.

[47] S.R. Islam, S.K. Manna, Lipidomic analysis of cancer cell and tumor tissues, in: Methods Mol. Biol., 2019. https://doi.org/10.1007/978-1-4939-9027-6_11.

[48] C. Johnson, S. Manna, K. Krausz, J. Bonzo, R. Divelbiss, M. Hollingshead, F. Gonzalez, Global Metabolomics Reveals Urinary Biomarkers of Breast Cancer in a MCF-7 Xenograft Mouse Model, Metabolites. (2013). https://doi.org/10.3390/metabo3030658.

[49] Y.P. Kang, J.H. Yoon, N.P. Long, G.B. Koo, H.J. Noh, S.J. Oh, S.B. Lee, H.M. Kim, J.Y. Hong, W.J. Lee, S.J. Lee, S.S. Hong, S.W. Kwon, Y.S. Kim, Spheroid-induced epithelial-mesenchymal transition provokes global alterations of breast cancer lipidome: A multi-layered omics analysis, Front. Oncol. (2019). https://doi.org/10.3389/fonc.2019.00145.

[50] H.Y. Kim, K.M. Lee, S.H. Kim, Y.J. Kwon, Y.J. Chun, H.K. Choi, Comparative metabolic and lipidomic profiling of human breast cancer cells with different metastatic potentials, Oncotarget. (2016). https://doi.org/10.18632/oncotarget.11560.

[51] T. Kind, K.H. Liu, D.Y. Lee, B. Defelice, J.K. Meissen, O. Fiehn, LipidBlast in silico tandem mass spectrometry database for lipid identification, Nat. Methods. (2013). https://doi.org/10.1038/nmeth.2551.

[52] C. Klose, M.A. Surma, M.J. Gerl, F. Meyenhofer, A. Shevchenko, K. Simons, Flexibility of a eukaryotic lipidome - insights from yeast lipidomics, PLoS One. (2012). https://doi.org/10.1371/journal.pone.0035063.

[53] J.P. Koelmel, N.M. Kroeger, C.Z. Ulmer, J.A. Bowden, R.E. Patterson, J.A. Cochran, C.W.W. Beecher, T.J. Garrett, R.A. Yost, LipidMatch: An automated workflow for rule-based lipid identification using untargeted high-resolution tandem mass spectrometry data, BMC Bioinformatics. (2017). https://doi.org/10.1186/s12859-017-1744-3.

[54] M.L. Kraft, Sphingolipid organization in the plasma membrane and the mechanisms that influence it, Front. Cell Dev. Biol. (2017). https://doi.org/10.3389/fcell.2016.00154.

[55] J.S. Kruger, N.S. Cleveland, R.Y. Yeap, T. Dong, K.J. Ramirez, N.J. Nagle, A.C. Lowell, G.T. Beckham, J.D. McMillan, M.J. Biddy, Recovery of Fuel-Precursor Lipids from Oleaginous Yeast, ACS Sustain. Chem. Eng. (2018). https://doi.org/10.1021/acssuschemeng.7b01874.

[56] A. V. Lee, S. Oesterreich, N.E. Davidson, MCF-7 Cells - Changing the Course of Breast Cancer Research and Care for 45 Years, J. Natl. Cancer Inst. (2015). https://doi.org/10.1093/jnci/djv073.

[57] J.Y. Lee, C. Yoo, S.Y. Jun, C.Y. Ahn, H.M. Oh, Comparison of several methods for effective lipid extraction from microalgae, in: Bioresour. Technol., 2010. https://doi.org/10.1016/j.biortech.2009.03.058.

[58] L. Li, J. Han, Z. Wang, J. Liu, J. Wei, S. Xiong, Z. Zhao, Mass spectrometry methodology in lipid analysis, Int. J. Mol. Sci. (2014). https://doi.org/10.3390/ijms150610492.

[59] C.T. Lim, E.H. Zhou, S.T. Quek, Mechanical models for living cells - A review, J. Biomech. (2006). https://doi.org/10.1016/j.jbiomech.2004.12.008.

[60] Z. Liu, A. Logan, B.G. Cocks, S. Rochfort, Seasonal variation of polar lipid content in bovine milk, Food Chem. (2017). https://doi.org/10.1016/j.foodchem.2017.06.038.

[61] J. Long, C.-J. Zhang, N. Zhu, K. Du, Y.-F. Yin, X. Tan, D.-F. Liao, L. Qin, Lipid metabolism and carcinogenesis, cancer development., Am. J. Cancer Res. (2018).

[62] X. Luo, L. Li, Metabolomics of Small Numbers of Cells: Metabolomic Profiling of 100, 1000, and 10000 Human Breast Cancer Cells, Anal. Chem. (2017). https://doi.org/10.1021/acs.analchem.7b03100.

[63] X. Luo, S. Zhao, T. Huan, D. Sun, R.M.N. Friis, M.C. Schultz, L. Li, High-performance chemical isotope labeling liquid chromatography-mass spectrometry for profiling the metabolomic reprogramming elicited by ammonium limitation in yeast, J. Proteome Res. (2016). https://doi.org/10.1021/acs.jproteome.6b00070.

[64] B. MacLean, D.M. Tomazela, S.E. Abbatiello, S. Zhang, J.R. Whiteaker, A.G. Paulovich, S.A. Carr, M.J. MacCoss, Effect of collision energy optimization on the measurement of peptides by

selected reaction monitoring (SRM) mass spectrometry, Anal. Chem. (2010). https://doi.org/10.1021/ac102179j.

[65] E.K. Matich, M. Ghafari, E. Camgoz, E. Caliskan, B.A. Pfeifer, B.Z. Haznedaroglu, G.E. Atilla-Gokcumen, Time-series lipidomic analysis of the oleaginous green microalga species Ettlia oleoabundans under nutrient stress, Biotechnol. Biofuels. (2018). https://doi.org/10.1186/s13068-018-1026-y.

[66] V. Matyash, G. Liebisch, T. V. Kurzchalia, A. Shevchenko, D. Schwudke, Lipid extraction by methyl-terf-butyl ether for high-throughput lipidomics, in: J. Lipid Res., 2008. https://doi.org/10.1194/jlr.D700041-JLR200.

[67] S. Mohammadi, B. Saberidokht, S. Subramaniam, A. Grama, Scope and limitations of yeast as a model organism for studying human tissue-specific pathways, BMC Syst. Biol. (2015). https://doi.org/10.1186/s12918-015-0253-0.

[68] E.. Morgan, Vogel's textbook of practical organic chemistry. 5th edn., Endeavour. (1990). https://doi.org/10.1016/0160-9327(90)90017-I.

[69] L.H. Münger, S. Boulos, L. Nyström, UPLC-MS/MS based identification of dietary steryl glucosides by investigation of corresponding free sterols, Front. Chem. (2018). https://doi.org/10.3389/fchem.2018.00342.

[70] S.A. Murphy, A. Nicolaou, Lipidomics applications in health, disease and nutrition research, Mol. Nutr. Food Res. (2013). https://doi.org/10.1002/mnfr.201200863.

[71] J.N. Myers, P. V. Rekhadevi, A. Ramesh, Comparative evaluation of different cell lysis and extraction methods for studying benzo(a)pyrene metabolism in HT-29 colon cancer cell cultures, Cell. Physiol. Biochem. (2011). https://doi.org/10.1159/000331732.

[72] A. V. Oliveira, R. Vilaça, C.N. Santos, V. Costa, R. Menezes, Exploring the power of yeast to model aging and age-related neurodegenerative disorders, Biogerontology. (2017). https://doi.org/10.1007/s10522-016-9666-4.

[73] C. Pitman, W. LaCourse, Desorption Atmospheric Pressure Chemical Ionization: A Brief Review, Anal. Chim. Acta. (2020). https://doi.org/https://doi.org/10.1016/j.aca.2020.05.073.

[74] E. Rampler, C. Coman, G. Hermann, A. Sickmann, R. Ahrends, G. Koellensperger, LILY-lipidome isotope labeling of yeast:: In vivo synthesis of 13C labeled reference lipids for quantification by mass spectrometry, Analyst. (2017). https://doi.org/10.1039/c7an00107j.

[75] M.L. Rodrigues, The multifunctional fungal ergosterol, MBio. (2018). https://doi.org/10.1128/mBio.01755-18.

[76] A. Rodríguez, M. Vaneechoutte, Comparison of the efficiency of different cell lysis methods and different commercial methods for RNA extraction from Candida albicans stored in RNAlater, BMC Microbiol. (2019). https://doi.org/10.1186/s12866-019-1473-z.

[77] L. Rodríguez-Berdini, B.L. Caputto, Lipid metabolism in neurons: A brief story of a novel c-Fos-dependent mechanism for the regulation of their synthesis, Front. Cell. Neurosci. (2019). https://doi.org/10.3389/fncel.2019.00198.

[78] E.R. Rojas, G. Billings, P.D. Odermatt, G.K. Auer, L. Zhu, A. Miguel, F. Chang, D.B. Weibel, J.A. Theriot, K.C. Huang, The outer membrane is an essential load-bearing element in Gram-negative bacteria, Nature. (2018). https://doi.org/10.1038/s41586-018-0344-3.

[79] J. Roy, P. Dibaeinia, T.M. Fan, S. Sinha, A. Das, Global analysis of osteosarcoma lipidomes reveal altered lipid profiles in metastatic versus nonmetastatic cells, J. Lipid Res. (2019). https://doi.org/10.1194/jlr.M088559.

[80] W. Runguphan, J.D. Keasling, Metabolic engineering of Saccharomyces cerevisiae for production of fatty acid-derived biofuels and chemicals, Metab. Eng. (2014). https://doi.org/10.1016/j.ymben.2013.07.003.

[81] S. Sakaguchi, T. Yamaguchi, T. Nomura, M. Ono, Regulatory T Cells and Immune Tolerance, Cell. (2008). https://doi.org/10.1016/j.cell.2008.05.009.

[82] R. Salari, R. Salari, Investigation of the Best Saccharomyces cerevisiae Growth Condition, Electron. Physician. (2017). https://doi.org/10.19082/3592.

[83] C. Schiffman, L. Petrick, K. Perttula, Y. Yano, H. Carlsson, T. Whitehead, C. Metayer, J. Hayes, S. Rappaport, S. Dudoit, Filtering procedures for untargeted lc-ms metabolomics data, BMC Bioinformatics. (2019). https://doi.org/10.1186/s12859-019-2871-9.

[84] S.W.J. Shields, C.R. Canez, K. V. Wasslen, H. Lee, D. Stalinski, L. Trouborst, S. Joudan, S. Whitton, H.P. Weinert, J.M. Manthorpe, J.C. Smith, Enhancing the analysis of complex lipid samples through developments in chromatography and chemical derivatization, in: NATO Sci. Peace Secur. Ser. A Chem. Biol., 2017. https://doi.org/10.1007/978-94-024-1113-3_11.

[85] K. Sidiropoulou, E.K. Pissadaki, P. Poirazi, Inside the brain of a neuron, EMBO Rep. (2006). https://doi.org/10.1038/sj.embor.7400789.

[86] B. Silva Barbosa Correia, R. Susana Torrinhas, W. Yutaka Ohashi, L. Tasic, Analytical Tools for Lipid Assessment in Biological Assays, in: Adv. Lipid Metab., 2020. https://doi.org/10.5772/intechopen.81523.

[87] R. Simstein, M. Burow, A. Parker, C. Weldon, B. Beckman, Apoptosis, chemoresistance, and breast cancer: Insights from the MCF-7 cell model system, Exp. Biol. Med. (2003). https://doi.org/10.1177/153537020322800903.

[88] P. Sun, S. Xia, B. Lal, X. Shi, K.S. Yang, P.A. Watkins, J. Laterra, Lipid metabolism enzyme ACSVL3 supports glioblastoma stem cell maintenance and tumorigenicity, BMC Cancer. (2014). https://doi.org/10.1186/1471-2407-14-401.

[89] A. Swiader, H. Nahapetyan, J. Faccini, R. D'Angelo, E. Mucher, M. Elbaz, P. Boya, C. Vindis, Mitophagy acts as a safeguard mechanism against human vascular smooth muscle cell apoptosis induced by atherogenic lipids, Oncotarget. (2016). https://doi.org/10.18632/oncotarget.8936.

[90] R.M. Taskova, H. Zorn, U. Krings, H. Bouws, R.G. Berger, A comparison of cell wall disruption techniques for the isolation of intracellular metabolites from Pleurotus and Lepista sp., Zeitschrift Fur Naturforsch. - Sect. C J. Biosci. (2006). https://doi.org/10.1515/znc-2006-5-608.

[91] A.J. Taylor, A. Dexter, J. Bunch, Exploring Ion Suppression in Mass Spectrometry Imaging of a Heterogeneous Tissue, Anal. Chem. (2018). https://doi.org/10.1021/acs.analchem.7b05005.

[92] G. Tiwari, R. Tiwari, Bioanalytical method validation: An updated review, Pharm. Methods. (2010). https://doi.org/10.4103/2229-4708.72226.

[93] T.H. Toh, B.A. Prior, M.J. Van Der Merwe, Quantification of plasma membrane ergosterol of Saccharomyces cerevisiae by direct-injection atmospheric pressure chemical ionization/tandem mass spectrometry, Anal. Biochem. (2001). https://doi.org/10.1006/abio.2000.4877.

[94] U.S. Department of Health and Human Services, Report on Carcinogens, 14th Edition, 2016.

[95] C.Z. Ulmer, C.M. Jones, R.A. Yost, T.J. Garrett, J.A. Bowden, Optimization of Folch, Bligh-Dyer, and Matyash sample-to-extraction solvent ratios for human plasma-based lipidomics studies, Anal. Chim. Acta. (2018). https://doi.org/10.1016/j.aca.2018.08.004.

[96] C.Z. Ulmer, R.E. Patterson, J.P. Koelmel, T.J. Garrett, R.A. Yost, A robust lipidomics workflow for mammalian cells, plasma, and tissue using liquid-chromatography high-resolution tandem mass spectrometry, Methods Mol. Biol. (2017). https://doi.org/10.1007/978-1-4939-6996-8_10.

[97] R.A. van den Berg, H.C.J. Hoefsloot, J.A. Westerhuis, A.K. Smilde, M.J. van der Werf, Centering, scaling, and transformations: Improving the biological information content of metabolomics data, BMC Genomics. (2006). https://doi.org/10.1186/1471-2164-7-142.

[98] G. Van Meer, D.R. Voelker, G.W. Feigenson, Membrane lipids: Where they are and how they behave, Nat. Rev. Mol. Cell Biol. (2008). https://doi.org/10.1038/nrm2330.

[99] D.L. Vaux, F. Fidler, G. Cumming, Replicates and repeats—what is the difference and is it significant?, EMBO Rep. (2012). https://doi.org/10.1038/embor.2012.36.

[100] F.M. Vaz, M. Pras-Raves, A.H. Bootsma, A.H.C. van Kampen, Principles and practice of lipidomics, J. Inherit. Metab. Dis. (2014). https://doi.org/10.1007/s10545-014-9792-6.

[101] A. Vermassen, S. Leroy, R. Talon, C. Provot, M. Popowska, M. Desvaux, Cell wall hydrolases in bacteria: Insight on the diversity of cell wall amidases, glycosidases and peptidases toward peptidoglycan, Front. Microbiol. (2019). https://doi.org/10.3389/fmicb.2019.00331.

[102] S. Vinter, Variations in internal standard: An inspector's perspective, Bioanalysis. (2019). https://doi.org/10.4155/bio-2019-0232.

[103] D. Wang, Y. Li, X. Hu, W. Su, M. Zhong, Combined enzymatic and mechanical cell disruption and lipid extraction of green alga Neochloris oleoabundans, Int. J. Mol. Sci. (2015). https://doi.org/10.3390/ijms16047707.

[104] X. Wang, S.P. Devaiah, W. Zhang, R. Welti, Signaling functions of phosphatidic acid, Prog. Lipid Res. (2006). https://doi.org/10.1016/j.plipres.2006.01.005.

[105] K. Watanabe, N. Yamagiwa, Y. Torisawa, Cyclopentyl methyl ether as a new and alternative process solvent, Org. Process Res. Dev. (2007). https://doi.org/10.1021/op0680136.

[106] L.J. Wei, C. Zhang, H. Zhang, X. Wei, S.X. Li, J.T. Liu, X.B. Ren, [A case-control study on the association between serum lipid level and the risk of breast cancer]., Zhonghua Yu Fang Yi Xue Za Zhi. 50 (2016) 1091–1095. https://doi.org/10.3760/cma.j.issn.0253-9624.2016.12.013.

[107] M.R. Wenk, Lipidomics: New tools and applications, Cell. (2010). https://doi.org/10.1016/j.cell.2010.11.033.

[108] B. Worley, R. Powers, Multivariate Analysis in Metabolomics, Curr. Metabolomics. (2013). https://doi.org/10.2174/2213235x11301010092.

[109] K. Yang, X. Han, Lipidomics: Techniques, Applications, and Outcomes Related to Biomedical Sciences, Trends Biochem. Sci. (2016). https://doi.org/10.1016/j.tibs.2016.08.010.

[110] W. Zhang, D. Zhang, Q. Chen, J. Wu, Z. Ouyang, Y. Xia, Online photochemical derivatization enables comprehensive mass spectrometric analysis of unsaturated phospholipid isomers, Nat. Commun. (2019). https://doi.org/10.1038/s41467-018-07963-8.

[111] Y.J. Zhou, N.A. Buijs, V. Siewers, J. Nielsen, Fatty acid-derived biofuels and chemicals production in Saccharomyces cerevisiae, Front. Bioeng. Biotechnol. (2014). https://doi.org/10.3389/fbioe.2014.00032.

Appendix

Appendix Table 1: Summary of MSMS methods used on the yeast samples for lipid identification. CE refers to collision energy.

Lipid Classes	Mass Range (m/z)	CE (eV)	ESI Mode
Phospholipids	150	15	Neg
	350	25	
	1450	40	
	1500	45	
PE-Cer, PI-Cer, Sulf	150	10	Neg
	450	20	
	675	35	
	800	60	
	1000	80	
	1500	90	
BMP, GDG, LSL, Sph	150	30	Neg
	300	45	
	400	54	
	700	55	
	1000	65	
	1500	70	
Cer, FA, Hex-Cer, Lac-Cer, NAA, WE	150	25	Neg
	800	35	
	1000	55	
	1500	60	
Cer, CL	150	10	Neg
	650	30	
	1200	35	
	1500	45	
GDG, Sph, Sulf, WE	150	13	Pos
	650	25	
	651	40	
	1300	60	
	1500	70	
BMP, LPG, LPI, LPS, PG, PI, PS	150	10	Pos
	450	15	
	700	30	
	1300	35	
	1500	40	
DG, MG, TG	150	15	Pos
	500	20	

	700	30	
	1500	40	
Ergo, FA, Lac-Cer	150	29	Pos
	400	31	
	600	55	
	1000	70	
	1500	85	
Hex-Cer	150	20	Pos
	400	45	
	1000	60	
	1500	70	
CholE, PI-Cer, Sulf-DG	150	10	Pos
	600	15	
	850	20	
	950	35	
	1500	50	
Car, Cer, CL, LSL, NAA, PE-Cer	150	18	Pos
	600	33	
	950	45	
	1100	40	
	1500	50	
LPA, LPC, LPE, PA, PC, PE, SM	150	15	Pos
	350	20	
	600	30	
	1300	45	
	1500	50	

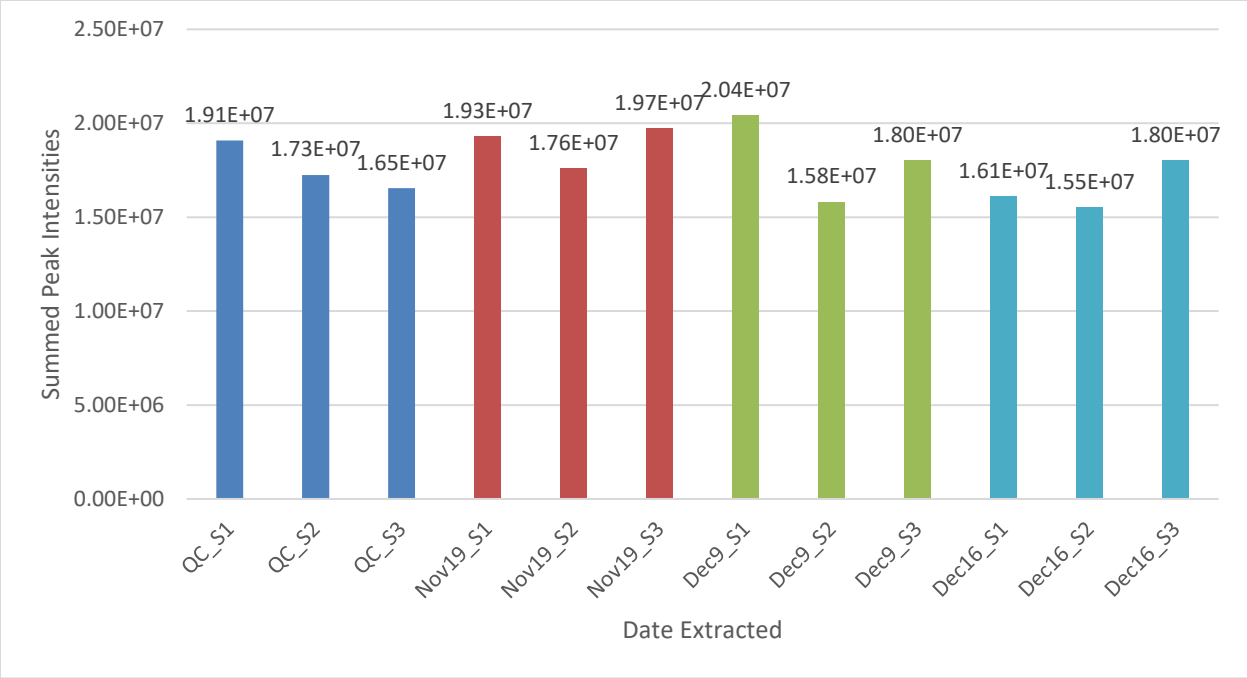

Appendix Figure 1: Summed signal intensities for all internal standards extracted from yeast cells using a modified Folch protocol. Samples were extracted on different days and run in both ESI modes.

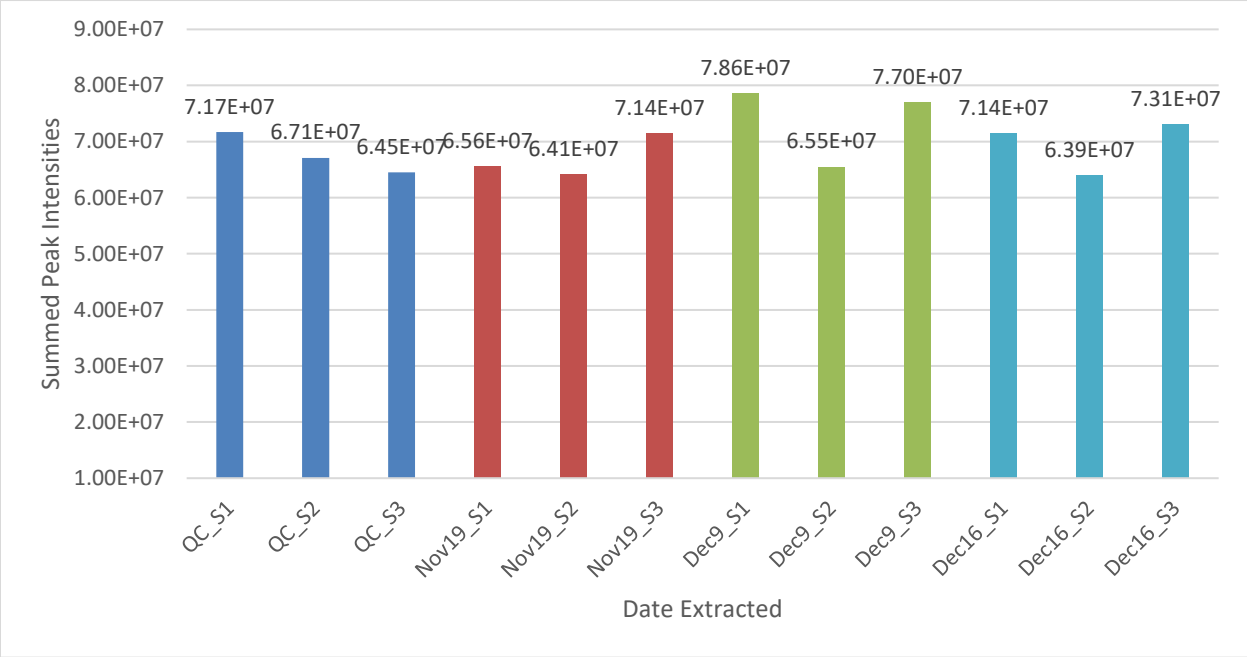

Appendix Figure 2: Summed signal intensities for putatively identified lipids extracted from yeast cells using a modified Folch protocol. Samples were extracted on different days and run in ESI positive mode.

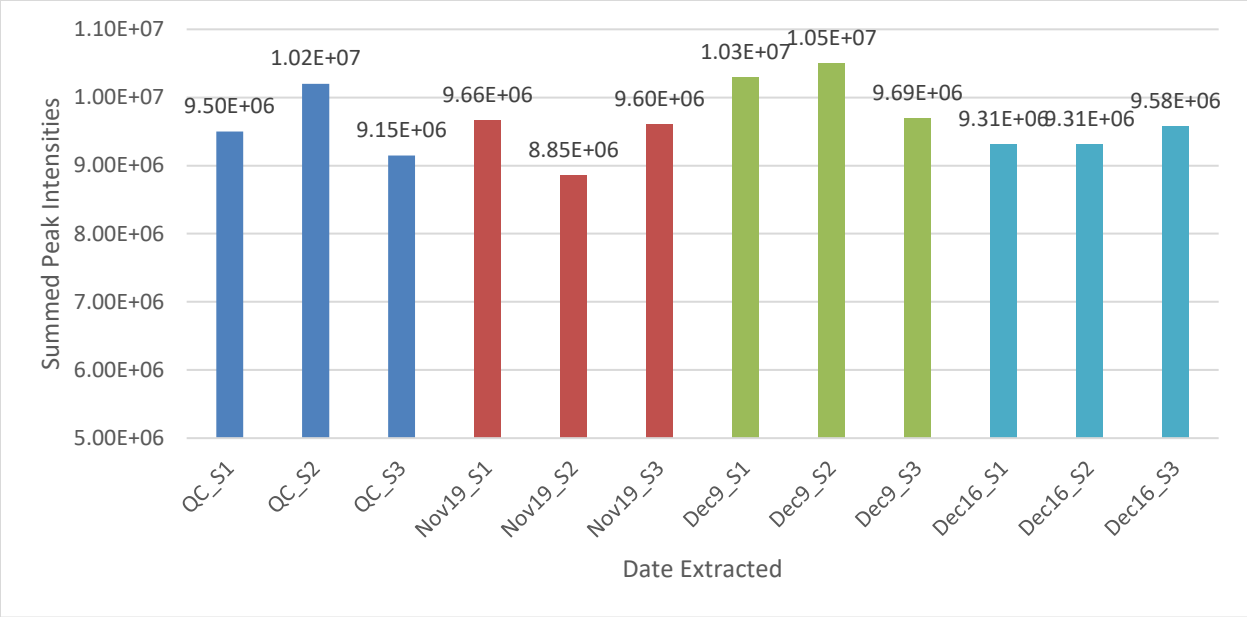

Appendix Figure 3: Summed signal intensities for putatively identified lipids extracted from yeast cells using a modified Folch protocol. Samples were extracted on different days and run in ESI negative mode.

Appendix Table 2: List of annotated lipid species detected in yeast cells through Metaboscape 4.0 libraries (LC-MS-MS Positive mode; LC-MS-MS Negative mode; MSDIAL; RIKEN Oxidized Phospholipids) and LipidMatch. Feature names in bold were detected through both annotation software.

RT [min]	Precursor Ion (m/z)	Name	Annotation Source/Library	MS/MS score	Ionization Mode
0.83	293.1791	NCGC00017248-12!2,5-dihydroxy-3-undecylcyclohexa-2,5-diene-1,4-dione	LC-MS-MS Negative Mode	997.2	Neg
0.9	213.0557	3-Phenoxybenzoic acid	LC-MS-MS Negative Mode	991.1	Neg
0.99	463.1307	NCGC00169618-04!6-[(6,8-dihydroxy-7-methoxy-3-methyl-1-oxo-3,4-dihydroisochromen-4-yl)oxy]-4,8-dihydroxy-7-methoxy-3-methyl-3,4-dihydroisochromen-1-one	LC-MS-MS Positive Mode	554.2	Pos
1.06	265.1117	4,7,8-trimethoxy-3,5-dimethylchromen-2-one	LC-MS-MS Positive Mode	401.9	Pos
1.07	344.2276	HYDROQUINIDINE	LC-MS-MS Positive Mode	116.2	Pos
1.07	256.1756	Tripelennamine	LC-MS-MS Positive Mode	210.8	Pos
1.14	272.1869	3-hydroxy-C10-homoserine lactone	LC-MS-MS Positive Mode	111	Pos
1.15	331.3114	MMV687273	LC-MS-MS Positive Mode	456.2	Pos
1.21	310.2025	Nadolol	LC-MS-MS Positive Mode	122.4	Pos

1.22	249.1498	2-[(2S,4aR,8aS)-2-hydroxy-4a-methyl-8-methylidene-3,4,5,6,7,8a-hexahydro-1H-naphthalen-2-yl]prop-2-enoic acid	LC-MS-MS Negative Mode	971.4	Neg
1.23	368.2459	Blonanserin (Lonasen)	LC-MS-MS Positive Mode	135	Pos
1.24	371.15	Arctigenin	LC-MS-MS Negative Mode	204.9	Neg
1.27	415.2118	MMV020623	LC-MS-MS Positive Mode	287.9	Pos
1.29	277.1809	C14-SAS (TENTATIVE)	LC-MS-MS Negative Mode	632	Neg
1.32	265.1479	Lauryl sulfate	LC-MS-MS Negative Mode	998.5	Neg
1.35	**510.3193**	**PC 16:0; PC 8:0-8:0; [M+H]+**	**MSDIAL-LipidDBs-VS34 /LipidMatch**	**431.9**	**Pos**
1.36	297.0823	aflatoxin B2	LC-MS-MS Positive Mode	113.8	Pos
1.37	223.0639	reticulol	LC-MS-MS Positive Mode	271.7	Pos
1.42	420.33	1_MG(22:6)+NH4	LipidMatch	N/A	Pos
1.42	343.2956	CocamidoprpylBetaine	LC-MS-MS Positive Mode	988.6	Pos
1.42	**440.2774**	**LPC 12:0; [M+H]+**	**MSDIAL-LipidDBs-VS34 /LipidMatch**	**853.6**	**Pos**
1.42	311.1688	Triptophenolide	LC-MS-MS Negative Mode	996.2	Neg
1.43	396.146	2-methoxy-3,5-dimethyl-6-[(4Z)-4-[(E)-2-methyl-3-(4-nitrophenyl)prop-2-enylidene]oxolan-2-yl]pyran-4-one	LC-MS-MS Negative Mode	217	Neg
1.45	484.27	1_LPC(12:0)+HCO2	LipidMatch	N/A	Neg
1.46	309.1742	C12-AE1S (TENTATIVE)	LC-MS-MS Negative Mode	602.7	Neg
1.49	334.3	1_MG(15:0)+NH4	LipidMatch	N/A	Pos
1.49	**466.2932**	**LPC 14:1; [M+H]+**	**MSDIAL-LipidDBs-VS34 /LipidMatch**	**869.3**	**Pos**
1.5	313.1435	Benzyl-butyl-phthalate	LC-MS-MS Positive Mode	475.2	Pos
1.5	**510.2844**	**LPC 14:1; [M+FA-H]-**	**MSDIAL-LipidDBs-VS34 /LipidMatch**	**782.7**	**Neg**
1.52	554.35	1_OxLPC(18:1(OO))+H	LipidMatch	N/A	Pos
1.53	598.34	1_OxLPC(18:1(OO))+HCO2	LipidMatch	N/A	Neg
1.53	297.0824	Flunixine	LC-MS-MS Positive Mode	501.4	Pos
1.53	221.1549	KOBUSONE	LC-MS-MS Negative Mode	127.9	Neg
1.54	306.24	1_MG(13:0)+NH4	LipidMatch	N/A	Pos
1.55	325.1845	Dodecylbenzenesulfonic acid	LC-MS-MS Negative Mode	969.7	Neg
1.57	267.1721	Tri-isobutylphosphate	LC-MS-MS Positive Mode	928.2	Pos
1.59	279.1591	Dibutyl phthalate	LC-MS-MS Positive Mode	996.9	Pos
1.59	293.1783	Tetradecylsulfate	LC-MS-MS Negative Mode	996.4	Neg
1.64	379.1917	LPA 14:1; [M-H]-	MSDIAL-LipidDBs-VS34	278.9	Neg
1.64	230.248	N,N-Dimethyldodecylamine N-oxide	LC-MS-MS Positive Mode	994.4	Pos
1.64	399.2509	Tri(butoxyethyl)phosphate	LC-MS-MS Positive Mode	958.2	Pos
1.67	369.1255	Tricresylphosphate	LC-MS-MS Positive Mode	289.5	Pos
1.69	273.1847	Galaxolidone	LC-MS-MS Positive Mode	812.3	Pos
1.71	576.41	1_LPC(22:2)+H	LipidMatch	N/A	Pos
1.71	620.44	1_OxLPC(24:1(Ke))+H	LipidMatch	N/A	Pos
1.72	339.2001	Canrenone	LC-MS-MS Negative Mode	996.5	Neg
1.73	538.32	1_LPC(16:1)+HCO2	LipidMatch	N/A	Neg

1.77	394.32	1_MG(20:5)+NH4	LipidMatch	N/A	Pos
1.77	**468.3089**	**LPC 14:0; [M+H]+**	**MSDIAL-LipidDBs-VS34 /LipidMatch**	**951.5**	**Pos**
1.78	512.3	1_LPC(14:0)+HCO2	LipidMatch	N/A	Neg
1.83	**538.3152**	**LPC 16:1; [M+FA-H]-**	**MSDIAL-LipidDBs-VS34 /LipidMatch**	**784.4**	**Neg**
1.83	**494.3244**	**PC 16:1e; PC 14:1e/2:0; [M+H]+**	**MSDIAL-LipidDBs-VS34 /LipidMatch**	**979.6**	**Pos**
1.85	**452.2774**	**LPE 16:1; [M+H]+**	**MSDIAL-LipidDBs-VS34 /LipidMatch**	**985.4**	**Pos**
1.85	463.1307	NCGC00384744-01!5-hydroxy-3-[4-hydroxy-2-[(2S,3R,4S,5S,6R)-3,4,5-trihydroxy-6-(hydroxymethyl)oxan-2-yl]oxyphenyl]-7-methoxychromen-4-one	MSDIAL-LipidDBs-VS34	711.2	Pos
1.86	450.26	1_LPE(16:1)-H	LipidMatch	N/A	Neg
1.86	288.2898	C17-Sphinganine	LC-MS-MS Positive Mode	940.3	Pos
1.86	**480.3091**	**LPC 15:1; [M+H]+**	**MSDIAL-LipidDBs-VS34 /LipidMatch**	**369.1**	**Pos**
1.87	309.2041	MLS000728650-01!	LC-MS-MS Positive Mode	273.4	Pos
1.87	297.2436	OxFA 18:0(1O(1Cyc)); [M-H]-	MSDIAL-LipidDBs-VS34	952.9	Neg
1.88	464.2785	PE 17:1e; PE 14:1e/3:0; [M-H]-	MSDIAL-LipidDBs-VS34	374.1	Neg
1.9	313.2385	FAHFA 18:0; FAHFA 2:0/16:0; [M-H]-	MSDIAL-LipidDBs-VS34	134.7	Neg
1.9	337.2351	NCGC00385898-01_C20H32O4_1-Naphthalenepentanoic acid, 5-carboxydecahydro-beta,5,8a-trimethyl-2-methylene-	LC-MS-MS Positive Mode	146.2	Pos
1.9	299.2591	OxFA 18:0(1O); [M-H]-	MSDIAL-LipidDBs-VS34	969.5	Neg
1.92	318.3004	Phytosphingosine (not validated, isomer of 1697)	LC-MS-MS Positive Mode	903	Pos
1.94	385.2372	Megestrol-17-acetate	LC-MS-MS Positive Mode	425.2	Pos
1.95	564.33	1_LPC(18:2)+HCO2	LipidMatch	N/A	Neg
2	379.1917	LPA 14:1; [M-H]-	MSDIAL-LipidDBs-VS34	276.3	Neg
2	272.2591	Myristoyl Ethanolamide	LC-MS-MS Positive Mode	396.8	Pos
2.01	**482.324**	**LPC 15:0; [M+H]+**	**MSDIAL-LipidDBs-VS34 /LipidMatch**	**400.9**	**Pos**
2.02	383.2228	5-[(Z)-12-(3,5-dihydroxyphenyl)dodec-8-enyl]benzene-1,3-diol	LC-MS-MS Negative Mode	983.3	Neg
2.02	**526.3154**	**LPC 15:0; [M+FA-H]-**	**MSDIAL-LipidDBs-VS34 /LipidMatch**	**680.5**	**Neg**
2.04	299.2017	FA 20:6; [M-H]-	MSDIAL-LipidDBs-VS34	977.7	Neg
2.09	371.1016	(E)-3-[6-[(2S,3R,4S,5S,6R)-3,4,5-trihydroxy-6-(hydroxymethyl)oxan-2-yl]oxy-1,3-benzodioxol-5-yl]prop-2-enoic acid	LC-MS-MS Positive Mode	109.1	Pos
2.09	552.33	1_LPC(17:1)+HCO2	LipidMatch	N/A	Neg
2.12	258.2794	N,N-Dimethyltetradecylamine-N-oxide	LC-MS-MS Positive Mode	997.4	Pos
2.14	513.3108	MGMG 18:3	LC-MS-MS Negative Mode	109.2	Neg
2.15	**508.3399**	**LPC 17:1; [M+H]+**	**MSDIAL-LipidDBs-VS34 /LipidMatch**	**482.9**	**Pos**
2.16	**496.3401**	**PC 16:0e; PC 14:0e/2:0; [M+H]+**	**MSDIAL-LipidDBs-VS34 /LipidMatch**	**991.5**	**Pos**
2.16	648.4682	PC 26:1; PC 10:0-16:1; [M+H]+	MSDIAL-LipidDBs-VS34	232	Pos
2.17	545.2914	MMV690028	LC-MS-MS Negative Mode	515.2	Neg
2.2	331.2843	Ceratodictyol	LC-MS-MS Positive Mode	892.4	Pos
2.21	599.3383	Deferrioxamine E	LC-MS-MS Negative Mode	869.3	Neg

2.22	452.28	1_LPE(16:0)-H	LipidMatch	N/A	Neg
2.24	566.35	1_LPC(18:1)+HCO2	LipidMatch	N/A	Neg
2.24	**522.3559**	**LPC 18:1; [M+H]+**	**MSDIAL-LipidDBs-VS34 /LipidMatch**	**986.3**	**Pos**
2.28	**480.3088**	**LPC 15:1; [M+H]+**	**MSDIAL-LipidDBs-VS34 /LipidMatch**	**457.6**	**Pos**
2.29	530.32	1_LPC(17:1)+Na	LipidMatch	N/A	Pos
2.3	636.42	1_OxLPC(24:1(Ke,OH))+H	LipidMatch	N/A	Pos
2.32	351.2511	5-(5-methoxycarbonyl-5,8a-dimethyl-2-methylidene-3,4,4a,6,7,8-hexahydro-1H-naphthalen-1-yl)-3-methylpentanoic acid	LC-MS-MS Positive Mode	181.5	Pos
2.32	301.2173	FA 20:5; [M-H]-	MSDIAL-LipidDBs-VS34	602	Neg
2.33	540.33	1_LPC(16:0)+HCO2	LipidMatch	N/A	Neg
2.33	255.233	FA 16:0; [M-H]-	MSDIAL-LipidDBs-VS34	977.1	Neg
2.33	**478.294**	**LPE 18:1; [M-H]-**	**MSDIAL-LipidDBs-VS34 /LipidMatch**	**977.5**	**Neg**
2.33	**496.3401**	**PC 16:0e; PC 14:0e/2:0; [M+H]+**	**MSDIAL-LipidDBs-VS34 /LipidMatch**	**978.6**	**Pos**
2.34	534.3	1_OxLPC(15:0(COOH))+Na	LipidMatch	N/A	Pos
2.37	452.28	1_LPE(16:0)-H	LipidMatch	N/A	Neg
2.42	**522.3559**	**LPC 18:1; [M+H]+**	**MSDIAL-LipidDBs-VS34 /LipidMatch**	**855**	**Pos**
2.45	**478.2942**	**LPE 18:1; [M-H]-**	**MSDIAL-LipidDBs-VS34 /LipidMatch**	**760.4**	**Neg**
2.45	227.2017	Myristic acid	LC-MS-MS Negative Mode	994.9	Neg
2.49	502.29	1_LPE(18:1)+Na	LipidMatch	N/A	Pos
2.5	492.31	PE 19:1e; PE 16:1e/3:0; [M-H]-	MSDIAL-LipidDBs-VS34	169.1	Neg
2.51	303.2329	FA 20:4; [M-H]-	MSDIAL-LipidDBs-VS34	778.1	Neg
2.51	754.5013	OxPE 36:4(1O); OxPE 18:1-18:3(1O) ; [M-H]-	MSDIAL-LipidDBs-VS34	202.7	Neg
2.53	253.2172	FA 16:1; [M-H]-	MSDIAL-LipidDBs-VS34	995.3	Neg
2.54	341.2699	FAHFA 20:0; FAHFA 2:0/18:0; [M-H]-	MSDIAL-LipidDBs-VS34	132.2	Neg
2.54	387.2485	Medroxyprogesteroneacetate	LC-MS-MS Positive Mode	782.4	Pos
2.6	463.2825	Methyl-mappain	LC-MS-MS Positive Mode	653.3	Pos
2.63	634.42	1_PE(13:0_15:1)+H	LipidMatch	N/A	Pos
2.72	279.233	FA 18:2; [M-H]-	MSDIAL-LipidDBs-VS34	993.2	Neg
2.74	367.2272	Drospirenone	LC-MS-MS Positive Mode	997.4	Pos
2.76	349.2416	5-(5-methoxycarbonyl-5,8a-dimethyl-2-methylidene-3,4,4a,6,7,8-hexahydro-1H-naphthalen-1-yl)-3-methylpentanoic acid	LC-MS-MS Negative Mode	982.6	Neg
2.95	396.2179	LPE 12:0; [M-H]-	MSDIAL-LipidDBs-VS34	192.6	Neg
2.99	**524.3715**	**PC 18:0e; PC 14:0e/4:0; [M+H]+**	**MSDIAL-LipidDBs-VS34 /LipidMatch**	**799.2**	**Pos**
3	282.2793	Dodemorph	LC-MS-MS Positive Mode	894.1	Pos
3.01	267.2329	FA 17:1; [M-H]-	MSDIAL-LipidDBs-VS34	991.6	Neg
3.13	617.3489	PG 25:3; PG 3:0-22:3; [M-H]-	MSDIAL-LipidDBs-VS34	155.7	Neg
3.18	305.2486	FA 20:3; [M-H]-	MSDIAL-LipidDBs-VS34	933.5	Neg
3.19	427.3896	3-Epilupeol	LC-MS-MS Positive Mode	887	Pos
3.27	**524.3715**	**PC 18:0e; PC 14:0e/4:0; [M+H]+**	**MSDIAL-LipidDBs-VS34 /LipidMatch**	**978.4**	**Pos**
3.28	**568.3624**	**LPC 18:0; [M+FA-H]-**	**MSDIAL-LipidDBs-VS34 /LipidMatch**	**664.3**	**Neg**

3.33	**480.3104**	**LPE 18:0; [M-H]-**	**MSDIAL-LipidDBs-VS34 /LipidMatch**	**895.7**	**Neg**
3.35	**550.387**	**LPC 20:1; [M+H]+**	**MSDIAL-LipidDBs-VS34 /LipidMatch**	**661**	**Pos**
3.46	255.2327	FA 16:0; [M-H]-	MSDIAL-LipidDBs-VS34	995.1	Neg
3.47	334.31	1_MG(15:0)+NH4	LipidMatch	N/A	Pos
3.47	338.3418	Erucamide	LC-MS-MS Positive Mode	979.3	Pos
3.48	421.2383	LPA 17:1; [M-H]-	MSDIAL-LipidDBs-VS34	106.9	Neg
3.51	543.3119	PA 25:3; PA 3:0-22:3; [M-H]-	MSDIAL-LipidDBs-VS34	224.1	Neg
3.53	**559.4711**	**FAHFA 36:3; FAHFA 18:1/18:2; [M-H]-**	**MSDIAL-LipidDBs-VS34 /LipidMatch**	**665.9**	**Neg**
3.54	587.3733	PA 28:2; PA 14:1-14:1; [M-H]-	MSDIAL-LipidDBs-VS34	325	Neg
3.55	362.33	1_MG(17:0)+NH4	LipidMatch	N/A	Pos
3.55	592.5307	Cer-AS d37:2; Cer-AS d19:2/18:0; [M-H]-	MSDIAL-LipidDBs-VS34	858.4	Neg
3.59	513.3007	LPA 24:4; [M-H]-	MSDIAL-LipidDBs-VS34	267.9	Neg
3.6	281.2483	FA 18:1; [M-H]-	MSDIAL-LipidDBs-VS34	993.5	Neg
3.66	402.3396	NCGC00160316-01!6,7-didehydro-26,28didemethyl-16,28-secosolanidan-3,16-diol	LC-MS-MS Positive Mode	242.6	Pos
3.79	429.336	Ergosterol Peroxide_120246	LC-MS-MS Positive Mode	116.9	Pos
4.06	774.5937	PC 35:1; PC 13:0-22:1; [M+H]+	MSDIAL-LipidDBs-VS34	246.3	Pos
4.12	**435.2541**	**LPA 18:1; [M-H]-**	**MSDIAL-LipidDBs-VS34 /LipidMatch**	**277.4**	**Neg**
4.18	269.2485	FA 17:0; [M-H]-	MSDIAL-LipidDBs-VS34	992.7	Neg
4.45	391.2846	Dioctylphthalate	LC-MS-MS Positive Mode	988.7	Pos
4.57	359.3161	1-Monostearin	LC-MS-MS Positive Mode	278.2	Pos
4.6	390.36	1_MG(19:0)+NH4	LipidMatch	N/A	Pos
4.82	465.3044	LPA 20:0; [M-H]-	MSDIAL-LipidDBs-VS34	276.6	Neg
4.83	961.606	PI 40:3; PI 20:1-20:2; [M-H]-	MSDIAL-LipidDBs-VS34	706.3	Neg
4.92	744.5834	PC 34:2e; PC 16:0e/18:2; [M+H]+	MSDIAL-LipidDBs-VS34	980.4	Pos
5.04	451.3184	(1S,2R,5R,6R,10R,13S,15S)-5-[(2R,3E,5R)-5,6-dimethylhept-3-en-2-yl]-6,10-dimethyl-16,17-dioxapentacyclo[13.2.2.0Â¹,â?¹.0Â²,â?¶.0Â¹â?°,Â¹â?µ]nonadec-18-en-13-ol	LC-MS-MS Positive Mode	991.4	Pos
5.05	**589.5179**	**FAHFA 38:2; FAHFA 18:0/20:2; [M-H]-**	**MSDIAL-LipidDBs-VS34 /LipidMatch**	**782.9**	**Neg**
5.06	297.1526	C10LAS	LC-MS-MS Negative Mode	978.6	Neg
5.06	283.2639	FA 18:0; [M-H]-	MSDIAL-LipidDBs-VS34	993.9	Neg
5.13	428.35	1_MG(22:2)+NH4	LipidMatch	N/A	Pos
5.31	749.4428	alpha-Hederin	LC-MS-MS Negative Mode	154.3	Neg
5.43	383.32	1_FAHFA(18:0/5:0)-H	LipidMatch	N/A	Neg
5.46	401.3421	7-Oxocholesterol	LC-MS-MS Positive Mode	478.3	Pos
5.6	725.43	1_PI(10:0_16:0)-H	LipidMatch	N/A	Neg
5.62	**622.4445**	**PC 24:0; PC 12:0-12:0; [M+H]+**	**MSDIAL-LipidDBs-VS34 /LipidMatch**	**748**	**Pos**
5.65	622.44	1_OxLPC(24:1(OH))+H	LipidMatch	N/A	Pos
5.72	865.5105	OxPI 34:2(2O); OxPI 16:0-18:2(2O); [M-H]-	MSDIAL-LipidDBs-VS34	802.1	Neg
5.77	751.4409	PI 28:1; PI 12:0-16:1; [M-H]-	MSDIAL-LipidDBs-VS34	885.4	Neg

5.8	583.3432	PA 28:4; PA 4:0-24:4; [M-H]-	MSDIAL-LipidDBs-VS34	254.7	Neg
5.82	648.46	1_PC(10:0_16:1)+H	LipidMatch	N/A	Pos
5.97	677.4348	PG 29:1; PG 12:0-17:1; [M-H]-	MSDIAL-LipidDBs-VS34	320.6	Neg
6.11	297.2798	FA 19:0; [M-H]-	MSDIAL-LipidDBs-VS34	756.5	Neg
6.28	674.4765	PC 28:2; PC 14:1-14:1; [M+H]+	MSDIAL-LipidDBs-VS34	902.8	Pos
6.3	790.52	1_OxPC(16:1_16:1(OH))+HCO2	LipidMatch	N/A	Neg
6.34	747.54	1_PG(17:1_17:1)+H	LipidMatch	N/A	Pos
6.39	702.47	1_OxPE(16:1_16:1(OH))-H	LipidMatch	N/A	Neg
6.46	659.48	1_PA(16:1_17:1)+H	LipidMatch	N/A	Pos
6.85	397.33	1_FAHFA(18:0/6:0)-H	LipidMatch	N/A	Neg
6.91	772.6148	PC 36:2e; PC 14:0e/22:2; [M+H]+	MSDIAL-LipidDBs-VS34	692.6	Pos
7.14	587.3742	PA 28:2; PA 14:1-14:1; [M-H]-	MSDIAL-LipidDBs-VS34	273.7	Neg
7.21	311.2954	FA 20:0; [M-H]-	MSDIAL-LipidDBs-VS34	908.3	Neg
7.28	337.3111	FA 22:1; [M-H]-	MSDIAL-LipidDBs-VS34	985.7	Neg
7.62	**753.4566**	**PI 28:0; PI 14:0-14:0; [M-H]-**	**MSDIAL-LipidDBs-VS34 /LipidMatch**	**896.3**	**Neg**
7.71	**650.4763**	**PC 26:0; PC 13:0-13:0; [M+H]+**	**MSDIAL-LipidDBs-VS34 /LipidMatch**	**955**	**Pos**
7.72	694.47	1_PC(10:0_16:0)+HCO2	LipidMatch	N/A	Neg
7.78	790.5597	PS 36:1; PS 20:0-16:1; [M+H]+	MSDIAL-LipidDBs-VS34	172	Pos
7.79	834.55	1_OxPC(16:1_18:1(OO))+HCO2	LipidMatch	N/A	Neg
7.84	**676.4917**	**PC 28:1; PC 12:0-16:1; [M+H]+**	**MSDIAL-LipidDBs-VS34 /LipidMatch**	**988.3**	**Pos**
7.84	**779.4729**	**PI 30:1; PI 14:0-16:1; [M-H]-**	**MSDIAL-LipidDBs-VS34 /LipidMatch**	**882.9**	**Neg**
7.86	**720.4824**	**PC 28:1; PC 12:0-16:1; [M+FA-H]-**	**MSDIAL-LipidDBs-VS34 /LipidMatch**	**795.6**	**Neg**
7.93	728.5229	PC 32:3; PC 12:0-20:3; [M+H]+	MSDIAL-LipidDBs-VS34	972.8	Pos
7.99	**805.4875**	**PI 32:2; PI 16:1-16:1; [M-H]-**	**MSDIAL-LipidDBs-VS34 /LipidMatch**	**892.7**	**Neg**
8.02	**634.4511**	**PE 28:1; PE 12:0-16:1; [M+H]+**	**MSDIAL-LipidDBs-VS34 /LipidMatch**	**974.7**	**Pos**
8.04	**632.4298**	**PE 28:1; PE 12:0-16:1; [M-H]-**	**MSDIAL-LipidDBs-VS34 /LipidMatch**	**763.2**	**Neg**
8.07	425.3632	DINCH	LC-MS-MS Positive Mode	102.5	Pos
8.12	**702.5073**	**PC 30:2; PC 15:1-15:1; [M+H]+**	**MSDIAL-LipidDBs-VS34 /LipidMatch**	**973.5**	**Pos**
8.13	746.5	1_PC(14:1_16:1)+HCO2	LipidMatch	N/A	Neg
8.3	**660.4611**	**PE 30:2; PE 15:1-15:1; [M+H]+**	**MSDIAL-LipidDBs-VS34 /LipidMatch**	**964**	**Pos**
8.31	**658.4456**	**PE 30:2; PE 14:1-16:1; [M-H]-**	**MSDIAL-LipidDBs-VS34 /LipidMatch**	**519.9**	**Neg**
8.33	736.51	1_BMP(16:1_16:1)+NH4	LipidMatch	N/A	Pos
8.38	791.5265	GlcADG 36:4; GlcADG 18:2-18:2; [M-H]-	MSDIAL-LipidDBs-VS34	470.2	Neg
8.41	**730.4665**	**PS 32:2; PS 16:1-16:1; [M-H]-**	**MSDIAL-LipidDBs-VS34 /LipidMatch**	**663.3**	**Neg**
8.45	714.47	1_Plasmenyl-PS(P-16:1/16:1)-H	LipidMatch	N/A	Neg
8.45	613.3906	PA 30:3; PA 13:1-17:2; [M-H]-	MSDIAL-LipidDBs-VS34	224	Neg
8.51	728.5228	PC 32:3; PC 16:1-16:2; [M+H]+	MSDIAL-LipidDBs-VS34	987.1	Pos
8.52	772.5135	PS 35:2; PS 16:1-19:1; [M-H]-	MSDIAL-LipidDBs-VS34	462.9	Neg
8.6	778.5412	PC 36:6; PC 18:3-18:3; [M+H]+	MSDIAL-LipidDBs-VS34	932.9	Pos
8.69	543.3114	PA 25:3; PA 3:0-22:3; [M-H]-	MSDIAL-LipidDBs-VS34	246.8	Neg

8.7	684.4613	PE 32:3; PE 16:1-16:2; [M-H]-	MSDIAL-LipidDBs-VS34	697.8	Neg
8.72	**717.4682**	**PG 32:2; PG 16:1-16:1; [M-H]-**	**MSDIAL-LipidDBs-VS34 /LipidMatch**	**348.5**	**Neg**
8.75	883.5202	OxPI 34:1(3O); OxPI 16:0-18:1(3O); [M-H]-	MSDIAL-LipidDBs-VS34	117.8	Neg
8.78	**793.479**	**PA 44:11; PA 22:5-22:6; [M-H]-**	**MSDIAL-LipidDBs-VS34 /LipidMatch**	**245.2**	**Neg**
8.79	**793.4885**	**PI 31:1; PI 15:0-16:1; [M-H]-**	**MSDIAL-LipidDBs-VS34 /LipidMatch**	**844.2**	**Neg**
8.94	**819.5022**	**PI 33:2; PI 15:1-18:1; [M-H]-**	**MSDIAL-LipidDBs-VS34 /LipidMatch**	**812.1**	**Neg**
8.96	**754.538**	**PC 34:4; PC 17:2-17:2; [M+H]+**	**MSDIAL-LipidDBs-VS34 /LipidMatch**	**952.6**	**Pos**
9.03	**716.523**	**PC 31:2; PC 15:1-16:1; [M+H]+**	**MSDIAL-LipidDBs-VS34 /LipidMatch**	**956.1**	**Pos**
9.04	**760.5137**	**PS 34:1; PS 19:0-15:1; [M-H]-**	**MSDIAL-LipidDBs-VS34 /LipidMatch**	**113.6**	**Neg**
9.06	606.335	PS 23:1; PS 7:0-16:1; [M-H]-	MSDIAL-LipidDBs-VS34	302.6	Neg
9.1	769.4671	Ginsenoside F3	LC-MS-MS Negative Mode	210.5	Neg
9.21	**672.4619**	**PE 31:2; PE 15:1-16:1; [M-H]-**	**MSDIAL-LipidDBs-VS34 /LipidMatch**	**814.6**	**Neg**
9.24	**674.4762**	**PE 31:2; PE 15:1-16:1; [M+H]+**	**MSDIAL-LipidDBs-VS34 /LipidMatch**	**962.8**	**Pos**
9.26	**732.4813**	**PS 32:2; PS 16:1-16:1; [M+H]+**	**MSDIAL-LipidDBs-VS34 /LipidMatch**	**948.4**	**Pos**
9.29	**712.4918**	**PE 34:4; PE 17:2-17:2; [M+H]+**	**MSDIAL-LipidDBs-VS34 /LipidMatch**	**944.1**	**Pos**
9.3	339.2001	Canrenone	LC-MS-MS Negative Mode	980.4	Neg
9.41	792.58	1_Plasmenyl-PC(P-16:1/22:4)+H	LipidMatch	N/A	Pos
9.42	698.5	1_MGDG(9:0_22:4)+NH4-CO	LipidMatch	N/A	Pos
9.42	339.3267	FA 22:0; [M-H]-	MSDIAL-LipidDBs-VS34	974.9	Neg
9.43	365.3423	Nervonic acid	LC-MS-MS Negative Mode	989.5	Neg
9.44	836.57	1_OxPC(16:0_18:1(OO))+HCO2	LipidMatch	N/A	Neg
9.51	1194.819	AcylGlcADG 64:15; AcylGlcADG 22:5-22:5-20:5; [M+NH4]+	MSDIAL-LipidDBs-VS34	194.8	Pos
9.52	1175.777	AcylGlcADG 64:15; AcylGlcADG 22:5-22:5-20:5; [M-H]-	MSDIAL-LipidDBs-VS34	740.4	Neg
9.53	643.4343	PA 32:2; PA 16:1-16:1; [M-H]-	MSDIAL-LipidDBs-VS34	590.8	Neg
9.56	862.58	1_OxPC(16:1_20:1(OO))+HCO2	LipidMatch	N/A	Neg
9.56	818.5912	PS 38:1; PS 22:0-16:1; [M+H]+	MSDIAL-LipidDBs-VS34	177.7	Pos
9.62	**722.4978**	**PC 28:0; PC 14:0-14:0; [M+FA-H]-**	**MSDIAL-LipidDBs-VS34 /LipidMatch**	**813.2**	**Neg**
9.64	**678.5073**	**PC 28:0; PC 14:0-14:0; [M+H]+**	**MSDIAL-LipidDBs-VS34 /LipidMatch**	**955**	**Pos**
9.68	**807.5042**	**PI 32:1; PI 16:0-16:1; [M-H]-**	**MSDIAL-LipidDBs-VS34 /LipidMatch**	**856.7**	**Neg**
9.77	**704.5227**	**PC 30:1; PC 14:0-16:1; [M+H]+**	**MSDIAL-LipidDBs-VS34 /LipidMatch**	**953**	**Pos**
9.78	**833.5197**	**PI 34:2; PI 17:1-17:1; [M-H]-**	**MSDIAL-LipidDBs-VS34 /LipidMatch**	**865.7**	**Neg**
9.79	748.51	1_PC(14:0_16:1)+HCO2	LipidMatch	N/A	Neg
9.82	780.5533	PC 36:5; PC 18:2-18:3; [M+H]+	MSDIAL-LipidDBs-VS34	967.4	Pos
9.84	**634.4453**	**HexCer-AP t27:0; HexCer-AP t15:0/12:0; [M-H]-**	**MSDIAL-LipidDBs-VS34 /LipidMatch**	**690.1**	**Neg**
9.9	749.51	1_MGDG(16:1_16:1)+Na	LipidMatch	N/A	Pos
9.9	**730.5382**	**PC 32:2; PC 16:1-16:1; [M+H]+**	**MSDIAL-LipidDBs-VS34 /LipidMatch**	**955**	**Pos**
9.91	**774.5304**	**PS 35:1; PS 19:0-16:1; [M-H]-**	**MSDIAL-LipidDBs-VS34 /LipidMatch**	**366.8**	**Neg**
9.95	752.52	1_PC(16:1_16:1)+Na	LipidMatch	N/A	Pos
9.98	662.48	1_PE(14:0_16:1)+H	LipidMatch	N/A	Pos

9.99	**660.4609**	**PE 30:1; PE 14:0-16:1; [M-H]-**	**MSDIAL-LipidDBs-VS34 /LipidMatch**	**895.2**	**Neg**
10.01	541.2958	PA 25:4; PA 9:0-16:4; [M-H]-	MSDIAL-LipidDBs-VS34	256.5	Neg
10.03	**732.483**	**PS 32:1; PS 16:0-16:1; [M-H]-**	**MSDIAL-LipidDBs-VS34 /LipidMatch**	**523.8**	**Neg**
10.04	676.4916	PC 28:1; PC 12:0-16:1; [M+H]+	MSDIAL-LipidDBs-VS34	159.5	Pos
10.07	764.54	1_PG(16:1_18:1)+NH4	LipidMatch	N/A	Pos
10.09	**758.4988**	**PS 34:2; PS 17:1-17:1; [M-H]-**	**MSDIAL-LipidDBs-VS34 /LipidMatch**	**541.9**	**Neg**
10.1	**688.4913**	**PE 32:2; PE 16:1-16:1; [M+H]+**	**MSDIAL-LipidDBs-VS34 /LipidMatch**	**124.5**	**Pos**
10.11	**686.4766**	**PE 32:2; PE 16:1-16:1; [M-H]-**	**MSDIAL-LipidDBs-VS34 /LipidMatch**	**944.2**	**Neg**
10.12	774.58	1_PC(15:1_20:0)+H	LipidMatch	N/A	Pos
10.13	**714.5075**	**PE 34:2; PE 16:1-18:1; [M-H]-**	**MSDIAL-LipidDBs-VS34 /LipidMatch**	**733.5**	**Neg**
10.15	**730.5382**	**PC 32:2; PC 16:1-16:1; [M+H]+**	**MSDIAL-LipidDBs-VS34 /LipidMatch**	**993**	**Pos**
10.17	**700.4917**	**PE 33:2; PE 16:1-17:1; [M-H]-**	**MSDIAL-LipidDBs-VS34 /LipidMatch**	**717.4**	**Neg**
10.22	756.55	1_PC(16:1_18:2)+H	LipidMatch	N/A	Pos
10.22	**800.5459**	**PS 37:2; PS 19:0-18:2; [M-H]-**	**MSDIAL-LipidDBs-VS34 /LipidMatch**	**108.5**	**Neg**
10.23	734.5	1_PS(16:0_16:1)+H	LipidMatch	N/A	Pos
10.23	**760.5124**	**PS 34:2; PS 16:1-18:1; [M+H]+**	**MSDIAL-LipidDBs-VS34 /LipidMatch**	**943.3**	**Pos**
10.27	**636.4969**	**PC 26:0e; PC 16:0e/10:0; [M+H]+**	**MSDIAL-LipidDBs-VS34 /LipidMatch**	**993.4**	**Pos**
10.28	**859.5356**	**PI(16:0e/15-HETE)**	**RIKEN_IMS_Oxidized_Phospholipids/LipidMatch**	**875.6**	**Neg**
10.35	**686.4768**	**PE 32:2; PE 16:1-16:1; [M-H]-**	**MSDIAL-LipidDBs-VS34 /LipidMatch**	**959.9**	**Neg**
10.39	**745.501**	**PG 34:2; PG 16:1-18:1; [M-H]-**	**MSDIAL-LipidDBs-VS34 /LipidMatch**	**863.9**	**Neg**
10.42	**712.4923**	**PC 32:3; PC 16:1-16:2; [M+FA-H]-**	**MSDIAL-LipidDBs-VS34 /LipidMatch**	**163.2**	**Neg**
10.48	**554.4784**	**DG 30:2; DG 14:1-16:1; [M+NH4]+**	**MSDIAL-LipidDBs-VS34 /LipidMatch**	**786**	**Pos**
10.51	714.51	1_PE(16:1_18:2)+H	LipidMatch	N/A	Pos
10.52	**821.5198**	**PI 33:1; PI 15:0-18:1; [M-H]-**	**MSDIAL-LipidDBs-VS34 /LipidMatch**	**744.9**	**Neg**
10.53	**760.5126**	**PS 34:2; PS 16:1-18:1; [M+H]+**	**MSDIAL-LipidDBs-VS34 /LipidMatch**	**944.9**	**Pos**
10.54	734.4971	PS 32:1; PS 6:0-26:1; [M+H]+	MSDIAL-LipidDBs-VS34	245.5	Pos
10.57	782.4952	PS 36:5; PS 18:1-18:4; [M+H]+	MSDIAL-LipidDBs-VS34	148.9	Pos
10.59	782.5696	PC 36:4; PC 18:2-18:2; [M+H]+	MSDIAL-LipidDBs-VS34	114	Pos
10.66	762.53	1_PC(15:0_16:1)+HCO2	LipidMatch	N/A	Neg
10.66	704.5219	PC 30:1; PC 8:0-22:1; [M+H]+	MSDIAL-LipidDBs-VS34	134.5	Pos
10.66	**718.538**	**PC 31:1; PC 15:0-16:1; [M+H]+**	**MSDIAL-LipidDBs-VS34 /LipidMatch**	**957.2**	**Pos**
10.75	**636.4968**	**LPC 26:0; [M+H]+**	**MSDIAL-LipidDBs-VS34 /LipidMatch**	**645.9**	**Pos**
10.75	**744.5549**	**PC 33:2; PC 16:1-17:1; [M+H]+**	**MSDIAL-LipidDBs-VS34 /LipidMatch**	**974.9**	**Pos**
10.77	**788.5458**	**PS 36:1; PS 19:0-17:1; [M-H]-**	**MSDIAL-LipidDBs-VS34 /LipidMatch**	**153**	**Neg**
10.85	**676.4918**	**PE 31:1; PE 13:0-18:1; [M+H]+**	**MSDIAL-LipidDBs-VS34 /LipidMatch**	**122.1**	**Pos**
10.86	**674.4768**	**PE 31:1; PE 15:0-16:1; [M-H]-**	**MSDIAL-LipidDBs-VS34 /LipidMatch**	**858.8**	**Neg**
10.88	**645.4496**	**PA 32:1; PA 16:0-16:1; [M-H]-**	**MSDIAL-LipidDBs-VS34 /LipidMatch**	**508.3**	**Neg**
10.9	**570.5103**	**Cer-AP t34:0; Cer-AP t18:0/16:0; [M-H]-**	**MSDIAL-LipidDBs-VS34 /LipidMatch**	**675.2**	**Neg**
10.95	702.5078	PE 33:2; PE 16:1-17:1; [M+H]+	MSDIAL-LipidDBs-VS34	947.3	Pos

10.96	**700.4913**	**PE 33:2; PE 16:1-17:1; [M-H]-**	**MSDIAL-LipidDBs-VS34 /LipidMatch**	**735**	**Neg**
10.99	605.4462	Ginsenoside Rh3	LC-MS-MS Positive Mode	163	Pos
11.01	820.61	1_Plasmenyl-PC(P-18:1/22:4)+H	LipidMatch	N/A	Pos
11.01	820.6067	PS 38:0; PS 19:0-19:0; [M+H]+	MSDIAL-LipidDBs-VS34	175.2	Pos
11.02	864.6	1_OxPC(18:0_18:1(OO))+HCO2	LipidMatch	N/A	Neg
11.03	**685.4477**	**GlcADG 28:1; GlcADG 12:0-16:1; [M-H]-**	**MSDIAL-LipidDBs-VS34 /LipidMatch**	**144.9**	**Neg**
11.05	890.62	1_OxPC(18:1_20:1(OO))+HCO2	LipidMatch	N/A	Neg
11.05	846.6222	PS 40:1; PS 20:0-20:1; [M+H]+	MSDIAL-LipidDBs-VS34	125.9	Pos
11.06	**671.4657**	**PA 34:2; PA 16:1-18:1; [M-H]-**	**MSDIAL-LipidDBs-VS34 /LipidMatch**	**489.7**	**Neg**
11.12	699.48	1_CL(16:1_16:1_18:1_18:1)-2H	LipidMatch	N/A	Neg
11.28	835.52	1_PI(16:0_18:1)-H	LipidMatch	N/A	Neg
11.28	835.54	1_PI(16:1_18:0)-H	LipidMatch	N/A	Neg
11.31	**706.5383**	**PC 30:0; PC 15:0-15:0; [M+H]+**	**MSDIAL-LipidDBs-VS34 /LipidMatch**	**982.9**	**Pos**
11.35	861.54	1_PI(18:1_18:1)-H	LipidMatch	N/A	Neg
11.35	**861.5508**	**PI 36:2; PI 18:1-18:1; [M-H]-**	**MSDIAL-LipidDBs-VS34 /LipidMatch**	**170.3**	**Neg**
11.36	808.5849	PC 38:5; PC 20:2-18:3; [M+H]+	MSDIAL-LipidDBs-VS34	512	Pos
11.42	790.61	1_PC(16:0_20:0)+H	LipidMatch	N/A	Pos
11.43	776.59	1_OxTG(16:1_18:1_9:2(COOH))+NH4	LipidMatch	N/A	Pos
11.44	776.53	1_PC(14:0_18:1)+HCO2	LipidMatch	N/A	Neg
11.44	**732.5537**	**PC 32:1; PC 16:0-16:1; [M+H]+**	**MSDIAL-LipidDBs-VS34 /LipidMatch**	**923.4**	**Pos**
11.45	**776.5459**	**PC 32:1; PC 16:0-16:1; [M+FA-H]-**	**MSDIAL-LipidDBs-VS34 /LipidMatch**	**815.6**	**Neg**
11.53	802.55	1_PC(16:1_18:1)+HCO2	LipidMatch	N/A	Neg
11.53	**758.5692**	**PC 34:2; PC 17:1-17:1; [M+H]+**	**MSDIAL-LipidDBs-VS34 /LipidMatch**	**953.2**	**Pos**
11.53	802.5618	PS 37:1; PS 19:0-18:1; [M-H]-	MSDIAL-LipidDBs-VS34	174.7	Neg
11.59	780.55	1_PC(16:1_18:1)+Na | 1_PC(14:0_20:2)+Na | 1_PC(16:0_18:2)+Na	LipidMatch	N/A	Pos
11.59	773.5335	PG 36:2; PG 18:1-18:1; [M-H]-	MSDIAL-LipidDBs-VS34	159.2	Neg
11.62	**760.5139**	**PS 34:1; PS 16:0-18:1; [M-H]-**	**MSDIAL-LipidDBs-VS34 /LipidMatch**	**525.7**	**Neg**
11.63	**762.5274**	**PS 34:1; PS 16:0-18:1; [M+H]+**	**MSDIAL-LipidDBs-VS34 /LipidMatch**	**856**	**Pos**
11.64	608.47	1_Co(Q6)+NH4	LipidMatch	N/A	Pos
11.66	690.51	1_PE(16:0_16:1)+H 1_PEtOH(16:0_16:2)+NH4	LipidMatch	N/A	Pos
11.66	756.4807	PS 34:3; PS 16:0-18:3; [M-H]-	MSDIAL-LipidDBs-VS34	268	Neg
11.67	**688.4921**	**PE 32:1; PE 16:0-16:1; [M-H]-**	**MSDIAL-LipidDBs-VS34 /LipidMatch**	**897.7**	**Neg**
11.69	732.5532	PC 32:1; PC 15:0-17:1; [M+H]+	MSDIAL-LipidDBs-VS34	364.2	Pos
11.69	**766.5353**	**PC 35:5; PC 17:1-18:4; [M+H]+**	**MSDIAL-LipidDBs-VS34 /LipidMatch**	**248**	**Pos**
11.71	802.61	1_PC(15:1_22:0)+H	LipidMatch	N/A	Pos
11.71	**742.5398**	**PE 36:2; PE 18:1-18:1; [M-H]-**	**MSDIAL-LipidDBs-VS34 /LipidMatch**	**881.8**	**Neg**
11.72	**716.5216**	**PE 34:2; PE 16:1-18:1; [M+H]+**	**MSDIAL-LipidDBs-VS34 /LipidMatch**	**718.2**	**Pos**
11.74	714.5	1_PE(16:1_18:1)-H	LipidMatch	N/A	Neg
11.74	**714.5091**	**PE 34:2; PE 16:1-18:1; [M-H]-**	**MSDIAL-LipidDBs-VS34 /LipidMatch**	**879**	**Neg**

11.75	**758.5689**	**PC 34:2; PC 17:1-17:1; [M+H]+**	**MSDIAL-LipidDBs-VS34 /LipidMatch**	**993.7**	**Pos**
11.77	**784.5844**	**PC 36:3; PC 18:1-18:2; [M+H]+**	**MSDIAL-LipidDBs-VS34 /LipidMatch**	**932**	**Pos**
11.78	**728.5245**	**PE 35:2; PE 17:1-18:1; [M-H]-**	**MSDIAL-LipidDBs-VS34 /LipidMatch**	**692.1**	**Neg**
11.78	788.5422	PS 36:2; PS 18:1-18:1; [M+H]+	MSDIAL-LipidDBs-VS34	102.1	Pos
11.81	796.5123	PS 37:4; PS 15:0-22:4; [M-H]-	MSDIAL-LipidDBs-VS34	272.7	Neg
11.84	**582.5097**	**DG 32:2; DG 16:1-16:1; [M+NH4]+**	**MSDIAL-LipidDBs-VS34 /LipidMatch**	**399.5**	**Pos**
11.85	760.5	1_PS(16:0_18:1)-H	LipidMatch	N/A	Neg
11.86	**760.5145**	**PS 34:1; PS 16:0-18:1; [M-H]-**	**MSDIAL-LipidDBs-VS34 /LipidMatch**	**527.9**	**Neg**
11.91	530.48	1_DG(12:0_16:0)+NH4	LipidMatch	N/A	Pos
11.92	**716.5223**	**PE 34:2; PE 16:1-18:1; [M+H]+**	**MSDIAL-LipidDBs-VS34 /LipidMatch**	**972.2**	**Pos**
11.92	685.4354	TG 39:9; TG 12:3-12:3-15:3; [M+Na]+	MSDIAL-LipidDBs-VS34	918.7	Pos
11.97	758.57	1_PC(16:1_18:1)+H	LipidMatch	N/A	Pos
11.98	**740.5251**	**PE 36:3; PE 18:1-18:2; [M-H]-**	**MSDIAL-LipidDBs-VS34 /LipidMatch**	**444.7**	**Neg**
12.02	**849.5518**	**PI 35:1; PI 17:0-18:1; [M-H]-**	**MSDIAL-LipidDBs-VS34 /LipidMatch**	**667.4**	**Neg**
12.06	791.5247	GlcADG 36:4; GlcADG 18:1-18:3; [M-H]-	MSDIAL-LipidDBs-VS34	270.5	Neg
12.07	**582.5096**	**DG 32:2; DG 16:1-16:1; [M+NH4]+**	**MSDIAL-LipidDBs-VS34 /LipidMatch**	**900.3**	**Pos**
12.09	797.6499	SM d41:3; SM d28:2/13:1; [M+H]+	MSDIAL-LipidDBs-VS34	914.9	Pos
12.1	811.6657	SM d42:3; SM d27:2/15:1; [M+H]+	MSDIAL-LipidDBs-VS34	483.8	Pos
12.22	797.6503	SM d41:3; SM d28:2/13:1; [M+H]+	MSDIAL-LipidDBs-VS34	906.4	Pos
12.23	746.57	1_PC(15:0_18:1)+H	LipidMatch	N/A	Pos
12.23	811.6658	SM d42:3; SM d27:2/15:1; [M+H]+	MSDIAL-LipidDBs-VS34	536	Pos
12.24	790.56	1_PC(15:0_18:1)+HCO2	LipidMatch	N/A	Neg
12.25	768.551	PC 35:4; PC 9:0-26:4; [M+H]+	MSDIAL-LipidDBs-VS34	161	Pos
12.29	760.5143	PS 34:1; PS 16:0-18:1; [M-H]-	MSDIAL-LipidDBs-VS34	132	Neg
12.3	**816.5777**	**PS 38:1; PS 20:0-18:1; [M-H]-**	**MSDIAL-LipidDBs-VS34 /LipidMatch**	**149.8**	**Neg**
12.36	769.6195	SM d39:3; SM d15:1/24:2; [M+H]+	MSDIAL-LipidDBs-VS34	209.6	Pos
12.42	**704.5229**	**PE 33:1; PE 15:0-18:1; [M+H]+**	**MSDIAL-LipidDBs-VS34 /LipidMatch**	**965.3**	**Pos**
12.42	**702.5079**	**PE 33:1; PE 15:0-18:1; [M-H]-**	**MSDIAL-LipidDBs-VS34 /LipidMatch**	**807.9**	**Neg**
12.42	848.6375	PS 40:0; PS 20:0-20:0; [M+H]+	MSDIAL-LipidDBs-VS34	185.2	Pos
12.43	892.63	1_OxPC(18:0_20:1(OO))+HCO2	LipidMatch	N/A	Neg
12.47	673.4815	PA 34:1; PA 16:0-18:1; [M-H]-	MSDIAL-LipidDBs-VS34	135.5	Neg
12.53	729.4537	PA 39:8; PA 17:2-22:6; [M-H]-	MSDIAL-LipidDBs-VS34	248.2	Neg
12.55	562.5198	Cer-NS d36:3; Cer-NS d18:2/18:1; [M+H]+	MSDIAL-LipidDBs-VS34	105.9	Pos
12.59	**598.5414**	**Cer-AP t36:0; Cer-AP t18:0/18:0; [M+FA-H]-**	**MSDIAL-LipidDBs-VS34 /LipidMatch**	**877.3**	**Neg**
12.66	889.5824	PI 38:2; PI 19:1-19:1; [M-H]-	MSDIAL-LipidDBs-VS34	868.6	Neg
12.67	239.0596	(3R,4S)-4,6,8-trihydroxy-7-methoxy-3-methyl-3,4-dihydroisochromen-1-one	LC-MS-MS Negative Mode	129.2	Neg
12.7	863.57	1_PI(18:0_18:1)-H	LipidMatch	N/A	Neg
12.71	863.55	1_PI(16:0_20:1)-H	LipidMatch	N/A	Neg
12.82	**734.4946**	**PS 32:1; PS 6:0-26:1; [M+H]+**	**MSDIAL-LipidDBs-VS34 /LipidMatch**	**252.2**	**Pos**

12.87	**734.5691**	**PC 32:0; PC 16:0-16:0; [M+H]+**	**MSDIAL-LipidDBs-VS34 /LipidMatch**	**990.7**	**Pos**
12.88	778.56	1_PC(16:0_16:0)+HCO2	LipidMatch	N/A	Neg
12.9	818.64	1_PC(16:0_22:0)+H	LipidMatch	N/A	Pos
12.9	782.5666	PC 36:4; PC 18:2-18:2; [M+H]+	MSDIAL-LipidDBs-VS34	250.2	Pos
12.92	**760.585**	**PC 34:1; PC 16:0-18:1; [M+H]+**	**MSDIAL-LipidDBs-VS34 /LipidMatch**	**956.4**	**Pos**
12.93	804.56	1_PC(16:0_18:1)+HCO2	LipidMatch	N/A	Neg
12.93	**804.5774**	**PC 34:1; PC 16:0-18:1; [M+FA-H]-**	**MSDIAL-LipidDBs-VS34 /LipidMatch**	**243.1**	**Neg**
12.96	**786.6003**	**PC 36:2; PC 18:1-18:1; [M+H]+**	**MSDIAL-LipidDBs-VS34 /LipidMatch**	**960.1**	**Pos**
12.97	**830.5923**	**PC 36:2; PC 18:1-18:1; [M+FA-H]-**	**MSDIAL-LipidDBs-VS34 /LipidMatch**	**929.8**	**Neg**
12.98	830.58	1_PC(18:1_18:1)+HCO2	LipidMatch	N/A	Neg
13.01	749.5123	Azithromycin	LC-MS-MS Positive Mode	723.1	Pos
13.09	692.522	PE 32:0; PE 16:0-16:0; [M+H]+	MSDIAL-LipidDBs-VS34	715.6	Pos
13.09	**744.5525**	**PE 36:1; PE 18:0-18:1; [M-H]-**	**MSDIAL-LipidDBs-VS34 /LipidMatch**	**492.7**	**Neg**
13.1	**746.5685**	**PC 33:1; PC 17:0-16:1; [M+H]+**	**MSDIAL-LipidDBs-VS34 /LipidMatch**	**953.2**	**Pos**
13.13	**760.5848**	**PC 34:1; PC 16:0-18:1; [M+H]+**	**MSDIAL-LipidDBs-VS34 /LipidMatch**	**925.9**	**Pos**
13.13	762.5035	PC 35:7; PC 13:1-22:6; [M+H]+	MSDIAL-LipidDBs-VS34	547	Pos
13.13	756.492	PC 36:10e; PC 18:5e/18:5; [M+H]+	MSDIAL-LipidDBs-VS34	528.9	Pos
13.13	**718.5381**	**PE 34:1; PE 16:0-18:1; [M+H]+**	**MSDIAL-LipidDBs-VS34 /LipidMatch**	**962.4**	**Pos**
13.14	716.51	1_PE(16:0_18:1)-H	LipidMatch	N/A	Neg
13.14	716.5246	HexCer-AP t33:1; HexCer-AP t18:0/15:1; [M-H]-	MSDIAL-LipidDBs-VS34	572	Neg
13.14	784.5116	PS 36:3; PS 18:1-18:2; [M-H]-	MSDIAL-LipidDBs-VS34	158.3	Neg
13.16	732.5537	PC 32:1; PC 15:0-17:1; [M+H]+	MSDIAL-LipidDBs-VS34	420.2	Pos
13.2	741.53	1_CL(18:1_18:1_18:1_20:1)-2H	LipidMatch	N/A	Neg
13.26	**762.5277**	**PS 34:1; PS 16:0-18:1; [M+H]+**	**MSDIAL-LipidDBs-VS34 /LipidMatch**	**893.7**	**Pos**
13.31	773.52	1_PG(18:1_18:1)-H	LipidMatch	N/A	Neg
13.38	669.591	FAHFA 44:4; FAHFA 18:0/26:4; [M-H]-	MSDIAL-LipidDBs-VS34	176.6	Neg
13.51	**584.5253**	**DG 32:1; DG 16:0-16:1; [M+NH4]+**	**MSDIAL-LipidDBs-VS34 /LipidMatch**	**822.5**	**Pos**
13.52	611.49	1_FAHFA(16:1/24:4)-H	LipidMatch	N/A	Neg
13.54	**610.5409**	**DG 34:2; DG 16:1-18:1; [M+NH4]+**	**MSDIAL-LipidDBs-VS34 /LipidMatch**	**903.3**	**Pos**
13.61	818.59	1_PC(17:0_18:1)+HCO2	LipidMatch	N/A	Neg
13.61	**774.6007**	**PC 35:1; PC 18:0-17:1; [M+H]+**	**MSDIAL-LipidDBs-VS34 /LipidMatch**	**917.2**	**Pos**
13.62	818.58	1_PC(17:0_18:1)+HCO2	LipidMatch	N/A	Neg
13.71	700.58	1_OxTG(16:0_16:0_5:0(COOH))+NH4	LipidMatch	N/A	Pos
13.81	**730.5405**	**PE 35:1; PE 17:0-18:1; [M-H]-**	**MSDIAL-LipidDBs-VS34 /LipidMatch**	**688.4**	**Neg**
13.85	757.485	PA 41:8; PA 19:2-22:6; [M-H]-	MSDIAL-LipidDBs-VS34	234.3	Neg
13.92	610.54	1_DG(16:1_18:1)+NH4	LipidMatch	N/A	Pos
13.96	891.59	1_PI(18:0_20:1)-H	LipidMatch	N/A	Neg
13.96	**891.5992**	**PI 38:1; PI 20:0-18:1; [M-H]-**	**MSDIAL-LipidDBs-VS34 /LipidMatch**	**885.9**	**Neg**
13.98	676.53	1_Co(Q7)+NH4	LipidMatch	N/A	Pos

14.02	700.59	1_OxTG(16:0_16:0_5:0(COOH))+NH4	LipidMatch	N/A	Pos
14.06	672.5787	Cer-AP t38:0; Cer-AP t20:0/18:0; [M+FA-H]-	MSDIAL-LipidDBs-VS34	864.5	Neg
14.19	**814.6319**	**PC 38:2; PC 19:1-19:1; [M+H]+**	**MSDIAL-LipidDBs-VS34 /LipidMatch**	**679.5**	**Pos**
14.19	**858.6246**	**PS 41:1; PS 23:0-18:1; [M-H]-**	**MSDIAL-LipidDBs-VS34 /LipidMatch**	**101.8**	**Neg**
14.22	806.59	1_PC(16:0_18:0)+HCO2	LipidMatch	N/A	Neg
14.22	**762.6006**	**PC 34:0; PC 17:0-17:0; [M+H]+**	**MSDIAL-LipidDBs-VS34 /LipidMatch**	**975.3**	**Pos**
14.23	832.6	1_PC(18:0_18:1)+HCO2	LipidMatch	N/A	Neg
14.23	846.67	1_PC(18:0_22:0)+H	LipidMatch	N/A	Pos
14.24	**832.6086**	**PC 36:1; PC 18:0-18:1; [M+FA-H]-**	**MSDIAL-LipidDBs-VS34 /LipidMatch**	**889.1**	**Neg**
14.24	**788.6161**	**PC 36:1; PC 18:0-18:1; [M+H]+**	**MSDIAL-LipidDBs-VS34 /LipidMatch**	**989.1**	**Pos**
14.38	774.6	1_PE(18:0_20:1)+H	LipidMatch	N/A	Pos
14.38	772.5869	PE 38:1; PE 20:0-18:1; [M-H]-	MSDIAL-LipidDBs-VS34	659.8	Neg
14.38	840.5752	PS 40:3; PS 18:1-22:2; [M-H]-	MSDIAL-LipidDBs-VS34	112.8	Neg
14.39	698.57	1_OxTG(16:0_16:0_6:0(CHO))+NH4	LipidMatch	N/A	Pos
14.44	746.57	1_PE(18:0_18:1)+H	LipidMatch	N/A	Pos
14.44	812.5436	PS 38:3; PS 18:1-20:2; [M-H]-	MSDIAL-LipidDBs-VS34	171.7	Neg
14.45	744.56	1_PE(18:0_18:1)-H	LipidMatch	N/A	Neg
14.46	744.54	1_PE(18:0_18:1)-H	LipidMatch	N/A	Neg
14.49	756.63	1_OxTG(16:0_16:0_9:0(COOH))+NH4	LipidMatch	N/A	Pos
14.55	716.4458	PS 31:2; PS 13:1-18:1; [M-H]-	MSDIAL-LipidDBs-VS34	308.4	Neg
14.64	639.52	1_FAHFA(18:1/24:4)-H	LipidMatch	N/A	Neg
14.83	638.57	1_DG(18:1_18:1)+NH4	LipidMatch	N/A	Pos
14.83	**612.5565**	**DG 34:1; DG 16:0-18:1; [M+NH4]+**	**MSDIAL-LipidDBs-VS34 /LipidMatch**	**909.2**	**Pos**
14.84	639.52	1_FAHFA(18:1/24:4)-H	LipidMatch	N/A	Neg
15.01	945.65	1_PI(18:1_24:1)-H	LipidMatch	N/A	Neg
15.02	945.63	1_PI(18:1_24:1)-H	LipidMatch	N/A	Neg
15.05	761.626	(2E,6E)-3,7,11,15,19,23,27,31,35-nonamethylhexatriaconta-2,6,34-triene-1,11,15,19,23,27,31-heptol	LC-MS-MS Positive Mode	309.3	Pos
15.07	919.6303	PI 40:1; PI 22:0-18:1; [M-H]-	MSDIAL-LipidDBs-VS34	398.8	Neg
15.11	726.63	1_Cer-AP(t18:1/24:0)+HCO2	LipidMatch	N/A	Neg
15.32	700.61	1_Cer-AP(t18:0/22:0)+HCO2	LipidMatch	N/A	Neg
15.34	700.6	1_Cer-AP(t18:0/22:0)+HCO2	LipidMatch	N/A	Neg
15.39	860.64	1_PC(16:1_22:0)+HCO2	LipidMatch	N/A	Neg
15.39	816.6476	PC 38:1; PC 23:0-15:1; [M+H]+	MSDIAL-LipidDBs-VS34	871.2	Pos
15.67	719.5	1_PG(16:0_16:1)-H	LipidMatch	N/A	Neg
15.87	**714.6258**	**Cer-AP t41:0; Cer-AP t17:0/24:0; [M+FA-H]-**	**MSDIAL-LipidDBs-VS34 /LipidMatch**	**858.9**	**Neg**
15.97	**614.5721**	**DG 34:0; DG 16:0-18:0; [M+NH4]+**	**MSDIAL-LipidDBs-VS34 /LipidMatch**	**933.8**	**Pos**
16	973.677	PI 44:2; PI 18:1-26:1; [M-H]-	MSDIAL-LipidDBs-VS34	312.2	Neg
16.02	667.55	1_FAHFA(18:1/26:4)-H	LipidMatch	N/A	Neg
16.02	**640.5878**	**DG 36:1; DG 18:0-18:1; [M+NH4]+**	**MSDIAL-LipidDBs-VS34 /LipidMatch**	**909.1**	**Pos**

16.07	**708.6139**	**TG 40:2; TG 12:0-12:1-16:1; [M+NH4]+**	**MSDIAL-LipidDBs-VS34 /LipidMatch**	**278.5**	**Pos**
16.1	**947.661**	**PI 42:1; PI 24:0-18:1; [M-H]-**	**MSDIAL-LipidDBs-VS34 /LipidMatch**	**823.4**	**Neg**
16.24	**734.6297**	**TG 42:3; TG 13:1-13:1-16:1; [M+NH4]+**	**MSDIAL-LipidDBs-VS34 /LipidMatch**	**659.8**	**Pos**
16.32	**754.6576**	**Cer-AP t44:1; Cer-AP t18:0/26:1; [M+FA-H]-**	**MSDIAL-LipidDBs-VS34 /LipidMatch**	**852.7**	**Neg**
16.35	870.6985	PC 42:2; PC 21:1-21:1; [M+H]+	MSDIAL-LipidDBs-VS34	591.9	Pos
16.42	818.6657	PC 38:0; PC 19:0-19:0; [M+H]+	MSDIAL-LipidDBs-VS34	900.9	Pos
16.43	728.64	1_Cer-AP(t18:0/24:0)+HCO2	LipidMatch	N/A	Neg
16.43	888.67	1_PC(16:1_24:0)+HCO2	LipidMatch	N/A	Neg
16.44	844.6799	PC 40:1; PC 18:0-22:1; [M+H]+	MSDIAL-LipidDBs-VS34	630.4	Pos
16.57	961.66	1_PI(18:1_25:0)-H	LipidMatch	N/A	Neg
16.58	961.68	1_PI(18:1_25:0)-H	LipidMatch	N/A	Neg
16.69	726.65	1_Cer_BS(d18:2/29:3)-H	LipidMatch	N/A	Neg
16.75	712.63	1_Cer-NP(t18:0/24:0)+HCO2	LipidMatch	N/A	Neg
16.75	**712.6464**	**Cer-ADS d42:0; Cer-ADS d17:0/25:0; [M+FA-H]-**	**MSDIAL-LipidDBs-VS34 /LipidMatch**	**931.2**	**Neg**
16.81	239.0601	Dinoseb	LC-MS-MS Negative Mode	192.5	Neg
16.81	767.5633	PA 41:3; PA 19:0-22:3; [M-H]-	MSDIAL-LipidDBs-VS34	224.6	Neg
16.94	**742.6572**	**Cer-AP t43:0; Cer-AP t18:0/25:0; [M+FA-H]-**	**MSDIAL-LipidDBs-VS34 /LipidMatch**	**853.8**	**Neg**
16.95	742.64	1_Cer-AP(t18:0/25:0)+HCO2	LipidMatch	N/A	Neg
16.97	710.61	1_TG(10:0_14:0_16:1)+NH4	LipidMatch	N/A	Pos
17.02	838.75	1_OxTG(16:0_16:0_16:1(OH))+NH4	LipidMatch	N/A	Pos
17.02	**975.6923**	**PI 44:1; PI 26:0-18:1; [M-H]-**	**MSDIAL-LipidDBs-VS34 /LipidMatch**	**727.2**	**Neg**
17.06	**710.6285**	**TG 40:1; TG 12:0-12:0-16:1; [M+NH4]+**	**MSDIAL-LipidDBs-VS34 /LipidMatch**	**205.2**	**Pos**
17.07	**642.6032**	**DG 36:0; DG 18:0-18:0; [M+NH4]+**	**MSDIAL-LipidDBs-VS34 /LipidMatch**	**859.4**	**Pos**
17.08	669.57	1_FAHFA(18:0/26:4)-H	LipidMatch	N/A	Neg
17.08	**736.6451**	**TG 42:2; TG 12:0-14:1-16:1; [M+NH4]+**	**MSDIAL-LipidDBs-VS34 /LipidMatch**	**324.1**	**Pos**
17.24	**726.6624**	**Cer-ADS d43:0; Cer-ADS d22:0/21:0; [M+FA-H]-**	**MSDIAL-LipidDBs-VS34 /LipidMatch**	**922.7**	**Neg**
17.25	866.72	1_MGDG(21:0_22:4)+NH4-CO	LipidMatch	N/A	Pos
17.34	694.6361	Cer-NDS d42:1; Cer-NDS d22:0/20:1; [M+FA-H]-	MSDIAL-LipidDBs-VS34	700.3	Neg
17.38	712.65	1_Cer-ADS(d16:0/26:0)+HCO2	LipidMatch	N/A	Neg
17.39	712.64	1_Cer-ADS(d16:0/26:0)+HCO2	LipidMatch	N/A	Neg
17.4	750.64	1_TG(12:0_15:1_16:1)+NH4	LipidMatch	N/A	Pos
17.42	712.68	1_Cer-NS(d29:3/18:2)+H	LipidMatch	N/A	Pos
17.43	**756.6729**	**Cer-AP t44:0; Cer-AP t18:0/26:0; [M+FA-H]-**	**MSDIAL-LipidDBs-VS34 /LipidMatch**	**816.4**	**Neg**
17.44	756.66	1_Cer-AP(t19:0/25:0)+HCO2	LipidMatch	N/A	Neg
17.45	796.72	1_OxTG(18:0_18:0_9:0(CHO))+NH4	LipidMatch	N/A	Pos
17.48	698.61	1_TG(12:0_12:0_15:0)+NH4	LipidMatch	N/A	Pos
17.54	743.5631	PA 39:1; PA 15:0-24:1; [M-H]-	MSDIAL-LipidDBs-VS34	244.4	Neg
17.56	**724.6447**	**TG 41:1; TG 12:0-13:0-16:1; [M+NH4]+**	**MSDIAL-LipidDBs-VS34 /LipidMatch**	**382.4**	**Pos**

17.66	696.64	1_Cer-NDS(d18:0/24:0)+HCO2	LipidMatch	N/A	Neg
17.69	696.65	1_Cer-NDS(d18:0/24:0)+HCO2	LipidMatch	N/A	Neg
17.69	**698.6449**	**Cer-NS d46:5; Cer-NS d22:3/24:2; [M+H]+**	**MSDIAL-LipidDBs-VS34 /LipidMatch**	**113.5**	**Pos**
17.72	**740.678**	**Cer-NP t44:0; Cer-NP t18:0/26:0; [M+FA-H]-**	**MSDIAL-LipidDBs-VS34 /LipidMatch**	**850.7**	**Neg**
17.74	740.67	1_Cer-NP(t18:0/26:0)+HCO2	LipidMatch	N/A	Neg
17.76	1317.87	1_CL(14:0_16:1_16:1_16:1)-H	LipidMatch	N/A	Neg
17.76	1317.89	1_CL(14:0_16:1_16:1_16:1)-H	LipidMatch	N/A	Neg
17.76	1336.93	1_CL(30:1)(32:2)+NH4	LipidMatch	N/A	Pos
17.77	1310.91	1_CL(28:0)(32:2)+NH4 | 1_CL(30:1)(30:1)+NH4	LipidMatch	N/A	Pos
17.78	**1343.906**	**CL 64:4; CL 16:1-16:1-16:1-16:1; [M-H]-**	**MSDIAL-LipidDBs-VS34 /LipidMatch**	**468.2**	**Neg**
17.91	**770.6889**	**Cer-AP t45:0; Cer-AP t20:0/25:0; [M+FA-H]-**	**MSDIAL-LipidDBs-VS34 /LipidMatch**	**848.7**	**Neg**
17.93	770.68	1_Cer-AP(t18:0/27:0)+HCO2	LipidMatch	N/A	Neg
17.94	963.6894	PI 43:0; PI 19:0-24:0; [M-H]-	MSDIAL-LipidDBs-VS34	789.6	Neg
17.98	906.78	1_OxTG(16:1_18:1_18:1(OO))+NH4	LipidMatch	N/A	Pos
18.01	764.68	1_TG(10:0_16:1_18:1)+NH4	LipidMatch	N/A	Pos
18.03	820.74	1_TG(12:0_18:1_18:1)+NH4	LipidMatch	N/A	Pos
18.04	790.69	1_TG(14:1_16:1_16:1)+NH4	LipidMatch	N/A	Pos
18.04	860.77	1_TG(17:1_17:1_17:1)+NH4	LipidMatch	N/A	Pos
18.04	**738.6605**	**TG 42:1; TG 13:0-13:0-16:1; [M+NH4]+**	**MSDIAL-LipidDBs-VS34 /LipidMatch**	**319.4**	**Pos**
18.1	624.63	1_Cer-NDS(d22:0/18:0)+H	LipidMatch	N/A	Pos
18.11	**871.6789**	**TG 52:7; TG 16:1-16:1-20:5; [M+Na]+**	**MSDIAL-LipidDBs-VS34 /LipidMatch**	**339.8**	**Pos**
18.16	**816.7078**	**TG 48:4; TG 16:1-16:1-16:2; [M+NH4]+**	**MSDIAL-LipidDBs-VS34 /LipidMatch**	**935.3**	**Pos**
18.26	944.73	1_PC(18:1_26:0)+HCO2	LipidMatch	N/A	Neg
18.26	874.7259	PC 42:0; PC 21:0-21:0; [M+H]+	MSDIAL-LipidDBs-VS34	531.4	Pos
18.27	**900.7417**	**PC 44:1; PC 26:0-18:1; [M+H]+**	**MSDIAL-LipidDBs-VS34 /LipidMatch**	**966.9**	**Pos**
18.28	944.72	1_PC(18:1_26:0)+HCO2	LipidMatch	N/A	Neg
18.32	**740.6779**	**Cer-ADS d44:0; Cer-ADS d18:0/26:0; [M+FA-H]-**	**MSDIAL-LipidDBs-VS34 /LipidMatch**	**910.8**	**Neg**
18.35	**784.7044**	**Cer-AP t46:0; Cer-AP t24:0/22:0; [M+FA-H]-**	**MSDIAL-LipidDBs-VS34 /LipidMatch**	**840.1**	**Neg**
18.46	809.66	1_TG(15:1_16:1_16:1)+Na	LipidMatch	N/A	Pos
18.47	804.71	1_TG(15:1_16:1_16:1)+NH4	LipidMatch	N/A	Pos
18.47	**1371.937**	**CL 66:4; CL 16:1-16:1-16:1-18:1; [M-H]-**	**MSDIAL-LipidDBs-VS34 /LipidMatch**	**559.3**	**Neg**
18.47	**1390.977**	**CL 66:4; CL 16:1-16:1-16:2-18:0; [M+NH4]+**	**MSDIAL-LipidDBs-VS34 /LipidMatch**	**967.3**	**Pos**
18.48	784.69	1_Cer-AP(t20:0/26:0)+HCO2	LipidMatch	N/A	Neg
18.48	**778.6919**	**TG 45:2; TG 15:0-15:1-15:1; [M+Na]+**	**MSDIAL-LipidDBs-VS34 /LipidMatch**	**916.9**	**Pos**
18.49	752.68	1_TG(12:0_15:0_16:1)+NH4	LipidMatch	N/A	Pos
18.5	**726.6593**	**TG 41:0; TG 13:0-13:0-15:0; [M+NH4]+**	**MSDIAL-LipidDBs-VS34 /LipidMatch**	**482.5**	**Pos**
18.6	**724.6832**	**Cer-NDS d44:0; Cer-NDS d18:0/26:0; [M+FA-H]-**	**MSDIAL-LipidDBs-VS34 /LipidMatch**	**764.8**	**Neg**
18.62	**768.7094**	**Cer-ADS d46:0; Cer-ADS d19:0/27:0; [M+FA-H]-**	**MSDIAL-LipidDBs-VS34 /LipidMatch**	**873.6**	**Neg**

18.81	934.81	1_OxTG(16:1_18:1_20:1(OO))+NH4	LipidMatch	N/A	Pos
18.82	**823.678**	**TG 48:3; TG 16:1-16:1-16:1; [M+Na]+**	**MSDIAL-LipidDBs-VS34 /LipidMatch**	**943.2**	**Pos**
18.88	818.72	1_TG(14:1_16:1_18:1)+NH4	LipidMatch	N/A	Pos
18.89	792.71	1_TG(12:0_16:1_18:1)+NH4	LipidMatch	N/A	Pos
18.92	766.69	1_TG(12:0_16:0_16:1)+NH4	LipidMatch	N/A	Pos
18.95	**740.676**	**TG 42:0; TG 13:0-13:0-16:0; [M+NH4]+**	**MSDIAL-LipidDBs-VS34 /LipidMatch**	**623.4**	**Pos**
18.98	**771.6471**	**TG 44:1; TG 12:0-16:0-16:1; [M+Na]+**	**MSDIAL-LipidDBs-VS34 /LipidMatch**	**320.8**	**Pos**
19.08	928.7729	PC 46:1; PC 26:0-20:1; [M+H]+	MSDIAL-LipidDBs-VS34	712.8	Pos
19.12	1373.93	1_CL(16:1_18:0_16:1_16:1)-H	LipidMatch	N/A	Neg
19.12	**1419.008**	**CL 68:4; CL 16:0-18:2-16:1-18:1; [M+NH4]+**	**MSDIAL-LipidDBs-VS34 /LipidMatch**	**917.6**	**Pos**
19.12	**1399.968**	**CL 68:4; CL 16:1-16:1-18:1-18:1; [M-H]-**	**MSDIAL-LipidDBs-VS34 /LipidMatch**	**539.4**	**Neg**
19.15	**1373.953**	**CL 66:3; CL 16:1-16:1-16:1-18:0; [M-H]-**	**MSDIAL-LipidDBs-VS34 /LipidMatch**	**511.9**	**Neg**
19.18	875.71	1_TG(16:1_18:1_18:3)+Na	LipidMatch	N/A	Pos
19.3	806.7236	TG 47:2; TG 15:0-16:1-16:1; [M+Na]+	MSDIAL-LipidDBs-VS34	924.1	Pos
19.31	**832.7391**	**TG 49:3; TG 16:1-16:1-17:1; [M+NH4]+**	**MSDIAL-LipidDBs-VS34 /LipidMatch**	**877.7**	**Pos**
19.33	780.71	1_TG(12:0_16:0_17:1)+NH4	LipidMatch	N/A	Pos
19.34	754.69	1_TG(13:0_14:0_16:0)+NH4	LipidMatch	N/A	Pos
19.55	901.73	1_TG(16:1_18:1_20:4)+Na	LipidMatch	N/A	Pos
19.62	851.71	1_TG(16:1_16:1_18:1)+Na	LipidMatch	N/A	Pos
19.66	846.75	1_TG(16:1_16:1_18:1)+NH4	LipidMatch	N/A	Pos
19.7	820.74	1_TG(16:0_16:1_16:1)+NH4	LipidMatch	N/A	Pos
19.74	1427.98	1_CL(16:1_18:1_18:1_18:1)-H	LipidMatch	N/A	Neg
19.74	**1428.001**	**CL 70:4; CL 16:1-18:1-18:1-18:1; [M-H]-**	**MSDIAL-LipidDBs-VS34 /LipidMatch**	**608.5**	**Neg**
19.75	1401.985	CL 68:3; CL 16:1-18:0-16:2-18:0; [M-H]-	MSDIAL-LipidDBs-VS34	467	Neg
19.75	**794.7225**	**TG 46:1; TG 12:0-16:0-18:1; [M+NH4]+**	**MSDIAL-LipidDBs-VS34 /LipidMatch**	**771.1**	**Pos**
19.77	1375.95	1_CL(16:0_16:0_16:1_18:1)-H	LipidMatch	N/A	Neg
19.77	**1375.969**	**CL 66:2; CL 14:0-18:1-16:0-18:1; [M-H]-**	**MSDIAL-LipidDBs-VS34 /LipidMatch**	**495.8**	**Neg**
19.77	**768.707**	**TG 44:0; TG 12:0-16:0-16:0; [M+NH4]+**	**MSDIAL-LipidDBs-VS34 /LipidMatch**	**749.1**	**Pos**
20.08	**834.7548**	**TG 49:2; TG 15:0-17:1-17:1; [M+Na]+**	**MSDIAL-LipidDBs-VS34 /LipidMatch**	**828.6**	**Pos**
20.09	**808.739**	**TG 47:1; TG 15:0-16:0-16:1; [M+NH4]+**	**MSDIAL-LipidDBs-VS34 /LipidMatch**	**535.7**	**Pos**
20.09	**860.7703**	**TG 51:3; TG 16:1-17:1-18:1; [M+NH4]+**	**MSDIAL-LipidDBs-VS34 /LipidMatch**	**973.8**	**Pos**
20.29	**1456.031**	**CL 72:4; CL 18:1-18:1-18:1-18:1; [M-H]-**	**MSDIAL-LipidDBs-VS34 /LipidMatch**	**601.1**	**Neg**
20.31	1456.01	1_CL(18:1_18:1_18:1_18:1)-H	LipidMatch	N/A	Neg
20.34	1403.98	1_CL(16:0_16:0_18:1_18:1)-H	LipidMatch	N/A	Neg
20.34	**1404**	**CL 68:2; CL 16:0-18:1-16:0-18:1; [M-H]-**	**MSDIAL-LipidDBs-VS34 /LipidMatch**	**444.5**	**Neg**
20.35	**879.7397**	**TG 52:3; TG 16:1-18:1-18:1; [M+Na]+**	**MSDIAL-LipidDBs-VS34 /LipidMatch**	**892.6**	**Pos**
20.41	874.78	1_TG(16:1_18:1_18:1)+NH4	LipidMatch	N/A	Pos
20.45	848.77	1_TG(16:0_16:1_18:1)+NH4	LipidMatch	N/A	Pos
20.47	822.75	1_TG(16:0_16:0_16:1)+NH4	LipidMatch	N/A	Pos
20.51	853.72	1_TG(16:0_16:1_18:1)+Na	LipidMatch	N/A	Pos

20.55	666.62	1_CE(18:2)+NH4	LipidMatch	N/A	Pos
20.69	678.62	1_DG(18:3_21:0)+NH4	LipidMatch	N/A	Pos
20.79	888.8	1_TG(17:1_18:1_18:1)+NH4	LipidMatch	N/A	Pos
20.81	**862.7856**	**TG 51:2; TG 16:0-17:1-18:1; [M+NH4]+**	**MSDIAL-LipidDBs-VS34 /LipidMatch**	**675.6**	**Pos**
20.82	810.75	1_TG(15:0_16:0_16:0)+NH4	LipidMatch	N/A	Pos
21.04	907.77	1_TG(16:1_18:1_20:1)+Na	LipidMatch	N/A	Pos
21.07	881.76	1_TG(16:1_18:0_18:1)+Na	LipidMatch	N/A	Pos
21.09	902.82	1_TG(16:1_18:1_20:1)+NH4	LipidMatch	N/A	Pos
21.12	876.8	1_TG(16:1_18:0_18:1)+NH4	LipidMatch	N/A	Pos
21.14	850.78	1_TG(16:0_16:1_18:0)+NH4	LipidMatch	N/A	Pos
21.17	824.77	1_TG(14:0_16:0_18:0)+NH4	LipidMatch	N/A	Pos
21.4	668.634	CE 18:1; [M+NH4]+	MSDIAL-LipidDBs-VS34	711.2	Pos
21.45	890.82	1_TG(17:1_18:0_18:1)+NH4	LipidMatch	N/A	Pos
21.46	864.8	1_TG(16:0_17:0_18:1)+NH4	LipidMatch	N/A	Pos
21.47	895.7725	TG 53:2; TG 17:0-18:1-18:1; [M+Na]+	MSDIAL-LipidDBs-VS34	903.9	Pos
21.49	**838.785**	**TG 49:0; TG 16:0-16:0-17:0; [M+NH4]+**	**MSDIAL-LipidDBs-VS34 /LipidMatch**	**868.6**	**Pos**
21.67	935.8	1_TG(16:1_20:1_20:1)+Na	LipidMatch	N/A	Pos
21.75	904.83	1_TG(18:0_18:1_18:1)+NH4	LipidMatch	N/A	Pos
21.77	878.82	1_TG(16:0_18:0_18:1)+NH4	LipidMatch	N/A	Pos
21.8	852.8	1_TG(16:0_16:0_18:0)+NH4	LipidMatch	N/A	Pos
21.81	**883.772**	**TG 52:1; TG 16:0-18:0-18:1; [M+Na]+**	**MSDIAL-LipidDBs-VS34 /LipidMatch**	**500.3**	**Pos**
21.95	710.68	1_DG(18:1_23:0)+NH4	LipidMatch	N/A	Pos
22.08	**892.832**	**TG 53:1; TG 13:1-20:0-20:0; [M+Na]+**	**MSDIAL-LipidDBs-VS34 /LipidMatch**	**886.7**	**Pos**
22.1	**866.817**	**TG 51:0; TG 17:0-17:0-17:0; [M+Na]+**	**MSDIAL-LipidDBs-VS34 /LipidMatch**	**936**	**Pos**
22.26	**958.8794**	**TG 58:3; TG 16:1-21:1-21:1; [M+NH4]+**	**MSDIAL-LipidDBs-VS34 /LipidMatch**	**552.9**	**Pos**
22.36	**906.8485**	**TG 54:1; TG 18:0-18:0-18:1; [M+NH4]+**	**MSDIAL-LipidDBs-VS34 /LipidMatch**	**897.1**	**Pos**
22.4	**880.8326**	**TG 52:0; TG 16:0-18:0-18:0; [M+NH4]+**	**MSDIAL-LipidDBs-VS34 /LipidMatch**	**459.8**	**Pos**
22.62	**946.8792**	**TG 57:2; TG 16:1-20:1-21:0; [M+NH4]+**	**MSDIAL-LipidDBs-VS34 /LipidMatch**	**446.2**	**Pos**
22.67	**894.8475**	**TG 53:0; TG 16:0-18:0-19:0; [M+NH4]+**	**MSDIAL-LipidDBs-VS34 /LipidMatch**	**589.6**	**Pos**
22.8	**986.9109**	**TG 60:3; TG 16:1-22:1-22:1; [M+NH4]+**	**MSDIAL-LipidDBs-VS34 /LipidMatch**	**380.8**	**Pos**
22.88	**960.8955**	**TG 58:2; TG 16:1-20:0-22:1; [M+NH4]+**	**MSDIAL-LipidDBs-VS34 /LipidMatch**	**462.1**	**Pos**
23.14	**974.9112**	**TG 59:2; TG 15:2-22:0-22:0; [M+Na]+**	**MSDIAL-LipidDBs-VS34 /LipidMatch**	**881.8**	**Pos**
23.15	**948.895**	**TG 57:1; TG 16:0-20:1-21:0; [M+NH4]+**	**MSDIAL-LipidDBs-VS34 /LipidMatch**	**308**	**Pos**
23.18	**922.8788**	**TG 55:0; TG 16:0-18:0-21:0; [M+NH4]+**	**MSDIAL-LipidDBs-VS34 /LipidMatch**	**468.8**	**Pos**
23.38	988.93	1_TG(16:1_18:1_26:0)+NH4	LipidMatch	N/A	Pos
23.4	**962.9111**	**TG 58:1; TG 19:0-19:0-20:1; [M+Na]+**	**MSDIAL-LipidDBs-VS34 /LipidMatch**	**876.5**	**Pos**
23.43	**936.8951**	**TG 56:0; TG 16:0-18:0-22:0; [M+NH4]+**	**MSDIAL-LipidDBs-VS34 /LipidMatch**	**580.8**	**Pos**
23.63	**1002.942**	**TG 61:2; TG 18:1-21:0-22:1; [M+NH4]+**	**MSDIAL-LipidDBs-VS34 /LipidMatch**	**292.3**	**Pos**
23.64	976.93	1_TG(16:0_18:1_25:0)+NH4	LipidMatch	N/A	Pos
23.64	**981.8815**	**TG 59:1; TG 15:1-22:0-22:0; [M+Na]+**	**MSDIAL-LipidDBs-VS34 /LipidMatch**	**874.2**	**Pos**

23.87	**1016.958**	**TG 62:2; TG 18:1-22:0-22:1; [M+NH4]+**	**MSDIAL-LipidDBs-VS34 /LipidMatch**	**446.2**	**Pos**
23.88	**990.9422**	**TG 60:1; TG 16:0-22:0-22:1; [M+NH4]+**	**MSDIAL-LipidDBs-VS34 /LipidMatch**	**325.2**	**Pos**
24.12	**1004.957**	**TG 61:1; TG 18:0-21:1-22:0; [M+NH4]+**	**MSDIAL-LipidDBs-VS34 /LipidMatch**	**171**	**Pos**
24.37	**1018.973**	**TG 62:1; TG 18:1-22:0-22:0; [M+NH4]+**	**MSDIAL-LipidDBs-VS34 /LipidMatch**	**319.4**	**Pos**
24.79	360.324	phenylethylamide 359	LC-MS-MS Positive Mode	245.4	Pos
24.88	1047.01	1_TG(18:1_20:0_26:0)+NH4	LipidMatch	N/A	Pos

Appendix Table 3: Summary of MSMS methods used on the MCF-7 samples for lipid identification. CE refers to collision energy.

Lipid Classes	Mass Range (m/z)	CE (eV)	ESI Mode
Phospholipids	150	15	Neg
	350	25	
	1450	40	
	1500	45	
MG, MIPC, PE-Cer, Sulf	150	10	Neg
	450	20	
	675	35	
	800	60	
	1000	80	
	1500	90	
BMP, Hex-Cer, SM, Sph	150	30	Neg
	700	40	
	1500	55	
Car, FA, Lac-Cer, NAA	150	25	Neg
	800	35	
	1000	55	
	1500	60	
Acer-Cer, CholE, CL, ST	150	20	Neg
	650	35	
	1500	45	
BMP, Sph, SPB	150	13	Pos
	650	25	
	651	40	
	1300	60	
	1500	70	
LPG, LPI, LPS, PG, PI, PS	150	10	Pos
	450	15	

	700	30	
	1300	35	
	1500	40	
DG, MG, TG	150	15	Pos
	500	20	
	700	30	
	1500	40	
FA, Hex-Cer, ST	150	25	Pos
	400	40	
	1000	60	
	1500	70	
CholE, MIPC, Sulf	150	10	Pos
	600	15	
	850	20	
	950	35	
	1500	50	
Acer-Cer, Car, Cer, NAA, PE-Cer	150	18	Pos
	600	33	
	950	45	
	1100	40	
	1500	50	
LPA, LPC, LPE, PA, PC, PE, SM	150	15	Pos
	350	20	
	600	30	
	1300	45	
	1500	50	

Appendix Table 4: List of annotated lipid species detected in MCF-7 breast cancer cells through Metaboscape 4.0 libraries (Bruker LipidBlast; Mass Bank; RIKEN Oxidized Phospholipids; LC-MSMS Positive; and LC-MSMS Negative) and LipidMatch. Feature names in bold were detected through both annotation software.

RT [min]	Precursor Ion [m/z]	Name	Annotation Source/Library	MSMS Score	Ionization Mode
0.75	646.47337	MGDG(7:0_20:2)+NH4-CO	LipidMatch	N/A	Pos
0.91	305.0438	Calycin	LC-MS-MS Negative Mode	325.8	Neg
0.93	704.51569	DG(20:5_22:6)+NH4	LipidMatch	N/A	Pos
0.99	463.13066	NCGC00169618-04!6-[(6,8-dihydroxy-7-methoxy-3-methyl-1-oxo-3,4-dihydroisochromen-4-yl)oxy]-4,8-dihydroxy-7-methoxy-3-methyl-3,4-dihydroisochromen-1-one	LC-MS-MS Positive Mode	528.3	Pos

1.01	268.10394	MMV687145	LC-MS-MS Positive Mode	199.3	Pos
1.11	242.13689	3-hydroxy-C8-homoserine lactone	MassBank	797.4	Neg
1.12	322.19093	MMV026550	LC-MS-MS Positive Mode	736.7	Pos
1.2	261.10972	MMV023233	LC-MS-MS Positive Mode	969.4	Pos
1.22	357.21002	4-hydroxy-2,5,5,9-tetramethylcycloundeca-2,9-dienyl 4-hydroxybenzoate	MassBank	982.3	Neg
1.33	297.11497	Enterolactone	LC-MS-MS Negative Mode	994.3	Neg
1.39	359.22014	NCGC00384872-01!4-[4-(3,4-dimethoxyphenyl)-2,3-dimethylbutyl]-1,2-dimethoxybenzene	LC-MS-MS Positive Mode	567.5	Pos
1.41	343.29556	CocamidoprpylBetaine	LC-MS-MS Positive Mode	966.3	Pos
1.43	311.13101	5-hydroxy-2,2-dimethyl-10-(2-methylbut-3-en-2-yl)pyrano[3,2-g]chromen-8-one	LC-MS-MS Negative Mode	993.6	Neg
1.43	279.15077	Mianserin-N-Oxide	MassBank	918.3	Neg
1.56	397.21532	Mitragynine	LC-MS-MS Negative Mode	788	Neg
1.57	279.15893	Dibutyl phthalate	LC-MS-MS Positive Mode	998.2	Pos
1.6	**646.47397**	**MGDG(10:0_17:2)+NH4-CO**	**LipidMatch/Bruker LipidBlast**	**574.1**	**Pos**
1.62	399.25067	Tri(butoxyethyl)phosphate	LC-MS-MS Positive Mode	891.8	Pos
1.69	372.31221	Tetradecanoyl-L-Carnitine	LC-MS-MS Positive Mode	617.1	Pos
1.71	315.17433	(2R,3R,4S,5S,6R)-2-[(2E)-4-ethenyl-2,5-dimethylhexa-2,5-dienoxy]-6-(hydroxymethyl)oxane-3,4,5-triol	LC-MS-MS Positive Mode	503.8	Pos
1.72	339.16322	NCGC00384544-01!2-hydroxy-4-methoxy-3-(3-methylbut-2-enyl)-6-(2-phenylethyl)benzoic acid	LC-MS-MS Negative Mode	540.4	Neg
1.76	468.30869	LPC(14:0)+H	LipidMatch	N/A	Pos
1.76	512.29704	LPC(14:0)+HCO2	LipidMatch	N/A	Neg
1.79	660.48986	Plasmenyl-PC(P-16:1/12:0)+H	LipidMatch	N/A	Pos
1.81	**494.32448**	**LPC(16:1)+H**	**LipidMatch/Bruker LipidBlast**	**923.1**	**Pos**
1.82	288.28973	C17-Sphinganine	LC-MS-MS Positive Mode	921	Pos
1.82	**538.3119**	**LPC(16:1)+HCO2**	**LipidMatch/Bruker LipidBlast**	**723**	**Neg**
1.82	538.30127	OxLPE(20:1(OO))-H	LipidMatch	N/A	Neg
1.84	463.13103	6-[(6,8-dihydroxy-7-methoxy-3-methyl-1-oxo-3,4-dihydroisochromen-4-yl)oxy]-4,8-dihydroxy-7-methoxy-3-methyl-3,4-dihydroisochromen-1-one	LC-MS-MS Positive Mode	250.1	Pos
1.84	452.27734	LPE 16:1; [M+H]+	Bruker LipidBlast	885.7	Pos
1.86	**450.2627**	**LPE(16:1)-H**	**LipidMatch/Bruker LipidBlast**	**985.6**	**Neg**
1.92	318.30029	Phytosphingosine	LC-MS-MS Positive Mode	854.7	Pos
1.94	655.40871	GlcADG 26:2; GlcADG 13:1-13:1; [M-H]-	Bruker LipidBlast	822.2	Neg
1.97	520.33899	PC 18:2e; PC 16:2e/2:0; [M+H]+	Bruker LipidBlast	848.9	Pos
2	**482.32447**	**LPC(15:0)+H**	**LipidMatch/Bruker LipidBlast**	**530.4**	**Pos**
2.01	526.31133	LPC(15:0)+HCO2	LipidMatch	N/A	Neg
2.04	674.50538	Plasmenyl-PC(P-16:1/13:0)+H	LipidMatch	N/A	Pos
2.06	**508.33984**	**LPC(17:1)+H**	**LipidMatch/Bruker LipidBlast**	**601.7**	**Pos**

2.15	**496.34009**	**LPC(16:0)+H**	**LipidMatch/Bruker LipidBlast**	**989.1**	**Pos**
2.15	540.3273	LPC(16:0)+HCO2	LipidMatch	N/A	Neg
2.16	648.46858	PC 26:1; PC 7:0-19:1; [M+H]+	Bruker LipidBlast	621.5	Pos
2.22	**522.356**	**MGDG(2:0_16:1)+NH4-CO**	**LipidMatch/Bruker LipidBlast**	**985.3**	**Pos**
2.25	**478.29183**	**LPE(18:1)-H**	**LipidMatch/Bruker LipidBlast**	**976.4**	**Neg**
2.26	327.22014	FA 18:2+3O	MassBank	844.3	Neg
2.27	426.35797	Oleoyl-L-Carnitine	LC-MS-MS Positive Mode	973.7	Pos
2.32	496.34011	PC(16:0/0:0)	LC-MS-MS Positive Mode	968.2	Pos
2.35	454.29306	LPE 16:0; [M+H]+	Bruker LipidBlast	985.5	Pos
2.35	454.29306	LPE(16:0)+H	LipidMatch	N/A	Pos
2.35	452.26484	LPE(16:0)-H	LipidMatch	N/A	Neg
2.36	452.24517	OxLPE(15:0(CHO))-H	LipidMatch	N/A	Neg
2.39	408.32324	MMV688990	LC-MS-MS Positive Mode	944.9	Pos
2.4	**522.35594**	**LPC(18:1)+H**	**LipidMatch/Bruker LipidBlast**	**608.9**	**Pos**
2.43	**480.30869**	**LPE(18:1)+H**	**LipidMatch/Bruker LipidBlast**	**950.5**	**Pos**
2.44	**478.29428**	**LPE(18:1)-H**	**LipidMatch/Bruker LipidBlast**	**970.9**	**Neg**
2.5	303.22034	Aleuretic Acid	LC-MS-MS Negative Mode	991.4	Neg
2.51	579.42526	FAHFA(20:4/18:3)-H	LipidMatch	N/A	Neg
2.53	529.40968	FAHFA(16:1/18:3)-H	LipidMatch	N/A	Neg
2.55	**510.35601**	**LPC(17:0)+H**	**LipidMatch/Bruker LipidBlast**	**575.2**	**Pos**
2.55	554.33269	LPC(17:0)+HCO2	LipidMatch	N/A	Neg
2.6	329.23585	FA 18:1+3O	MassBank	648.7	Neg
2.62	329.21117	17alpha-Hydroxyprogesterone	MassBank	888.4	Neg
2.64	367.21504	OxFA 20:4(4O(2Cyc)); [M-H]-	Bruker LipidBlast	988.9	Neg
2.65	367.19198	LPA 13:0; [M-H]-	Bruker LipidBlast	279.5	Neg
2.65	504.29615	LPE(20:2)-H	LipidMatch	N/A	Neg
2.7	480.34477	Plasmenyl-LPC(P-16:0)+H	LipidMatch	N/A	Pos
2.82	396.21742	LPE 12:0; [M-H]-	Bruker LipidBlast	191.8	Neg
2.87	241.22434	Pentadecanoic acid	LC-MS-MS Negative Mode	992.1	Neg
2.94	396.18262	PE 11:0; PE 3:0-8:0; [M-H]-	Bruker LipidBlast	435.8	Neg
3.14	331.28432	Ceratodictyol	LC-MS-MS Positive Mode	158	Pos
3.17	351.22014	OxFA 20:4(3O(2Cyc)); [M-H]-	Bruker LipidBlast	984.9	Neg
3.26	**524.37153**	**LPC(18:0)+H**	**LipidMatch/Bruker LipidBlast**	**979.4**	**Pos**
3.26	568.34945	LPC(18:0)+HCO2	LipidMatch	N/A	Neg
3.31	482.32438	LPE(18:0)+H	LipidMatch	N/A	Pos
3.32	**480.30744**	**LPE(18:0)-H**	**LipidMatch/Bruker LipidBlast**	**171**	**Neg**
3.33	**550.38737**	**LPC(20:1)+H**	**LipidMatch/Bruker LipidBlast**	**454.6**	**Pos**

3.34	480.27765	OxLPE(17:1(OH))-H	LipidMatch	N/A	Neg
3.39	**508.34003**	**LPE(20:1)+H**	**LipidMatch/Bruker LipidBlast**	**989**	**Pos**
3.46	540.44747	DG(14:1_15:1)+NH4	LipidMatch	N/A	Pos
3.59	281.25388	Oleic acid	MassBank	994.2	Neg
3.64	990.56448	OxPC(22:3(OOO)_22:6(Ke))+HCO2	LipidMatch	N/A	Neg
3.73	494.31163	LPE(19:0)-H	LipidMatch	N/A	Neg
3.73	494.29404	PE 18:0; PE 9:0-9:0; [M-H]-	Bruker LipidBlast	195.9	Neg
3.88	508.37659	Plasmanyl-LPC(O-18:1)+H	LipidMatch	N/A	Pos
3.89	552.35371	Plasmanyl-LPC(O-18:0)+HCO2	LipidMatch	N/A	Neg
3.91	269.25448	FA 17:0; [M-H]-	Bruker LipidBlast	996	Neg
3.92	464.30109	GLYCOCHOLATE	LC-MS-MS Negative Mode	890.4	Neg
4.05	464.06289	(Methylsulfinyl)hexyl glucosinolate	MassBank	384.7	Neg
4.05	464.28198	PE 17:1e; PE 14:1e/3:0; [M-H]-	Bruker LipidBlast	388.1	Neg
4.07	464.30204	Plasmenyl-LPE(P-18:0)-H	LipidMatch	N/A	Neg
4.08	730.56801	MGDG(11:0_22:2)+NH4-CO	LipidMatch	N/A	Pos
4.11	435.24077	LPA(18:0)-H	LipidMatch	N/A	Neg
4.13	435.25413	LPA 18:1; [M-H]-	Bruker LipidBlast	278.4	Neg
4.14	284.29493	Stearamide	LC-MS-MS Positive Mode	993.8	Pos
4.25	295.22581	OxFA 18:1(1O(1Cyc)); [M-H]-	Bruker LipidBlast	993.4	Neg
4.45	391.28448	Dioctylphthalate	LC-MS-MS Positive Mode	992.5	Pos
4.74	**552.40302**	**LPC(20:0)+H**	**LipidMatch/Bruker LipidBlast**	**677.5**	**Pos**
4.79	**465.30328**	**LPA(20:0)-H**	**LipidMatch/Bruker LipidBlast**	**276.5**	**Neg**
4.81	401.34153	7-Oxocholesterol	LC-MS-MS Positive Mode	682.8	Pos
4.81	934.64028	PS(22:6_25:0)+H	LipidMatch	N/A	Pos
4.89	**534.35227**	**LPE(22:1)-H**	**LipidMatch/Bruker LipidBlast**	**801.5**	**Neg**
4.89	788.60969	PEtOH(15:0_24:2)+NH4	LipidMatch	N/A	Pos
4.92	**744.58329**	**MGDG(14:0_20:2)+NH4-CO**	**LipidMatch/Bruker LipidBlast**	**959.2**	**Pos**
4.97	536.37206	LPE 22:1; [M+H]+	Bruker LipidBlast	921	Pos
5.05	283.27407	Stearic acid	LC-MS-MS Negative Mode	998.9	Neg
5.06	604.43449	LPC 24:2; [M+H]+	Bruker LipidBlast	464.1	Pos
5.53	492.33164	Plasmenyl-LPE(P-20:0)-H	LipidMatch	N/A	Neg
5.61	587.36203	PA(14:1_14:1)-H	LipidMatch	N/A	Neg
5.66	536.4072	Plasmanyl-LPC(O-20:1)+H	LipidMatch	N/A	Pos
5.68	580.3862	Plasmanyl-LPC(O-20:0)+HCO2	LipidMatch	N/A	Neg
5.7	884.54404	PG(22:6_22:6)+NH4	LipidMatch	N/A	Pos
5.7	**865.48963**	**PG(22:6_22:6)-H**	**LipidMatch/Bruker LipidBlast**	**574.7**	**Neg**
5.71	297.28477	FA 19:0; [M-H]-	Bruker LipidBlast	928.2	Neg
5.77	459.07095	NCGC00386097-01!	LC-MS-MS Negative Mode	964.1	Neg
5.87	494.36068	CerP(d15:0/10:0)+H	LipidMatch	N/A	Pos

5.87	382.20189	LPE 11:0; [M-H]-	Bruker LipidBlast	190.3	Neg
5.88	492.31447	PE 19:1e; PE 14:1e/5:0; [M-H]-	Bruker LipidBlast	430.6	Neg
5.88	492.33241	Plasmenyl-LPE(P-20:0)-H	LipidMatch	N/A	Neg
5.92	865.49059	PI 37:7; PI 19:2-18:5; [M-H]-	Bruker LipidBlast	675.6	Neg
5.93	677.42062	PA 35:6; PA 13:1-22:5; [M-H]-	Bruker LipidBlast	242.2	Neg
6.1	297.24157	OxFA 18:0(1O(1Cyc)); [M-H]-	Bruker LipidBlast	887.8	Neg
6.12	810.52901	BMP(16:1_22:6)+NH4	LipidMatch	N/A	Pos
6.13	791.47357	OxCL(16:1_22:6(OOH)2_18:1_22:6)-2H	LipidMatch	N/A	Neg
6.25	813.57491	PG(17:2_22:2)+H	LipidMatch	N/A	Pos
6.27	791.56224	PA(21:0_22:6)+H	LipidMatch	N/A	Pos
6.29	650.42666	LPC(24:1)+HCO2	LipidMatch	N/A	Neg
6.34	747.5355	SM(d20:4/18:3)+H	LipidMatch	N/A	Pos
6.35	691.44123	PG(14:0_16:1)-H	LipidMatch	N/A	Neg
6.35	867.50516	PG(22:5_22:6)-H	LipidMatch	N/A	Neg
6.37	725.52201	PEtOH(20:0_16:3)-H	LipidMatch	N/A	Pos
6.4	703.50911	PA(16:1_20:0)+H	LipidMatch	N/A	Pos
6.53	615.45672	SM(d20:3/8:0)+H	LipidMatch	N/A	Pos
6.6	717.45746	OxCL(16:0_22:6_16:1_16:1(OH))-2H	LipidMatch	N/A	Neg
6.61	767.47321	PG(16:1_20:4)-H	LipidMatch	N/A	Neg
6.63	549.4172	TG(12:0_8:0_8:0)+Na	LipidMatch	N/A	Pos
6.64	843.50485	OxCL(18:2(OOH)2_22:6(OOH)_20:3_22:3(OH))-2H	LipidMatch	N/A	Neg
6.69	483.21024	PA 21:5; PA 3:0-18:5; [M-H]-	Bruker LipidBlast	255.5	Neg
6.74	948.71957	OxTG(14:1(OH)_22:4(OOOO)_16:1)+NH4	LipidMatch	N/A	Pos
6.78	904.69372	PG(18:2_26:0)+NH4	LipidMatch	N/A	Pos
6.78	793.48856	PI 31:1; PI 16:0-15:1; [M-H]-	Bruker LipidBlast	740.2	Neg
6.8	**606.45032**	**LPC(24:1)+H**	**LipidMatch/Bruker LipidBlast**	**978.3**	**Pos**
6.8	**817.48921**	**PG(18:2_22:6)-H**	**LipidMatch/Bruker LipidBlast**	**768.1**	**Neg**
6.82	650.42645	LPC(24:1)+HCO2	LipidMatch	N/A	Neg
6.82	860.66726	OxTG(18:4(OO)_14:1(Ke)_16:0)+NH4	LipidMatch	N/A	Pos
6.86	816.64124	PC(16:1_22:0)+H	LipidMatch	N/A	Pos
6.87	536.35853	LPE(22:0)-H	LipidMatch	N/A	Neg
6.9	**564.40342**	**LPE(24:1)+H**	**LipidMatch/Bruker LipidBlast**	**967.1**	**Pos**
6.91	**772.61468**	**Plasmenyl-PC(P-20:0/16:1)+H**	**LipidMatch/Bruker LipidBlast**	**630.2**	**Pos**
6.92	**562.38416**	**LPE(24:1)-H**	**LipidMatch/Bruker LipidBlast**	**761.6**	**Neg**
6.95	728.58871	TG(14:1_20:5_8:0)+NH4	LipidMatch	N/A	Pos
6.98	867.50553	OxPG(18:1_22:6(3O))-H	LipidMatch	N/A	Neg
6.99	684.5625	DG(18:2_22:5)+NH4	LipidMatch	N/A	Pos
7.02	632.46563	PC 26:2e; PC 16:2e/10:0; [M+H]+	Bruker LipidBlast	462	Pos
7.04	640.53651	TG(10:0_17:1_8:0)+NH4	LipidMatch	N/A	Pos
7.08	596.51038	DG(16:1_17:1)+NH4	LipidMatch	N/A	Pos
7.11	769.48862	OxCL(16:0_18:1_22:5_22:6(OH))-2H	LipidMatch	N/A	Neg

7.19	311.30003	Arachidic acid	LC-MS-MS Negative Mode	993.2	Neg
7.26	337.31495	FA 22:1; [M-H]-	Bruker LipidBlast	986.2	Neg
7.3	351.22018	OxFA 20:4(3O(2Cyc)); [M-H]-	Bruker LipidBlast	906	Neg
7.39	748.54719	Plasmenyl-PS(P-16:0/18:0)+H	LipidMatch	N/A	Pos
7.4	792.52633	OxPC(17:0_15:0(CHO))+HCO2	LipidMatch	N/A	Neg
7.55	731.47354	PG(16:1_17:1)-H	LipidMatch	N/A	Neg
7.58	722.53258	CerP(d18:1/24:4)+H	LipidMatch	N/A	Pos
7.69	694.37322	OxPC(15:1(OH)_8:1(COOH))+HCO2	LipidMatch	N/A	Neg
7.7	**650.47625**	**PC(12:0_14:0)+H**	**LipidMatch/Bruker LipidBlast**	**986.8**	**Pos**
7.71	694.45279	PC(12:0_14:0)+HCO2	LipidMatch	N/A	Neg
7.83	793.48932	PG(16:0_22:6)-H	LipidMatch	N/A	Neg
7.88	**779.45803**	**PI(14:0_16:1)-H**	**LipidMatch/LC-MS-MS Negative Mode**	**946.2**	**Neg**
7.96	**676.49171**	**PC(12:0_16:1)+H**	**LipidMatch/Bruker LipidBlast**	**953**	**Pos**
7.97	720.46858	PC(10:0_18:1)+HCO2	LipidMatch	N/A	Neg
8.01	819.46954	CL(22:6_22:6_22:6_22:6)-2H	LipidMatch	N/A	Neg
8.01	**838.55983**	**PG(18:1_22:6)+NH4**	**LipidMatch/Bruker LipidBlast**	**903.8**	**Pos**
8.02	**819.50448**	**PG(18:1_22:6)-H**	**LipidMatch/Bruker LipidBlast**	**758**	**Neg**
8.12	**702.50741**	**PC(14:1_16:1)+H**	**LipidMatch/Bruker LipidBlast**	**955**	**Pos**
8.12	693.45828	PG(14:0_16:0)-H	LipidMatch	N/A	Neg
8.13	746.48419	OxCL(16:0_18:1(OOH)_18:1_18:1(OOH))-2H	LipidMatch	N/A	Neg
8.21	230.24851	N,N-Dimethyldodecylamine N-oxide	LC-MS-MS Positive Mode	999.6	Pos
8.26	**664.49203**	**PMeOH(13:0_18:1)+NH4**	**LipidMatch/Bruker LipidBlast**	**989.8**	**Pos**
8.3	736.51258	BMP(16:1_16:1)+NH4	LipidMatch	N/A	Pos
8.32	**717.45734**	**PG(16:1_16:1)-H**	**LipidMatch/Bruker LipidBlast**	**202.7**	**Neg**
8.36	**676.49169**	**PC(14:0_14:1)+H**	**LipidMatch/Bruker LipidBlast**	**989.8**	**Pos**
8.45	734.48424	CL(16:0_16:1_20:4_22:6)-2H	LipidMatch	N/A	Neg
8.46	**764.54392**	**PG(16:1_18:1)+NH4**	**LipidMatch/Bruker LipidBlast**	**982.6**	**Pos**
8.47	752.52258	PC 34:5; PC 14:1-20:4; [M+H]+	Bruker LipidBlast	951.6	Pos
8.47	**702.50785**	**PC(14:1_16:1)+H**	**LipidMatch/Bruker LipidBlast**	**993.6**	**Pos**
8.48	745.48872	PG(14:1_20:1)-H	LipidMatch	N/A	Neg
8.51	881.50477	PI(18:1_20:5)-H	LipidMatch	N/A	Neg
8.54	831.48937	PI(16:1_18:2)-H	LipidMatch	N/A	Neg
8.58	840.57548	BMP(18:1_22:5)+NH4	LipidMatch	N/A	Pos
8.62	**778.5389**	**PMeOH(20:3_20:4)+NH4**	**LipidMatch/Bruker LipidBlast**	**963.9**	**Pos**
8.66	743.4734	PG(16:1_18:2)-H	LipidMatch	N/A	Neg
8.7	**664.49208**	**PC(13:0_14:0)+H**	**LipidMatch/Bruker LipidBlast**	**952**	**Pos**
8.71	708.46711	PC(13:0_14:0)+HCO2	LipidMatch	N/A	Neg
8.73	745.48844	PG(16:1_18:1)-H	LipidMatch	N/A	Neg

8.8	**736.49178**	**PE(16:1_20:5)+H**	**LipidMatch/Bruker LipidBlast**	**333.2**	**Pos**
8.81	734.46411	PE(16:1_20:5)-H	LipidMatch	N/A	Neg
8.85	634.48125	PC 26:1e; PC 16:1e/10:0; [M+H]+	Bruker LipidBlast	978.1	Pos
8.9	**728.52264**	**PMeOH(18:1_18:3)+NH4**	**LipidMatch/Bruker LipidBlast**	**965.8**	**Pos**
8.91	847.53651	PG(20:2_22:5)-H	LipidMatch	N/A	Neg
8.92	**690.50768**	**PC(14:1_15:0)+H**	**LipidMatch/Bruker LipidBlast**	**990.3**	**Pos**
8.92	797.51968	PG(18:1_20:3)-H	LipidMatch	N/A	Neg
8.98	564.38969	LPE(24:0)-H	LipidMatch	N/A	Neg
9.03	**716.52276**	**PC(15:1_16:1)+H**	**LipidMatch/Bruker LipidBlast**	**952.3**	**Pos**
9.06	771.50454	PG(18:1_18:2)-H	LipidMatch	N/A	Neg
9.12	881.50526	PI(16:0_22:6)-H	LipidMatch	N/A	Neg
9.15	854.57011	PC 42:10; PC 20:4-22:6; [M+H]+	Bruker LipidBlast	904	Pos
9.17	**778.53911**	**PC(14:0_22:6)+H**	**LipidMatch/Bruker LipidBlast**	**954.8**	**Pos**
9.18	907.52104	PI(18:1_22:6)-H	LipidMatch	N/A	Neg
9.21	**804.55421**	**PC(16:1_22:6)+H**	**LipidMatch/Bruker LipidBlast**	**952.8**	**Pos**
9.23	**678.50693**	**PMeOH(14:0_18:1)+NH4**	**LipidMatch/Bruker LipidBlast**	**977**	**Pos**
9.25	848.53163	PC(16:1_22:6)+HCO2	LipidMatch	N/A	Neg
9.3	**804.55433**	**PC(16:1_22:6)+H**	**LipidMatch/Bruker LipidBlast**	**953.2**	**Pos**
9.36	**736.4919**	**PE(14:0_22:6)+H**	**LipidMatch/Bruker LipidBlast**	**954.7**	**Pos**
9.5	760.42584	OxPC(14:1_15:2(COOH))+HCO2	LipidMatch	N/A	Neg
9.5	**762.50757**	**PE(16:1_22:6)+H**	**LipidMatch/Bruker LipidBlast**	**592.8**	**Pos**
9.51	760.47865	PE(16:1_22:6)-H	LipidMatch	N/A	Neg
9.53	1194.8184	AcylGlcADG 64:15; AcylGlcADG 22:6-22:6-20:3; [M+NH4]+	Bruker LipidBlast	194.8	Pos
9.6	**857.47905**	**OxPG(16:0_22:6(4O))-H**	**LipidMatch/Bruker LipidBlast**	**412.7**	**Neg**
9.65	**678.50743**	**PC(14:0_14:0)+H**	**LipidMatch/Bruker LipidBlast**	**993.5**	**Pos**
9.65	807.48861	PI(16:0_16:1)-H	LipidMatch	N/A	Neg
9.66	722.48357	PC(14:0_14:0)+HCO2	LipidMatch	N/A	Neg
9.68	722.41562	OxPC(14:0_12:1(COOH))+HCO2	LipidMatch	N/A	Neg
9.68	830.56988	PC 40:8; PC 20:4-20:4; [M+H]+	Bruker LipidBlast	923.8	Pos
9.7	754.53831	PC 34:4; PC 17:2-17:2; [M+H]+	Bruker LipidBlast	975.8	Pos
9.71	833.5039	PI(16:1_18:1)-H	LipidMatch	N/A	Neg
9.78	**704.52335**	**PC(14:0_16:1)+H**	**LipidMatch/Bruker LipidBlast**	**971.9**	**Pos**
9.79	748.49964	PC(14:0_16:1)+HCO2	LipidMatch	N/A	Neg
9.83	**780.55437**	**PC(16:1_20:4)+H**	**LipidMatch/Bruker LipidBlast**	**914.7**	**Pos**
9.84	824.53044	PC(16:1_20:4)+HCO2	LipidMatch	N/A	Neg
9.89	**806.57053**	**PC(16:1_22:5)+H**	**LipidMatch/Bruker LipidBlast**	**988.1**	**Pos**
9.91	**730.5392**	**PC(16:1_16:1)+H**	**LipidMatch/Bruker LipidBlast**	**960.9**	**Pos**

9.91	831.65946	TG(10:0_17:2_22:4)+Na	LipidMatch	N/A	Pos
9.92	774.51605	PC(16:1_16:1)+HCO2	LipidMatch	N/A	Neg
9.97	752.52096	PC(16:1_16:1)+Na	LipidMatch	N/A	Pos
9.99	**662.47676**	**PE(14:0_16:1)+H**	**LipidMatch/Bruker LipidBlast**	**824.6**	**Pos**
9.99	**701.56008**	**SM(d18:2/16:0)+H**	**LipidMatch/Bruker LipidBlast**	**980.7**	**Pos**
10	**726.50582**	**PC(14:0_16:1)+Na**	**LipidMatch/Bruker LipidBlast**	**649.8**	**Pos**
10	660.44651	PE(14:0_16:1)-H	LipidMatch	N/A	Neg
10.01	764.5443	BMP(16:1_18:1)+NH4	LipidMatch	N/A	Pos
10.01	732.46829	PS(16:0_16:1)-H	LipidMatch	N/A	Neg
10.02	**738.50824**	**PE(16:1_20:4)+H**	**LipidMatch/Bruker LipidBlast**	**337.1**	**Pos**
10.04	736.47813	CL(16:1_18:1_18:2_22:5)-2H	LipidMatch	N/A	Neg
10.09	792.57515	BMP 36:2; BMP 18:1-18:1; [M+NH4]+	Bruker LipidBlast	712.6	Pos
10.1	**818.5705**	**PC(17:1_22:6)+H**	**LipidMatch/Bruker LipidBlast**	**947.6**	**Pos**
10.1	**688.49223**	**PE(16:1_16:1)+H**	**LipidMatch/Bruker LipidBlast**	**789.2**	**Pos**
10.1	**764.52528**	**PE(18:1_20:5)+H**	**LipidMatch/Bruker LipidBlast**	**261.9**	**Pos**
10.12	686.46235	PE(16:1_16:1)-H	LipidMatch	N/A	Neg
10.16	**692.52349**	**PC(14:0_15:0)+H**	**LipidMatch/Bruker LipidBlast**	**952.9**	**Pos**
10.17	736.49863	PE(16:1_20:4)-H	LipidMatch	N/A	Neg
10.2	704.5234	PC 30:1; PC 6:0-24:1; [M+H]+	Bruker LipidBlast	970.9	Pos
10.22	**756.55474**	**PC(16:1_18:2)+H**	**LipidMatch/Bruker LipidBlast**	**952.9**	**Pos**
10.26	780.5539	PC 36:5; PC 14:1-22:4; [M+H]+	Bruker LipidBlast	922.2	Pos
10.3	762.46224	OxPC(16:1_13:1(COOH))+HCO2	LipidMatch	N/A	Neg
10.3	**718.53911**	**PC(14:1_17:0)+H**	**LipidMatch/Bruker LipidBlast**	**953.1**	**Pos**
10.31	762.5147	PE(16:0_22:6)-H	LipidMatch	N/A	Neg
10.32	**806.57052**	**PC(18:1_20:5)+H**	**LipidMatch/Bruker LipidBlast**	**952.8**	**Pos**
10.32	**714.50666**	**PE(16:1_18:2)+H**	**LipidMatch/Bruker LipidBlast**	**973.8**	**Pos**
10.37	792.57577	BMP 36:2; BMP 18:1-18:1; [M+NH4]+	Bruker LipidBlast	698.1	Pos
10.39	740.56401	PC 34:4e; PC 14:1e/20:3; [M+H]+	Bruker LipidBlast	195.9	Pos
10.42	**756.55465**	**PC(16:1_18:2)+H**	**LipidMatch/Bruker LipidBlast**	**953.1**	**Pos**
10.42	677.56016	SM d32:0; SM d15:0/17:0; [M+H]+	Bruker LipidBlast	982	Pos
10.43	800.53213	PC(16:1_18:2)+HCO2	LipidMatch	N/A	Neg
10.43	721.53612	SM(d18:0/14:0)+HCO2	LipidMatch	N/A	Neg
10.54	764.52359	PE(18:1_20:5)+H	LipidMatch	N/A	Pos
10.55	736.43615	OxPC(14:0_13:1(COOH))+HCO2	LipidMatch	N/A	Neg
10.55	692.52336	PC 29:0; PC 14:0-15:0; [M+H]+	Bruker LipidBlast	953	Pos
10.55	736.49862	PC(14:0_15:0)+HCO2	LipidMatch	N/A	Neg
10.56	**703.57567**	**SM(d18:1/16:0)+H**	**LipidMatch/Bruker LipidBlast**	**979.4**	**Pos**
10.57	730.53879	PC 32:2; PC 16:1-16:1; [M+H]+	Bruker LipidBlast	918.5	Pos

10.58	**714.50671**	**PE(16:1_18:2)+H**	**LipidMatch/Bruker LipidBlast**	**932.6**	**Pos**
10.59	762.49493	DMPE(16:1_20:5)-H	LipidMatch	N/A	Neg
10.59	**790.53849**	**PE(18:1_22:6)+H**	**LipidMatch/Bruker LipidBlast**	**408.4**	**Pos**
10.6	762.44227	OxPC(13:0_16:2(COOH))+HCO2	LipidMatch	N/A	Neg
10.6	736.49186	PC 33:6; PC 15:1-18:5; [M+H]+	Bruker LipidBlast	272.5	Pos
10.6	**782.57009**	**PC(16:1_20:3)+H**	**LipidMatch/Bruker LipidBlast**	**994.2**	**Pos**
10.6	734.49902	PS(16:0_16:1)+H	LipidMatch	N/A	Pos
10.63	762.70463	Cer-EODS(d19:0/13:0-O-16:1)-H	LipidMatch	N/A	Neg
10.64	794.57032	PC 37:5; PC 17:2-20:3; [M+H]+	Bruker LipidBlast	916.6	Pos
10.64	**718.53893**	**PC(15:0_16:1)+H**	**LipidMatch/Bruker LipidBlast**	**950.7**	**Pos**
10.65	762.51372	PC(15:0_16:1)+HCO2	LipidMatch	N/A	Neg
10.65	762.46165	Plasmenyl-PS(P-16:1/20:5)-H	LipidMatch	N/A	Neg
10.66	762.7224	Cer-AS(d15:1/34:0)-H	LipidMatch	N/A	Neg
10.67	**740.4719**	**Plasmenyl-PS(P-16:1/18:2)-H**	**LipidMatch/Bruker LipidBlast**	**317**	**Neg**
10.68	740.53234	DMPE(16:1_18:2)-H	LipidMatch	N/A	Neg
10.69	820.58946	PC 39:6; PC 17:0-22:6; [M+H]+	Bruker LipidBlast	911.7	Pos
10.74	**744.55477**	**PC(16:1_17:1)+H**	**LipidMatch/Bruker LipidBlast**	**952.9**	**Pos**
10.76	909.53588	PI(18:0_22:6)-H	LipidMatch	N/A	Neg
10.77	909.52009	OxPI(18:1_18:1(3O))-H	LipidMatch	N/A	Neg
10.77	750.51348	PC(15:0_15:0)+HCO2	LipidMatch	N/A	Neg
10.84	690.5445	PC 30:1e; PC 14:0e/16:1; [M+H]+	Bruker LipidBlast	858.6	Pos
10.86	750.49498	DMPE(15:0_20:5)-H	LipidMatch	N/A	Neg
10.88	**806.5707**	**PC(16:0_22:6)+H**	**LipidMatch/Bruker LipidBlast**	**953.2**	**Pos**
10.88	**832.58631**	**PC(18:1_22:6)+H**	**LipidMatch/Bruker LipidBlast**	**953.1**	**Pos**
10.89	850.54617	PC(16:0_22:6)+HCO2	LipidMatch	N/A	Neg
10.9	876.56209	PC(18:1_22:6)+HCO2	LipidMatch	N/A	Neg
10.94	**702.508**	**PE(16:1_17:1)+H**	**LipidMatch/Bruker LipidBlast**	**872**	**Pos**
10.95	**700.478**	**PE(16:1_17:1)-H**	**LipidMatch/Bruker LipidBlast**	**122.1**	**Neg**
10.98	716.56278	PC 32:2e; PC 16:1e/16:1; [M+H]+	Bruker LipidBlast	957.8	Pos
11.01	750.5147	HexCer-NS(d15:3/20:2)+HCO2	LipidMatch	N/A	Neg
11.01	750.45767	OxCL(16:1(OH)_18:3(OOH)2_18:1_18:2)-2H	LipidMatch	N/A	Neg
11.01	**706.53899**	**PC(15:0_15:0)+H**	**LipidMatch/Bruker LipidBlast**	**955**	**Pos**
11.07	**764.52335**	**PE(16:0_22:6)+H**	**LipidMatch/Bruker LipidBlast**	**689.2**	**Pos**
11.08	782.57059	PC 36:4; PC 18:2-18:2; [M+H]+	Bruker LipidBlast	807.5	Pos
11.08	762.49394	PE(16:0_22:6)-H	LipidMatch	N/A	Neg
11.13	788.5096	PE(18:1_22:6)-H	LipidMatch	N/A	Neg
11.14	788.46579	OxPC(15:1_16:2(COOH))+HCO2	LipidMatch	N/A	Neg
11.14	**790.53895**	**PE(18:1_22:6)+H**	**LipidMatch/Bruker LipidBlast**	**754.9**	**Pos**

11.15	**754.53544**	**PC(16:1_18:3)+H**	**LipidMatch/Bruker LipidBlast**	**547.5**	**Pos**
11.21	834.60171	PC 40:6; PC 20:3-20:3; [M+H]+	Bruker LipidBlast	955.1	Pos
11.23	770.56989	PC 35:3; PC 17:1-18:2; [M+H]+	Bruker LipidBlast	916.4	Pos
11.23	808.58594	PC 38:5; PC 18:0-20:5; [M+H]+	Bruker LipidBlast	904.7	Pos
11.23	703.57548	SM d34:1; SM d16:1/18:0; [M+H]+	Bruker LipidBlast	965.8	Pos
11.27	835.5204	PI(16:1_18:0)-H	LipidMatch	N/A	Neg
11.29	842.57131	PE 44:9; PE 26:4-18:5; [M+H]+	Bruker LipidBlast	192.2	Pos
11.32	728.52094	PC 32:3; PC 10:0-22:3; [M+H]+	Bruker LipidBlast	845.8	Pos
11.36	750.45824	OxPC(16:0_12:1(COOH))+HCO2	LipidMatch	N/A	Neg
11.36	782.56992	PC 36:4; PC 18:2-18:2; [M+H]+	Bruker LipidBlast	920.6	Pos
11.36	**706.53907**	**PC(14:0_16:0)+H**	**LipidMatch/Bruker LipidBlast**	**950.9**	**Pos**
11.37	750.51519	PC(14:0_16:0)+HCO2	LipidMatch	N/A	Neg
11.38	808.58553	PC 38:5; PC 18:0-20:5; [M+H]+	Bruker LipidBlast	855.8	Pos
11.42	766.55841	PG(16:0_18:1)+NH4	LipidMatch	N/A	Pos
11.45	**732.55545**	**PC(16:0_16:1)+H**	**LipidMatch/Bruker LipidBlast**	**634.3**	**Pos**
11.46	776.48323	OxPC(16:1_14:1(COOH))+HCO2	LipidMatch	N/A	Neg
11.46	776.53114	PC(16:0_16:1)+HCO2	LipidMatch	N/A	Neg
11.5	**703.57655**	**SM(d18:1/16:0)+H**	**LipidMatch/Bruker LipidBlast**	**978.3**	**Pos**
11.51	747.55212	SM(d18:1/16:0)+HCO2	LipidMatch	N/A	Neg
11.53	**758.57094**	**PC(16:1_18:1)+H**	**LipidMatch/Bruker LipidBlast**	**947.6**	**Pos**
11.54	802.50683	OxPC(16:1_16:2(COOH))+HCO2	LipidMatch	N/A	Neg
11.54	802.54676	PC(16:1_18:1)+HCO2	LipidMatch	N/A	Neg
11.56	**788.54127**	**PS(18:1_18:1)+H**	**LipidMatch/Bruker LipidBlast**	**168.3**	**Pos**
11.6	773.5676	SM(d20:1/16:1)+HCO2	LipidMatch	N/A	Neg
11.62	**766.53957**	**PE(18:1_20:4)+H**	**LipidMatch/Bruker LipidBlast**	**413.2**	**Pos**
11.62	**762.52945**	**PS(16:0_18:1)+H**	**LipidMatch/Bruker LipidBlast**	**652.7**	**Pos**
11.63	764.45757	OxPE(20:4_16:2(COOH))-H	LipidMatch	N/A	Neg
11.63	764.50974	PE(18:1_20:4)-H	LipidMatch	N/A	Neg
11.64	792.5555	PC 37:6; PC 15:1-22:5; [M+H]+	Bruker LipidBlast	943.8	Pos
11.67	690.50844	PE 32:1; PE 16:0-16:1; [M+H]+	Bruker LipidBlast	131.9	Pos
11.71	**788.54122**	**PS(18:1_18:1)+H**	**LipidMatch/Bruker LipidBlast**	**494.4**	**Pos**
11.72	**716.52408**	**PE(16:1_18:1)+H**	**LipidMatch/Bruker LipidBlast**	**827.9**	**Pos**
11.73	714.42275	OxPE(16:1_16:2(COOH))-H	LipidMatch	N/A	Neg
11.75	714.49423	PE(16:1_18:1)-H	LipidMatch	N/A	Neg
11.76	**784.58655**	**PC(18:1_18:2)+H**	**LipidMatch/Bruker LipidBlast**	**991.8**	**Pos**
11.8	796.58601	PC 37:4; PC 17:0-20:4; [M+H]+	Bruker LipidBlast	961	Pos
11.8	**720.5553**	**PC(15:0_16:0)+H**	**LipidMatch/Bruker LipidBlast**	**952.9**	**Pos**
11.83	764.73258	Cer-EODS(d18:0/15:0-O-15:0)-H	LipidMatch	N/A	Neg
11.83	764.47804	OxPE(20:4_17:1(Ke))-H	LipidMatch	N/A	Neg

11.83	764.53015	PE(18:1_20:4)-H	LipidMatch	N/A	Neg
11.87	721.50851	PG(16:0_16:1)+H	LipidMatch	N/A	Pos
11.91	790.50261	OxPC(16:1_15:1(COOH))+HCO2	LipidMatch	N/A	Neg
11.91	**808.58505**	**PC(16:0_22:5)+H**	**LipidMatch/Bruker LipidBlast**	**963**	**Pos**
11.92	790.54594	PC(16:1_17:0)+HCO2	LipidMatch	N/A	Neg
11.94	**746.57096**	**PC(16:1_17:0)+H**	**LipidMatch/Bruker LipidBlast**	**980.1**	**Pos**
11.95	758.57086	PC 34:2; PC 17:1-17:1; [M+H]+	Bruker LipidBlast	555.5	Pos
11.95	**806.5692**	**PC(18:1_18:2)+Na**	**LipidMatch/Bruker LipidBlast**	**838.9**	**Pos**
11.96	834.60252	PC 40:6; PC 20:3-20:3; [M+H]+	Bruker LipidBlast	941.6	Pos
11.98	**784.58659**	**PC(18:1_18:2)+H**	**LipidMatch/Bruker LipidBlast**	**953**	**Pos**
11.99	**742.53944**	**PE(18:1_18:2)+H**	**LipidMatch/Bruker LipidBlast**	**966**	**Pos**
12	740.50918	PE(18:1_18:2)-H	LipidMatch	N/A	Neg
12.01	556.49537	DAG 30:1; DAG 14:0-16:1; [M+NH4]+	Bruker LipidBlast	503.4	Pos
12.02	792.58838	PC 38:6e; PC 16:0e/22:6; [M+H]+	Bruker LipidBlast	817.5	Pos
12.04	230.24863	N,N-Dimethyldodecylamine N-oxide	LC-MS-MS Positive Mode	992.1	Pos
12.04	**754.53877**	**PE(17:0_20:4)+H**	**LipidMatch/Bruker LipidBlast**	**887.9**	**Pos**
12.05	764.50994	MMPE(15:0_22:5)-H	LipidMatch	N/A	Neg
12.07	582.51078	DAG 32:2; DAG 16:1-16:1; [M+NH4]+	Bruker LipidBlast	557.9	Pos
12.07	**810.60209**	**PC(18:1_20:3)+H**	**LipidMatch/Bruker LipidBlast**	**933.5**	**Pos**
12.07	818.57182	PE 42:7; PE 22:3-20:4; [M+H]+	Bruker LipidBlast	786.1	Pos
12.07	702.49368	PE(16:1_17:0)-H	LipidMatch	N/A	Neg
12.09	727.57379	SM d36:3; SM d14:2/22:1; [M+H]+	Bruker LipidBlast	158.1	Pos
12.1	716.55868	PC 32:2e; PC 16:1e/16:1; [M+H]+	Bruker LipidBlast	962.6	Pos
12.1	822.60215	PC 39:5; PC 19:2-20:3; [M+H]+	Bruker LipidBlast	941.7	Pos
12.12	797.65172	SM d41:3; SM d28:2/13:1; [M+H]+	Bruker LipidBlast	832.3	Pos
12.14	705.59188	SM d34:0; SM d19:0/15:0; [M+H]+	Bruker LipidBlast	979.9	Pos
12.15	749.56733	SM(d20:0/14:0)+HCO2	LipidMatch	N/A	Neg
12.22	**746.57089**	**PC(16:0_17:1)+H**	**LipidMatch/Bruker LipidBlast**	**952.7**	**Pos**
12.23	790.54613	PC(16:0_17:1)+HCO2	LipidMatch	N/A	Neg
12.25	790.50282	OxPC(17:1_14:1(COOH))+HCO2	LipidMatch	N/A	Neg
12.26	**772.58642**	**PC(17:1_18:1)+H**	**LipidMatch/Bruker LipidBlast**	**953.2**	**Pos**
12.26	**836.61775**	**PC(18:1_22:4)+H**	**LipidMatch/Bruker LipidBlast**	**880.1**	**Pos**
12.27	768.55385	PC 35:4; PC 17:1-18:3; [M+H]+	Bruker LipidBlast	893.3	Pos
12.27	816.56149	PC(17:1_18:1)+HCO2	LipidMatch	N/A	Neg
12.28	816.52588	OxPC(17:1_17:2(OH))+HCO2	LipidMatch	N/A	Neg
12.32	887.53243	GlcADG 44:12; GlcADG 22:6-22:6; [M-H]-	Bruker LipidBlast	833.5	Neg
12.32	734.57062	PC 32:0; PC 16:0-16:0; [M+H]+	Bruker LipidBlast	954.9	Pos
12.32	887.55155	PI(18:0_20:3)-H	LipidMatch	N/A	Neg
12.33	780.55492	PC 36:5; PC 14:1-22:4; [M+H]+	Bruker LipidBlast	626	Pos

12.33	754.53841	PC(14:0_20:4)+H	LipidMatch	N/A	Pos
12.36	**538.52099**	**Cer-NS(d18:1/16:0)+H**	**LipidMatch/Bruker LipidBlast**	**975.3**	**Pos**
12.37	582.49644	Cer-NS(d18:1/16:0)+HCO2	LipidMatch	N/A	Neg
12.41	**740.55879**	**BMP(16:0_16:0)+NH4**	**LipidMatch/Bruker LipidBlast**	**250**	**Pos**
12.43	856.58644	PC 42:9; PC 24:4-18:5; [M+H]+	Bruker LipidBlast	503.5	Pos
12.46	**730.53942**	**PE(17:1_18:1)+H**	**LipidMatch/Bruker LipidBlast**	**889.6**	**Pos**
12.47	728.44414	OxPE(17:1_16:2(COOH))-H	LipidMatch	N/A	Neg
12.47	728.50947	PE(17:1_18:1)-H	LipidMatch	N/A	Neg
12.49	810.60218	PC 38:4; PC 19:2-19:2; [M+H]+	Bruker LipidBlast	933.5	Pos
12.54	778.54579	PC(16:0_16:0)+HCO2	LipidMatch	N/A	Neg
12.56	**734.57046**	**PC(16:0_16:0)+H**	**LipidMatch/Bruker LipidBlast**	**955.1**	**Pos**
12.58	**792.5553**	**PE(18:0_22:6)+H**	**LipidMatch/Bruker LipidBlast**	**826.5**	**Pos**
12.59	**790.52522**	**PE(18:0_22:6)-H**	**LipidMatch/Bruker LipidBlast**	**436.9**	**Neg**
12.6	836.6176	PC 40:5; PC 18:1-22:4; [M+H]+	Bruker LipidBlast	909.9	Pos
12.63	862.63334	PC 42:6; PC 20:1-22:5; [M+H]+	Bruker LipidBlast	953	Pos
12.68	760.58614	PC(16:0_18:1)+H	LipidMatch	N/A	Pos
12.69	798.60119	PC 37:3; PC 18:1-19:2; [M+H]+	Bruker LipidBlast	952.1	Pos
12.69	**863.5522**	**PI(18:0_18:1)-H**	**LipidMatch/Bruker LipidBlast**	**746.6**	**Neg**
12.72	**768.55477**	**PE(18:1_20:3)+H**	**LipidMatch/Bruker LipidBlast**	**455.9**	**Pos**
12.75	858.59929	PC 42:8; PC 20:3-22:5; [M+H]+	Bruker LipidBlast	292.5	Pos
12.77	766.47366	OxCL(18:2_18:3_18:3(OOH)2_20:3)-2H	LipidMatch	N/A	Neg
12.77	766.52482	PE(18:1_20:3)-H	LipidMatch	N/A	Neg
12.8	836.61708	PC 40:5; PC 18:1-22:4; [M+H]+	Bruker LipidBlast	939.6	Pos
12.81	818.55632	OxPE(18:1_20:1(OOO))-H	LipidMatch	N/A	Neg
12.81	**820.5852**	**PE(20:1_20:2)+Na**	**LipidMatch/Bruker LipidBlast**	**950.6**	**Pos**
12.82	810.60057	PC 38:4; PC 19:2-19:2; [M+H]+	Bruker LipidBlast	945.2	Pos
12.87	**734.57073**	**PC(14:0_18:0)+H**	**LipidMatch/Bruker LipidBlast**	**988.7**	**Pos**
12.9	**786.60214**	**PC(18:1_18:1)+H**	**LipidMatch/Bruker LipidBlast**	**929.5**	**Pos**
12.9	830.57823	PC(18:1_18:1)+HCO2	LipidMatch	N/A	Neg
12.93	**760.58696**	**PC(16:1_18:0)+H**	**LipidMatch/Bruker LipidBlast**	**970.9**	**Pos**
12.94	804.5629	PC(16:0_18:1)+HCO2	LipidMatch	N/A	Neg
12.97	784.58216	PC(18:1_18:2)+H	LipidMatch	N/A	Pos
13.02	801.59953	SM(d20:1/18:1)+HCO2	LipidMatch	N/A	Neg
13.04	**768.55529**	**PE(18:0_20:4)+H**	**LipidMatch/Bruker LipidBlast**	**386**	**Pos**
13.04	**816.57276**	**PS(18:1_20:1)+H**	**LipidMatch/Bruker LipidBlast**	**382.1**	**Pos**
13.05	794.5711	PC 37:5; PC 17:2-20:3; [M+H]+	Bruker LipidBlast	416.2	Pos
13.06	766.52554	PE(18:0_20:4)-H	LipidMatch	N/A	Neg
13.06	731.60801	SM d36:1; SM d14:0/22:1; [M+H]+	Bruker LipidBlast	521.9	Pos

13.06	775.58315	SM(d20:1/16:0)+HCO2	LipidMatch	N/A	Neg
13.08	**790.55878**	**PS(18:0_18:1)+H**	**LipidMatch/Bruker LipidBlast**	**295.4**	**Pos**
13.12	812.61807	PC 38:3; PC 22:0-16:3; [M+H]+	Bruker LipidBlast	948	Pos
13.15	**744.55557**	**PE(18:1_18:1)+H**	**LipidMatch/Bruker LipidBlast**	**760.7**	**Pos**
13.17	835.67178	SM d44:5; SM d26:3/18:2; [M+H]+	Bruker LipidBlast	973.9	Pos
13.18	742.52598	DMPE(16:1_18:1)-H	LipidMatch	N/A	Neg
13.24	790.56136	PS(18:0_18:1)+H	LipidMatch	N/A	Pos
13.26	**748.5868**	**PC(16:0_17:0)+H**	**LipidMatch/Bruker LipidBlast**	**953.1**	**Pos**
13.26	**774.6025**	**PC(17:0_18:1)+H**	**LipidMatch/Bruker LipidBlast**	**953.2**	**Pos**
13.29	792.51928	OxPC(17:0_14:1(Ke,OH))+HCO2	LipidMatch	N/A	Neg
13.29	792.56219	PC(16:0_17:0)+HCO2	LipidMatch	N/A	Neg
13.33	802.54344	PS(18:1_19:0)-H	LipidMatch	N/A	Neg
13.34	818.54223	OxPC(17:0_17:2(OH))+HCO2	LipidMatch	N/A	Neg
13.34	818.57775	PC(17:0_18:1)+HCO2	LipidMatch	N/A	Neg
13.36	**796.58437**	**PC(17:0_18:1)+Na**	**LipidMatch/Bruker LipidBlast**	**135**	**Pos**
13.37	**812.6181**	**PC(18:1_20:2)+H**	**LipidMatch/Bruker LipidBlast**	**949.7**	**Pos**
13.38	820.62127	PC 40:6e; PC 22:3e/18:3; [M+H]+	Bruker LipidBlast	671.1	Pos
13.38	742.52414	PE(18:1_18:1)-H	LipidMatch	N/A	Neg
13.39	820.59629	PE(20:5_22:1)+H	LipidMatch	N/A	Pos
13.41	686.57275	DAG 40:6; DAG 18:1-22:5; [M+NH4]+	Bruker LipidBlast	623.3	Pos
13.51	**584.52627**	**DG(16:0_16:1)+NH4**	**LipidMatch/Bruker LipidBlast**	**923.6**	**Pos**
13.52	718.57534	PC 32:1e; PC 14:1e/18:0; [M+H]+	Bruker LipidBlast	924.1	Pos
13.53	**732.55499**	**PE(17:0_18:1)+H**	**LipidMatch/Bruker LipidBlast**	**977.9**	**Pos**
13.54	**610.5418**	**DG(16:1_18:1)+NH4**	**LipidMatch/Bruker LipidBlast**	**938.2**	**Pos**
13.54	838.63328	PC 40:4; PC 20:2-20:2; [M+H]+	Bruker LipidBlast	949.2	Pos
13.55	730.52523	PE(17:0_18:1)-H	LipidMatch	N/A	Neg
13.56	730.46034	OxPE(18:1_15:1(COOH))-H	LipidMatch	N/A	Neg
13.57	**800.61775**	**PC(17:1_20:1)+H**	**LipidMatch/Bruker LipidBlast**	**953**	**Pos**
13.58	822.6006	PC 39:5; PC 19:2-20:3; [M+H]+	Bruker LipidBlast	890.5	Pos
13.58	864.649	PC 42:5; PC 24:1-18:4; [M+H]+	Bruker LipidBlast	895.3	Pos
13.58	844.59337	PC(17:1_20:1)+HCO2	LipidMatch	N/A	Neg
13.58	781.62193	SM d40:4; SM d15:3/25:1; [M+H]+	Bruker LipidBlast	111.6	Pos
13.59	844.56434	OxPC(18:1_18:2(OH))+HCO2	LipidMatch	N/A	Neg
13.62	**774.6021**	**PC(17:1_18:0)+H**	**LipidMatch/Bruker LipidBlast**	**953.3**	**Pos**
13.62	818.57774	PC(17:1_18:0)+HCO2	LipidMatch	N/A	Neg
13.64	733.62298	SM d36:0; SM d23:0/13:0; [M+H]+	Bruker LipidBlast	979.8	Pos
13.65	777.599	SM(d20:0/16:0)+HCO2	LipidMatch	N/A	Neg
13.66	770.57148	PC 35:3; PC 17:0-18:3; [M+H]+	Bruker LipidBlast	912.7	Pos
13.71	797.65037	SM d41:3; SM d28:2/13:1; [M+H]+	Bruker LipidBlast	978.7	Pos

13.73	**762.60157**	**PC(16:0_18:0)+H**	**LipidMatch/Bruker LipidBlast**	**954.8**	**Pos**
13.73	806.57726	PC(16:0_18:0)+HCO2	LipidMatch	N/A	Neg
13.74	806.53898	OxPS(18:0_18:0(1O))-H	LipidMatch	N/A	Neg
13.76	811.66963	SM d42:3; SM d21:3/21:0; [M+H]+	Bruker LipidBlast	973.2	Pos
13.77	758.57072	PC 34:2; PC 17:1-17:1; [M+H]+	Bruker LipidBlast	664.5	Pos
13.78	826.63318	MGDG(18:1_20:2)+NH4	LipidMatch	N/A	Pos
13.78	756.48605	OxCL(18:1_18:1(OOH)_18:2_18:3(OOH))-2H	LipidMatch	N/A	Neg
13.78	826.63318	PC 39:3; PC 20:1-19:2; [M+H]+	Bruker LipidBlast	799.4	Pos
13.78	**746.60701**	**Plasmanyl-PC(O-16:1/18:0)+H**	**LipidMatch/Bruker LipidBlast**	**979.7**	**Pos**
13.79	756.54088	DMPE(17:1_18:1)-H	LipidMatch	N/A	Neg
13.79	890.66417	PC 44:6; PC 22:3-22:3; [M+H]+	Bruker LipidBlast	891.3	Pos
13.79	870.60943	PC(19:0_20:3)+HCO2	LipidMatch	N/A	Neg
13.81	**732.55461**	**PE(17:0_18:1)+H**	**LipidMatch/Bruker LipidBlast**	**492.8**	**Pos**
13.83	730.52501	CL(18:0_18:0_18:0_18:1)-2H	LipidMatch	N/A	Neg
13.85	846.60178	PC 41:7; PC 19:2-22:5; [M+H]+	Bruker LipidBlast	789.6	Pos
13.86	891.56436	GlcADG 44:10; GlcADG 22:5-22:5; [M-H]-	Bruker LipidBlast	834.1	Neg
13.87	891.58304	PI(18:0_20:1)-H	LipidMatch	N/A	Neg
13.9	788.61716	PC 36:1; PC 14:0-22:1; [M+H]+	Bruker LipidBlast	952.8	Pos
13.92	864.64825	PC 42:5; PC 24:1-18:4; [M+H]+	Bruker LipidBlast	887.4	Pos
13.93	610.54077	DG(16:0_18:2)+NH4	LipidMatch	N/A	Pos
14	**796.58581**	**PE(18:0_22:4)+H**	**LipidMatch/Bruker LipidBlast**	**960.7**	**Pos**
14.01	794.55683	PE(18:0_22:4)-H	LipidMatch	N/A	Neg
14.07	**770.57015**	**PE(18:0_20:3)+H**	**LipidMatch/Bruker LipidBlast**	**948.8**	**Pos**
14.08	768.54098	PE(18:0_20:3)-H	LipidMatch	N/A	Neg
14.18	**814.63263**	**PC(18:1_20:1)+H**	**LipidMatch/Bruker LipidBlast**	**955.3**	**Pos**
14.19	858.60911	PC(18:1_20:1)+HCO2	LipidMatch	N/A	Neg
14.25	**788.61701**	**PC(18:0_18:1)+H**	**LipidMatch/Bruker LipidBlast**	**952.8**	**Pos**
14.3	**785.65378**	**SM(d18:1/22:1)+H**	**LipidMatch/Bruker LipidBlast**	**979.9**	**Pos**
14.3	829.62976	SM(d22:1/18:1)+HCO2	LipidMatch	N/A	Neg
14.34	832.60173	PC(18:0_18:1)+HCO2	LipidMatch	N/A	Neg
14.37	**811.66935**	**SM(d18:2/24:1)+H**	**LipidMatch/Bruker LipidBlast**	**979.9**	**Pos**
14.38	**840.64821**	**PC(18:1_22:2)+H**	**LipidMatch/Bruker LipidBlast**	**879.5**	**Pos**
14.38	**772.5856**	**PE(18:1_20:1)+H**	**LipidMatch/Bruker LipidBlast**	**922.3**	**Pos**
14.39	770.55626	PE(18:1_20:1)-H	LipidMatch	N/A	Neg
14.45	**746.56998**	**PE(18:0_18:1)+H**	**LipidMatch/Bruker LipidBlast**	**910.4**	**Pos**
14.46	744.54116	PE(18:0_18:1)-H	LipidMatch	N/A	Neg
14.48	848.65596	PC 42:6e; PC 18:5e/24:1; [M+H]+	Bruker LipidBlast	964.2	Pos
14.48	**802.63281**	**PC(18:1_19:0)+H**	**LipidMatch/Bruker LipidBlast**	**952.9**	**Pos**

14.52	824.61444	PC 39:4; PC 17:0-22:4; [M+H]+	Bruker LipidBlast	776.7	Pos
14.53	**776.61665**	**PC(17:0_18:0)+H**	**LipidMatch/Bruker LipidBlast**	**953**	**Pos**
14.54	846.6087	PC(18:1_19:0)+HCO2	LipidMatch	N/A	Neg
14.61	888.66489	HexCer-AP(t18:0/24:1)+HCO2	LipidMatch	N/A	Neg
14.61	856.59345	PC(18:1_20:2)+HCO2	LipidMatch	N/A	Neg
14.72	758.55644	PE(18:1_19:0)-H	LipidMatch	N/A	Neg
14.77	872.6256	PC(17:0_22:2)+HCO2	LipidMatch	N/A	Neg
14.8	772.62069	PC 36:2e; PC 14:0e/22:2; [M+H]+	Bruker LipidBlast	943.8	Pos
14.8	787.66943	SM d40:1; SM d21:0/19:1; [M+H]+	Bruker LipidBlast	980.1	Pos
14.81	828.65165	PC 39:2; PC 20:0-19:2; [M+H]+	Bruker LipidBlast	940	Pos
14.82	265.1362	(1S,8R,9R)-8-hydroxy-4-(propan-2-ylidene)-10-oxatricyclo[7.2.1.01,5]dodecane-8-carboxylic acid	LC-MS-MS Negative Mode	978	Neg
14.82	831.64574	SM(d24:1/16:0)+HCO2	LipidMatch	N/A	Neg
14.83	638.57249	DAG 36:2; DAG 18:1-18:1; [M+NH4]+	Bruker LipidBlast	540.1	Pos
14.84	**612.55688**	**DG(16:0_18:1)+NH4**	**LipidMatch/Bruker LipidBlast**	**833.5**	**Pos**
14.9	780.59194	PE 40:5e; PE 20:5e/20:0; [M+H]+	Bruker LipidBlast	217.6	Pos
14.91	**799.66945**	**SM(d17:1/24:1)+H**	**LipidMatch/Bruker LipidBlast**	**980**	**Pos**
14.91	843.64621	SM(d17:1/24:1)+HCO2	LipidMatch	N/A	Neg
14.92	813.68494	SM d42:2; SM d22:0/20:2; [M+H]+	Bruker LipidBlast	964.5	Pos
14.94	761.65375	SM d38:0; SM d22:0/16:0; [M+H]+	Bruker LipidBlast	979.8	Pos
14.94	835.66727	SM d44:5; SM d26:3/18:2; [M+H]+	Bruker LipidBlast	221.4	Pos
15.02	774.63986	PC 36:1e; PC 16:1e/20:0; [M+H]+	Bruker LipidBlast	938.8	Pos
15.02	818.61791	Plasmanyl-PC(O-20:0/16:1)+HCO2	LipidMatch	N/A	Neg
15.05	728.54614	Plasmenyl-PE(P-18:0/18:1)-H	LipidMatch	N/A	Neg
15.08	664.57445	Cer-NS(d18:1/22:1)+HCO2	LipidMatch	N/A	Neg
15.15	690.59012	Cer-NS(d18:2/24:1)+HCO2	LipidMatch	N/A	Neg
15.24	918.69399	PC 46:6; PC 22:2-24:4; [M+H]+	Bruker LipidBlast	674	Pos
15.27	822.64402	PC 38:2e; PC 18:1e/20:1; [M+H]+	Bruker LipidBlast	521.2	Pos
15.31	886.64085	PC(16:1_24:1)+HCO2	LipidMatch	N/A	Neg
15.32	**842.66399**	**PC(18:1_22:1)+H**	**LipidMatch/Bruker LipidBlast**	**740.9**	**Pos**
15.37	868.67955	PC 42:3; PC 26:1-16:2; [M+H]+	Bruker LipidBlast	875.5	Pos
15.39	801.68456	SM d41:1; SM d25:1/16:0; [M+H]+	Bruker LipidBlast	349.2	Pos
15.39	845.66125	SM(d17:0/24:1)+HCO2	LipidMatch	N/A	Neg
15.4	**816.64847**	**PC(14:0_24:1)+H**	**LipidMatch/Bruker LipidBlast**	**959.3**	**Pos**
15.4	848.60408	PE(20:4_24:1)-H	LipidMatch	N/A	Neg
15.42	876.64695	PC 43:6; PC 19:2-24:4; [M+H]+	Bruker LipidBlast	777.6	Pos
15.47	**813.68475**	**SM(d18:1/24:1)+H**	**LipidMatch/Bruker LipidBlast**	**997.7**	**Pos**
15.47	857.66205	SM(d24:1/18:1)+HCO2	LipidMatch	N/A	Neg
15.52	800.61697	PC 37:2; PC 17:0-20:2; [M+H]+	Bruker LipidBlast	339.6	Pos
15.59	**787.66946**	**SM(d18:1/22:0)+H**	**LipidMatch/Bruker LipidBlast**	**997.9**	**Pos**
15.59	831.64559	SM(d22:0/18:1)+HCO2	LipidMatch	N/A	Neg

15.81	827.7003	SM d43:2; SM d14:1/29:1; [M+H]+	Bruker LipidBlast	994.6	Pos
15.84	258.27924	N,N-Dimethyltetradecylamine-N-oxide	LC-MS-MS Positive Mode	982.1	Pos
15.85	856.6801	PC 41:2; PC 17:0-24:2; [M+H]+	Bruker LipidBlast	836.6	Pos
15.93	**815.70069**	**SM(d18:1/24:0)+H**	**LipidMatch/Bruker LipidBlast**	**980.1**	**Pos**
16	852.68895	PC 42:4e; PC 18:2e/24:2; [M+H]+	Bruker LipidBlast	725.7	Pos
16.03	640.58812	DAG 36:1; DAG 18:0-18:1; [M+NH4]+	Bruker LipidBlast	280.6	Pos
16.03	827.70076	SM d43:2; SM d14:1/29:1; [M+H]+	Bruker LipidBlast	980.1	Pos
16.04	789.685	SM d40:0; SM d17:0/23:0; [M+H]+	Bruker LipidBlast	979.8	Pos
16.12	**802.67639**	**Plasmanyl-PC(O-20:0/18:1)+H**	**LipidMatch/Bruker LipidBlast**	**979.5**	**Pos**
16.13	845.66175	SM(d23:0/18:1)+HCO2	LipidMatch	N/A	Neg
16.15	758.60596	PC 35:2e; PC 18:1e/17:1; [M+H]+	Bruker LipidBlast	432.5	Pos
16.22	**648.6295**	**Cer-NS(d18:1/24:1)+H**	**LipidMatch/Bruker LipidBlast**	**972.5**	**Pos**
16.23	692.60565	Cer-NS(d18:1/24:1)+HCO2	LipidMatch	N/A	Neg
16.27	920.70989	PC 46:5; PC 24:0-22:5; [M+H]+	Bruker LipidBlast	944.2	Pos
16.36	896.71071	PC 44:3; PC 20:1-24:2; [M+H]+	Bruker LipidBlast	651.1	Pos
16.36	**870.6953**	**PC(18:1_24:1)+H**	**LipidMatch/Bruker LipidBlast**	**955.4**	**Pos**
16.37	914.67211	PC(18:1_24:1)+HCO2	LipidMatch	N/A	Neg
16.45	**844.67987**	**PC(16:1_24:0)+H**	**LipidMatch/Bruker LipidBlast**	**952.4**	**Pos**
16.48	**829.71524**	**SM(d20:1/23:0)+H**	**LipidMatch/Bruker LipidBlast**	**981.3**	**Pos**
16.53	882.68965	HexCer-NS(d20:1/24:1)+HCO2	LipidMatch	N/A	Neg
16.56	841.7162	SM d44:2; SM d20:1/24:1; [M+H]+	Bruker LipidBlast	980	Pos
16.56	**841.7162**	**SM(d20:1/24:1)+H**	**LipidMatch/Bruker LipidBlast**	**925.6**	**Pos**
16.57	885.693	SM(d20:1/24:1)+HCO2	LipidMatch	N/A	Neg
16.65	859.67714	SM(d24:0/18:1)+HCO2	LipidMatch	N/A	Neg
16.66	**815.70066**	**SM(d18:1/24:0)+H**	**LipidMatch/Bruker LipidBlast**	**980.1**	**Pos**
16.69	738.64679	Cer-NP(t20:0/24:1)+HCO2	LipidMatch	N/A	Neg
16.72	**624.63031**	**Cer-NDS(d18:0/22:0)+H**	**LipidMatch/Bruker LipidBlast**	**489.1**	**Pos**
16.77	706.62297	Cer-NS(d18:1/25:1)+HCO2	LipidMatch	N/A	Neg
16.84	884.71079	PC 43:2; PC 21:1-22:1; [M+H]+	Bruker LipidBlast	947.6	Pos
16.93	647.55899	DAG 36:0; DAG 18:0-18:0; [M+NH4]+	Bruker LipidBlast	907	Pos
16.94	829.71529	SM d43:1; SM d27:0/16:1; [M+H]+	Bruker LipidBlast	931.3	Pos
16.98	**843.73182**	**SM(d20:1/24:0)+H**	**LipidMatch/Bruker LipidBlast**	**980**	**Pos**
17.02	884.70624	HexCer-NS(d22:1/22:0)+HCO2	LipidMatch	N/A	Neg
17.03	858.73906	PC 42:1e; PC 16:0e/26:1; [M+H]+	Bruker LipidBlast	257.8	Pos
17.05	817.71616	SM d42:0; SM d14:0/28:0; [M+H]+	Bruker LipidBlast	979.8	Pos
17.11	**830.70564**	**Plasmanyl-PC(O-22:0/18:1)+H**	**LipidMatch/Bruker LipidBlast**	**986.3**	**Pos**
17.28	720.63694	Cer-NS(d20:1/24:1)+HCO2	LipidMatch	N/A	Neg
17.3	898.72641	PC 44:2; PC 22:1-22:1; [M+H]+	Bruker LipidBlast	617.7	Pos
17.31	942.70261	PC(20:1_24:1)+HCO2	LipidMatch	N/A	Neg

17.36	694.62143	Cer-NS(d18:1/24:0)+HCO2	LipidMatch	N/A	Neg
17.38	**1011.75095**	**HBMP(16:0_18:1_18:1)-H**	**LipidMatch/Bruker LipidBlast**	**687.7**	**Neg**
17.4	**872.71104**	**PC(18:1_24:0)+H**	**LipidMatch/Bruker LipidBlast**	**952.9**	**Pos**
17.47	854.65104	DMPE(18:1_24:1)-H	LipidMatch	N/A	Neg
17.51	869.74748	SM d46:2; SM d21:2/25:0; [M+H]+	Bruker LipidBlast	991.3	Pos
17.57	828.63516	PE(18:1_24:0)-H	LipidMatch	N/A	Neg
17.62	722.65257	Cer-NDS(d20:0/24:1)+HCO2	LipidMatch	N/A	Neg
17.62	843.73208	SM d44:1; SM d21:0/23:1; [M+H]+	Bruker LipidBlast	997.9	Pos
17.71	674.64252	Cer-NS(d20:1/24:2)+H	LipidMatch	N/A	Pos
17.77	**1362.94389**	**CL(32:2)(32:2)+NH4**	**LipidMatch/Bruker LipidBlast**	**944.7**	**Pos**
17.78	1343.89088	CL(16:1_16:1_16:1_16:1)-H	LipidMatch	N/A	Neg
17.87	1369.90688	CL(16:1_16:1_16:1_18:2)-H	LipidMatch	N/A	Neg
18.06	**795.64762**	**TG(14:1_16:1_16:1)+Na**	**LipidMatch/Bruker LipidBlast**	**858.6**	**Pos**
18.13	1058.83492	HBMP(16:0_20:1_18:1)+NH4	LipidMatch	N/A	Pos
18.14	1039.78228	HBMP(18:1_18:1_18:0)-H	LipidMatch	N/A	Neg
18.27	900.74192	PC 44:1; PC 23:0-21:1; [M+H]+	Bruker LipidBlast	951.6	Pos
18.28	944.71845	PC(18:1_26:0)+HCO2	LipidMatch	N/A	Neg
18.39	871.67866	TG 52:7; TG 14:1-19:3-19:3; [M+Na]+	Bruker LipidBlast	881.3	Pos
18.45	1371.9227	CL(16:1_16:1_16:1_18:1)-H	LipidMatch	N/A	Neg
18.45	1390.97501	CL(32:2)(34:2)+NH4	LipidMatch	N/A	Pos
18.55	1397.93871	CL(16:1_16:1_18:1_18:2)-H	LipidMatch	N/A	Neg
18.61	**680.69227**	**Cer-NDS(d20:0/24:0)+H**	**LipidMatch/Bruker LipidBlast**	**128.4**	**Pos**
18.74	873.69487	TG(14:0_16:1_22:5)+Na	LipidMatch	N/A	Pos
18.85	**880.71819**	**Co(Q10)+NH4**	**LipidMatch/LC-MS-MS Positive Mode**	**854.2**	**Pos**
18.91	**792.70795**	**TG(14:0_16:1_16:1)+NH4**	**LipidMatch/Bruker LipidBlast**	**834.3**	**Pos**
18.91	**818.72365**	**TG(14:1_16:1_18:1)+NH4**	**LipidMatch/Bruker LipidBlast**	**893.3**	**Pos**
18.92	766.69254	TG 44:1; TG 12:0-16:0-16:1; [M+NH4]+	Bruker LipidBlast	200	Pos
19.08	1399.95403	CL(16:1_16:1_18:1_18:1)-H	LipidMatch	N/A	Neg
19.09	849.6952	TG 50:4; TG 16:1-16:1-18:2; [M+NH4]+	Bruker LipidBlast	624.7	Pos
19.22	**925.72593**	**TG(16:1_18:1_22:6)+Na**	**LipidMatch/Bruker LipidBlast**	**778.5**	**Pos**
19.24	**899.70766**	**TG(16:0_16:1_22:6)+Na**	**LipidMatch/Bruker LipidBlast**	**801.6**	**Pos**
19.32	806.72341	TG 47:2; TG 14:0-16:1-17:1; [M+NH4]+	Bruker LipidBlast	378.4	Pos
19.52	**927.74179**	**TG(16:1_18:1_22:5)+Na**	**LipidMatch/Bruker LipidBlast**	**713.3**	**Pos**
19.55	**901.72498**	**TG(16:1_18:1_20:4)+Na**	**LipidMatch/Bruker LipidBlast**	**899.3**	**Pos**
19.57	875.70941	TG 52:5; TG 16:2-18:0-18:3; [M+NH4]+	Bruker LipidBlast	600	Pos
19.67	**846.7549**	**TG(16:1_16:1_18:1)+NH4**	**LipidMatch/Bruker LipidBlast**	**757.8**	**Pos**
19.68	1427.9864	CL(16:1_18:1_18:1_18:1)-H	LipidMatch	N/A	Neg
19.71	**820.73933**	**TG(14:0_16:1_18:1)+NH4**	**LipidMatch/Bruker LipidBlast**	**832.9**	**Pos**

19.73	**794.72353**	**TG(14:0_16:0_16:1)+NH4**	**LipidMatch/Bruker LipidBlast**	**824.5**	**Pos**
19.85	**872.76983**	**TG(16:1_18:1_18:2)+NH4**	**LipidMatch/Bruker LipidBlast**	**874.7**	**Pos**
19.98	**953.75721**	**TG(18:1_18:1_22:6)+Na**	**LipidMatch/Bruker LipidBlast**	**832.7**	**Pos**
20.02	**927.74048**	**TG(16:0_18:1_22:6)+Na**	**LipidMatch/Bruker LipidBlast**	**896.9**	**Pos**
20.06	860.77082	TG(16:1_17:1_18:1)+NH4	LipidMatch	N/A	Pos
20.08	**834.75491**	**TG(15:0_16:1_18:1)+NH4**	**LipidMatch/Bruker LipidBlast**	**659.9**	**Pos**
20.1	808.73915	TG 47:1; TG 15:0-16:0-16:1; [M+NH4]+	Bruker LipidBlast	727.7	Pos
20.25	695.57415	CE 20:4; [M+NH4]+	Bruker LipidBlast	502.9	Pos
20.25	**955.7717**	**TG(18:1_18:1_22:5)+Na**	**LipidMatch/Bruker LipidBlast**	**774**	**Pos**
20.28	**929.75648**	**TG(16:0_18:1_22:5)+Na**	**LipidMatch/Bruker LipidBlast**	**510.1**	**Pos**
20.31	898.78554	TG 54:5; TG 16:0-16:0-22:5; [M+Na]+	Bruker LipidBlast	862.3	Pos
20.41	874.78597	TG(16:1_18:1_18:1)+NH4	LipidMatch	N/A	Pos
20.44	848.77032	TG(16:0_16:1_18:1)+NH4	LipidMatch	N/A	Pos
20.46	822.75471	TG(14:0_16:0_18:1)+NH4	LipidMatch	N/A	Pos
20.5	**796.73895**	**TG(14:0_16:0_16:0)+NH4**	**LipidMatch/Bruker LipidBlast**	**930.9**	**Pos**
20.5	853.72583	TG(16:0_16:1_18:1)+Na	LipidMatch	N/A	Pos
20.5	900.80093	TG(18:1_18:1_18:2)+NH4	LipidMatch	N/A	Pos
20.51	**827.7103**	**TG(14:0_16:0_18:1)+Na**	**LipidMatch/Bruker LipidBlast**	**707.7**	**Pos**
20.57	**905.75734**	**TG(18:1_18:1_18:2)+Na**	**LipidMatch/Bruker LipidBlast**	**864.9**	**Pos**
20.67	841.72599	TG(14:0_17:0_18:1)+Na	LipidMatch	N/A	Pos
20.71	836.77047	TG(15:0_16:0_18:1)+NH4	LipidMatch	N/A	Pos
20.75	**888.80234**	**TG(17:1_18:1_18:1)+NH4**	**LipidMatch/Bruker LipidBlast**	**819.6**	**Pos**
20.78	**862.78619**	**TG(16:0_17:1_18:1)+NH4**	**LipidMatch/Bruker LipidBlast**	**821.1**	**Pos**
20.83	**978.84819**	**OxTG(18:1_18:1_20:1(OOO))+NH4**	**LipidMatch/Bruker LipidBlast**	**407.3**	**Pos**
20.85	**952.83279**	**OxTG(16:0_18:1_20:1(OOO))+NH4**	**LipidMatch/Bruker LipidBlast**	**566.3**	**Pos**
21.05	907.77267	TG(18:1_18:1_18:1)+Na	LipidMatch	N/A	Pos
21.07	**881.75653**	**TG(16:0_18:1_18:1)+Na**	**LipidMatch/Bruker LipidBlast**	**792.6**	**Pos**
21.08	902.81756	TG(16:1_18:1_20:1)+NH4	LipidMatch	N/A	Pos
21.12	**881.75728**	**TG(16:0_18:1_18:1)+Na**	**LipidMatch/Bruker LipidBlast**	**792.6**	**Pos**
21.12	**876.80208**	**TG(16:0_18:1_18:1)+NH4**	**LipidMatch/Bruker LipidBlast**	**865.2**	**Pos**
21.16	**850.78626**	**TG(16:0_16:0_18:1)+NH4**	**LipidMatch/Bruker LipidBlast**	**896.1**	**Pos**
21.18	824.77053	TG(15:0_16:0_17:0)+NH4	LipidMatch	N/A	Pos
21.26	895.77283	TG(17:0_18:1_18:1)+Na	LipidMatch	N/A	Pos
21.29	864.80202	TG 51:1; TG 15:1-18:0-18:0; [M+Na]+	Bruker LipidBlast	887.2	Pos
21.35	890.81736	TG(17:0_18:1_18:1)+NH4	LipidMatch	N/A	Pos
21.37	668.63436	CE(18:1)+NH4	LipidMatch	N/A	Pos

21.39	**916.83177**	**TG(17:1_18:1_20:1)+NH4**	**LipidMatch/Bruker LipidBlast**	**814.2**	**Pos**
21.68	**930.84884**	**TG(18:1_18:1_20:1)+NH4**	**LipidMatch/Bruker LipidBlast**	**874.2**	**Pos**
21.74	**904.83332**	**TG(16:0_18:1_20:1)+NH4**	**LipidMatch/Bruker LipidBlast**	**886.5**	**Pos**
21.78	**878.81767**	**TG(16:0_18:0_18:1)+NH4**	**LipidMatch/Bruker LipidBlast**	**654.2**	**Pos**
21.82	**852.80189**	**TG(16:0_16:0_18:0)+NH4**	**LipidMatch/Bruker LipidBlast**	**958.2**	**Pos**
22.26	**958.87998**	**TG(16:1_18:1_24:1)+NH4**	**LipidMatch/Bruker LipidBlast**	**699.4**	**Pos**
22.3	**932.86438**	**TG(16:0_18:1_22:1)+NH4**	**LipidMatch/Bruker LipidBlast**	**729.5**	**Pos**
22.36	**906.84885**	**TG(16:0_18:0_20:1)+NH4**	**LipidMatch/Bruker LipidBlast**	**815.6**	**Pos**
22.41	**880.83295**	**TG(16:0_18:0_18:0)+NH4**	**LipidMatch/Bruker LipidBlast**	**360.7**	**Pos**
22.79	**986.91099**	**TG(18:1_18:1_24:1)+NH4**	**LipidMatch/Bruker LipidBlast**	**750.4**	**Pos**
22.83	**960.89576**	**TG(16:0_18:1_24:1)+NH4**	**LipidMatch/Bruker LipidBlast**	**432.2**	**Pos**
23.3	**1014.94192**	**TG(18:1_20:1_24:1)+NH4**	**LipidMatch/Bruker LipidBlast**	**571.1**	**Pos**
24.37	338.34176	Erucamide	LC-MS-MS Positive Mode	966.7	Pos